AALBORG UNIVERSITY
STUDENT REPORT

ELECTRICITY GENERATION FOR OFF-GRID HOUSES IN DENMARK

In collaboration with 'Project Grobund'

Andreas Mølsted
&
Uffe Schifter-Holm

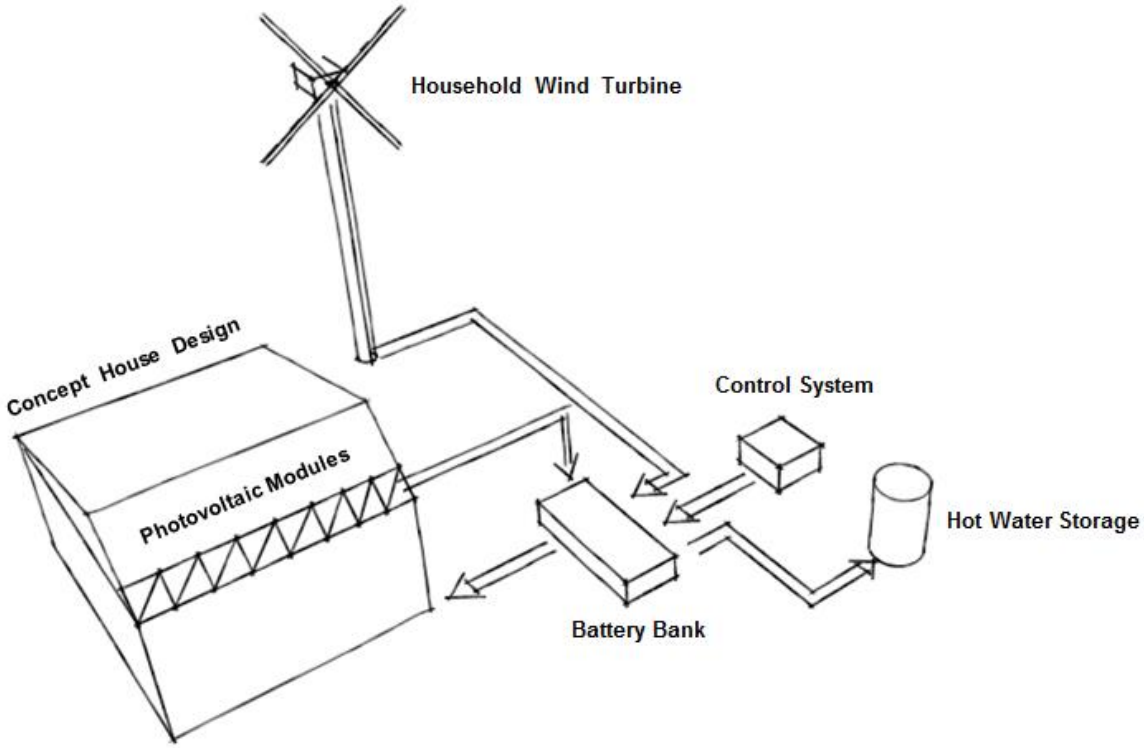

AALBORG UNIVERSITY
STUDENT REPORT

School of Engineering and Science
Department of Civil Engineering
Thomas Manns Vej 23
9220 Aalborg Ø, Denmark
Phone: +45 99 40 84 84
www.civil.aau.dk

Title:
Electricity generation for off-grid houses in Denmark

Study programme:
Master of Science in Technology in Building Energy Design

Project:
Master's Thesis
30 ECTS credits

Project period:
01-09-2016 to 13-01-2017

Supervisors:
Peter V. Nielsen <pvn@civil.aau.dk>
Chen Zhang <cz@civil.aau.dk>

Report pages: 105
Appendix pages: 50
Printed copies: 3
Included USB flash drives: 1 per copy

Synopsis:

The subject of this project is to analyze and design a solution for electricity generation for sustainable off-grid houses, that is currently under development as a part of a larger project called *Project Grobund*.

The report contains the following main topics:
A discussion of off-grid electricity systems and possible technologies for local electricity production.
Calculations/estimations of the energy demands for the conceptual off-grid house.
An investigation of the potential of thermoelectric elements on a mass oven through laboratory and in-field tests.
The development of an Excel-based *Off-grid Simulation Tool* (enclosed on flash drive), that can simulate the balance between electricity demand, production and storage for a system with photovoltaic panels, wind turbine and batteries.
The design of an energy system for the off-grid houses in *Project Grobund*.
An overview of Danish legislation that can affect the possibilities for off-grid living, with a detailed discussion of the circumstances at the intended location for *Project Grobund*.

Authors:

Andreas Mølsted <amoelsted@gmail.com >

Uffe H. Schifter-Holm <uffe.hjortshoej@gmail.com>

Abstract in Danish

Dette speciale beskriver en analyse- og designproces for et energisystem til et bæredygtigt off-grid hus, der er under udvikling som en del af et større projekt kaldet *Project Grobund*. Da en masseovn til rumvarme- og brugsvandsproduktion er en del af huskonceptets grunddesign, er specialets formål er at undersøge mulighederne for produktion og lagring af elektricitet, så beboernes behov er dækket.
Rapporten indledes med en beskrivelse af *Project Grobund* og konceptet for off-grid huset, hvorefter husets energiforbrug fastlægges.
Herefter præsenteres en undersøgelse af erfaringer med off-grid el-systemer samt en overordnet analyse af potentialet i forskellige teknologier til elektricitetsproduktion. Det konkluderes, at solceller og mikro-vindmøller er de teknologier, som har størst potentiale ift. kravene til systemet i *Project Grobund* samt at der kunne være et potentiale i termoelektriske elementer ifm. at udnytte varmeafgivelse fra masseovnen til strømproduktion.
Den næste del af rapporten beskriver derfor en række laboratorie tests af termoelektriske elementer samt praktiske tests, hvor elementerne placeres på en masseovn. Analysen viser, at denne teknologi ikke er anvendelig i forbindelse med masseovnen pga. dennes opbygning og anvendelsesmønter. Der kan dog være et potentiale for elproduktion med termoelektriske elementer, såfremt et forbrændingssystem blev designet til dette formål.
Derefter beskrives en proces, hvis formål er at udvikle et Excel-baseret værktøj (kan findes på vedlagte USB-stik) som kan benyttes til at simulere elproduktion, -lagring og -forbrug i et off-grid system bestående af solceller, vindmølle og batterilager. Teorien for beregning af timebaseret elproduktion fra solceller og vindmølle på en given lokation gennemgås, og det samlede simuleringsværktøj beskrives.
Simuleringsværktøjet benyttes herefter til at designe et energisystem for off-grid huset med udgangspunkt i, at der skal være 100 % dækning af elektricitetsbehovet. Til lokationen for *Project Grobund* syd for Ebeltoft på Djursland anbefales et system med følgende komponenter og værdier:

- Et jævnstrøms-system bestående af 5 m² solcellepaneler kombineret med en 1 kW vindmølle (10 meter højde) og 10.1 kWh batterikapacitet.
  Systemets årlige elproduktion er beregnet til 2055 kWh. Da el-behovet er estimeret til 713 kWh, resulterer dette i en del overskydende elproduktion, som det vælges at anvende til produktion af varmt brugsvand via en elpatron.
- En masseovn der dækker varmebehovet på 2195 kWh (som strækker sig fra november til april) samt producerer varmt brugsvand i samme periode, da der ikke er tilstrækkeligt elektricitet til dette.
- En 200 liter varmtvandsbeholder til lagring af varmt brugsvand. Fra april til og med oktober dækkes hele varmtvandsbehov på 769 kWh af elektricitet. Fra november indtil starten af april dækkes 387 kWh af elektricitet og de resterende 188 kWh af masseovnen.
- Systemets elpris er estimeret til 8.07 DKK/kWh, som dog kan reduceres til 7.06 DKK/kWh ved at implementere en generator i systemet (der kan dække el-behovet i perioder med lav produktion) og reducere batterikapaciteten til 1 kWh.

Herefter gives en oversigt/analyse af de lovgivningsmæssige rammer i Danmark i forbindelse med at leve off-grid samt af de konkrete bestemmelser (lokal- og kommuneplan) for området ved Ebeltoft.
Rapporten afsluttes med en diskussion af processen, forslag til emner der kunne arbejdes mere med og en konklusion, som beskriver det designede off-grid system.

Table of contents

1 Introduction

1.1 Problem Analysis – Background and Purpose

The work performed during this master thesis relates to a current development project named *Project Grobund* (Grobund, 2017). One of the purposes *Project Grobund* is the development of off-grid houses mainly constructed of processed straw elements. The project focuses on sustainable dwellings and the occupant's independency of the building sector and energy grids. The idea is to design a house which the occupants can build themselves, and mainly with sustainable and cheap materials, that can be produced locally. The houses are designed for families of 2-4 people and cover approximately 60 m². Each house is energy independent, implying that the entire energy consumption of the household is covered by on-house or on-site energy production. The plan is to build the first houses at a location near Ebeltoft and this location will be used as case for the analysis in the master thesis. The houses are intended to be cheap in both investment cost and annual maintenance and operation costs, so the annual payments for the house can be kept low.

The results of this project will possibly be applied to the dwellings developed by *Project Grobund* and therefore, the current ideas and concepts developed by *Project Grobund* will be discussed and evaluated as a part of this thesis. *Project Grobund* builds on a range of ideals, which are very important to understand and relate to, in order to understand the purpose of this master thesis.

The vision of *Project Grobund* is to enable people to live sustainable and to take responsibility of the development and job-creation in rural area. In context to the off-grid houses the ideals/values of the project are: energy and construction independency, sustainable construction and building methods, sustainable energy production, ownership of energy production, participation in the construction phase and interest in surveying local energy consumption and generation.

This master thesis aims at supporting *Project Grobund* with ideas and suggestions to the design of the off-grid energy system and additionally to design more energy efficient houses. The primary requirements to the energy system are, that it must be off-grid, as sustainable as possible and be able to cover the energy demand at all times. Further, it must be relatively simple in design and easy to understand, use and maintain, so that this can be done by the occupants.

1.2 Problem Formulation

The purpose of this master thesis is to identify potential energy system designs for the suggested off-grid houses by looking into the currently suggested energy system by *Project Grobund* and furthermore analyzing and specifying alternative energy solutions suited to the specific requirements of the houses.

The following is the problem statement, describing the topics that will be investigated and discussed within this thesis:

- Simulation of energy demand for the designed dwellings
    - Heating demand simulation in BSim as a function of the current conceptual design
    - Electricity demand in BSim through daylight calculations of the current conceptual design and assumption of intended appliances in the dwellings
    - Domestic hot water demand calculations through previous studies and user behavior
- Simulation, estimation and testing of suitable off-grid energy technologies
    - Investigation of suitable technologies to cover electricity demand, including the following:
        - Literature study of current available and popular systems
        - Overview of suitable technologies for this specific project
        - Detailed analysis of the technology or technologies found to be most suitable through the overview, including:
            - Hourly simulation of performance
            - Laboratory tests of technologies
            - In-field tests of technologies
- Development of a simulation tool to calculate the balance between the hourly user demand and the hourly electricity generation and DHW production in an off-grid system.
- Analysis of different solutions and designs of a suitable off-grid energy system that fulfills the requirements for *Project Grobund*.

1.3 Requirement Specification

The following presents the main requirements for the energy system in the houses at *Project Grobund*:

- Sustainable or renewable energy sources
- Simplicity in terms of construction and installation
- Low technical knowledge needed to maintain and repair system
- Reasonable investment and operational costs for the systems
    - Lifetime cost of the technologies and the proposed system will be evaluated as the 'Cost of Electricity' over a 20-year period. The most economic feasible technology will not necessarily be suggested as 'the best' solution.

1.4 Delimitation and General Assumptions

The scope of this master thesis is to investigate solutions for an off-grid energy system and evaluate the energy coverage (balance between demand and generation) for the current conceptual house design from *Project Grobund*. A firewood mass oven (stove) is an integrated part of the conceptual design and therefore other space heating technologies will not be investigated. The domestic hot water is intended to be produced by the mass oven during periods with a space heating demand and as such only technologies to cover the domestic hot water demand during periods without space heating will be investigated.

The thesis mainly focuses on the energy balance in the off-grid system and not on the technical details of the systems. This means, that the system elements are described in general with regard to energy generation, function and cost. The detailed designs concerning specific wires, fuses, pipes and the like is not evaluated.

The house proposed by *Project Grobund* currently contains ideas regarding fresh water supply and on-site handling of sewerage. This thesis will not evaluate these ideas nor investigate or proposed alternative ones.

General assumptions:

- The processed straw elements will conform to current fire and structural regulations.
- The mass oven will conform to current fire and other building regulatory instances.
- Assumptions and design intentions from Steen Møller from *Project Grobund* regarding the electrical system and appliances in the house will be applied in the energy simulations of the house. These assumptions can be found in Appendix D .

1.5 Methodology

The overall methods or work processes used in the report are:

- Determination on energy demands (space heating, electricity and domestic hot water (DHW)) based on Bsim simulations, references to other studies and information from *Project Grobund*
- Investigation and analysis of suitable off-grid electricity generation technologies through literature reviews and in the case of thermoelectric elements through laboratory and field tests
- Development of an Excel-based energy balance simulation tool to assist the process of off-grid system design. Theory for photovoltaic and wind turbine electricity generation are implemented in the tool together with functions for storage of electricity and domestic hot water (DHW).
- Design of a suitable energy system for the Off-grid houses in *Project Grobund* by use of the simulation tool and the obtained knowledge about off grid energy systems.

2 Project Grobund

2.1 Introduction

Project Grobund is an independent project initiated by Steen Møller, Jens Randrup and Henrik Moeslund. The vision of the project is to buy an old factory building south of Ebeltoft, Djursland, and start a production of off-grid houses (among other things). Beside the factory, the vision is to build a sustainable living-community with the houses, so that the participants in the project can work and live together in the area. The project initiators are as of the fall 2016 gathering funds and interested people to initiate the project. The first practical step is the construction of an off-grid processed straw element house, which is to be built at *Brenderup Højskole* on Funen during the spring and summer of 2017.

After this demonstration project, a large-scale production of the processed straw elements is to be initiated in Ebeltoft, Djursland, where *Project Grobund* hopes to be able to produce straw elements for 4-5 houses per day. One of the pillars of the project is the commitment and engagement from the people who are to inhabit the houses later on. The inhabitants are supposed to help construct the houses from the beginning. Not only does this encourage a stronger feeling of ownership of the house, but also requires the inhabitants to investigate the construction materials, understand the energy balance and learn how to use and engage in the house in the most efficient way.

The project also has a political vision and hopes to initiate a discussion about sustainable buildings and -living. The Danish Building Regulations from 2015 requires houses to be built with extremely low yearly energy consumption. This limits choice of material and construction methods, as the requirements and regulations leaves little to no choice for the construction companies, mostly due to cost-effectiveness.

The requirements lead to concrete, steel, mineral wool and glass being the main building materials in new houses and buildings in Denmark. While these materials are the cheapest and most available choices for construction companies and are easy to use in order to conform to the regulations, important factors are being neglected. Sustainability in terms of; material life time expectancy, embodied energy, demolition and recycling potential of materials are not being considered in the current Building Regulation.

One of the main purposes of *Project Grobund* is to show the Danish Government that it is possible to construct sustainable houses with sustainable materials, while also conforming to requirements such as annual energy consumption, indoor climate, building tightness etc. Therefore, by constructing a series of off-grid houses *Project Grobund* hopes to demonstrate an alternative and sustainable building method.

2.2 Conceptual Design

This section contains the conceptual design and ideas presented by *Project Grobund* in the beginning of September 2016. This is presented to clarify the overall design and systems of the house and also to establish the starting point, from where this master thesis began.
The design and especially the energy systems have since then been changed, as will be discussed throughout this report.

2.2.1 Conceptual Drawings

The conceptual or overall design of the initial off-grid house is illustrated in Figure 2.1. The load bearing elements of the house consist of processed straw elements as exterior walls and ceiling, while timber beams and columns support the greenhouse to the south as well as the polyethene (plastic) roof. The polyethene roof creates an unheated ceiling space between the processed straw element and the polyethene roofing which can be used for storage or technical utilities. The greenhouse will be unheated and for this reason high insulating glazing will be placed between the greenhouse and the interior. The greenhouse is as such not intended as living space, but rather for growing of vegetables and fruits. Additionally, the ground below the greenhouse is a part of the sewerage system, wherein grey and black water is filtered and used as fermentation of the earth in the greenhouse. For the conceptual design by *Project Grobund* the intended areas for photovoltaic and solar thermal collectors have been indicated on the figure.

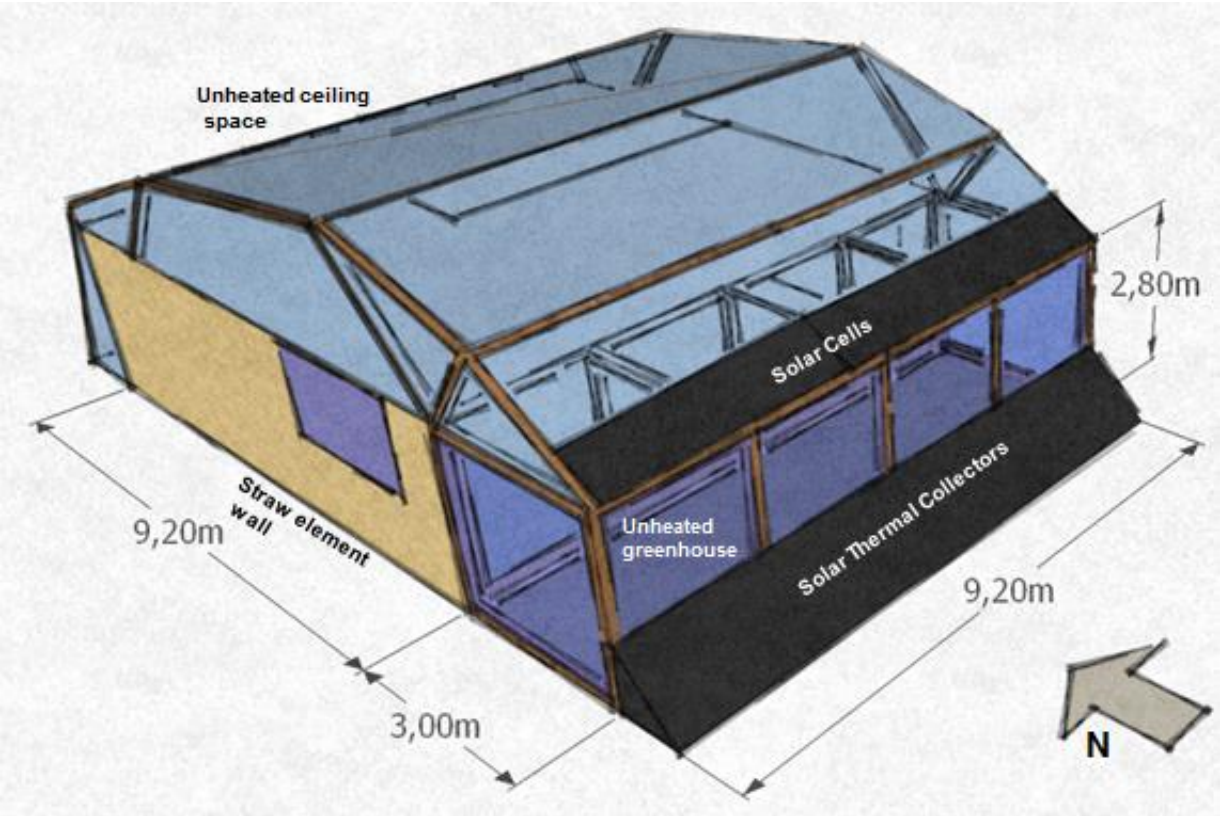

Figure 2.1 – Current house design 'Conceptual Design'

The construction materials can be divided into five categories: Straw elements, timber beams, glazing, polyethene and clay bricks for interior walls.

Compared to concrete, steel and aluminium, which composes the largest parts of modern houses and buildings, these materials have a low embodied energy, implying that a fairly low amount of energy is required to process the materials (YourHome, Australian Government).

Furthermore, the demolition or recycling for these materials are highly sustainable due to the material composition and mounting process, where everything will be mounted by screws and bolts. As such, recycling or re-use of the materials is made possible, increasing the overall sustainability of the house.

2.2.2 Energy Production

The overall energy system in the conceptual design is illustrated in Figure 2.2. The vision is to create a house which is entirely energy independent, hence the expression off-grid house. In order to fulfill this vision, several renewable energy technologies must be applied. As the house is designed to conform to the low energy consumption requirements of BR2015, the annual space heating and electricity consumptions must be relatively low. The energy system in the house will be designed to operate under seasonal conditions, meaning different systems will be used in different periods of the year.

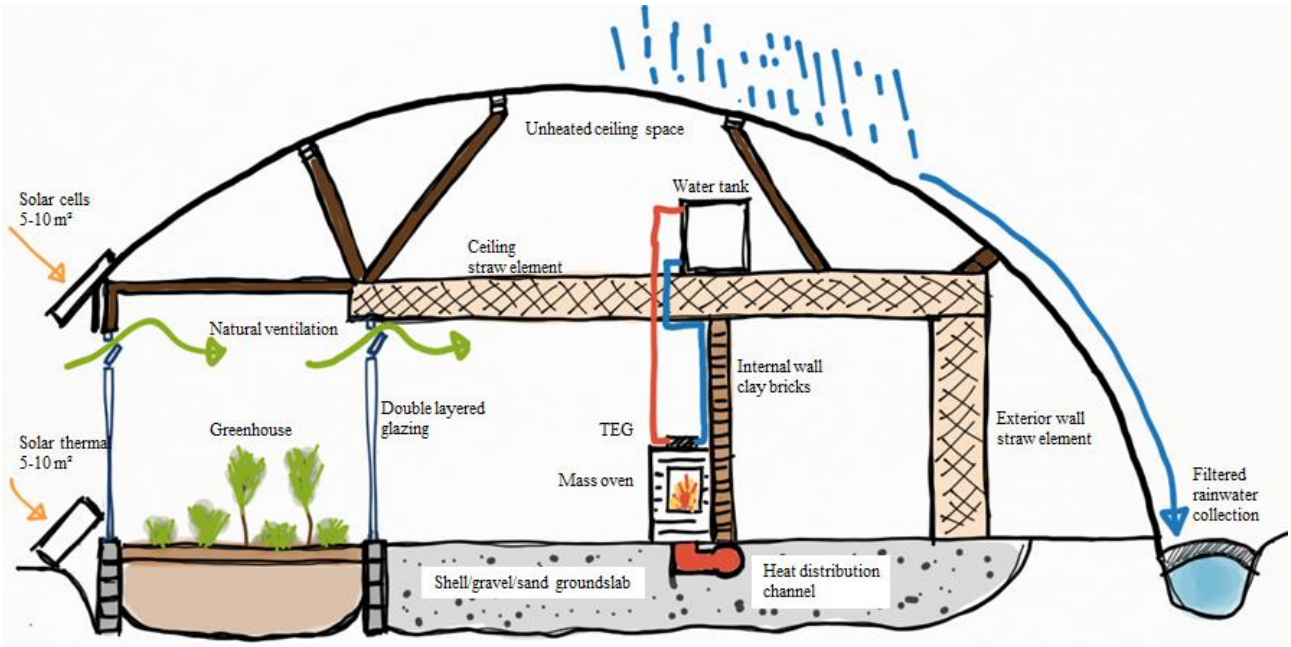

Figure 2.2 – System design and function by *Project Grobund*

In winter, space heating and domestic hot water is intended to be covered by an integrated mass oven and possibly supplemented by solar thermal collectors. Electricity demand is intended to be covered by thermoelectric generators on the mass oven and supplemented by a photovoltaic system. During summer, domestic hot water will be supplied by the solar thermal collectors, while electricity will be supplied by the photovoltaic system.

As the house is currently in a conceptual design phase, all of the above mentioned are ideas which are to be further designed, analyzed and tested. These investigations may consist of; simulation of photovoltaic and solar thermal collector area, simulation and test of thermoelectric generator performance, calculation of battery capacity for storage of generated electricity and also investigations and analysis of other suitable technologies.

3 Determination of Energy Consumption for Off-grid house

The following calculations and assumptions are based on the current conceptual house design, along with notes from *Project Grobund* regarding materials, construction methods, appliances and general use of the house – these can be found in Appendix D .

The calculated demands of space heating, domestic hot water and electricity will be applied throughout this thesis when assessing different energy technologies and systems.

3.1 Assumptions

In order to evaluate the energy consumption of the suggested design, a few assumptions must be made to develop the simulation models.

- Processed straw elements: Thickness of 0.6 meter, thermal conductivity of 0.068 W/mK, density of 250 kg/m³, thermal heat capacity of 800 J/kgK.
  As an additional support for Project Grobund, the thermal conductivity of five different straw elements samples has been tested as a part of the thesis. The thermal conductivity is based on these tests, that can be found in Appendix O .
- Excess production of electricity cannot be sold or send to the electricity grid

3.2 Electricity

In the conceptual design phase, the following electrical appliances and demands are included in the household:

- LED light fixtures in every room: 85 Watts according to Table 3.1 – Lighting levels
- Outlets for appliances, such as chargers for phones and computers: 200 watts assumed to be used six hours per day resulting in 438 kWh/year.
- Refrigerator - installed in the wall with the back outside the building in order to reduce cooling demand and thus electricity consumption: Approx. 100 kWh/year corresponding to A+++ energy class

The house is designed without a dishwater, dryer, microwave oven, toaster, etc. and uses a gas-oven. This reduces or eliminates several of the typically most energy demanding household appliances. Assumptions are based on Appendix D .

Room type	Area [m²]	Illuminance [Lux]	Luminous flux	Luminous efficacy [lm/w]	Power [W]
Bedroom	15	150	2250	150	15
Kitchen	20	300	6000	150	40
Living room	20	150	3000	150	20
Bathroom	5	300	1500	150	10
Total					**85**

Table 3.1 – Lighting levels

Hourly lighting levels have been simulated in a BSim model, more information about this model can be found in the section 3.3. Electricity use for lighting according to BSim model: 174 kWh.

Thereby reaching an annual total of 713 kWh for all electrical appliances, with an average daily total of 1.95 kWh. By applying the work of (Jensen., et al., 2011) the electricity consumption can be distributed over the hours of the year (based on the distribution in a normal household) as illustrated by Figure 3.1 and Figure 3.1.

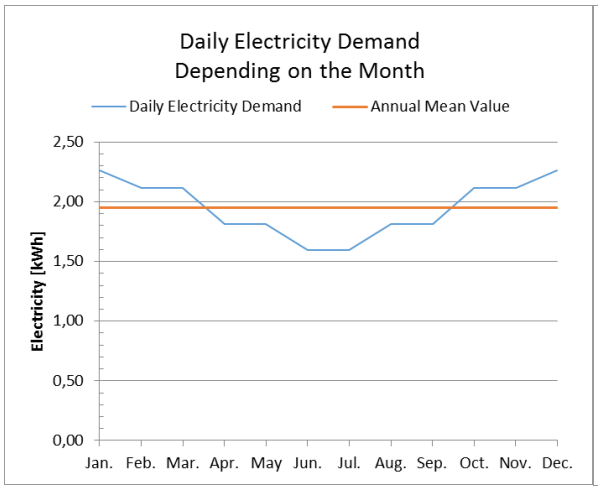

Figure 3.1 – Daily Electricity Demand

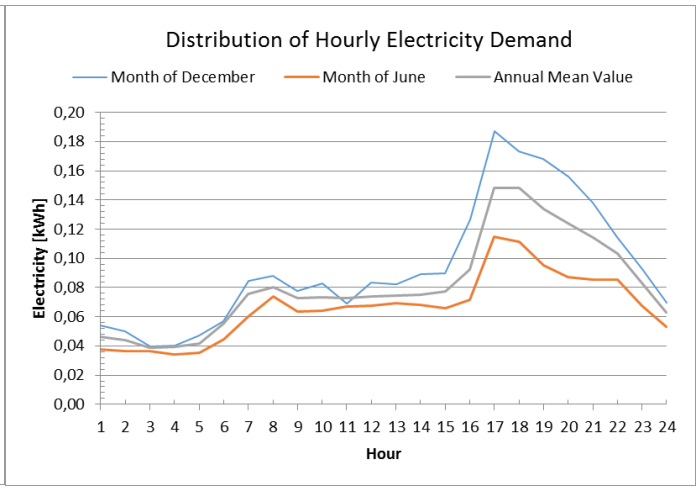

Figure 3.2 – Hourly Distribution of Electricity Demand

Figure 3.1 illustrates the variation in daily electricity demand over the year, where the highest demand can be found in December and January. Figure 3.2 illustrates the hourly distribution of the electricity demand for December and June (winter and summer solstice). The biggest deviation can be found between hours 16-18. On the 21st of December (winter solstice) the sun rises at 08:36 and sets at 15:38 in Denmark, whereas the sun rises at 04:25 and sets at 21:58 on the 21st of June (summer solstice). This large difference in day length is the main reason for the deviation throughout the year as the winter months require a much greater amount of artificial lighting than summer months.

3.3 Simulation of Space Heating

A BSim model of the house according to the current design in *Project Grobund* has been established. The geometry of the house can be seen in Figure 3.3.

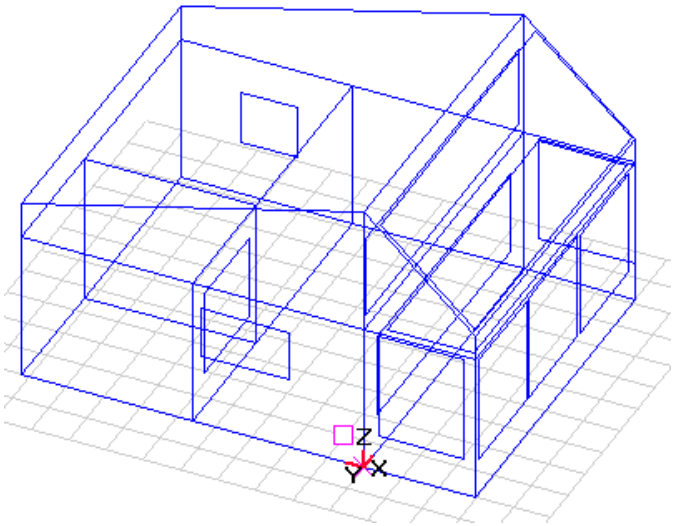

Figure 3.3 – Geometry of BSim model

The following is a list of the essential input which has been applied to the model:

- Infiltration rate: 0.04 h^{-1} (James & James, 2016)
    - A small ventilator of 50 m^3/h is installed in the chimney of the mass oven to ensure proper combustion temperatures and high efficiency. The fan operates between 7 and 9 am and increases the infiltration rate to 0.32 h^{-1} during that period.
- Natural ventilation: max 3 h^{-1}
- Equipment: 0.187 kW – Hourly loading profile according to section 3.2
- Lighting: 0.085 kW – Day- and sunlight controlled
- Occupants: 2 people – Hourly loading profile according to the work of (Jensen., et al., 2011)
- Windows: U-value 1.5 W/m^2K, G-value 0,63, LT-value 0.65
- Walls: U-value 0.11 W/m^2K (Appendix O)
- Ceiling: U-value 0.11 W/m^2K (Appendix O)
- Floor slab: U-value 0.095 W/m^2K (Munch-Andersen & Andersen, 2004)
- Solar shading: None
- Greenhouse: Unheated, natural ventilation max 3 h^{-1}, infiltration rate: 0.3 h^{-1}

The building envelope mainly consists of the straw elements, which are currently designed with a thickness of 0.60 meters, corresponding to a U-value of 0.11 W/m^2K (Appendix O)

The ground slab will be made up of a mix of shells, gravel and sand with a depth of approx. 1 meter, corresponding to a U-value of 0.095 W/m^2K.

The design suggests approx. 30% of the façade to be glazing, allowing for plenty of daylight as well as a view to the surroundings. The U-value of the double glazing is assumed to be 1.5 W/m²K, while the glazing for the greenhouse is assumed to have an U-value of 2.5 W/m²K.

Natural ventilation can be performed by opening windows to the outside for cooling of the indoor temperature, or to the greenhouse for pre-heating of the air depending on indoor and greenhouse temperatures.

3.3.1 Simulating the Mass Oven in BSim

The mass oven enables the occupants to ignite the oven for a short period of one or two hours per day. In this short operating period the mass oven reaches a combustion temperature of approximately 1000 °C, resulting in a high efficiency. The term 'mass' is used because the exhaust gasses is drawn through a 'path' made of materials with good thermal mass. In *Project Grobund* this path is through the brick-made oven and then a concrete pipe in the ground slab, as seen in Figure 2.2.

In this case, the exhaust gasses from the mass oven heats the floor of the house very similar to a floor heating system. The high thermal mass of the floor allows the heat from the oven to be stored and released slowly throughout the day. This is the core principle of the mass oven, which allows a very short operating period for each day and a more uniform heat dissipation compared to normal wood burning stoves.

In the BSim model, it is assumed that the mass oven is ignited at 7 am, if this is necessary according to the temperature in the house. The mass oven is simulated as a floor heating system, with a set point temperature of 20 °C, meaning that if the temperature at 7 am is lower than 20 °C, the mass oven is ignited. The simple nature of the mass oven means that there is no heating control system as is the case in typical modern houses, where circulation pumps, valves and thermostats very accurately control the indoor temperature. Instead, the occupants will ignite the oven with an amount of firewood up to 10 kg (due to the volume capacity of the oven). Table 3.2 shows the maximum heating capacity simulated in the floor heating system in BSim (the value of 5 kg firewood is found through multiple simulations to identify a suitable required heating power).

Firewood Added [kg]	Burn Value of Wood [kWh]	Heating Value Eff. of 0,90 [kWh]	Heating Power [kW]
5	20	18	9,0

Table 3.2 – Heating power in firewood (9 kW = 18 kWh over 2 hours)

Table 3.2 shows that firewood with the weight of 5 kilogram corresponds to a heating power of 9.0 kW over a two hour period. Therefore, the floor heating system is simulated to operate between 7-9 am with a heating power ranging from 0-9 kW depending on the operative temperature.

The heating results of the BSim model are seen in Table 3.3.

	Maximum Heating Power [kW]	Total Heating Energy [kWh]	Mass Oven Operating Cycles [-]
Bedroom	1.2	322.4	
Living Room	7.8	1872.5	
House Total	9	2194.9	143

Table 3.3 – Simulated annual heating results

The monthly distribution of the 2195 kWh is as follows:

Month	Jan.	Feb.	Mar.	Apr.		Nov.	Dec.
Space heating demand [kWh]	516	429	308	116		338	488

The mass oven operates a total of 143 times, or 39% of the days in a year with a maximum capacity of 9 kW, the period occurs from November till March (plus once in April and 3 times in October). The minimum operative temperature in the living room is 15.0 °C (early morning), while the average temperature is 22.3 °C. The low temperatures (15-18 °C), which occur a few times a year during the morning, can be avoided by igniting the mass oven at night in cold periods. Figure 3.4 illustrates the heating power and operating temperature for the month of January.

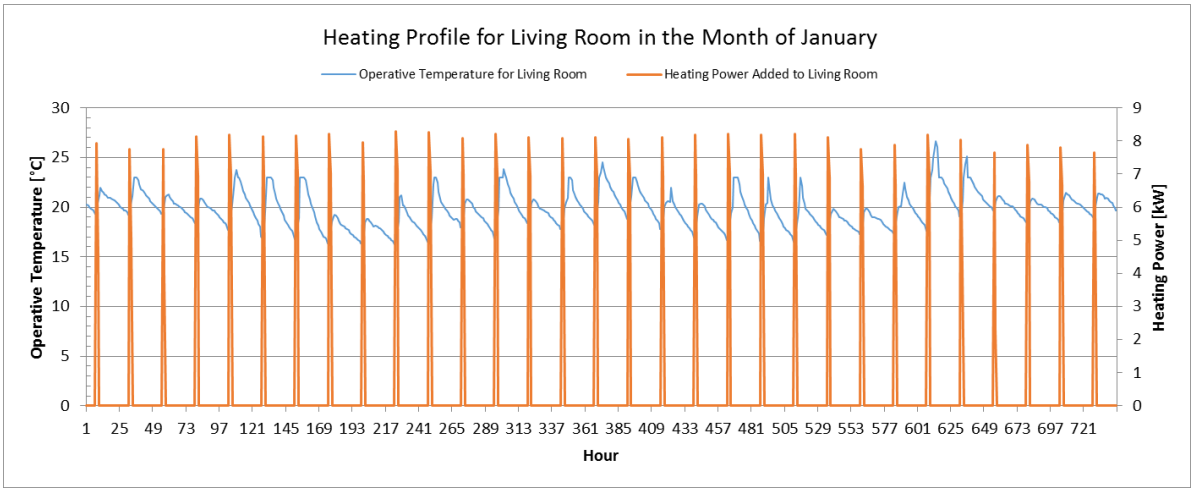

Figure 3.4 – Heating demand and operative temperature for living room in January

As can be seen in Figure 3.4, the mass oven operates every morning in January due to the operative temperature falling below 20°C every night. The high operative temperature around 12 pm on the 26th and 27th of January is due to a high solar gain from 11 am to 3 pm. This illustrates one of the issue with the mass oven, on days with a cold morning temperature the heat is already released and cannot be adjusted continuously throughout the day in case of large heat gains as solar radiation. The profile for the 1st of January is illustrated in Figure 3.5.

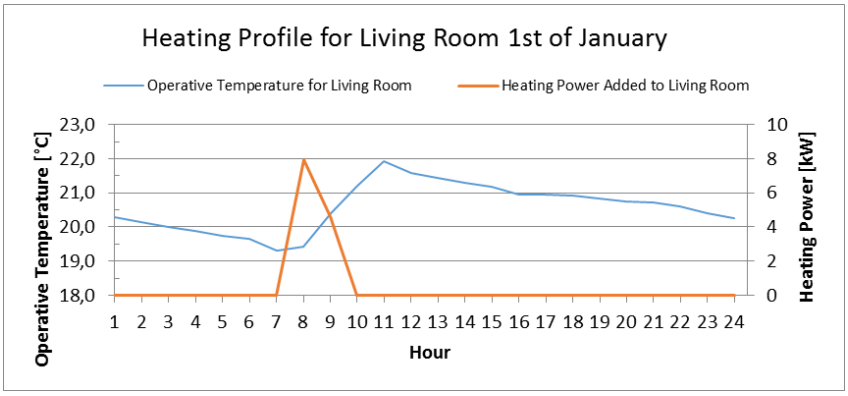

Figure 3.5 - Heating demand and operative temperature for living room on the 1st of January

On the 1st of January, which is similar to most days during the heating period, the coldest operative temperature occurs just before 7 am. The temperature then slowly increases as the mass oven is ignited and reaches its maximum of 22°C around 12 am. This slow increase occurs due to the slow release of heat from the floor as well as an increase in outdoor temperature and solar gains.

The simulated heating demand according to the BSim model will be used throughout this report.

Appendix C contains a alternative house design which can significantly decrease the heating demand of the house.

3.4 Domestic Hot Water

Determining the amount of daily usage of domestic hot water can be difficult as this will vary greatly depending on the individual needs of the inhabitants.

Key numbers from the Danish energy simulation program BE10 (Aggerholm & Grau, 2016) suggests a value of 250 liters/m² per year for an average household, assuming an average household is approx. 150 m² and 3 people, this comes out to **34,3 liters/person/day** for a single household.

SBi 260 (Ginnerup, 2015) suggests a domestic hot water use of **46 l/person/day.**

SBi 129 (Grønvold, et al., 1982) suggests a domestic hot water use of **40 l/person/day**.

Meanwhile, the projects of *Energi Parcel* (Larsen, et al., 2011) and *Komforthusene* (Larsen, 2010) recorded between 16-38 l/person/day, with an average of **27 l/person/day**.

The most important factor in regards to domestic hot water usage is human behavior. As previously defined, the inhabitants of these houses are going to have an interest in sustainability and low energy and water usage. Therefore it must be assumed that these individuals will use significantly less water and hot water than the average person. The projects of *Energi Parcel* (Larsen, et al., 2011) and *Komforthusene* (Larsen, 2010) are fairly newly established low-energy houses in Denmark, which can be assumed to be similar in water appliances and user behavior to the houses in *Project Grobund*.

Therefore, the average value of **27 l/person/day** will be applied in this project. The houses are assumed to have 2 occupants, resulting in a daily total of 54 liters of domestic hot water. Applying these values to the work of (Jensen., et al., 2011) an hourly distribution of DHW usage can be generated, as presented by Figure 3.6 can be produced.

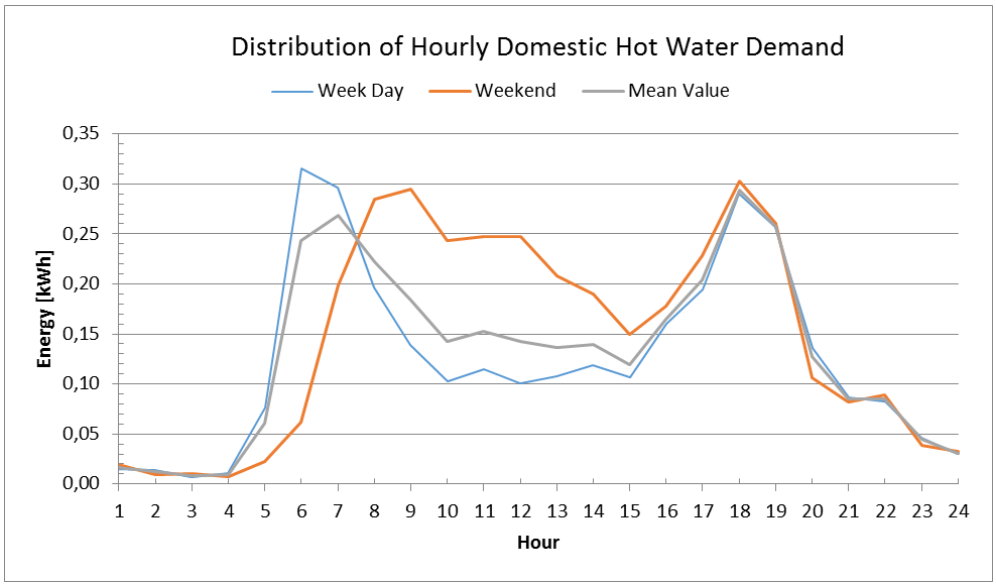

Figure 3.6 – Hourly distribution of domestic hot water demand

The results in Figure 3.6 are based on a daily demand of 54 liters corresponding to average daily demand of 3.15 kWh (water temperature difference of 50K). This results in an annual consumption of 1150 kWh for the household. If the water storage tank in the household is significantly larger than the daily demand of 54 liters, the hourly distribution becomes less significant, therefore the mean hourly distribution seen in Figure 3.6 will be applied for all days in the energy simulations with domestic hot water.

4 Literature Review of Stand-Alone Energy Systems

In order to learn from previous studies, get inspired by similar researches as well as avoid past mistakes, a literature review of off-grid energy systems has been performed. Herein, published papers have been studied in order to establish an overview of already tested experiments, setups and elements.

Stand-alone hybrid systems consisting of several renewable energy technologies have been tested and documented for decades. Recent published studies have been reviewed to identify the most common systems including their economic feasibility, their assets and their flaws or issues.

Almost all the studies, that are described in this chapter, indicates that a hybrid system composed of a photovoltaic system, one or more wind turbines, battery storage and possibly an auxiliary generator is the best solution for off-grid electricity generation in areas with sufficient solar and wind resources.

According to (Chong, et al., 2016) the combination of renewable energy power sources (REPS) and hybrid energy storages systems (HESS) can yield the following advantages:

- Optimization of the energy storage capacity as a reduction of the peak current demand
- Total system efficiency improvement
- Increase of system life time by optimizing operation and dynamic stress on the storage
- Better economic efficiency

The most common combination is a wind turbine, a photovoltaic (PV) array, a battery bank and a back-up diesel generator, as seen in (Kavadias, 2012). In this study, it is found that renewable energy systems require an oversized storage in order to fulfill the energy demand in all periods. Therefore, a back-up systems as a thermal power unit (typically diesel or gasoline generator) is usually advantageous., although wind and solar complement each other well, as the intermittency of both resources can help smooth out the electricity generation, as seen in Figure 4.1, in this specific case the measurement took place in the Greek islands. Carrying out a similar analysis for regions of Denmark would be resourceful in order to determine the potential for a combination of wind and solar power.

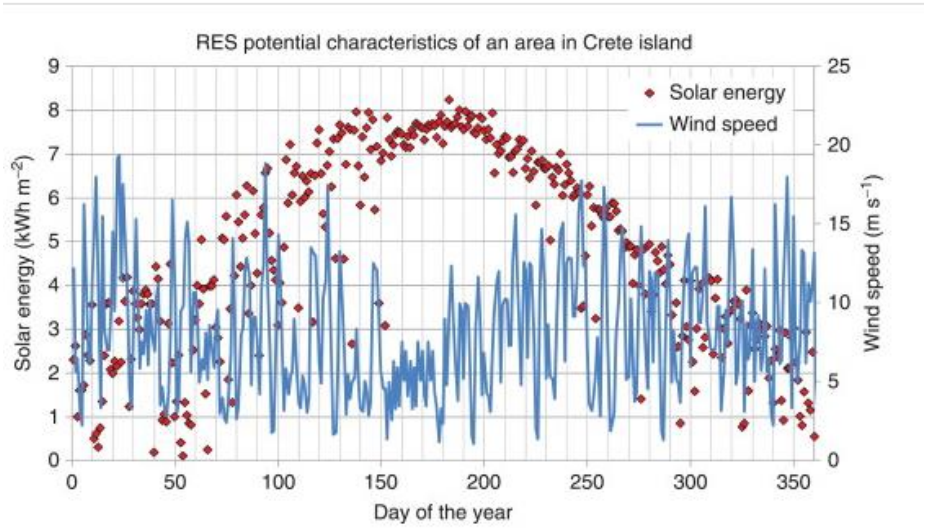

Figure 4.1 – Renewable Energy Characteristics (Kavadias, 2012)

In the study of (Nema, et al., 2009) the optimal system for rural households are found to be a combination of solar, wind, storage and auxiliary energy - as in the previous study. In this study the economic feasibility cannot compete with that of conventional fossil fuels systems, but it is stated that the technologies and the combination of these bear good potential for the future, especially for rural households and developing countries where high quality grid-connections are limited. This combination is also found to be the best solution for resident household in (Ogunjuyigbe, et al., 2016), where five scenarios (PV + battery, wind power + battery, single big diesel generator, 3-split diesel generators and PV+wind+split-diesel+battery) was analyzed.

In another study (Hossain, et al., 2016) of stand-alone systems the best electricity option for a large resort center in Malaysia is found to be 700 kW of photovoltaic arrays, 5 wind turbines, 240 batteries and 3 diesel generator units. The combination is found to have reasonable Cost of Electricity (CoE) and Net Present Value (NPV) compared to a grid connection.

(Bianchini, et al., 2014) set out to optimize a PV-wind-diesel-battery hybrid system for remote area application. Figure 4.2 and Figure 4.2 illustrates the findings of long terms savings for the system, where a systems without battery and with battery is examined. The results show that an increase in battery capacity is feasible until a certain point, where as a system without any storage capacity is the least feasible option. The absolute values and long term savings are only applicable to the exact area where the study took place, but the fact that an increase in battery capacity increases the economic feasibility are most likely applicable to all regions.

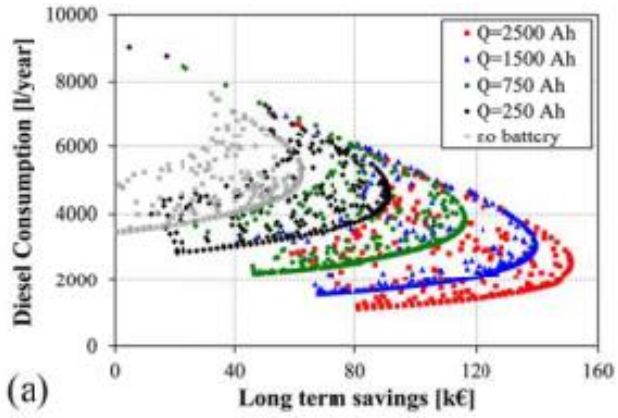

Figure 4.2 – Long term savings (Bianchini, et al., 2014)

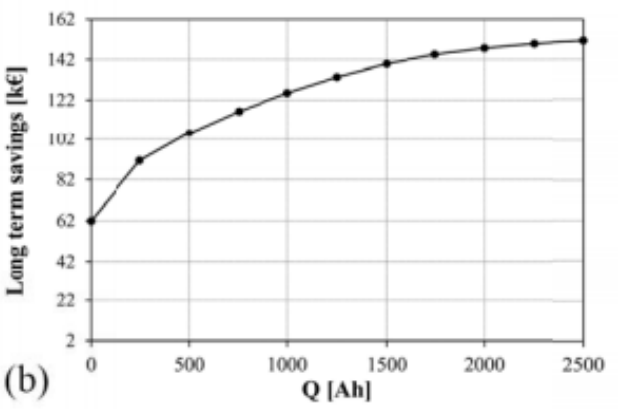

Figure 4.3 – Battery Size (Bianchini, et al., 2014)

The study concludes that in areas where natural resources, in this case wind and solar power, are available and reaches sufficient levels, a properly sized system can compete with conventional fossil fuel system. Also, the optimal system is a balance between smart dimensioning of the renewable energy systems and of the storage capacity, as an increase in the energy producing systems can lead to wasted energy production which nullifies the benefits of the system.

In Brazil, a hybrid system consisting of PV arrays, fuel cells and a battery bank was investigated (Silva, S. B.; Severino, M. M.; de Oliveira, M. A. G.;, 2013). The fuel cells have the advantage of being environmental friendly as it is fossil fuel free, but it was found that the fuel cell technology is currently too expensive and not as efficient as hoped. It was concluded that a system including fuel cell technology was not yet viable and further research to improve the technology and also decrease the cost was needed.

Propane exchange membrane fuel cells, a technology based on the reverse reaction of electrolysis, combined with PV and wind was investigated in (Madaci, et al., 2016). The PEMFC technology allows for heat generation and high efficiency and combined with PV and wind and a dump load in form of an electrolyzer for excess generation, the system was found to work very well. No economic analysis was conducted in order to identify the feasibility compared to other systems.

One study was found where a combination of PV and fuel cell achieved the lowest CoE and highest NPV (Rezk & Dousoky, 2016). Six systems were analyzed and rated as follows based on economic feasibility:

1. Photovoltaic and fuel cells
2. Photovoltaic and wind turbine generator
3. Photovoltaic, wind turbine generator and fuel cells
4. Photovoltaic and battery storage
5. Wind turbine generator and battery storage
6. Stand-alone diesel generator

The applied investment price of the fuel cells was around 5.5 DKK/W (nominal power), the same as a photovoltaic system, currently it seems impossible to locate a similar fuel cell price in the Danish or European market. Therefore, it seems the reason the combination of PV+FC does so well in this study, is the low investment price applied to the fuel cells.

Overall the studies agree that a combination of a photovoltaic system, a wind turbine, battery storage and an auxiliary unit is the best solution in terms of full coverage with the lowest cost of electricity.

5 Overview of Electricity Generation and Storage Systems

Figure 5.1 illustrates a number of technologies which will be examined as a supplement to a photovoltaic system, including known advantages and disadvantages of each technology. Following is a very short description of each technology. The technologies will be examined and consequently either disregarded or further analyzed in the project.

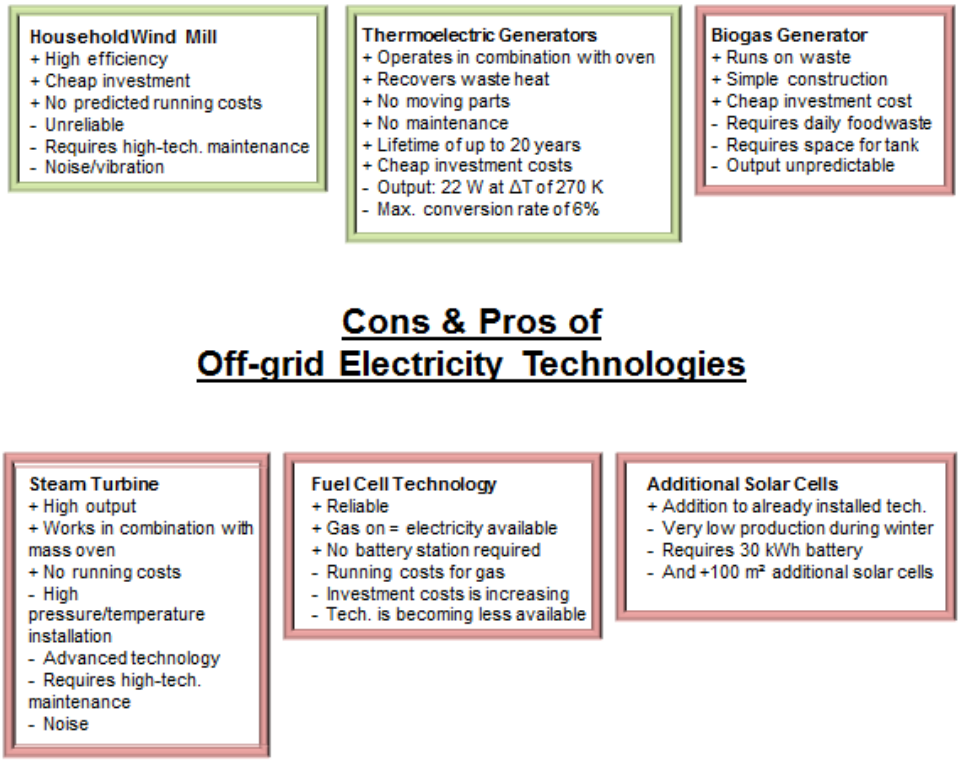

Figure 5.1 – Overview of investigated off-grid electricity technologies including cons and pros

5.1 Overview of Technologies

In this chapter the above technologies (Figure 5.1) will be shortly described in order to determine the main advantages and disadvantages of the technologies. In addition, energy storage systems will also be discussed. Depending on the outcome of this study, the most promising technology or technologies will be thoroughly analyzed following this.

5.2 Energy Storage System

Due to the fluctuating nature of most renewable energy sources, an energy storage system is often necessary to meet the load demand during all hours of the year. While some technologies already rely on stored energy, such a fuel cells running on methanol, wind and solar energy does not naturally have a source of storage. Therefore, an energy storage system will be necessary for the household. The most common storage type of electricity is batteries made of lead acid, lithium ion etc. Electrical batteries are easily usable and widely spread, but do come with some environmental drawbacks, as breaking down the batteries releases toxins. Additionally, the lifetime of the batteries can be fairly short depending on the usage or average depth of discharge (DoD). This indicates that heavy use of a battery will lead to a higher number of batteries used in an installation during a certain period, increasing investment cost and environmental impact. As such, batteries will be applied in the system for the proposed household, but system design and use will focus on increasing battery lifetime as much as possible.

Another type of energy storage is use of fossil fuels in combination with a diesel or gasoline generator to generate electricity when needed. While this technology is not renewable, it might have the same or less environmental impacts as the use of batteries.

5.3 Photovoltaic System

For small-scale installations, i.e. a household installation, a photovoltaic system is commonly an ideal choice among renewable energy sources for multiple reasons, such annual energy output, installation price, maintenance, noise, predictability, degradation, visual impact etc. Small systems of up to 6 kW are a popular choice for an increasing number of households in Denmark, as the subsidies from the government are beneficial, while the installation has minimal impact on the surroundings besides a visual change to the roof. But as the literature study suggested, an installation of only PV and a battery bank is not the optimal solution due to the intermittency of solar radiation. Using DRY data, Figure 5.2 illustrates the required size of a PV/Battery system to cover an annual electricity consumption of 713 kWh. The investment cost of such a system would range from approximately 100,000 to 500,000 DKK depending on size and battery type.

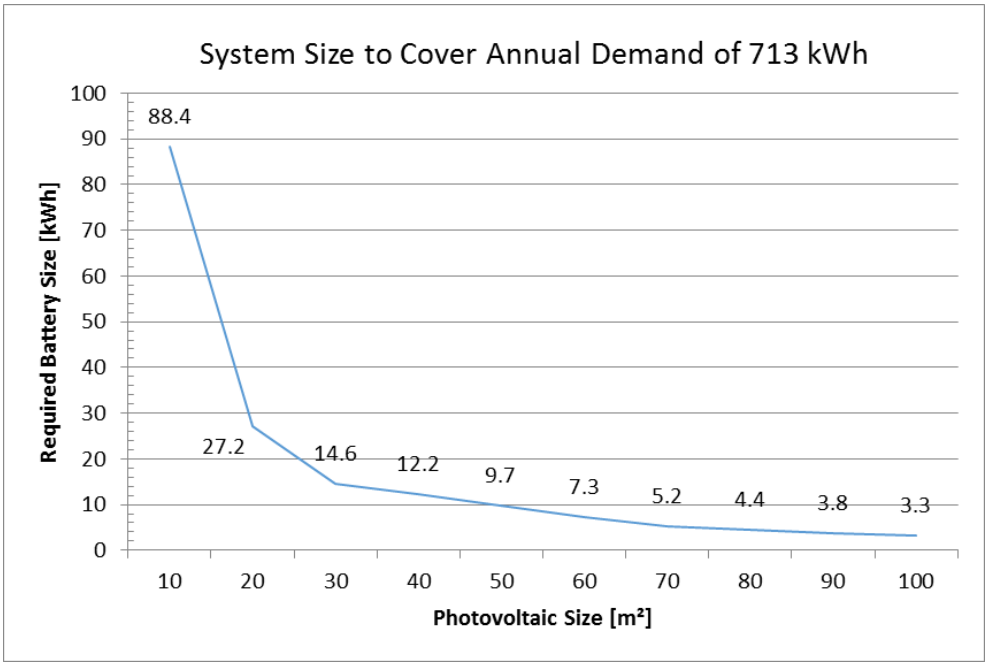

Figure 5.2 - Size of PV system and battery to cover annual electricity demand of 713 kWh

Besides the investment price, the required area is a limiting factor and as such, a PV+Battery system is not an option. Therefore, a second electricity source is required to supply a photovoltaic system.

5.4 Thermoelectric Generators

The full literature study of thermoelectric generators can be found in Appendix I .

As it is considered to integrate thermoelectric generators with the proposed house-integrated mass oven, a short literature study regarding the thermoelectric technology is performed in order to better assess the potential of this technology as an integrated part of the household's energy production.

Only a few papers have focused on electricity generation in combination with heating of water, which is the intended function of the TEG's in the household – i.e. the water is used to remove heat from the cold side of the TEG. As early as in 1996 a study of a system fairly similar was conducted in Northern Sweden.

Most papers report little to no economic value in the technology as of the current state, unless the TEG's are combined with a form of heat recovery, in which case 4-8% electrical efficiency and 50-80% thermal efficiency can be achieved (Zheng, Yan, & Simpson, 2013), (Zheng, Liu, Yan, & Wang, 2014).

Overall, the papers are positive towards the future of the thermoelectric generator technology and believe it can be become an important element in the future energy generation on a global level. This is both in the context of large scale solar power plants and waste heat recovery systems, as well as small scale generators for rural villages or off-grid houses.

5.5 Steam Engine / Turbine

A steam engine or steam turbine converts the pressure (work-potential) of heated water vapor to mechanical energy by moving a piston or turbine. When connected to a generator most of the mechanical energy can be converted to electricity, as generators can have efficiencies up to 95 %. Thus, the efficiency of the system (from thermal energy to electricity) depends primarily on the conversion from steam to mechanical energy.

Many examples of small homemade steam engines/turbines exist on the internet and some are made into commercial products like those produced by (Green steam engine) illustrated in Figure 5.3.

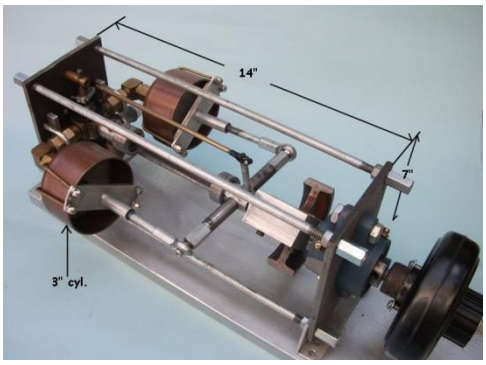

Figure 5.3 – Steam engine (Green Steam Engine)

To evaluate whether a steam engine/turbine could be a solution in context of producing electricity in combination with an oven system in the off-grid house, a calculation of the potential energy in saturated steam at different pressures/temperatures are presented in Table 5.1. To take an example, the Green Steam Engine operates at a steam pressure up to around 14 bar.

Assuming a boiler pressure of 15.54 bar (to fit the table) the available energy in the steam is 117.1 kJ/kg if the entire pressure drop to 1 atm is assumed to be utilized. At 10 ℃ the enthalpy of water is 42.01 kJ/kg which means that heating the water to 200 ℃ and evaporating it takes 2751 kJ/kg. This gives a theoretical efficiency from the energy in the steam to mechanical power of only 4.26 % without including losses in the steam generation process. To use a steam engine like this to produce electricity off-grid based on sustainable fuel, would require a special wood-fired boiler. Further, if most of the energy should not be lost, it would take a condensation unit where the heat is transferred to the building and the water is ejected or reused in the steam engine. A system like this begins to be quite complicated and is thought to be outside the concept of the off-grid house in *Project Grobund*.

Temp. [C]	Pressure [bar]	Enthalpy of sat. liquid [kJ/kg]	Evap. enthalpy [kJ/kg]	Enthalpy of sat. vapor [kJ/kg]	Pot. energy relative to 1 atm. [kJ/kg]
100	1.014	419.04	2257.0	2676.1	0
110	1.433	461.30	2230.2	2691.5	15.4
120	1.985	503.71	2202.6	2706.3	30.2
130	2.701	546.31	2174.2	2720.5	44.4
140	3.613	589.13	2144.7	2733.9	57.8
150	4.758	632.2	2114.3	2746.5	70.4
160	6.178	675.55	2082.6	2758.1	82
170	7.917	719.21	2049.5	2768.7	92.6
180	10.02	763.22	2015.0	2778.2	102.1
190	12.54	807.62	1978.8	2786.4	110.3
200	15.54	852.45	1940.7	2793.2	117.1

Table 5.1 - Potential energy in saturated steam at different pressures/temperatures. Values from (J. Moran, et al., 2012).

5.6 Biogas Generator

Biogas is the product of an anaerobic digestion process of organic materials producing methane (CH_4), CO_2, H_2S and H_2O. The main gas for energy production is methane, which is usually 60-70% of the produced gasses during digestion of the organic matter. Organic matter is commonly food waste. The methane gas can be used in a combustion engine or gas turbine to drive a generator. This process also releases heat as the transformation from chemical to electrical energy is not 100% efficient, thus heat energy is created as a bi-product in the combustion phase. The main advantages of this technology is the use of waste products to generate electricity without a running cost and also the reliability this entails, as the methane can be used in a generator system when electricity is needed by the user. As a bi-product of the digestion process, fertilizer is created which can be used in the green house to enhance plant growth.

The system requires a steady and fairly high amount of organic matter, which in a household would mostly consist of food waste. As such, the daily input to the system would be fairly low which would result in a very low amount of methane. The entire system is technical and requires technical knowledge to install, maintain and repair. Besides this, the combustion engine and generator are expensive which will result in a very high cost of electricity, as the total electricity production is estimated to be very low due to low input of organic matter. The technology is disregarded until the potential of more promising technologies have been analyzed further.

5.7 Fuel Cell Technology

Fuel cells use an electrochemical reaction to produce electricity from fuels such as hydrogen, methanol or gas. The advantage of a fuel cell is that it can deliver electricity continuously and whenever it is needed. The disadvantages are fuel must be bought for the system in order to use it and that both the fuel cell and the fuel are quite expensive.

It seems that there is only one commercial fuel cell available on the market (Rivers, Collyn. Fuel cells.), which is the EFOY methanol fuel cell (Efoy). The EFOY fuel cell is available in models from 40 to 105 W electricity production (up to 0.96 to 2.52 kWh per day) at a price of around 20,000-43,000 DKK in Denmark. The methanol use is stated to be 0.9 l/kWh and the price is around 37 DKK/l, which gives a fuel price of 33 DKK/kWh. The fuel cell is maintenance-free and full automatic with a 5-year warranty (Mobil energi)

Figure 5.4 – Efoy Fuel Cell

From 2013 to 2015 the company Truma sold natural gas fuel cells, that could produce 23 kWh electricity (12 V, 250 watt) from 9 kg propane/butane gas. The price of December 2016 for 11 kg gas in Denmark is around 180 kr. or around 125 kr. at the borders shops. This gives a fuel price of respectively 6.4 DKK/kWh and 4.5 DKK/kWh, which is substantially less than the fuel price for the EFOY methanol cell. However, the price of the unit was around 68,000 DKK which showed not to be viable on the market and after increases in component costs the production was ceased. (Rivers, Collyn. Truma.)

The main reason for the high price of the gas fuel cells is the prices of the materials and components used.

Research are made in this area and different companies have claimed to be developing gas fuel cells from cheap materials, that could reduce the price substantially.
An example is the company Redox, which in 2013 claimed to have a system that would cost around 5,500 DKK per kilowatt and be ready for sale by the end of 2014. As of December 2016, the system is still not on the market so the actual price and efficiency are not known. (Bullis)

Because of the high price of all the fuel cell systems (hydrogen, gas, methanol), they are mainly used for special applications, where power is needed off grid – such as remote communication- or weather stations. The companies struggle to make the technologies commercial viable, but in the future fuel cells could become an interesting off-grid solution. Off course, the production of the fuels most be considered if sustainability is a relevant parameter in the considerations. (LaMonica)

5.8 Household Wind Turbine

Wind energy, along with solar, is one of the most prominent renewable energy sources in the world with one of the lowest price/kWh cost – which is forecasted to decrease even further as the technology improves. Therefore, a small turbine installed at the house along with photovoltaic panels could be a possible energy option. In order to assess the suitability, a small literature study of household wind turbines is conducted. Studies include:

> *The Warwick Wind Trials Report, UK; 26 building-mounted wind turbines, estimated wind speeds of 4,5 – 6,5 m/s. Average performance of 214 Wh and consumption of 80 Wh, corresponding to an average in-use capacity factor of 0.85%.* (Warwick Wind Trials)
>
> *The Zeeland Small Wind Turbine Test, The Netherlands; 41.5% average net production compared to projected.* (Windworks)
>
> *The CADMUS Group Report, Massachusetts U.S.A; 21 wind energy systems of 21 kW or smaller with an average production of 29% compared to predicted.* (Shaw, et al., 2008)
>
> *NREL Report – Deployment of Wind Turbines in the Built Environment; Most successful project of four 2.1 kW installed turbines at a roof of 13 meters delivers 58% of predicted output at a turbine cost of 60.000$.* (Fields, et al., 2016)

These studies all indicate underperformance of small turbines installed at or near buildings, due to numerous factors such as; wind map inaccuracy, variation in wind speed, faulty estimation of wind obstacles and terrain, inaccurate turbine data etc. Additionally, several of the studies find it difficult to predict the turbine performance and also discover a high level of down-time due to maintenance and repairs, making the turbines fairly unreliable.

Therefore, a thorough analysis of the specific site is necessary to identify the potential of a wind turbine. Referring back to the literature study, a combination of wind and solar power was found in nearly every case to make the most optimal solution and therefore wind power will be investigated in more detail during this study.

5.9 Micro hydropower system

Micro hydropower systems are only possible if a stream is available at the site and are probably not relevant to consider in most off-grid cases. If the conditions are right however, hydropower can be the best off-grid electricity production method. The productions will be relatively constant all year, and the electricity output relative to the investment can be up to 100 times higher than for wind- and solar systems (Energy Alternatives LTD). The available power from a hydropower system depends on the height difference that can be utilized and the amount of water. Depending on the location micro hydropower systems can have a power of up to 100 kW or simply be a drop-in-the-stream unit with a nominal power of 100 W that utilizes the velocity of the water (U.S. Department of Energy). However, a simple drop-in turbine such as the Ampair 100 demands a minimum water flow velocity of around 2 m/s to produce any useful power (Ampair). According to a report from the Danish government, the mean water velocity in streams in Denmark varies from 0.1 to 1 m/s (Ovesen, et al., 2000). Due to this and the fact that significant height differences are rare in Denmark, micro hydropower is not thought to be relevant and will not be considered further.

5.10 Conclusion on Technology Overview

The cost of electricity (CoE) has been calculated for each technology to estimate the economic feasibility. The cost of electricity is calculated as:

$$CoE = \frac{Investment\ Cost + Operational\ Cost\ \cdot Time\ Period + Maintenance\ Cost\ \cdot Time\ Period}{Annual\ Electricity\ Generation\ \cdot Time\ Period}$$

The time period is the period of evaluation, which is typically the lifetime expectancy of the system. In the following Table 5.2 a 20 year period has been applied.

Technology	Total Investment Cost [DKK]	Operational Cost [DKK/kWh]	Maintenance Cost [DKK]	Total Annual Electricity Generation [kWh]	Cost of Electricity Over 20 Years [DKK/kWh]	Usable Annual Electricity Generation [kWh]	Effective Cost of Electricity [DKK/kWh]
Photovoltaic [750 W]	11,000	0	0	767.0	0.7	356.5	**1.5**
Thermoelectic Generator [35 modules -760 W]	10,500	0	600	255.7	4.4	356.5	**4.4**
Steam Engine [3000 W]	15,000	0	1,500	500.0	4.5	356.5	**4.5**
Biogas Generator [-]	-	-	-	-	-	-	**-**
Fuel Cell [105 W]	43,000	33		500.0	37.3	356.5	**37.3**
Wind Turbine [1000 W]	50,000	0	500	1287.0	2.3	356.5	**8.4**

Table 5.2 - Cost of electricity for individual technologies (assumptions can be seen in Appendix E.1)

The CoE calculations are based on an annual electricity demand of 713 kWh. All technologies are estimated to contribute to 50 % of the annual electricity demand, meaning all technologies are expected to be combined into a hybrid system. Based on the design sizes specified for photovoltaic [750W] and the wind turbine [1000W], the technologies will generate significantly more electricity than what can be used, due to electricity demand and battery capacity.

Therefore, 'Effective Cost of Electricity' values have been calculated, which takes into consideration the usable electricity generation instead of the total electricity generation. More information about the prices can be found in Appendix E.1.

5.11 Conclusion on Technology Overview

Based on the project specific requirements stated in the introduction (such as simplicity) and the estimated cost of electricity, a photovoltaic system supplemented by either thermoelectric generators or a household wind turbine shows the highest potential for future implementation in the project.

These technologies will be assessed thoroughly to identify which can best fulfill the requirements for off-grid electricity generation for the houses suggested by *Project Grobund*.

6 Laboratory Test of Thermoelectric Generator's

6.1 Theory for thermoelectric generator

A thermoelectric generator converts heat energy to electrical energy due to a thermoelectric effect called the Seebeck effect. When two conducting / semiconducting materials are joined in two places forming a loop, a temperature difference between the joints will cause a voltage difference and thus a current. The voltage difference is created because the electron energy level in the materials are affected differently due to the temperature difference. The materials used in a thermoelectric generator should have a high electrical conductivity and a relatively low thermal conductivity so a high temperature difference can be obtained. Only a limited number of semiconducting alloys based on some relatively rare materials such as bismuth, tellurium, lead and silicon-germanium have these properties. Researchers working within this subject are trying to improve or make new thermoelectric semiconductors for example by changing the nanostructure of the materials. (Adroja, et al., 2015) (Wikipedia. Thermoelectric.)

A thermoelectric generator consists of several junctions between the two semiconductors put together in a series as illustrated by Figure 6.1. The more junctions in series the higher voltage difference over the output cables.

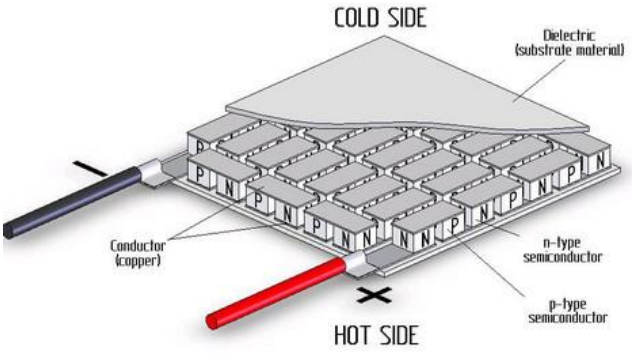

Figure 6.1 – Structure of thermoelectric generator (Close-up engineering, u.d.)

6.2 Preliminary Analysis of Thermoelectric Generators

The electricity generation potential of thermoelectric generators will be theoretically assessed by applying the knowledge and values from the literature study (section 5.4) to the current house concept. The thermo-electric elements are intended to be placed on the mass oven.

According to the BSim model (section 3.3), the heating season of the house starts in November and ends in April. With an assumed efficiency for the TEG's of 8 % and the maximum heat output from the mass oven of 9 kW, the maximum electrical output of the TEG modules is 720 Watts. As the mass oven is assumed to burn for two hours, this gives a maximum electricity generation of 1.44 kWh per day. This assumes that all the energy for space heating is lead from the mass oven through the TEG's before it is dissipated into the house. It also assumes that the TEG's operate at maximum efficiency (the heat is removed effectively from the cold side) and that around 35 TEG modules are installed on the oven. Figure 6.2 illustrates the space heating and TEG generation over the year, while Figure 6.3 zooms in the month of January. Each spike on the figures corresponds to the two hours, where the mass oven is burning.

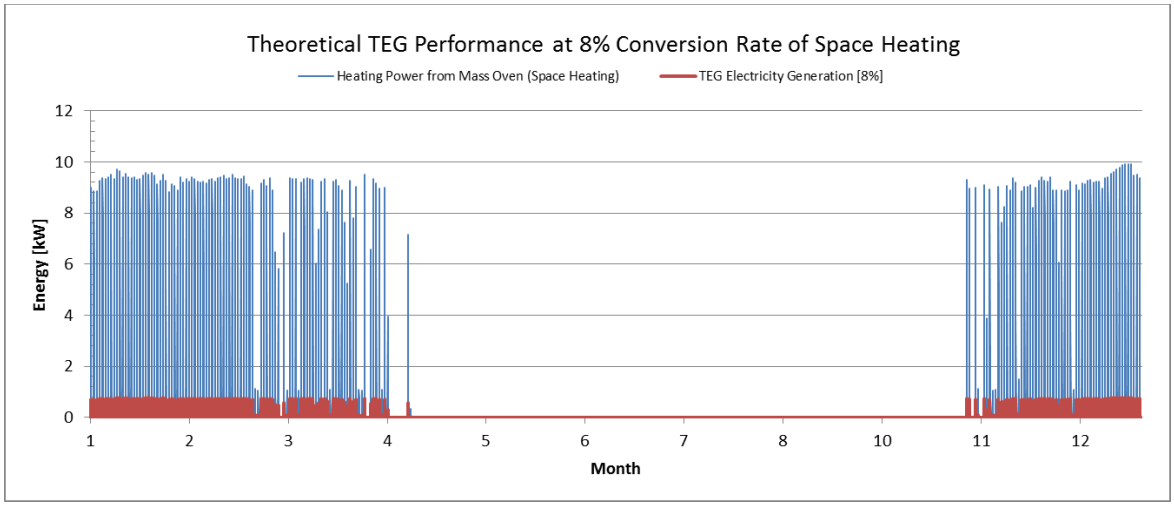

Figure 6.2 – Heating Power and Thermoelectric Generation at a 8% Efficiency

It can be observed, that from April till November almost no thermoelectric generation occurs and therefore the technology must be supplemented during the entire year. For the month of January the heating power and consequently electricity generation is illustrated in Figure 6.3.

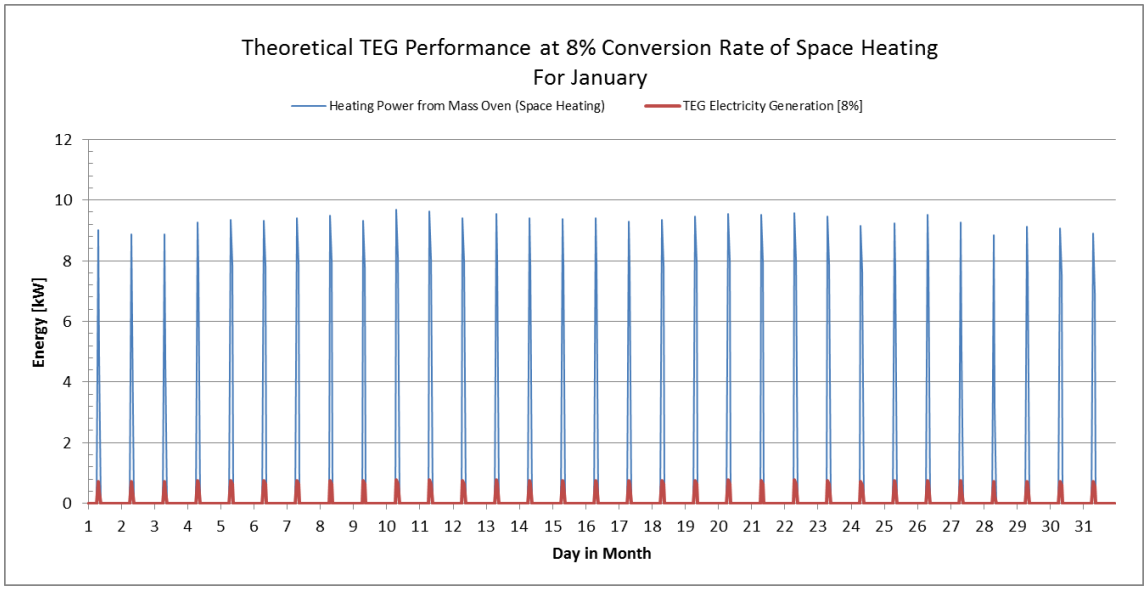

Figure 6.3 - Heating Power and Thermoelectric Generation at a 8% Efficiency for January

In the month of January, which is similar to the remaining winter months, the electricity output is highly reliable, generating approximately 1-1.8 kWh every morning (high value is including heat to domestic hot water). This indicates that the TEG's, in combination with a photovoltaic battery system, have potential to make a reliable off-grid electricity system.

The mass oven provides not only the space heating, but also the domestic hot water during the heating season from November to April. If a 50% efficiency (acc. to literature study) can be achieved in transferring heat from the mass oven to the domestic hot water, the hourly theoretical TEG performance can be calculated as:

$$TEG_{Elec}[W] = \left[Q_{Space} + \frac{Q_{DHW}}{\eta_{Heat\_DHW}}\right] \cdot \eta_{TEG} = \left[Q_{Space} + \frac{Q_{DHW}}{50\%}\right] \cdot 8\%$$

This further increases the thermoelectric output, as the heat release from the mass oven is increased in order to produce domestic hot water. Applying this equation, the maximum theoretical monthly output can be calculated, as seen in Figure 6.4.

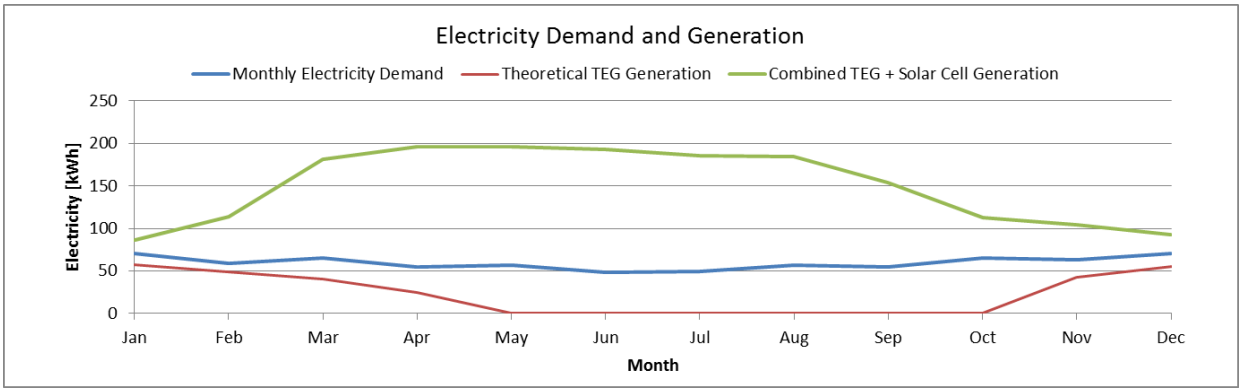

Figure 6.4 – Theoretical electricity generation for TEG's at 8% efficiency

Figure 6.4 also illustrates the combined TEG and photovoltaic generation. The photovoltaic system consists of 10 m² modules which are found to be a fair estimate of the required size for the household. The PV size will be analyzed further later in the report.

The theoretical electricity generation from TEG's at an 8% efficiency in combination with a small PV system is sufficient to cover the annual electricity demand of 713 kWh.

Based on this preliminary analysis a thorough test of the performance of thermoelectric generators will be performed under laboratory conditions to identify the actual efficiency for a specific high quality thermoelectric module in order to verify the findings of the theoretical performance analysis.

6.3 Laboratory Test: Aim of the Experiment

The main purpose of this experiment is to assess the performance of the proposed thermoelectric generator under various conditions. The tests are performed in order to identify the electricity potential by using TEG's in combination with a mass oven for off-grid houses. Therefore, the approach to these experiments will be of such a fashion as to create the best ideas and optimization for further in-field tests, which will be conducted with a mass oven (located at the home of Steen Møller from *Project Grobund*). The main purpose is therefore not solely to reproduce the manufacturer's stated output values, but instead to create results which can be realistically applied to a mass oven setup. Secondly, these results will be used to compare the performance of the tested TEG element to the data stated by the manufacturer.

6.4 Measurements

The performance of a thermoelectric generator type 'Tegpro High Temperature TEG Power Module – 22 Watt, 7 Volt' measuring 56x56x5mm, is tested. Test data for the TEG is available at the manufactures homepage, tegmart.com, which will be compared to the test results.

The performance of the TEG depends entirely on the temperature difference across the module, defining a 'hot' and a 'cold' side of the module. According to the manufacturer, the specifications are stated by Table 6.1. The graph illustrates conversion rates of heat to electricity as a function of cold and hot side temperatures, indicating that a cold side temperature of 30°C and hot side of 225°C yields the highest conversion rate.

Hot side temperature [°C]	300
Cold side temperature [°C]	30
Open circuit voltage [V]	14.4
Matched load resistance [ohm]	2.4
Matched load output voltage [V]	7.2
Matched load output current [A]	3.0
Matched load output power [W]	21.6
Heat flow across the module [W]	415
Heat flow density [W/m²]	13.2
AC resistance [ohm] measured under 27°C at 1000Hz	1.1-1.35

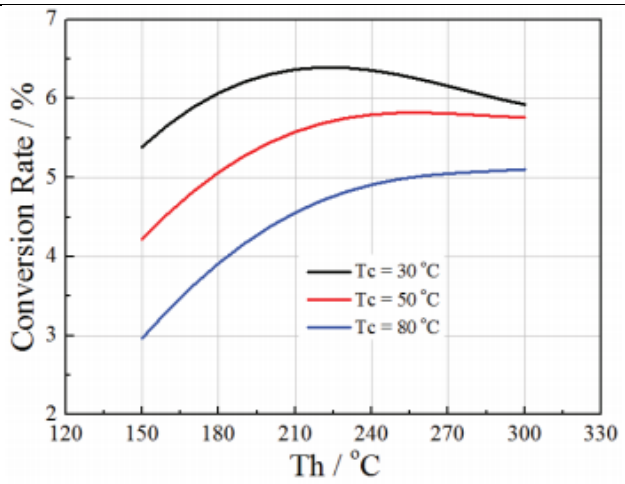

Figure 6.5 – Conversion rate (tegmart)

Table 6.1 – Thermoelectric Generator module specifications (tegmart)

To assess the module the following will be measured during the tests:

- Cold and hot side temperatures
- Water cooling inlet and outlet temperatures
- Surface temperature of the heating element used on the hot side
- Matched load voltage output
- Matched load current output

Through these measurements the efficiency and electricity generation potential of the TEG module can be assessed on a laboratory level. The results from these tests will later be compared to in-field results of the TEG module performed in Rønde, where the available mass oven is currently located. The mass oven in Rønde will be utilized in order to assess the TEG performance placed on a mass oven very similar to the system which will be installed in the off-grid houses.

6.5 Setup

In order to test the TEG element, a small test setup was established in the Aalborg University Laboratories at Sohnholmgårdsvej. The setup consisted of an electric heating element with temperature control, the TEG with water cooling held in position between two metal plates and equipment for measuring temperature and power. The water cooling is through a copper cooler designed for the thermoelectric module, allowing for constant water flow over the cold side of the module. The setup can be viewed in Figure 6.6 and Figure 6.7.

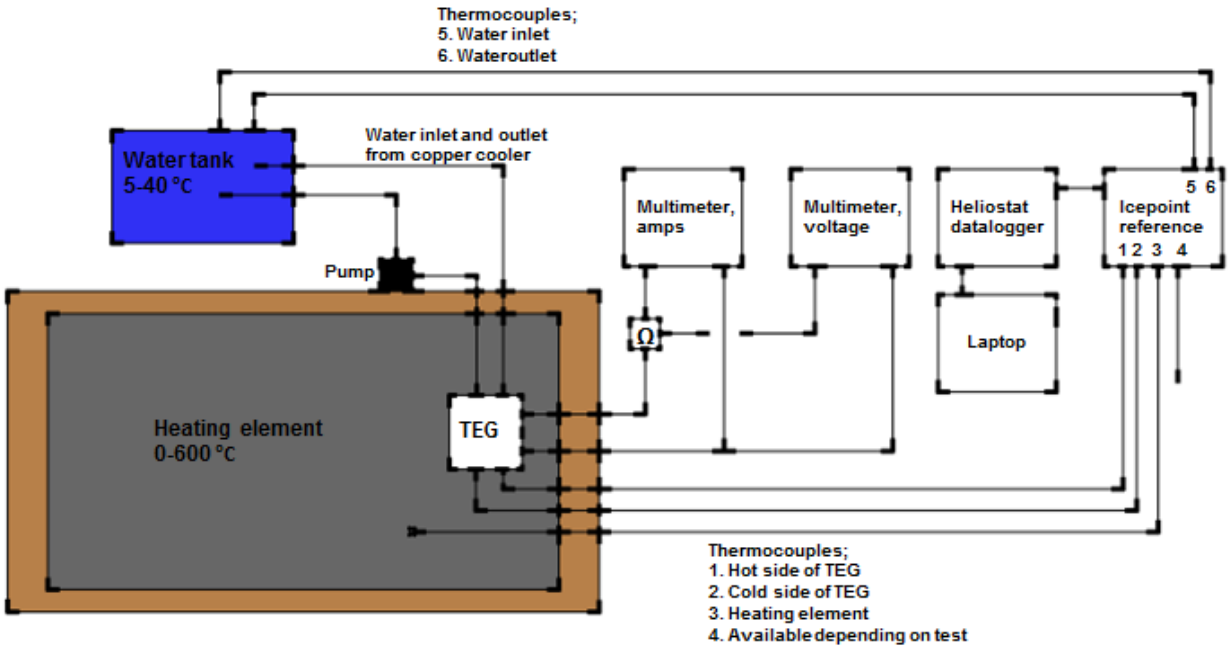

Figure 6.6 – Setup of laboratory test of thermoelectric generator

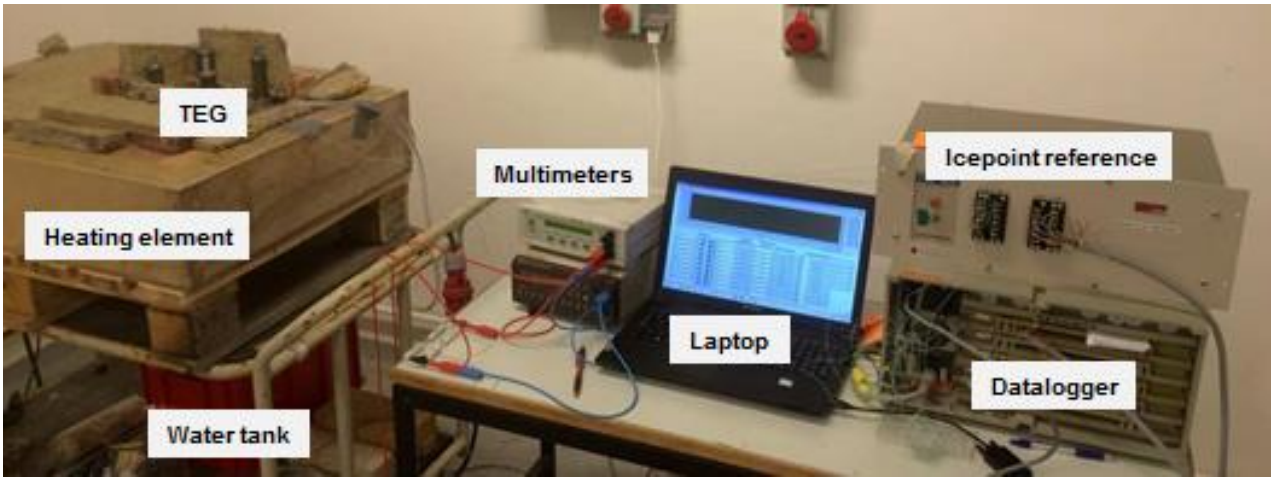

Figure 6.7 – Picture of laboratory setup

Table 6.2 shows a list of the equipment used for measurements.

Measurement	Device	Unit	Conversion
Voltage	Philips Multimeter	V	None
Current	Digital Multimeter	A	None
Hot side temperature	Thermocouple type K, 1	°C	25000 mV/K
Cold side temp.	Thermocouple type K, 2	°C	25000 mV/K
Heating element temp.	Thermocouple type K, 3	°C	25000 mV/K
Available temp. de-pending on test	Thermocouple type K, 4	°C	25000 mV/K
Water inlet temp.	Thermocouple type K, 5	°C	25000 mV/K
Water outlet temp.	Thermocouple type K, 6	°C	25000 mV/K

Table 6.2 – Specification of equipment for measurements

Additional equipment used in the setup, Table 6.3.

Device	Function
Heating element, temp. range 0-600°C	Heating of module hot side Function as mass oven
Water tank 5 liters, temp. range 5-40°C	Cooling of module cold side Function as domestic hot water tank
Water pump	Supply of water for cooling of module cold side

Table 6.3 – Additional equipment used

An important factor for the heat transfer from the heating element to the hot side of the TEG module is a high thermal conductivity and proper contact respectively between the heating element and the hot TEG side and between the cold TEG side and the copper cooler. To ensure good contact between these surfaces, a specific construction for the TEG has been developed, Figure 6.8.

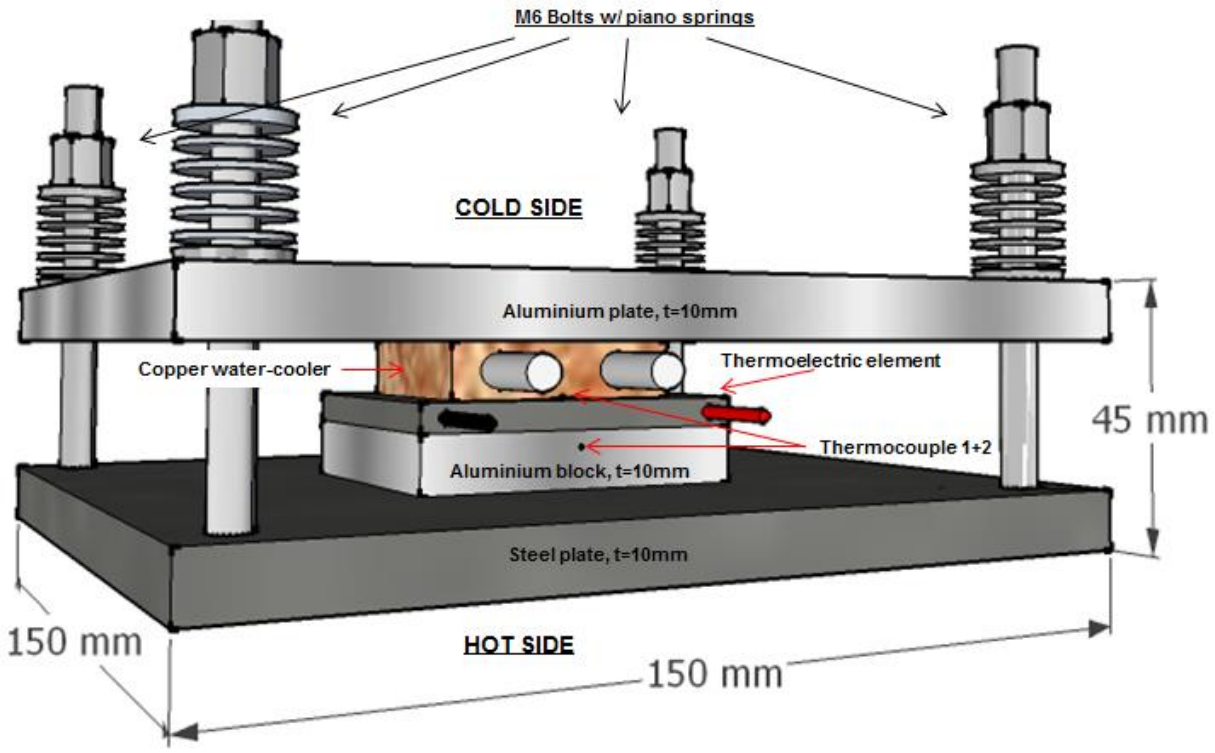

Figure 6.8 – Construction made to assemble TEG and cooler with constant pressure

The TEG construction in Figure 6.8 is assembled with a steel plate on the hot side and an aluminium plate on the cold side. While aluminium allows for a better heat transfer, steel must be used on the hot side, as a test with aluminium showed that the aluminium plate degraded and deformed under high temperature and pressure. The plates are pressed together by four M6 threaded rods and bolts combined with piano springs and plastic nuts. The plastic ensures a low heat transfer between the hot steel plate and the cold aluminium plate through the threaded rods. An aluminium block is placed beneath the TEG element in order to get the wires and cooling tubes away from the hot steel plate and to make space for insulation between the plates.

As the steel plate increases in temperature so does the M6 threaded rods, which makes them expand and become longer. This could significantly decrease the pressure across the construction and thereby decreases contact between the individual elements. Therefore, springs have been placed on the rods in order to maintain the pressure under temperature fluctuations. Thermal paste is applied to all surfaces to ensure good heat transfer between the elements.

Another function of the springs is regulation and analysis of applied pressure, as this effects the connection and thus heat transfer between the surfaces. One round/turn on each bolt, equals 21 kg of additional applied pressure across the module (determined from the spring constant). The springs thereby allow for an analysis of applied pressure versus electricity output, which can help identify the optimum pressure needed in the final tests with the mass oven.

6.6 Assumptions

The following assumptions have been made for the tests and calculations with the presented experimental set-up.

The thermal conductivity of aluminium at 300°C is 250 W/mK.

The thermal conductivity of thermal paste at 300°C is 5 W/mK, thickness of paste is assumed to be 0.1 mm.

Thermocouple 1, placed on the hot side of the module as seen from Figure 6.6 and Figure 6.7, is placed close to the upper-surface of a 10 mm aluminium plate (2.5mm from the top). Therefore, the measured temperature of thermocouple 1 will be higher than the actual temperature of the hot side of the TEG element (due to the temperature gradient through the aluminium). The difference in temperature between the measured point and the hot side is assumed to be as calculated in the following. As the surrounding area is well insulated, a one-dimensional approach is assumed to be sufficient for the calculation.

$$\Delta T = \frac{Q}{\frac{1}{\frac{d_{alu}}{k_{alu}} + \frac{d_{paste}}{k_{paste}}} \cdot A}$$

Where, Q is the maximum heat flow through the module (as specified by the manufacturer), A is the area of the module, d is the thickness of the layers and k is the thermal conductivity of the materials. This gives a temperature difference of:

$$\Delta T = \frac{415W}{\frac{1}{\frac{2.5mm}{250\ W/mK} + \frac{0.1mm}{5\ W/mk}} \cdot (56mm)^2} = 3.97K$$

In the following analysis, a temperature difference of $4\ K$ is assumed between the measurements of thermocouple 1 and the actual temperature on the hot side of the module. For the cold side, a layer of 0.2 mm paste is applied between the TEG cold side and the thermocouple, a temperature difference of 5.3 K is therefore assumed. These values are added and subtracted proportionally to the temperature difference, so that the full 3.97 K and 5.3 K is used at a heat flow of 415W, while no temperature compensation is made at 0 W.

6.7 Procedure

The general procedure used for the tests in the laboratory is as follows.

1. A water tank is filled with tap water and plastic pipes are placed in the tank and connected to a small pump and the copper cooler. Thermocouples 5+6 are placed in inlet and outlet water pipes.
2. TEG module is assembled in construction – as illustrated by Figure 6.8 and with insulation between the steel and aluminium plates.
3. Thermocouples 1+2 are placed on hot and cold side of the element.
4. Construction is placed on heating element, as shown in Figure 6.7. Thermocouple 3 is placed between heating element and TEG construction. The TEG construction is insulated on all sides with fireproof insulation.
5. Wires for measuring of voltage and current are connected to the TEG module.
6. The heating element is turned on - temperature is controlled manually.
7. Temperatures from thermocouples are logged by Heliostat datalogger.
8. Voltage and current is recorded on laptop.

The procedure may vary depending on the individual test at the time, i.e. varying applied pressure or experiments with brick between heating element and the construction.

6.8 Results and Discussion

In this section the most essential results from the laboratory tests are included. A lot of experiments and setups were conducted in the laboratory to reach an optimal setup for the following analysis. Changes were made to the TEG construction and different heating elements, thermal pastes and cooling devices were tried. The following sections present the best results in order to:

- Assess the performance of the thermoelectric generators and compare it with the manufacturer's data
- Identify the optimal setup for further in-field testing with the mass oven

6.8.1 Performance Test of Thermoelectric Generator

The TEG construction was placed directly on the heating element. Freezing elements were placed in the water tank to reach a starting water temperature of 6.7 °C. Pressure setting was 12 rounds equal to a total weight of 253 kg.

Figure 6.9 shows the measured and corrected hot and cold side temperatures. The corrected temperatures are based on the actual measurements corrected according to the assumptions (section 6.6). As such, at a heat flow of 415 W (maximum rated heat flow), the corrected hot and cold side temperatures are calculated as:

$$T_{Hot,Corr} = T_{Hot,Meas} - \Delta T, \quad where\ \Delta T = 3.97K$$

$$T_{Cold,Corr} = T_{Cold,Meas} + \Delta T, \quad where\ \Delta T = 5.29K$$

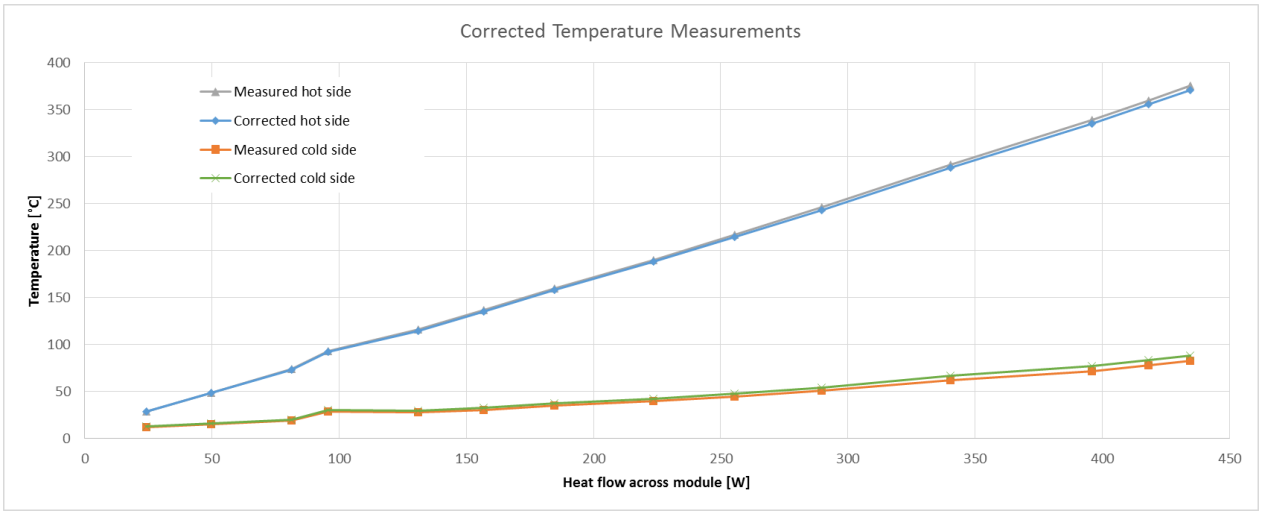

Figure 6.9 – Heat flow [W] across module as a function of temperature difference [K]

Correcting the cold and hot side temperatures leads to a corrected temperature difference 10.5K lower than the measured. By applying the corrected temperature difference [K] and comparing these to the measured output [W] a higher [W/K] (conversion rate) can be calculated, as the measured output remains the same, but the total temperature difference is decreased. Figure 6.10 shows the corrected output as a function of measured output and the corrected data set for temperature difference.

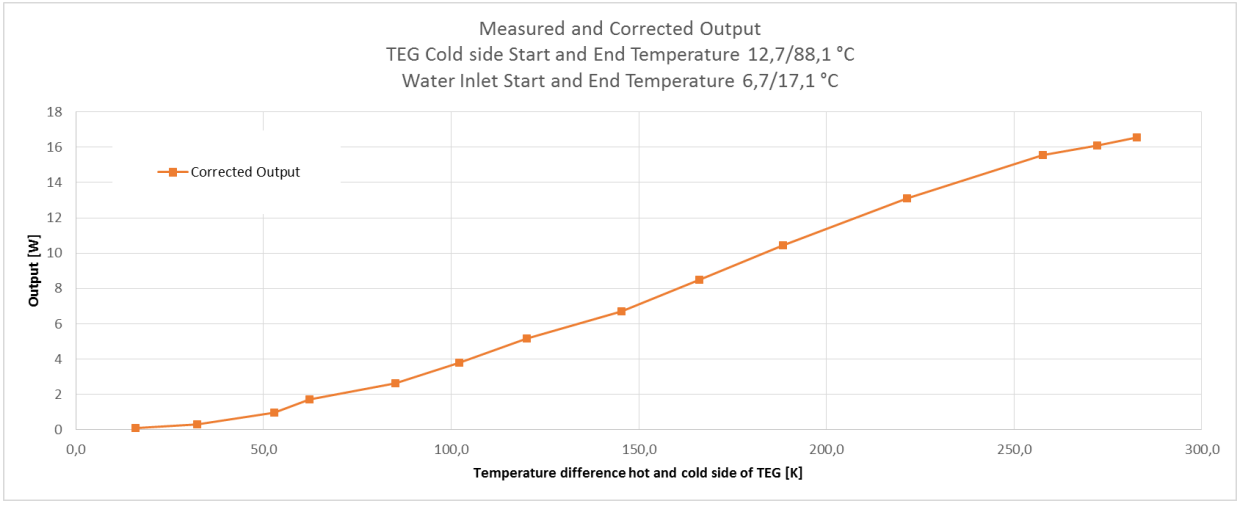

Figure 6.10 – TEG output [W] as a function of temperature difference [K]

Note: See graph title; Increase in cold side temperature does not correspond to increase in water supply temperature.

At a corrected temperature difference of 282.8K an output of 16.6W can be achieved. The high increase in cold side temperature of 70K indicates insufficient capacity to cool the cold side during operation, which can significantly decrease performance according to the manufacturer data (Figure 6.5).

Figure 6.11 shows the conversion rate as stated by the manufacturer (at cold side temperature of 30, 50 and 80°C) and the conversion rate as tested in the laboratory. The conversion rate is the percentage of heat flow

across the module converted to electricity. The cold side temperature of the tested TEG starts at 12.7°C and ends at 88.1°C.

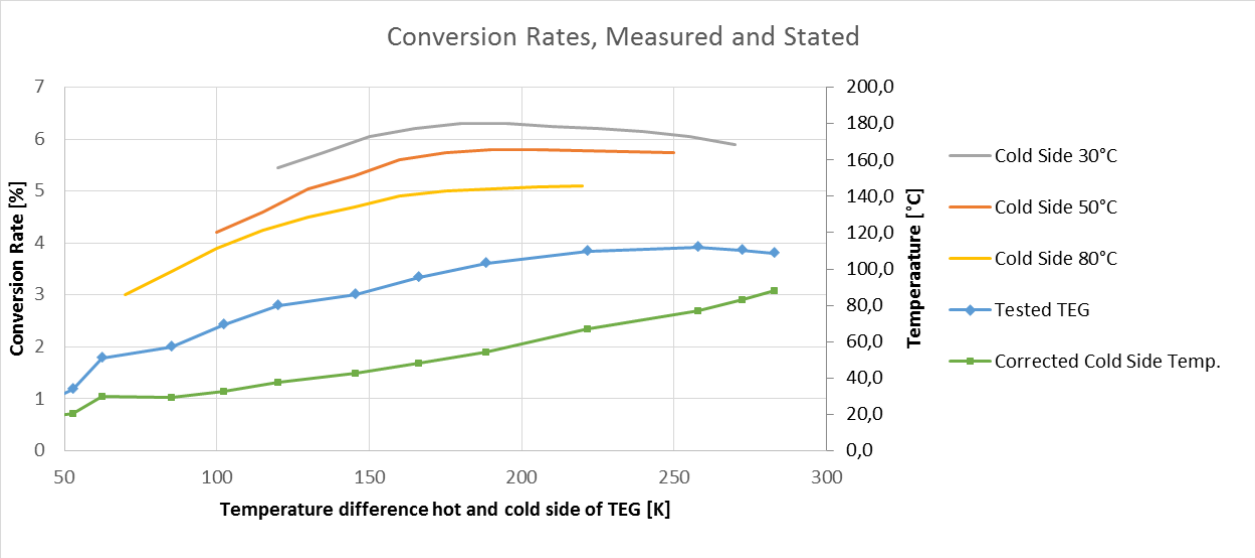

Figure 6.11 – Conversion rate of tested TEG module

The tested TEG element reaches a maximum conversion rate of 3.92% at a temperature difference of 257.6K. The manufacturer states a maximum conversion rate of 6.3% with a constant cold side temperature of 30°C and a temperature difference of 195K. The tested TEG achieves a performance of 0.06 W/K, while the manufacturer reaches up to 0.097 W/K. This corresponds to a difference of up to 33% in performance at peak conversion rate.

Figure 6.11 clearly indicates how the cold side temperature increases significantly throughout the test. Observing the three plotted functions from the manufacturer, it is clear how an increase in cold side temperature decreases performance [W/K]. If a construction was created to supply sufficient cooled water to maintain a temperature of 30°C on the cold side of the element, performance could be greatly improved, but as this is not realistic for the further application of the TEG (in terms of mass oven application), proceedings towards maintaining a lower and constant cold side temperature are not taken.

6.8.2 Assessment of Applied Pressure

Applying the spring-pressure relation in Table 18.10 in Appendix O , the impact of applied pressure on the performance of the TEG can be assessed.

Figure 6.12 shows how the increase in pressure on the TEG also increases the output. By adding 253 kg (end point on the graph) an increase of 34.5 % in power output can be gained compared to zero applied pressure. A pressure increase from 126-253 kg only increases performance by 4.1% which indicates, that the first amount of pressure has the highest impact – this is also illustrated by Figure 6.12.

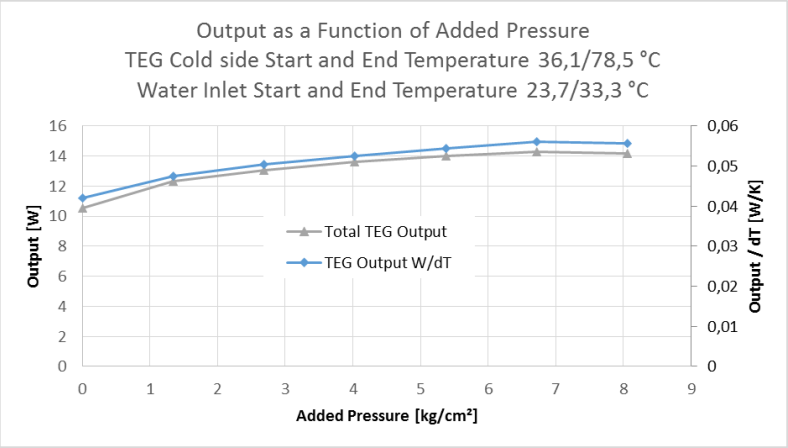

Figure 6.12 – TEG output [W] as a function of added pressure [kg/cm²]

6.8.3 Performance of TEG Placed on Bricks

This section initially presents the results when one layer of bricks is placed between the heating element and the TEG construction. Secondly the temperature increase through two layers of bricks placed on the heating element is presented. The main purpose of using bricks is to simulate the conditions of placing the TEG on the surface of a mass oven.

Figure 6.13 shows the temperature progression measured over the span of one hour. Exposed surface areas of the brick reaches 330°C after one hour, while the temperature between brick and steel plate (bottom of TEG construction) reaches only 130°C, resulting in a temperature of 83°C on the hot side of the TEG. The hot side temperature of 83°C resulted in a TEG output of less than 0.25 W.

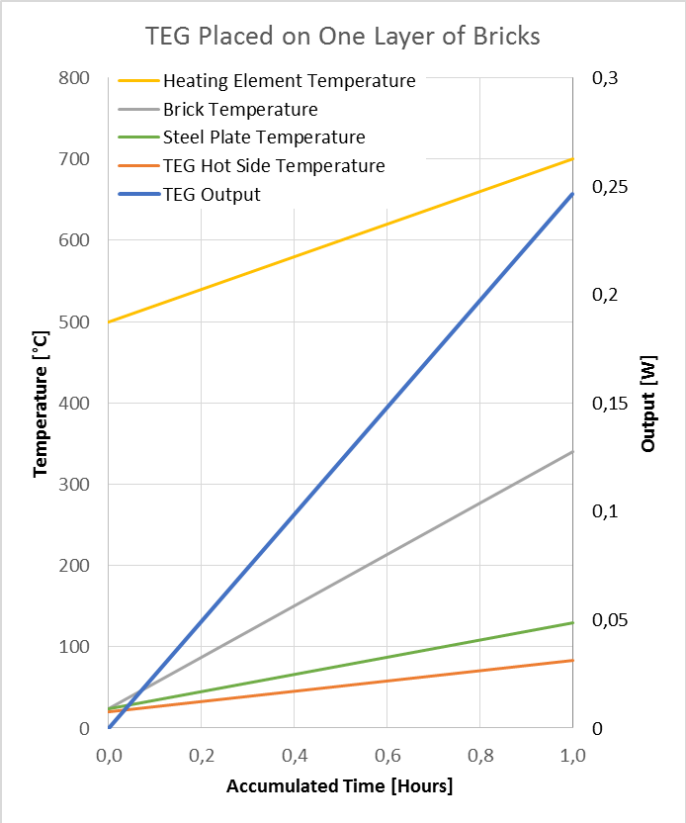

Figure 6.13 – Increase in temperature, TEG on one brick layer

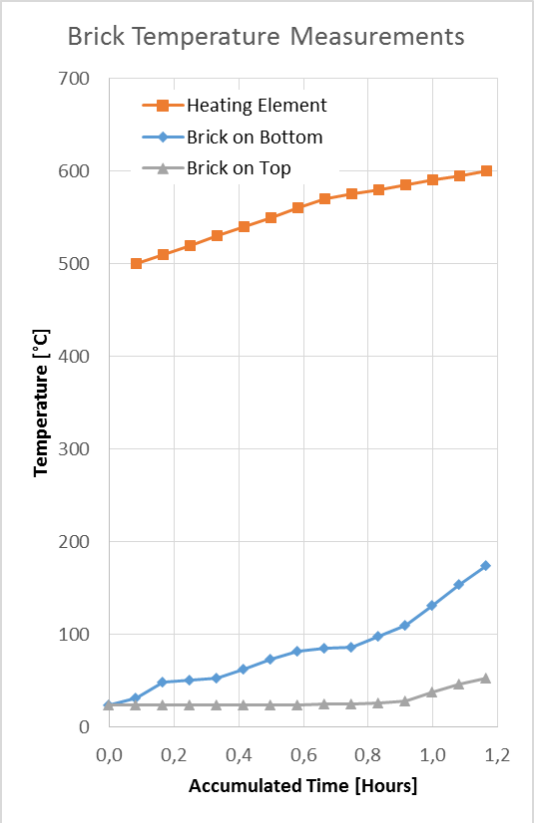

Figure 6.14 – Temperature profile for 2 layers of brick

A temperature difference of 200K is found across the brick, the layer of brick is insulated with 25mm of fire insulation, which significantly reduces heat loss, thus increasing the temperatures ('Brick Temperature' and 'Steel Plate Temperature'. The high horizontal temperature difference across the brick (between the surface under the element and the free surface) indicates that the thermal conductivity of the brick is too low to deliver the same amount of heat that is removed by the TEG construction. This results in a high temperature difference across the brick, a low temperature difference across the TEG element, a low amount of heat through the TEG element and thus a low performance.

Figure 6-14 shows the measurements from the test with two layers of brick with thermal paste added between each brick shows a maximum temperature on the top of the two layers of less than 50°C after more than one hour of heating, further indicating the low performance potential of TEG elements on bricks or other materials with low thermal conductivity.

6.9 Sources of Error

The following items can have affected the results of the laboratory test.

- Irradiative heat transfer from heating element to construction parts on cold side
    - Insulation is placed around the TEG construction as seen in Figure 6.7
- Irradiative and convective heat transfer from steel plate to construction parts on cold side
    - Insulation is placed between the steel plate and the aluminum plate surrounding the TEG module in the TEG construction
- Conductive heat transfer from hot to cold side through bolts and springs
    - Plastic rings are placed underneath springs to break metal connection from hot to cold side

The above three points can cause significantly higher cold side temperature and thereby reduce performance.

- Manual recording of both multi meters
    - Can cause human recording errors and creates less 'measurement points' than automatic recording
- Continuously temperature increment of water supply increasing cold side temperature
    - Could be avoided by water supply from tap or sufficiently large tank
- Low flow and uncontrolled/un-monitored water supply
    - A decrease in water supply can cause less cooling of the TEG in periods, which will affect performance
- Insufficient cooling by copper water cooler as explained in Figure 6.15

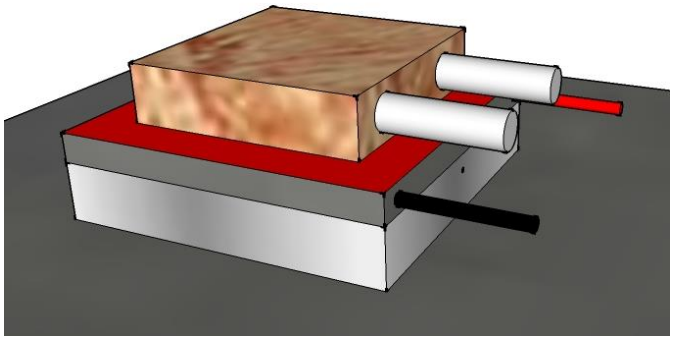

Figure 6.15 – TEG module area (in red) not covered by copper cooler

Figure 6.15 illustrates the copper cooler on the cold side of the TEG module. The red area indicates TEG surface which is not covered by cooling. The copper cooler measures 4x4cm and the TEG 5.6x5.6cm. As such, 49% of the cold side of the TEG module is not covered by the copper cooler which significantly reduces cooling power thus increasing the average cold side temperature of the TEG module. A 2.5mm copper plate of 5.6x5.6cm was placed between the TEG module and the cooler in order to enhance heat transfer. This addition was performed in the early phases of the experiment before any of the tests discussed in this chapter were conducted.

6.10 Conclusion and Further Process

The tested thermoelectric generator, rated by the manufacturer to 21.7W at a temperature difference of 270K, has been tested under various conditions.

With a ΔT of 270K the measured output is 16.0 W and a maximum conversion rate of 3.92% is achieved. This is a performance of 73.7% of that stated by the manufacturer.

At best, an output of 16.6W is recorded, with a difference in temperature of 282.8K (T_{cold} = 88.1°C, T_{hot} = 370.9°C).

If a constant cold side temperature at 30°C could be maintained, the TEG could possibly perform as stated by the manufacturer, but under realistic conditions it seems difficult to achieve the maximum rated output.

A significant increase in output is found by applying pressure to ensure better connection between the elements. A 34.5% increase in performance can be achieved by applying a total weight of 253 kg or 8.06 kg/cm². Once good contact has been established as a function of added pressure, only a small increase in performance can be observed by adding more pressure, indicating that only a small amount of pressure is necessary in order optimize the performance, i.e.:

A 10.7% increase can be achieved by increasing the pressure from 42 to 126 kg of total weight while only a 4% increase can be achieved by increasing the pressure additionally from 126 to 253 kg of total weight.

Placing one or more layers of brick between the heating source and the TEG construction is seen to insulate the heat flow in such a degree, that any electrical output is neglectable. A heating element between 500-600°C is only able to produce a hot side element temperature of 83°C after one hour, if one layer of brick is placed on the heating element. This results in a TEG output of less than 0.25W.

The result found in the laboratory shows that a performance similar or very close to that stated of the manufacturer is probably possible to achieve under ideal circumstances with sufficient pressure and cooling. Meanwhile, bricks are found to be inadequate conductors from heating source to TEG, even under prolonged conditions, as the heat energy is simply extracted faster from the surface of the brick than it can be transferred through it.

To further test the TEG's, a mass oven will be used as a heat source in order to assess the practical performance outside of ideal laboratory conditions.

7 Thermoelectric generators: Test on Mass Oven

7.1 Introduction

The mass oven is constructed as shown in Figure 7.1. Typically 2-10 kg of firewood is added to the firewood chamber. In order to ensure a high combustion temperature and thus a high thermal efficiency, constant air flow is secured by a small fan at the end of the exhaust pipe. The fan ensures air flow regardless of temperature and also removes the need for a vertical exhaust pipe, which is typical for most stoves.

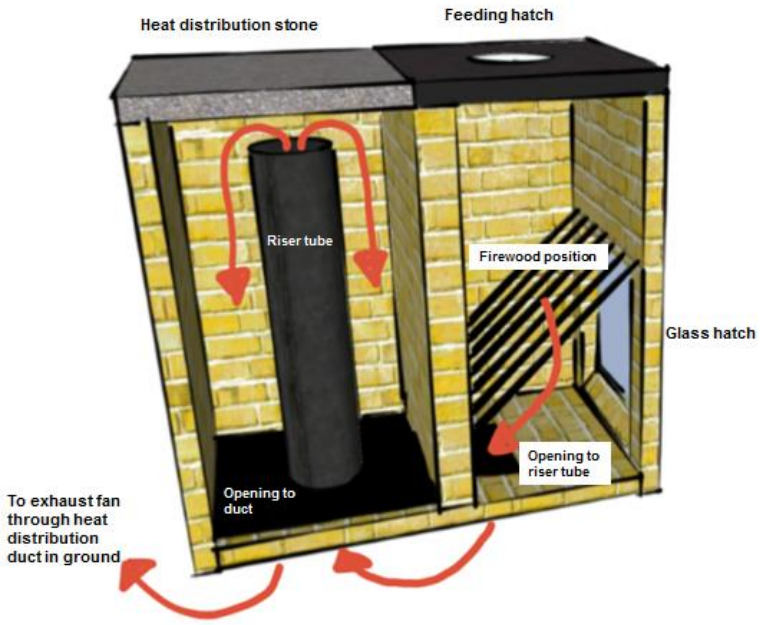

Figure 7.1 – Function of the mass oven

Figure 7.2 – Picture of the mass oven used in test

The mass oven works by placing the firewood through the feeding hatch and on to the steel grill, from where the wood can be reached and ignited through the glass hatch. As air flow is created by the exhaust fan at the end of the system, the combusted air is drawn through the grill and into a small opening in the ground from where the hot air rises through the riser tube where air temperatures reaches close to 1000°. The hot air is then drawn back into another opening (the two openings in the ground are not connected) and continuous into a concrete pipe running under the floor, which is utilized as a form of air-ground-heat system. At the end of the concrete pipe a charcoal filter is placed along with the exhaust fan.

7.2 Aims of the Experiment

The testing of the mass oven is done to assess the electricity generation potential through TEG's and to test the domestic hot water production. The results of previous laboratory experiments indicate that very little electricity generation can be achieved by applying the TEG's directly on a brick surface. Initially, the idea was to place the TEG's on the top of the *heat distribution stone* as this is the hottest (exterior) surface of the mass oven.

7.3 Experiment Setups with Mass Oven

7.3.1 Thermoelectric Generator

The output of the TEG is measured by placing the TEG construction from the laboratory directly on the *heat distribution stone*. The electricity output is measured by recording the voltage over a 2.2 ohm resistor with a hand-held multimeter. Temperature measurements are conducted with two thermocouples placed underneath the TEG construction and on an exposed area of the *heat distribution stone*.

7.3.2 Domestic Hot Water

To estimate the domestic hot water production of the mass oven, and also to estimate how much heat can be drawn from the mass oven for thermoelectric generation, a radiator is placed underneath the *heat distribution stone*. Figure 7.3 illustrates the setup where the radiator is placed directly above the riser tube underneath the *heat distribution stone*. On top of the radiator 50 mm of insulation is placed along with the heat distribution stone to ensure the chamber is fully closed and also to reduce heat loss from the radiator.

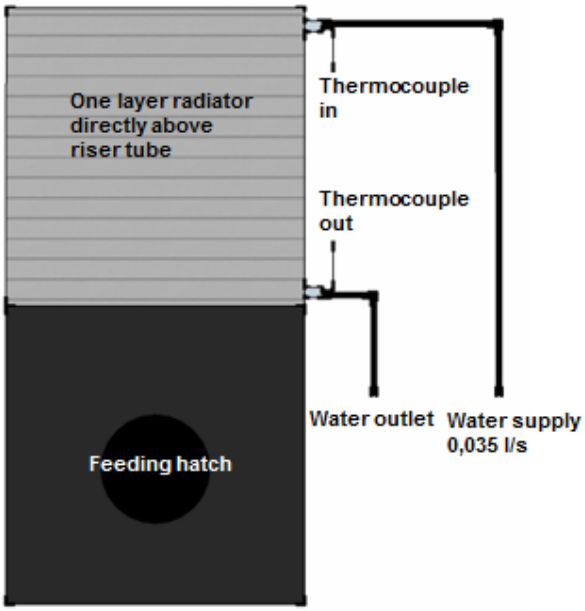

Figure 7.3 – Radiator setup on mass oven

Figure 7.4 – Picture of water pipe connected to radiator

Plastic pipes are connected to the in- and outlet of the radiator, both connections are placed on the same side, as such this is a type E-F radiator. In each connection, a thermocouple is placed to ensure measurements of the water temperature directly before/after entering the radiator.

The fresh water supply is directly from tap. Calculation of the water flow is performed by measuring the output from the water outlet.

According to Steen Møller (the initiator of *Project Grobund)*, a 'normal' supply of firewood is added to the chamber, consisting of 8 kg of wood with the burning value of approximately 4 kWh/kg, resulting in a total of 32 kWh.

7.4 Results and Discussion

7.4.1 TEG Directly on Heat distribution stone

The first test was conducted by placing the TEG directly on the heat distribution stone. The stone reached up to 150°C on an exposed (free) surface area after approximately 30 minutes. No output was measured from the TEG, as the surface temperature of the stone where the TEG was placed, was reduced significantly as soon as the TEG was placed on it. This indicates and confirms the same results as in the laboratory, showing that heat is removed from the stone at a much higher rate than the heat can be transferred through it. Therefore, no further tests or analysis was conducted with the TEG placed on the heat distribution stone.

7.4.2 Domestic Hot Water Test

Figure 7.5 shows the results of the domestic hot water test using a radiator as the heat receiving element.

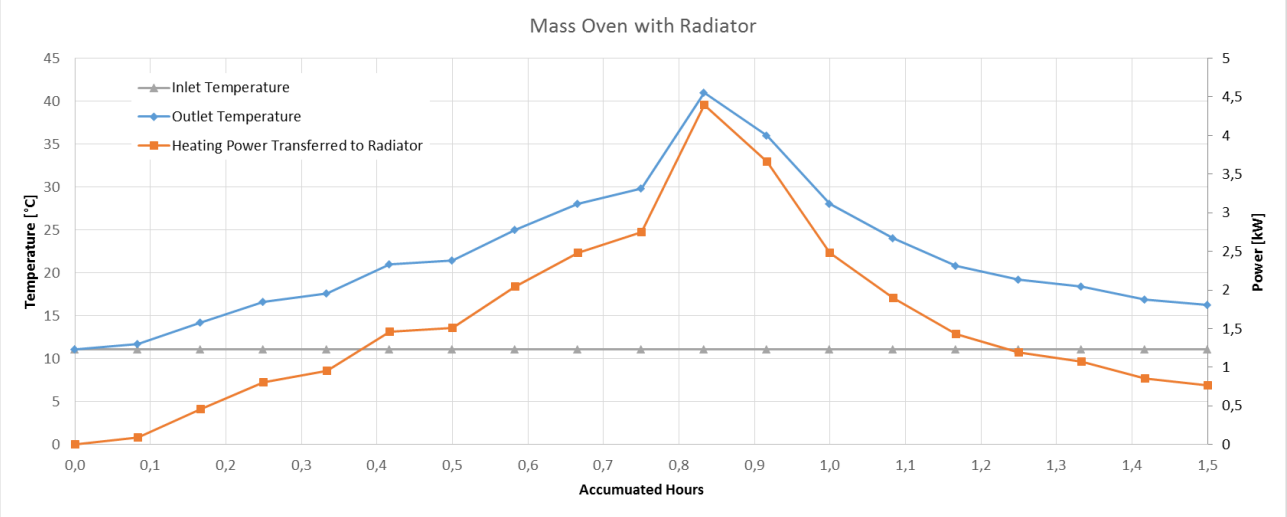

Figure 7.5 – Calculated heating power and measured inlet and outlet water temperatures

The timer was started as firewood was added and ignited in the mass oven and stopped after 1.5 hours when the outlet temperature of the water was close to that of the inlet. Peak power occurs around the 50 minute mark and an effect of 4.4 kW is calculated based on difference in temperature and water flow.

Table 7.1 shows the total amount of energy delivered to the water over the measured period and the corresponding efficiency of energy from the firewood to the water. Assuming the bottom side of the radiator (hot side) is covered in TEG elements, and thus all the absorbed heat by the water was transferred through the TEG elements as well, the energy delivered to the water can be multiplied by an appropriate conversion rate to estimate the maximum electricity potential. By applying a conversion rate of 3% (from section 6.8) for a TEG element, the potential electricity generation can be estimated.

Source	Energy [kWh]	Efficiency [%]
Wood	32	-
DHW	2,52	7,88
TEG	0,08	3

Table 7.1 – Calculated efficiency of heat to DHW and heat to TEG

As such, TEG elements covering the entire bottom side of the radiator, resulting in 100 TEG elements, could potentially generate 0.08 kWh during one mass oven ignition, which occurs once per day during the heating season.

7.5 Sources of Error

The following items could have affected the results of the mass oven tests.

- In-accurate measurements of temperature as simple measurement tools were used
- Inadequate insulation of radiator – heat loss to surrounding causing lower outlet temperature
- Insufficient mixing of water inside the radiator, as it is designed for vertical and not horizontal installation
    - Water boiling could be observed at the center of the radiator during ignition (yet the maximum observed temperature is 40 °C)
    - After the experiment was ended, insulation was removed from the radiator and a horizontal temperature difference across the surface of 30K was observed between center and edges

The sources of error can have impacted the results in such a way, that the actual potential for transferring heat from the oven to the radiator under better conditions could be significantly higher than what was measured and calculated.

7.6 Conclusion and Further Process

Testing the thermoelectric generator directly on the heat distribution stone clearly shows that such a setup is not a solution, indicating that the TEG must be placed on a material with high thermal conductivity similar to steel, aluminum or copper. As such, an estimation of replacing the heat distribution stone with a similar material to these metals can give an indication of the potential heat transfer.

Replacing the heat distribution stone with a cast-iron radiator produces sufficient domestic hot water (2.52 kWh over 90 minutes with a peak effect of 4.4 kW) to cover the households daily demand. Assuming the 2.52 kWh of heat energy could be transferred through TEG's with a conversion rate of 3% before reaching the radiator, a total amount of 0.08 kWh of electricity could potentially be generated each day.

The potential electricity generation is extremely low, corresponding to a 0.2 % conversion rate from heat energy released in the mass oven to electricity. Because of these findings no further tests with thermoelectric generators and the mass oven are considered. Instead, other options to cover the electricity demand will be considered.

8 Evaluation of Photovoltaic System

In order to evaluate the photovoltaic performance, the solar radiation on the photovoltaic (PV) modules must be calculated. After the total incident radiation is calculated, the electrical output depends on several performance factors of the specific photovoltaic modules. In this chapter the calculation methods used in the calculations for the design of the PV system will be explained. The theory is implemented in an Excel based *Off-grid Simulation Tool,* that can simulate the hourly energy balance for an off-grid system with PV-panels, wind turbine and battery storage.

Solar cells are made up by two layers of silicon. In both layers the silicon atoms are doped, meaning they contain an impurity. This impurity is an added atom either containing more or less electrons than the silicon atom, thus creating a negative or positive charge, known as n-type (negative type) or p-type (positive type). By combining a n-type and p-type conductor, a PN-type junction is created, at this junction an electric field develops, as the electrons from the positive layer combines with 'holes' from the negative layer. When solar energy in form photons are absorbed by the conductors, the electrons and holes in the electric field are released and this creates a potential difference, or voltage. If the conductors are connected to an external circuit, this flow of electrons and holes forms an electrical current, known as electricity.

8.1 Solar Resources

The solar resources applied in this project are hourly measured data of global and diffuse radiation from the Danish Design Reference Year (abbreviated 'DRY') (Wang, et al., 2013). In the DRY data Denmark is divided into 6 different zones according to measured radiation values from 6 weather stations, the zones are illustrated in Figure 8.1. The annual global radiation varies from 2.78 to 3.01 kWh/m² per day on average. The maximum variation across zones are +8.2% annually which can result in a significant difference in PV performance over a 20 year period. Therefore, the location of the photovoltaic system will be identified and radiation data will be adjusted accordingly when PV performance is calculated.

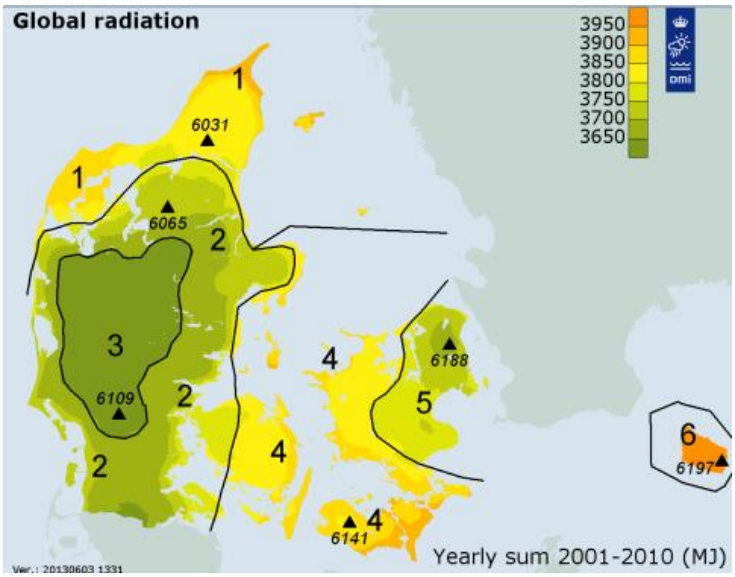

Figure 8.1 – Global radiation [MJ/year] measurements (Wang, et al., 2013)

8.2 Solar Radiation on Tilted Surface

8.2.1 Assumptions

Hourly values of global and diffuse radiation in [W/m²] from the Danish Design Reference Year data 2001-2010 are applied in order to calculate hourly values for the PV electricity generation. The radiation data varies according to six specific zones in the weather data. According to (Dragsted & Furbo, 2012) the measurements were performed with a CM11 pyranometer from 'Kipp&Zonen'. Based on the user manual available for the CM11, it is assumed that reflected radiation is not included in global radiation measurements. As such, the global radiation measurements is made up of direct beam and diffuse radiation, allowing the user to simply calculate the hourly values for beam radiation, as both global and diffuse radiation is given.

8.2.2 Calculation of Radiation

In the developed *Off-grid Simulation Tool* the user is asked to inform of solar module tilt angle and azimuth angle (orientation). Therefore the calculations will allow for simultaneous change of these two values. The following method is applied in order to calculate the hourly total radiation on an inclined surface, by calculating the ratio between angles of incidence beam radiation of an incline and horizontal surface, respectively.

The angle of the incidence beam radiation can be calculated as:

$$cos\theta = sin\delta \cdot sin\emptyset \cdot cosS - sin\delta \cdot cos\emptyset \cdot sinS \cdot cos\gamma + cos\delta \cdot cos\emptyset \cdot cosS \cdot cos\omega +$$

$$cos\delta \cdot sin\emptyset \cdot sinS \cdot cos\gamma \cdot cos\omega + cos\delta \cdot cosS \cdot sin\gamma \cdot sin\omega$$

Where;
S, is the angle between the tilted surface and horizontal
δ, is the declination angle of the sun
∅, is the latitude, positive for the Northern hemisphere
γ, is the azimuth angle of the modules, 0 for South facing components in the Northern hemisphere, and
ω, is the hour angle, changes by 15° every hour, solar noon = 0, morning is negative and afternoon positive

The declination angle can be calculated as:

$$\delta = 23.45 \cdot \sin[360 \cdot \frac{284 + N}{365}]$$

Where; N is the day of the year.

The sun hour angle is calculated as:

$$\omega = 15° \cdot solar\ hour - 120°$$

The solar hour can be calculated as:

$$Solar\ hour = local\ time[hours] + E[minutes] + 4 \cdot (L_{ST} - L_{Loc})[minutes]$$

Where;
L_{ST}, is the longitude for the standard time
L_{Loc}, is the longitude of the location, and

E, is the equation of time
The solar hour must be corrected in periods with daylight saving time (-1 hour)

The equation of time can be calculated as (in minutes):

$$E = 0{,}01719 + 0{,}4281\cos(B) - 7{,}352\sin(B) - 3{,}349\cos(2B) - 9{,}732\sin(2B)$$

$$B = 2\pi\frac{(N-1)}{364}, \text{ radians}$$

The ratio of beam radiation on an inclined surface to beam radiation on a horizontal surface can be calculated as:

$$R_b = \frac{I_{incl}}{I_{hori}} = \frac{cos\theta_T}{cos\theta_z}$$

Where the angle of incidence beam radiation of the horizontal surface can be simplified to:

$$cos\theta_z = sin\delta \cdot sin\emptyset + cos\delta \cdot cos\emptyset \cdot cosS \cdot cos\omega$$

And the angle of incidence beam radiation of the incline surface can be calculated as previously for $cos\theta$.

Finally the direct, diffuse and reflected radiation components on the incline surface can be calculated:

$$I_i = I_b \cdot R_b + I_d \cdot \frac{1 + cosS}{2} + (I_b \cdot I_d) \cdot (\frac{1 - cosS}{2}) \cdot \rho$$

(Total radiation on inclined surface = Direct + Diffuse + Reflected components)

Where;
ρ, is the reflectance of the ground
I_b and I_d are the direct and diffuse components of measured sky radiation, and
I_i, is the total radiation on the inclined surface

In the simulation tool these three components (direct, diffuse and reflected) are calculated hourly depending on the chosen tilt and azimuth angle, and also the latitude and longitude angles. The total radiation, in W/m², on the modules is then multiplied by the total module area, performance ratio for the system and efficiency of the modules to calculate the hourly solar cell system performance.

This method is described in *Solar Thermal Energy Design, MECH9720, Graham Morrison and Gary Rosengarten*.

8.3 Photovoltaic Performance

The electrical output generated by a PV system can be described as:

$$P_{PV} = A_{PV} \cdot I_T \cdot PR \cdot \eta_{eff}$$

Where:
P_{PV} is the power [W]
A_{PV} is the area of the solar modules [m²]
I_T is the total incidence solar radiation [W/m²]
η_{eff} is the efficiency of the modules specified by the individual manufacturer
PR is the performance ratio [%]

The performance ratio can be calculated as:

$$PR = (1 - \eta_{soil}) \cdot (1 - \eta_{shading}) \cdot (1 - \eta_{wiring}) \cdot (1 - \eta_{degradation}) \cdot (1 - \eta_{rating})$$

Where:
η_{soil} is the loss factor due to soiling on the modules
$\eta_{shading}$ is the loss factor due to partial shading on the modules
η_{wiring} is loss factor due to mismatches in connection and resistive losses in the wiring
$\eta_{degradation}$ is loss factor due to light-induced reduction of the efficiency of the cells
η_{rating} is the loss factor due to a difference between performance achieved under Standard Test Conditions (STC) and actual conditions

In order to maximize the output of the PV system, the I-V (current-voltage) and P-V (power-voltage) characteristics of the specific system must be evaluated. Figure 8.2 and Figure 8.23 illustrates the characteristics for a PV system.

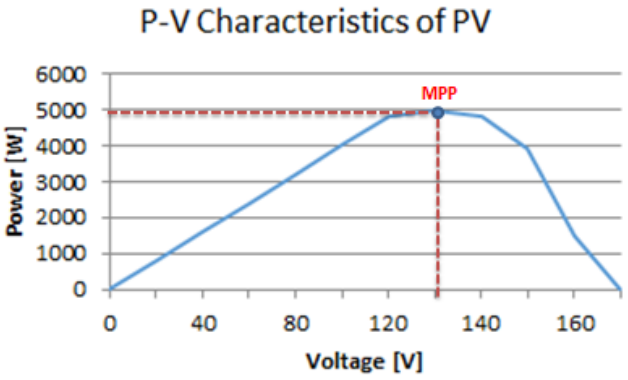

Figure 8.2 – P-V characteristics of a PV system

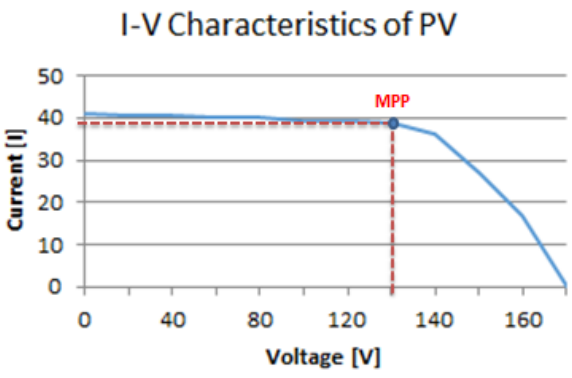

Figure 8.3 – I-V characteristics of a PV system

The P-V-curve illustrates the relationship between output voltage and power, while the I-V-curve illustrates the relationship between output voltage and current, the terms can be calculated as:

$$V_{OC} = \frac{\eta \cdot K \cdot T}{q} ln\left(\frac{I_{SC}}{I_O} + 1\right)$$

Where:
V is the open current voltage
K is a constant of 1.38×10^{-23} J/K
T is the cell temperature in Kelvin
q is the elementary charge of 1.6×10^{-19} Coulombs
I_O is the saturation current
I is the short circuit current of the cell
η is the efficiency, typically ranges between 0.14-0.17, and can be calculated as:

$$\eta = \frac{V_{OC} \cdot I_{SC} \cdot FF}{P_{in}} = \frac{V_{MPP} \cdot I_{MPP}}{P_{in}}$$

Where:
FF is the fill factor, describing the relationship between maximum and theoretical output. Typical fill factors range between 0.5 to 0.85.
V_{MPP} is the specific voltage at the max power point
I_{MPP} is the specific current at the max power point
P_{in} is the radiation on the cell

The P-V characteristics can be used to identify the max power point (MPP) which will result in a specific output voltage. By applying this voltage to the I-V curve, a specific current can be identified. A system with the specifically identified current and voltage will yield the highest output.

The current and voltage output of a system consisting of several PV modules can be manipulated by combining a number of modules in series and parallel. In example, 6 modules of 10 A and 12 V each, can be combined with 3 parallel strings, thus 2 modules in series, resulting in a total output of 30 A and 24 V. To achieve the best output, a max power point tracker (MPPT) can be applied to the system, which will constantly calculate the MPP and adjust the output voltage accordingly. A MPPT is especially effective during low radiation periods where the output voltage is low, if the output voltage of the system is lower than that of the battery, the system becomes extremely inefficient. In this case, a MPPT will adjust the output voltage, thus decreasing the current, to achieve a voltage which will yield a higher system efficiency.

The design performance, specific characteristics of the modules and number of modules must be identified to design and optimize the system, including design of a controller such as an MPPT. This will not be analyzed in this report.

8.4 Photovoltaic Tracking System

In advanced PV systems, axis tracking can be incorporated to enhance the performance. Dual tracking allows automatic change of the tilt and orientation angles of the PV modules according to position of the sun, resulting in higher irradiance for all hours during the year. While dual axis tracking systems are expensive, a simple system could be implemented, where adjustment of the tilt angle of the modules could be changed according to the optimal angle for each month.

The generation in same months can be increased by up to 11.87% by adjusting the tilt angle of the PV panels. This results in an annual increase of 70.4 kWh or 4.54%. The optimal tilt angle of the modules for each month can be seen in Table 8.1. Further details of the calculation can be found in Appendix G .

Month	Jan.	Feb.	Mar.	Apr.	May	June	July	Aug.	Sep.	Oct.	Nov.	Dec.
Tilt Angle °	80	70	65	45	25	0	0	35	55	70	75	80

Table 8.1 – Module tilt angle for optimal monthly PV output

A system where the PV modules can be changed manually by the user increases not only the investment cost but also the risk of additional repairs on the system due to the added complexity. By upgrading the system from 10 to 11 m², approximately 1500 DKK additional investment price, the annual electricity generation can be increased by 9.98% or 154.9 kWh, which is more than the manual tracking method.

The single tracking system allowing the tilt angle of the photovoltaic system to be manually adjusted is found not to yield an increase in electricity generation which can justify the added investment cost and increased risk of reparation and maintenance work.

8.5 Dual-Directional Modules

A PV system made up of two sections with different orientation has been assessed in order to see if dual orientation can yield a higher annual usable PV generation. For example, the annual electricity coverage of two sections of 1m m² both facing directly south has been assessed and compared to two sections of 1 m², where one section is faced due south and one due west. In total nine different combinations of orientation was assessed, the results are found in Appendix G . The combination with the highest performance is 50% of the modules facing south and 50% of the modules facing southwest. This combination yields a 3.7% higher annual generation and reduces the battery capacity by less than 1%, compared to 100% of the modules facing south. It is therefore assessed that construction of dual-directional modules is not a cost-beneficial optimization.

8.6 Validation of Calculation Method

In order to validate the calculation method described within this chapter, the monthly photovoltaic electricity generation for a specific system will be simulated in the simulation program PVsyst (PVsyst). The simulation results from PVsyst will be compared to the results of the described calculation method.

PVsyst allows for monthly weather data input, therefore the global and diffuse radiation in W/m² from the DRY data file will be inserted into the PVsyst model. The following system is the input information for both the PVsyst program and the described calculation method:

- Photovoltaic Size: 1500 Wp
- System performance ratio: 80%
- Tilt angle: 50°
- Orientation: South
- Location: Copenhagen. Longitude 12.4°. Latitude 55.7°

The results from PVsyst compared to the results of the described calculation method can be seen in Figure 8.4. The deviation in incident radiation is directly correlated to the deviation in electricity generation. Therefore the calculation methods for the electricity generation from the incident radiation are found to be similar.

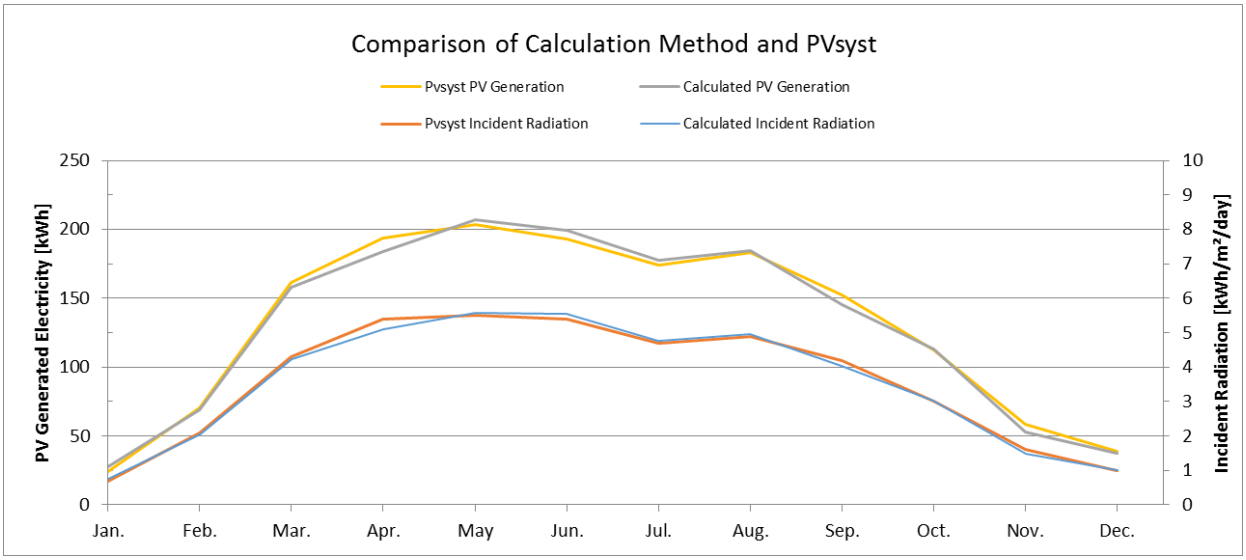

Figure 8.4 – Comparison of incident radiation and electricity generation between PVsyst and applied method

The incident radiation describes the total solar radiation onto the PV modules. The average annual incident radiation is 0.6% higher in PVsyst than the calculation method, see Table 8.2.

PVsyst also simulates an annual electricity generation 0.6% higher than the calculation method, see Table 8.2.

	Calculated Incident Rad. [kWh/m²/day]	PVSyst Incident Rad. [kWh/m²/day]	Deviation [%]	Calculated PV Generated [kWh]	PVSyst PV Generated [kWh]	Deviation %
Annually	3.54	3.6	0.6	1555.6	1565.3	0.6

Table 8.2 – Deviation between PVsyst simulation and applied calculation method

The monthly deviation in incident radiation ranges from -6.1% in January to +7.8% in November, the error over the entire year is off-set as a result of varying negative and positive deviations.

The slight deviation between PVsyst and the calculation method can occur due to the weather data. The weather data are inserted into PVsyst in monthly values. Therefore, PVsyst must create an hourly distribution profile based on assumptions programmed in PVsyst. The hourly values have great influence on the hourly incident radiation even if the monthly or daily values are similar, because the incident radiation relies heavily on the position of the sun and the corresponding global and diffuse radiation for each hour.

The variation in the distribution profile of weather data in PVsyst (which is not available to the user) is most likely the cause of the annual deviation of 0.6%.

9 Theory for Estimation of Wind Conditions

This chapter describes the theory for estimation of wind conditions at different locations in Denmark.
The purpose is to implement the theory in an *Off-grid Simulation Tool* that can simulate the electricity production for an off-grid system, with wind turbine, solar panels and battery storage. Besides describing general theory regarding wind conditions and performance, this chapter will also focus on the estimation of wind conditions at a location near Ebeltoft, as this is a possible building site for Project Grobund, but the theory can be applied to other locations.

9.1 Applied Wind Data

When considering grid connected wind turbine projects, a statistical Weibull-distribution, based on overall information about the wind conditions in a specific area, is normally used for the wind estimation. This is sufficient because it is the yearly electricity production that is important for the feasibility of the project (DWIA - Weibull). Defining the exact wind power in each hour is not critical. Further, grid wind turbines today are so tall, that they are not significantly affected by local obstacles in the landscape around the location. This means, that the wind conditions can be estimated only based on the general roughness of the terrain (normally up to 20 km around the location) as this affects the wind profile. (DWIA - Wind estimation)

In the context of simulating a small off-grid system however, the actual wind velocity in each hour is important, as it - together with solar panels and batteries - should be able to cover the electricity demand the entire year. Further, in order to estimate the wind velocity each hour at the relatively low height of a household wind turbine, it is necessary to make detailed calculations based on the terrain roughness and the obstacles around the location. The by far best case of course, is to have actual wind speed measurements from the exact location.

9.1.1 Wind data - Danish Design Reference Year (2001–2010)

The wind data used in the *Off-grid Simulation Tool* is the public available data from the Danish Design Reference year 2001-2010 (DRY) published by the Danish Meteorological Institute (DMI. DRY-data.). This is a reference climate dataset that has hourly mean values for different weather parameters such as wind speed and wind direction. This is the only publically available hourly wind data available from DMI and probably in general.

In the reference year data Denmark is divided into five wind zones, as illustrated by Figure 9.1, to take into account, that the wind conditions depend on the location. For each of these zones a representative dataset of wind speed and wind direction from a specific measurement station is used. These measurement stations are indicated on Figure 9.1 by a small triangle and a number. The stations are at Thyborøn, Karup, Assens, Holbæk and Nexø (Bornholm).

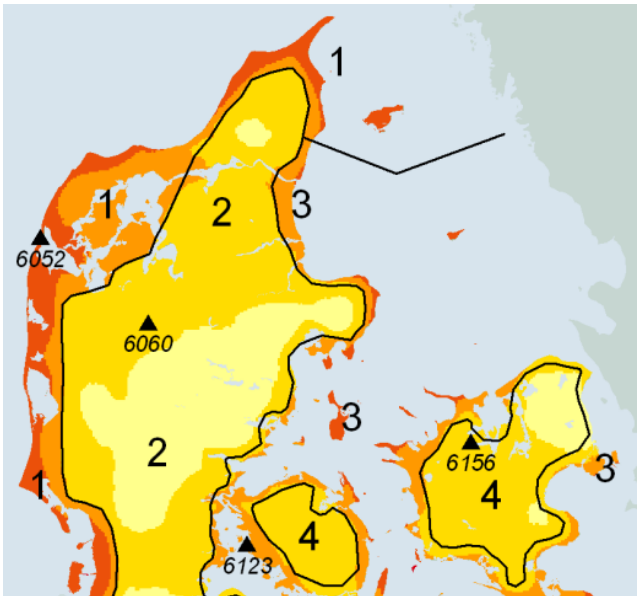

Figure 9.1 – DRY-data wind zones and measurement stations in Denmark (DMI. DRY-data.)

Even though the data from one measurement station is thought to be representative as meteorological weather data care must be taken, when using the data for wind turbine calculations. The meteorological wind data is measured at a height of 10 meter and thus, it is affected significantly by the surrounding terrain roughness and possible obstacles. This means, that unless the wind data is corrected according to the local conditions at the measurement station and again according to the local conditions at the place of interest, it is not necessarily representative for the specific location in this context. This is true even if the data is measured close to the location, as there can be significant local differences. Because of this, the wind data will be adjusted according to local conditions in the *Off-grid Simulation Tool* based on the theory for terrain roughness and shelter of obstacles, that will be described in the following sections of this chapter. (DWIA - Meteorological wind)

The focus will be to estimate the wind conditions at a location near Ebeltoft, as this is a possible building site for *Project Grobund*, but the theory can be applied to other locations. To calculate the wind conditions at Ebeltoft, the DRY wind data from the measurement station at Assens will be used, as this is the most representative of the five stations (both location are near the coast respectively on the east side of Jutland and west side of Funen).

9.2 Parameters and Methods for Estimation of Local Wind Conditions

Together with the efficiency of a wind turbine to turn wind energy into electrical energy, the actual wind conditions at a given location are critical for the electricity yield. In this chapter, the conditions which affect the wind speed at a specific location will be discussed briefly and the calculation methods that are implemented in the developed *Off-grid Simulation Tool* will be presented.

The wind speed at a specific location is a result of the following parameters:

- The geostrophic wind – which is the global wind patterns caused by pressure differences (due to temperature differences).
- The general roughness of the terrain, which slows down the wind by friction.
- Contours of the landscape (orography), that can speed up or slow down the wind.
- Local obstacles that slows down the wind – such as specific trees and buildings.

The geostrophic wind and the orography are briefly explained in Appendix J , while the terrain roughness and influence of obstacles are discussed more detailed in the following, as the theories for these are used in the *Off-grid Simulation Tool.*

To give an overview over why the theory explained in the following sections are implemented in the *Off-grid Simulation Tool*, Figure 9.2 illustrates the complete method for detailed wind data adjustment in the *Off-grid simulation tool.* The DRY wind data from Assens is mentioned in the figure, as this is the wind date adjusted to Ebeltoft in the simulation tool. Assens is chosen, as the terrain here is the most representative compared to Ebeltoft (both locations are near the coast respectively on the east side of Jutland and west side of Funen).

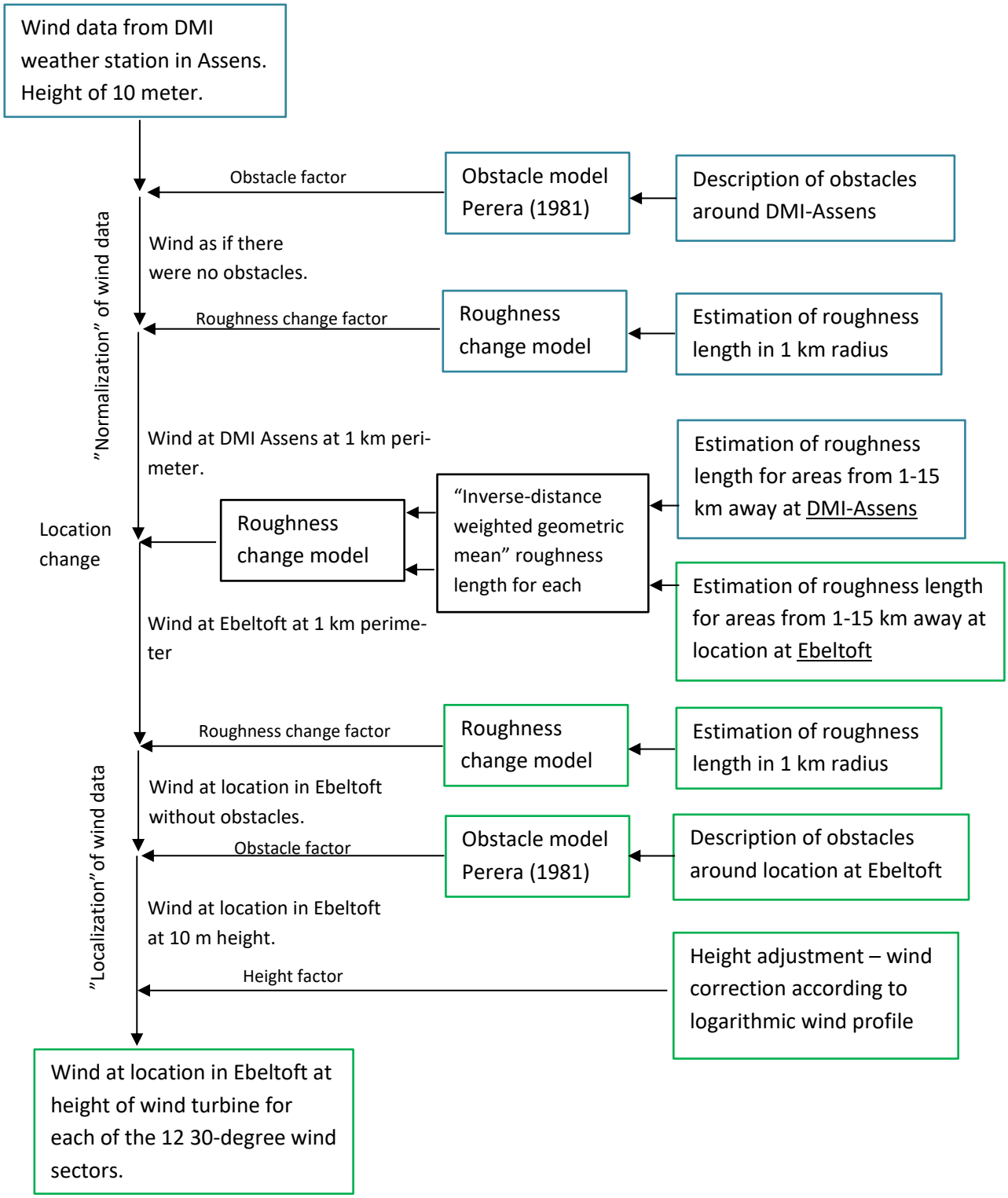

Figure 9.2 - Overview of the detailed method for wind calculations in the *Off-grid simulation tool*

9.2.1 Roughness classes and wind gradient

When the wind moves over the terrain the air-layer close to the ground is slowed down by the obstacles such as trees and buildings. Due to the shear forces between the molecules in the air, this friction causes a wind speed gradient that extent upwards from the ground. That is, the wind speed is lowest at ground and increases with height.

To describe this wind gradient in a specific area, the general roughness of the terrain is described by roughness classes depending on the amount and form of obstacles. These classes correspond to different *roughness lengths,* which is a theoretical height over ground were wind speed is calculated to be zero, this is used to calculate the wind gradient. Table 9.1 shows the roughness classes, lengths and corresponding terrain types.

Roughness classes, lengths and corresponding terrain types		
Class	**Length [m]**	**Terrain type**
0	0.0002	Water surface
0.5	0.0024	Smooth surfaces, such as concrete runways and mowed grass.
1	0.03	Open, almost level agricultural land without fences and hedgerows and very scattered buildings.
1.5	0.055	Agricultural land with some houses and few 8-meter-tall hedgerows (1250 meters between).
2	0.1	Agricultural land with some houses and 8-meter-tall hedgerows (500 meters between).
2.5	0.2	Agricultural land with many houses or a lot of 8-meter-tall hedgerows (250 meters).
3	0.4	Villages, small towns, agricultural land with a lot of tall hedgerows or forests.
3.5	0.8	Large cities with tall buildings.
4	1.6	Very large cities with tall buildings and sky scrapers.

Table 9.1 - Rougness classes, lengths and corresponding terrain types. **(DWIA - Roughness)**

Under neutral atmospheric stability conditions (i.e. there is no temperature difference between the surface of the ground and the air) the wind gradient can be described by the following equation (DWIA - Wind gradient, u.d.):

$$v = v_{ref} \cdot \frac{\ln(h/Rl)}{\ln(h_{ref}/Rl)}$$

Equation 9-1

where v is the unknown wind speed at the height h, v_{ref} is the known wind speed at the height h_{ref} and Rl is the roughness length for the terrain.

Graph 1 shows the wind gradient calculated with Equation 9-1 for roughness lengths corresponding to the classes 0, 2 and 4, when the wind speed is 14 m/s at a height of 100 m. It is clear, that the higher the roughness class for the terrain is, the more the wind is slowed down when the height is decreased. At the typical heights for micro wind turbines of 10-25 meter, the effect of the terrain roughness is significant. Remember that the energy in the wind depends on the third power of the wind speed. To give an example, the energy at a height of 10 meter is approximately: 993, 488 and $143\ W/m^2$ for the three curves on the graph.

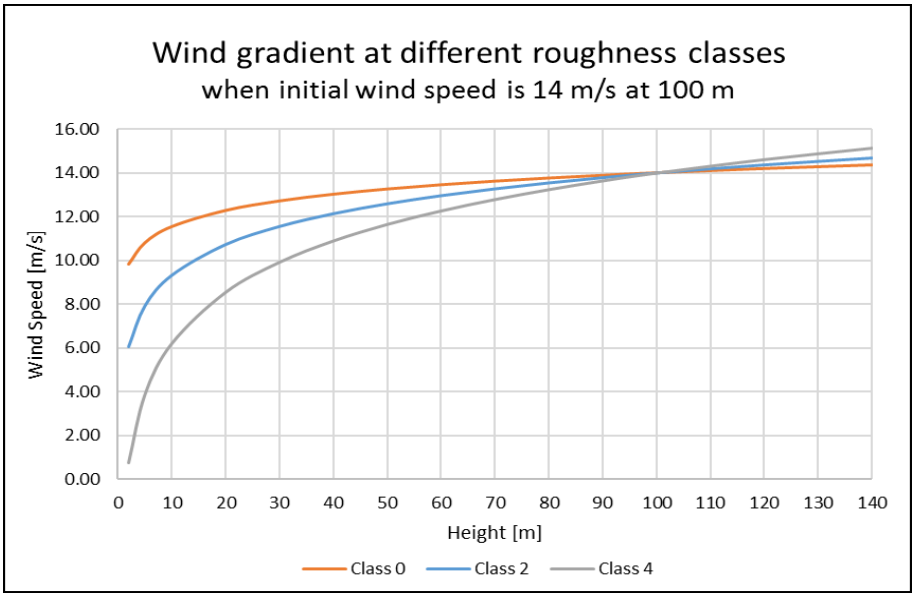

Graph 1 – Wind gradient at different roughness classes based on Equation 9-1

9.2.2 Roughness Change Model in the Off-grid Simulation Tool

In Appendix K , the theory for adjustments of wind speed due to a roughness change is described. This section gives an overview of the theory, as it is implemented in the *Off-grid Simulation Tool* in order to adjust wind data from one location to another. For each of the twelve 30-degree sectors around a location an inverse-distance weighted geometric mean roughness length ($\widetilde{Rl}$) are calculated for respectively the first kilometer and the 1-15 kilometers. These roughness lengths are used to adjust the wind data between the locations by applying the roughness change equation (Equation 18-1) in a sequence as illustrated by Figure 9.3.

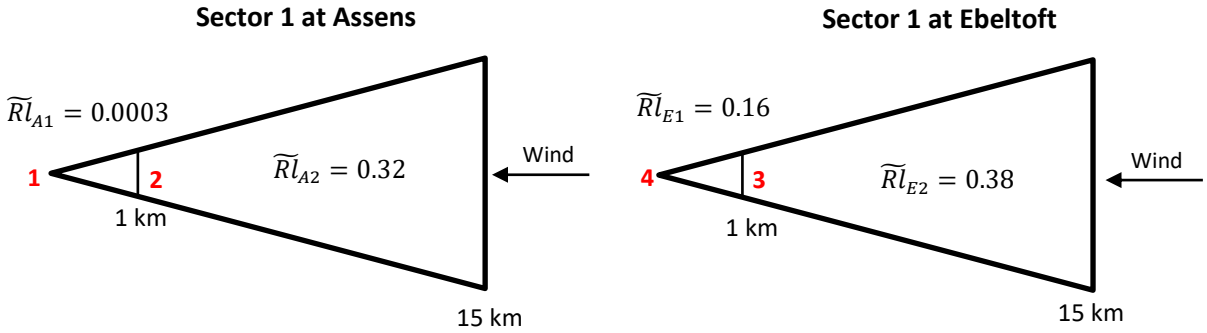

Figure 9.3 – Method for change of wind data between locations

First the influence of the last kilometer (0-1 km from the location) at Assens is removed by using the roughness change equation as if the roughness changed from $\widetilde{Rl}_{A2} = 0.32$ to $\widetilde{Rl}_{A1} = 0.0003$ and dividing the wind velocity with the obtained factor. This gives the wind velocity at point 2 on the figure, which in this case will be lower than at point 1, due to the very low roughness of the last kilometer (mainly water), which increases the wind speed. Now the equation is used again with $\widetilde{Rl}_{E2} = 0.38$ and $\widetilde{Rl}_{E1} = 0.16$ to change the roughness from point 2 to point 3 – i.e. from the general roughness condition at Assens to the general condition at Ebeltoft. At last the equation is used from point 3 to point 4 to adjust for the last kilometer (0-1 km) before the location at Ebeltoft.

9.2.3 Adjustment of Wind Data due to Obstacles

In addition to the roughness differences between two locations, the amount and type of obstacles/shelters close to the location can also be different and must be considered. As a rule of thumb, obstacles in a radius of 1 km around the locations should be considered, as these can have a significant impact on the wind – especially if the obstacles are higher than the wind turbine. (DWIA - Shelters) (EMD - Map, 2001)

The method used in the *Off-grid Simulation Tool* to calculate the effect of shelters is an empirical expression called *The 2D infinite fence model* by Perera (1981). It is basically the same model that is used in the European Wind Altlas software WAsP, but implemented in a more refined way than in the *Off-grid Simulation Tool.*
The model is described in (Bechmann, et al., 2015) and calculates the wind deficit behind a 2D shelter of infinite lateral dimensions (i.e. an infinite wall). The theory implemented in the *Off-grid Simulation Tool* can be found in Appendix F .

Validation of the obstacle function

Figure 9.4 shows an example of a 20-meter-wide, 6-meter-high house placed 150 meter from a 12-meter-high wind turbine. The roughness length of the terrain is estimated to be 0.03 and the porosity of the obstacle is 0 (solid).
With the *Off-grid Simulation Tool* this gives a reduction in the wind speed at the turbine of 4.4 %.
To validate the model the same calculation is made with an online shelter calculation tool from the Danish Wind Industry Association (DWIA - Tool), which gives a reduction of 4 % (result is stated without decimals). This might not sound as a lot, but it results in a decrease of the energy in the wind of 11-12 %, which indicates that even obstacles that are relatively low compared to the wind turbine, can have a significant impact. The online tool generates a matrix with the reduction calculated for each field, as presented by Figure 9.5. The numbers illustrate the wind speed in percent of the undisturbed wind speed as a function of distance and height. When comparing the calculations for other obstacles, the two models show very similar results, which indicates that the theory is implemented correctly in the *Off-grid Simulation Tool*.

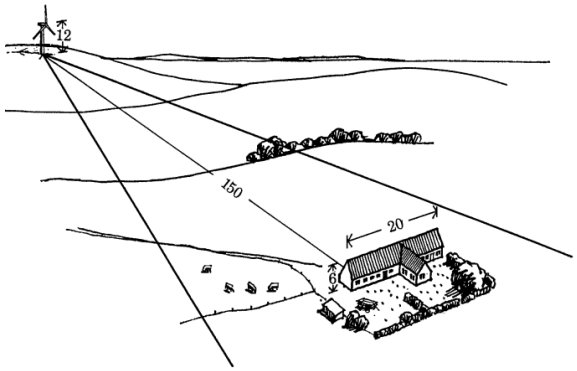

Figure 9.4 – Obstacle in the upwind direction of a wind turbine (Troen & Petersen, 1989, p. 86)

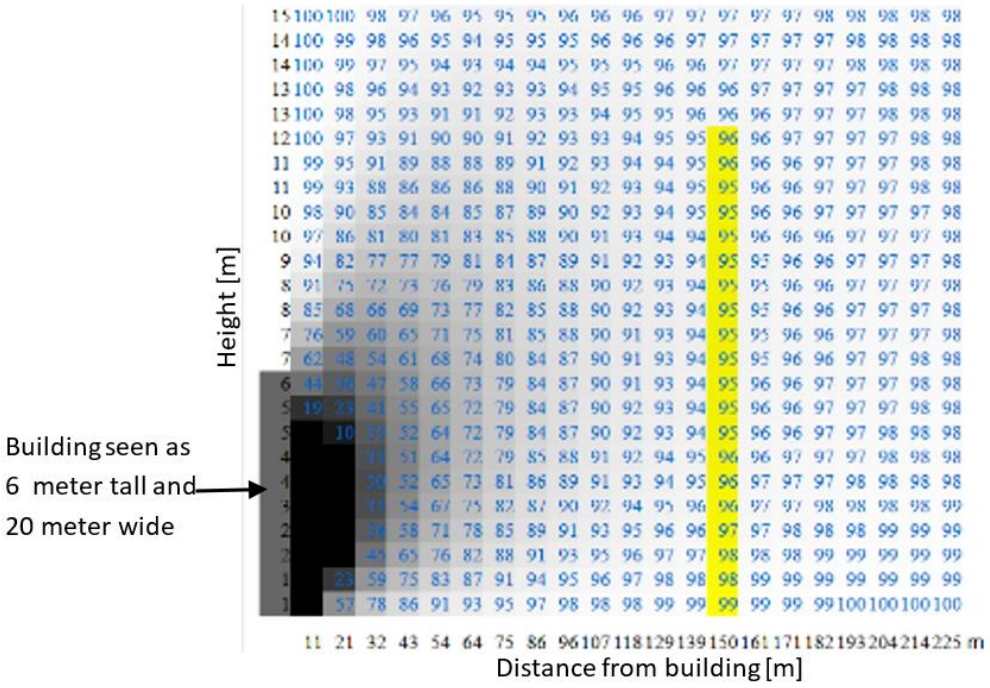

Figure 9.5 – Reduction of wind speed behind a 6-meter-tall, 20-meter-wide building. (DWIA - Tool)

9.2.4 Presentation and Validation of Results of Wind Data Estimation at Ebeltoft

In the previous sections, it has been described how the *Off-grid Simulation Tool* adjusts the wind data from the DMI measurement station at Assens to the possible building location at Ebeltoft.

The mean wind speed of the measurements from Assens is $5.74\ m/s$ and the distribution of velocities is indicated by the blue bars at Figure 9.6. After the adjustments, the mean of the calculated wind speed at Ebeltoft is $4.85\ m/s$ and the distribution is shown by the orange bars at Figure 9.6. As the energy in the wind depends on the third power of the wind velocity, it is interesting to look at how much lower the energy content is because of the lower wind speed. When the energy is calculated and summed up over the different wind speeds, the difference of 1.11 m/s in mean wind speed results in the wind power at Ebeltoft being 64% of the wind power at Assens.

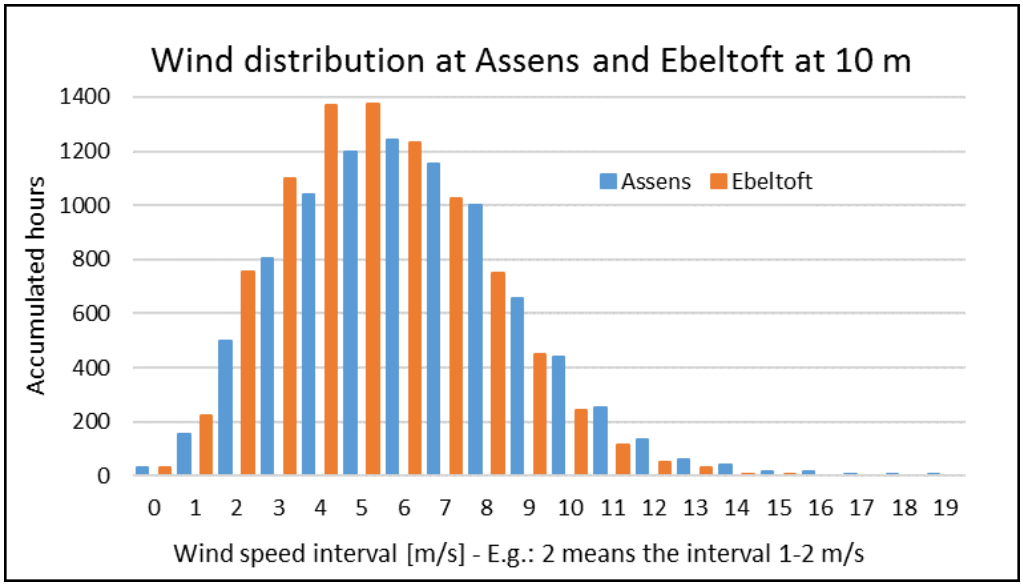

Figure 9.6 – Wind distribution at Assens (DMI measurement) and Ebeltoft (calculated) at 10 m

It is difficult to validate the calculated wind data at Ebeltoft without actual measurements or simulations with a commercial wind software that can simulate local conditions – such as WindPRO (EMD - WindPro).

A way to get an idea of whether the calculation are correct, is to look at the general wind conditions for the two areas and the amount of obstacles. Figure 9.7 shows the two locations on the Danish wind resource map (developed by Energy- and Environment data, EMD, and Risø). The map shows the mean wind speed at a height of 25 meter calculated based on the roughness of the terrain. Local obstacles are not taken into account.

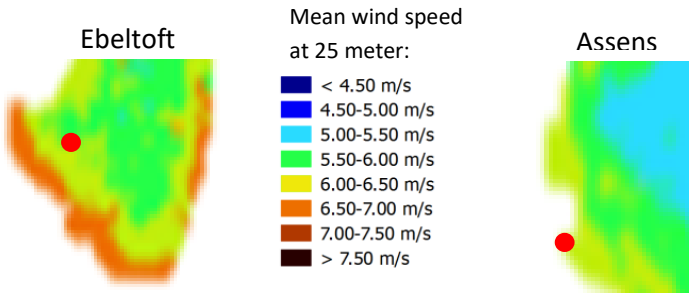

Figure 9.7 – Sections from wind resource map (25-meter height) over location near Ebeltoft and measurement station at Assens (EMD & Risø)

At Assens the measurement station is situated close to the coast in very open terrain and the wind resource map indicates a mean wind of 6-6.5 m/s at a height of 25 meter. The data from the measurement station at Assens is measured at a height of 10 meter. When it is adjusted with the logarithmic wind profile from 10 to 25-meter height, the mean wind speed is increased from $5.74\ m/s$ to $6.6\ m/s$. After this adjustment, the calculated mean wind can be compared to the wind resource map.
At Ebeltoft the location is situated with at least 1.5 km to the coast in each direction, and with some relatively rough terrain in the north to south directions. On the wind resource map, the location is at the borderline

between mean wind from 6-6.5 m/s to 5.5-6 m/s. When the height is changed to 25 meter in the simulation tool, the mean wind at Ebeltoft is calculated to be 5.7 m/s.
Based on the wind resource map, it is realistic that the wind speed is lower at Ebeltoft due to the higher roughness of the terrain around the location. This indicates, that the results from the *Off-grid Simulation Tool* show the right trend, but how precise it is, cannot be evaluated with the, in this project, available data and software.

Another evaluation that can indicate whether the tendency in the calculations are realistic is to look at the local obstacles, that affects the wind speed. Figure 9.8 indicates the position of obstacles around the location near Ebeltoft and at the measurement station in Assens. As seen, there are significantly more obstacles around the location at Ebeltoft.

Figure 9.8 – Obstacles at Ebeltoft and Assens implemented in the calculation

Figure 9.9 shows the reduction of wind speed in percent due to obstacles for each of the 12 sectors at both locations and the number of hours with wind from the directions. As seen, there is significantly higher reduction at Ebeltoft for the north and south directed sectors.

9.2.5 Factors not included in the wind estimation in the *Off-grid Simulation Tool*

As the description of wind behavior is quite complicated, a number of factors are not included in the developed calculation method. The most important of these are the orography at a location (contours of the landscape), conditions with atmospheric instability (vertical air flow due to temperature differences) and wind displacement height (vertical displacement of the wind profile of the wind over forests, etc.). These factors are discussed in Appendix N .

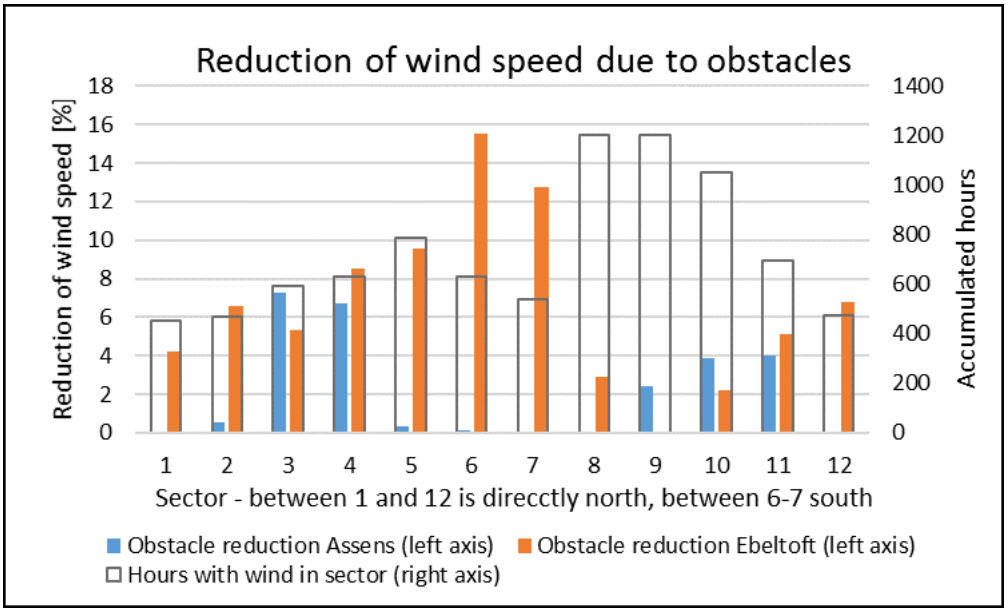

Figure 9.9 – Reduction of wind speed due to obstacles at location near Ebeltoft and measurement station at Assens.

As the wind is prevailing in some directions, it is obstacles in these sectors that have the highest influence on the mean wind speed over the year. Bars named 'Direction' in Figure 9.9 indicates accumulated hours in the respective direction. The directions are the same in the calculated data for Ebeltoft, as the directions are not adjusted. As seen, the prevailing wind is from the sectors 8, 9 and 10 which corresponds to west-southwest. When looking at the number of wind-hours in each sector and the reductions due to obstacles it is clear, that overall the influence of obstacles are highest at the location at Ebeltoft.

10 Theory for Estimating Wind Turbine Generation

This chapter describes the theory for calculation of wind turbine generation implemented in the *Off-grid Simulation Tool*. The purpose of the described method is to calculate the generation based on the wind data described in Chapter 0. Two different methods can be chosen in the simulation tool to define a wind turbines generation. In the first method, the efficiency of the wind turbine is defined for different wind speeds - i.e. how much of the energy in the wind the turbine can convert to electrical energy. In the other method, a power curve is stated for the wind turbine defining the electricity generation at different wind speeds. This is actually the same as defining the efficiencies, but often the power curve is stated by the manufacturer.

10.1 Calculating/defining wind turbine generation from efficiencies

A wind turbine converts the kinetic energy in the wind to a mechanical rotational power that can be used to turn a generator and produce electricity. The amount of generated electricity depends mainly on the energy in the wind and the efficiency of the conversion from kinetic wind energy to mechanical rotation.
The energy in the wind is kinetic energy in the form of the air mass in motion. The kinetic energy of any mass in motion can be calculated based on the mass m and the velocity v as:

$$E = \frac{1}{2} \cdot m \cdot v^2 \; [J]$$

Equation 10-1

For a defined plane, the mass flow of air through it depends on the density and velocity of the air flow and the area of the plane:

$$\dot{m}_{air} = \rho_{air} \cdot A \cdot v_{air} \ [kg/s]$$

Equation 10-2

By replacing the specific mass in Equation 10-1 with the mass flow defined by Equation 10-2, the power in the wind passing through the defined plane can be found:

$$P_{air} = \frac{1}{2} \cdot \rho_{air} \cdot A \cdot v_{air}^3 \ [J/s]$$

Equation 10-3

The energy captured by a wind turbine is the difference in the kinetic energy (due to velocity) in the wind before and after the turbine. As the wind cannot be stopped completely after the turbine – this would stop the air flow past it – the entire energy in the wind defined by Equation 10-3 cannot be harvested.

In 1919 the German physicist Albert Betz derived the maximum theoretical efficiency for a wind turbine converting kinetic wind energy into mechanical energy is 59.3 %. This value is known as the *Betz Limit* or the *maximum power coefficient,* $C_{p,max}$.
In the real world, a wind turbine cannot operate at this theoretical limit due to practical/mechanical requirements. In practice the limit with today's technology is up to 45-50 % at peak efficiency for utility scale wind turbines (above 1 MW nominal power) (NSW Government, 2010). For a specific wind turbine, the available power in the wind can be found by multiplying Equation 10-3 with the specific *power coefficient* C_p (efficiency) for the turbine. When the C_p for a wind turbine is known, the power generated by the turbine can be calculated with Equation 10-3 as:

$$P_{wind\ turbine} = \frac{1}{2} \cdot \rho_{air} \cdot A \cdot v_{air}^3 \cdot C_p \ [J/s]$$

Equation 10-4

As discussed in Appendix R , the efficiency of wind turbines varies with the wind speed which means, it is necessary to define efficiencies at different speeds. Examples and references to realistic efficiency-distributions for small wind turbines can be found in the appendix. With the efficiencies at different wind speeds, the power curve of the wind turbine can be defined from Equation 10-4.

10.2 Defining wind turbine generation from stated power curve

As described in previous section 10.1 there is both a theoretical limit and a practical limit to the efficiency of a wind turbine. As the practical efficiency depends on the specific design and system, the best way to estimate the potential electricity production of a specific wind turbine is with a power curve that shows the true relationship between wind speed and electricity generation tested under real conditions. If the specific power curve is not known, the efficiency method described in previous section can be used with estimated efficiencies.

To give an example Figure 10.1 shows the power curve for a 1 kW (24 V) wind turbine called Air Force 1 produced by (Future Energy). From this power curve, the electricity generation at different wind speeds can be calculated. It must be remembered, that there is a generation initiation wind speed – here 3 m/s – which is the limit, where the turbine starts generating electricity. Further, the turbine will have a maximum power limit (here the maximum stated point is 1142 W) – above which higher wind speeds does not generates higher output – and probably a cut-off wind speed, where the turbine stops due to safety or a survival wind speed (here 52 m/s) above which the turbine will probably break.

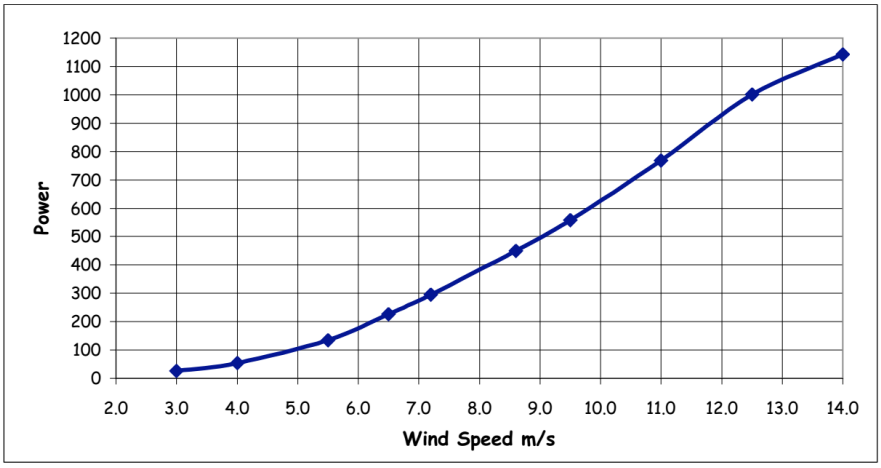

Figure 10.1 – Power curve for Air Force 1, 1 kW micro wind turbine (Future Energy, u.d.)

When using a power curve like this stated by the manufacturer, it is always a good idea to calculate the efficiencies at the different points – i.e. the stated power in relation to the power in the wind. As discussed in Appendix R , the stated power curve for the Air Force 1 (Figure 10.1) is unrealistic as it shows efficiencies of above 60 %. In reality, the efficiency of a small wind turbine is around 20-30 % with peak efficiencies up to 35 % (WindpowerProgram). In Appendix R , it is estimated, that the realistic production from the Air Force 1 is around half of what the power curve claims.

10.3 Calculation of wind turbine generation in the *Off-grid Simulation Tool*

In the *Off-grid Simulation Tool* the wind turbine electricity generation is calculated for each hour from the hourly mean wind speed (at the height of the wind turbine) and a function describing the power curve (i.e. defining generation as a function of wind speed). Depending on the chosen method, the power curve function is calculated as a sixth-degree polynomial regression based on either the stated power curve or a calculated power curve based on the stated efficiencies at different wind speeds.
To take the Air Force 1 as an example, Equation 10-5 shows the regression for the power curve shown at Figure 10.1 in the previous section.

$$\text{Power [W]} = -0.008 \cdot v^6 + 0.36 \cdot v^5 - 6.6 \cdot v^4 + 60.9 \cdot v^3 - 286.4 \cdot v^2 + 677 \cdot v - 620.8 \quad (R^2 = 1)$$

Equation 10-5

where Power [W] *is the power generated by the generator in the wind turbine (before losses in wires, etc.) and* v *is the stated wind speed.*

Table 10.1 shows the generation points stated by the manufacturer, the calculated power from the equation and the deviation between the two.

Wind [m/s]	Stated power [W]	Regression power [W]	Deviation [%]
3	26	26.3	1.0
4	55	54.0	-1.8
5.5	135	137.5	1.9
6.5	227	224.9	-0.9
7.2	296	295.6	-0.1
8.6	450	450.5	0.1
9.5	558	559.0	0.2
11	768	766.8	-0.2
12.5	1002	1002.5	0.1
14	1142	1141.9	0.0

Table 10.1 – Stated power curve and regression curve for Air Force One, 1 kW wind turbine

As seen in Table 10.1, the deviations are in the order of 2 % at the low wind speeds and very low at the higher speeds. As the generation is very low at the lowest wind speed, and the deviation is alternating between a positive and negative value, the regression is thought to be sufficiently precise to calculate the generation. Different power curves have been tried in the simulation tool and the sixth-degree polynomial regression has been found to give very good fits.

In the *Off-grid Simulation Tool*, the wind speed is evaluated as a mean hourly value. When the mean wind speed for a specific hour is used with Equation 10-5, the equation gives the hourly electricity generation in watt-hours (Wh) and this is the value calculated by the tool.

10.3.1 Parameters for wind calculation in the *Off-grid Simulation Tool*

Before the simulation tool can calculate the wind turbine generation several parameters must be defined. The generation is calculated from the stated power curve or efficiencies as explained in the previous section. In addition, the following parameters must be defined:

- A generation initiation wind speed – below this generation is defined as zero
- A cut-off wind speed – above this generation is defined as zero
- A maximum power generation – this overwrites values calculated by the power curve, if they should be higher.
- A tower height – used in the wind calculation to estimate the wind speed at different heights
- A rotor diameter – used in the calculation of energy in the wind for the swept area, when the efficiency method is used to state the power curve
- A system loss (from turbine to battery)

10.3.2 Validation of the wind turbine generation method

In Section 13.3 and Appendix Q results from the *Off-grid Simulation Tool* are compared to results from the commercial energy system analysis tool 'Homer Pro'. The Air Force 1 wind turbine is used as example for the validation (with the information stated by the manufacturer).

The Off-grid Simulation Tool calculates a yearly generation of 1287 kWh, while the Homer Pro software calculates a generation of 1309 kWh – a deviation of only 1.7 %. Figure 10.2 shows the simulated generations during January for respectively the simulation tool and Homer Pro. As they are very similar, the simulation tool can be assumed to produce realistic results.

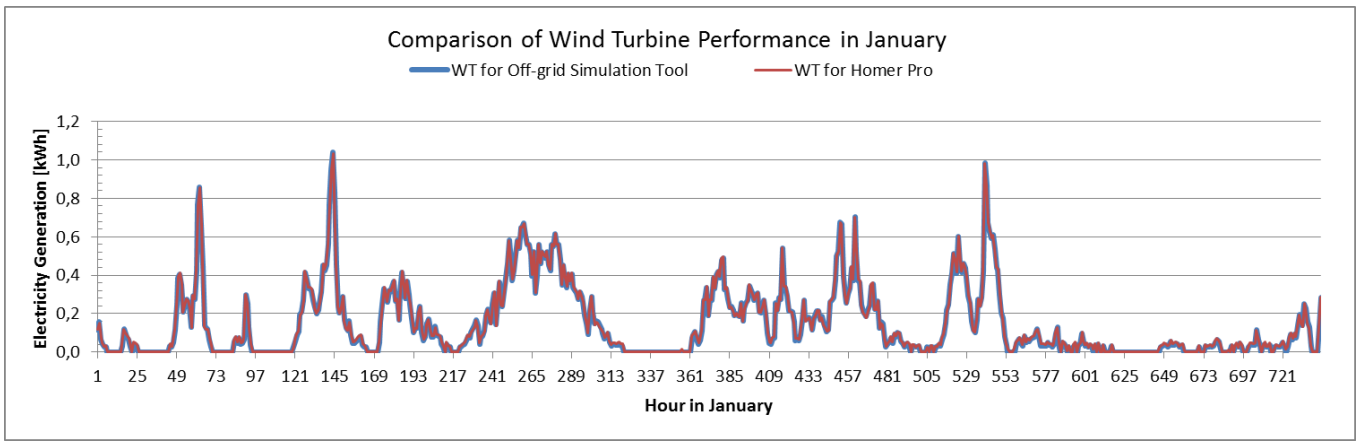

Figure 10.2 – Comparison of wind turbine generation for validation of simulation tool

10.3.3 Discussion errors/uncertainties in the calculation method

Error due to hourly mean wind speeds

As mentioned the *Off-grid Simulation Tool* calculates the wind turbine production based on the measured/calculated mean hourly wind speed. As the power in the wind depends on the third power of the wind speed, this can result in an underestimation of the generation. The magnitude of the deviation depends on the actual distribution of wind speeds during the hour and the more the wind speed varies during the hour, the larger the error. To estimate the impact of the error, the deviation has been investigated for the Air Force 1 wind turbine by calculating the generation on a minute-basis and comparing it to the hourly mean calculation. For a distribution where the wind speed is fairly uniform (5, 6 and 7 m/s – each for 20 min) the underestimation of energy in the wind is only 2.3 %. For a distribution where the variation is large (3, 5, 7, 9, 11 and 13 m/s – each for 10 min) the deviation is 17 %. The last calculation is thought to be a rare change of wind speeds during an hour. On the other hand, due to the nature of the wind and possible increased turbulence at a specific location, the wind speed can vary significantly at the rotor of a small wind turbine. The actual impact of the hour-mean-error in the yearly simulations is very difficult to estimate, but as it results in an underestimation of the electricity generation, it is not thought to be a critical uncertainty.

Error due to the density of air at different temperatures

As Equation 10-3 shows, the energy in the wind is proportional to the density of the air. At -10 ℃ the density of air is 1.34 kg/m^3 and at 30 ℃ it is 1.17 kg/m^3 (Gribble). Compared to the density of 1.25 kg/m^3 at the yearly mean temperature of around 8.5 ℃ (DMI - Mean temp.) the density is 7.2 % higher at -10 ℃ and 6.4 % lower at 30 ℃. The impact of this effect on the calculations for the Air Force 1 wind turbine is not known, as the company does not explain the conditions/assumptions for the stated power curve. If the power curve is measured on a cold winter day, the yearly error in the calculation could be an overestimation of the generation of up to 7.2 % and for specific hours in the summer up to 13 %.

It is thought to be unlikely that the power curve is stated at a very low temperature, as this would be misleading and could result in customer complaints. If it is the case, the deviation is still lowest in the winter, when the generation from the wind turbine is most important (due to low PV-panel generation).
In other cases, where the temperature behind the power curve is known, the error could be corrected by using the hourly mean temperatures in the Design Reference Year.
Due to these considerations, the impact of a potential error is not thought to be significant. Further, as the error due to hourly mean wind speeds underestimated the production, this deviation would probably make the resulting error over longer periods smaller.

Correctness of stated power curve

The method is based on the power curves stated by the manufacturers of the wind turbines. If the power curve for a wind turbine is not correct, the method will calculate wrong generation values. As discussed in Appendix R , the stated power curves for small wind turbines can be quite overestimated and result in unrealistic calculated electricity generations.

10.4 A note on charge controllers for wind turbines

In an off-grid energy system with a wind turbine and battery storage, a charge controller is needed for more reasons. Many small wind turbines are designed to output a voltage around either 12, 24 or 48 V. With peak power up to 1-2 kW depending on the turbine, this can give high currents in the order of 40-80 A. As the battery can be destroyed by overcharging (when it is full) or by too high currents, a charge controller is needed to monitor the charging and adjust it when necessary, by directing the excess current to another load, called the 'dump load'. This load could be a submersion heater in a DHW tank or just an air-cooled resistor. In addition, a wind turbine must be connected to a load in order not to 'run loose' and possible destroy itself. The reason for this is, that it is the magnetic fields in the generator due to the induced current, that gives the rotor a mechanical resistance. If the turbine is not connected to a dump load, it is necessary to brake it with a mechanical brake or electrical brake (short cut the generator). Different charge controllers based on different technologies and with different functions exist, but a popular one for small wind systems is the Tristar controllers made by Morningstar. This controller is install in parallel to the battery, so the charging current does not go through the controller, which reduces the energy losses and the wear on the controller. Only when there is an excess current, this is diverted through the controller to the dump load. The controller can also be used in combined solar and wind turbine systems. The way to use it is explained at (Piggott, Hugh - Tristar, 2017).

11 Energy Storage System

Two types of energy storage will be applied in the *Off-grid Simulation Tool* and system design; electrical batteries and a hot water tank. Electricity generation which cannot be instantaneously used will be utilized to charge the electrical batteries. If the electrical batteries are at maximum capacity, the hot water tank will be used to store excess energy by heating domestic hot water through an immersion heater in the tank.
The lifetime of a battery heavily depends on the quality of use. Correct charging of a battery, in terms of charging voltage, can increase the lifetime significantly. This can be achieved by installing a charge controller which adjusts the input voltage according to the current battery state. The depth of discharge (DoD), which is how much of the battery's relative capacity is utilized, also has great impact on the lifetime. Illustrated in Figure 11.1 and Figure 11-2 is the retailer's (Viva Energi - GEL) expected cycles for two types of batteries as a function of the depth of discharge.

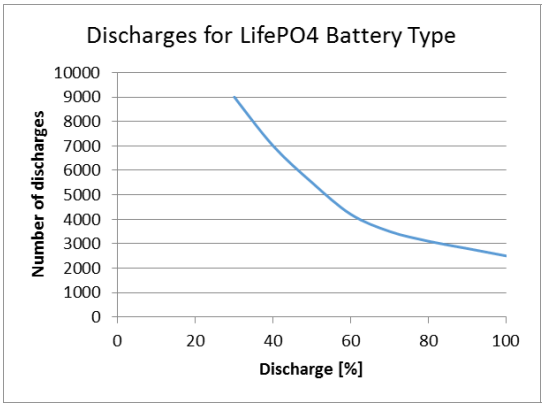

Figure 11.1 – LifePO4 battery discharges depending on DoD

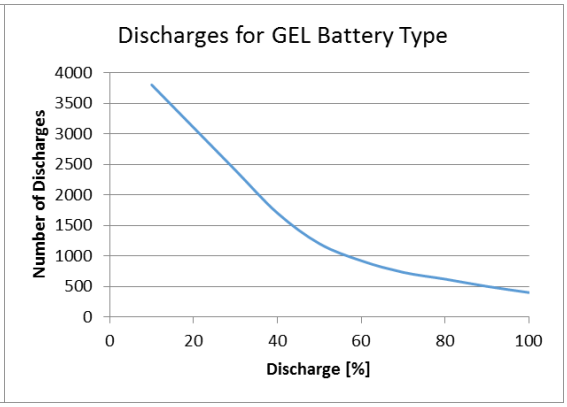

Figure 11.2 - GEL battery discharges depending on DoD

If the average discharge is increased from 30 to 60%, both batteries decrease their expected lifetime cycles by more than 50%. This means that two batteries with an average discharge of 30% will yield more lifetime capacity than one battery with an average of 60%. On the other hand, batteries can be expensive and it might show to be more economical sustainable to increase the average charge in order to decrease the number of batteries in the system. In the *Off-grid Simulation Tool* the number and depth of discharges during the year is used to estimate the lifespan of the battery storage as described in the next section. From the lifespan and the investment price of the batteries for a specific design, the long term cost can be evaluated and compared with other solutions.

11.1 Battery Capacity Calculations

In order to assess the state of the battery, the following calculation process has been applied. It is based on the hourly demand value, hourly PV-panel generation and hourly wind turbine (WT) generation:

$$hourly\ total\ generation = PV\ generation + WT\ generation$$

$$if: hourly\ total\ generation > consumption = battery\ is\ unused$$

$$if\ above\ is\ false:$$

$$battery\ stored\ energy = stored\ energy\ in\ previous\ hour - [consumption - total\ generation]$$

$$for\ above: if\ battery\ stored\ energy > battery\ capacity, excess\ electricity\ is\ used\ for\ DHW$$

Based on the above equations, the amount discharged for every hour, if discharged at all, can be calculated. The amount discharged results in a specific depth of discharge for each discharge cycle in the year. An example of this is illustrated in Figure 11.3.

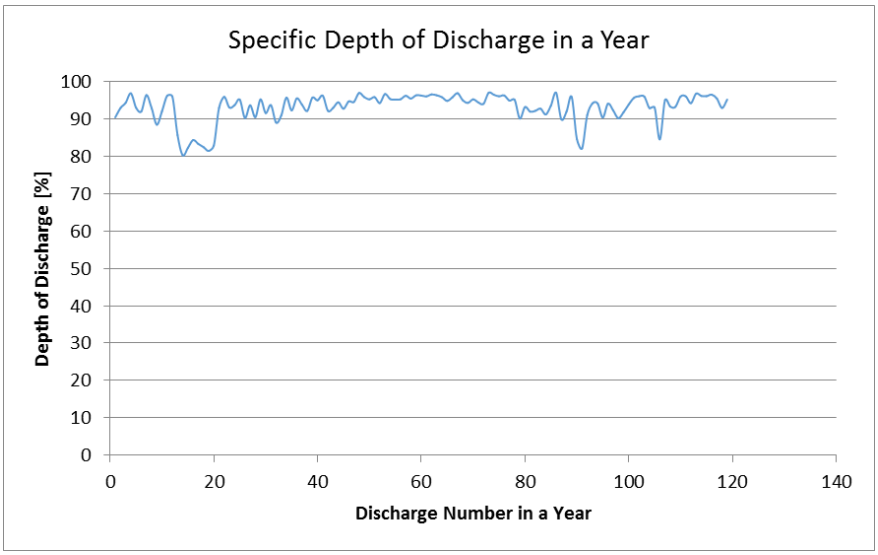

Figure 11.3 – Specific DoD for every discharge in a year

This graph is the result of each discharged occurring in a one year period for the specific system. The x-axis shows the number of discharges per year. This information is used in order to calculate an expected lifetime of the battery by calculating an average DoD and using the manufacturer information from Figure 11.1 or Figure 11-2, resulting in a total number of discharges for the battery before it should be replaced. Having identified the absolute number of discharges in the battery, the total battery investment cost can be calculated for a 20-year period.

In the *Off-grid Simulation Tool* the user can adjust the actual installed battery capacity in order to estimate which combination of batteries will be the cheapest solution in a year 20 period.

12 Overview of the Off-grid Simulation Tool

The theory discussed in the previous Chapters 8 to 11 are implemented in the *Off-grid Simulation Tool,* that allows the user to simulate the hourly balance of an off-grid electricity generation system composed of a photovoltaic system, a wind turbine, a battery bank, a domestic hot water tank and potentially a diesel or gasoline generator. The user is required to input annual electricity and domestic hot water consumption along with site and system specific data. Based on this input, the simulation tool calculates hourly demand profiles and hourly electricity generation values.

The simple nature of the tool creates a platform from where users without great technical knowledge can identify or optimize the sizes of the individual components in an off-grid electricity system intended for a single household.

For the printed copies of this report, the Off-grid Simulation Tool can be found on the enclosed flash drive.

12.1 Main Components

The main components of the system are illustrated in Figure 12.1. The technical composition of a photovoltaic system generates a direct current (DC) output. Direct current is also capable of being electrically stored, while alternating current (AC) is not. Therefore, an inverter is necesarry if the user requires an AC output for appliances, which is the output form in a typical grid system. An inverter will increase the investment cost and the complexity of the system significantly. The requirement of alternating current does not impact the Excel tool in anyway, but the illustrated and proposed system is a direct current system.

The calculations in the *Off-grid Simulation Tool* revolve around the hourly outputs of the photovoltaic system and the wind turbine in balance with the battery capacity and electricity demand.

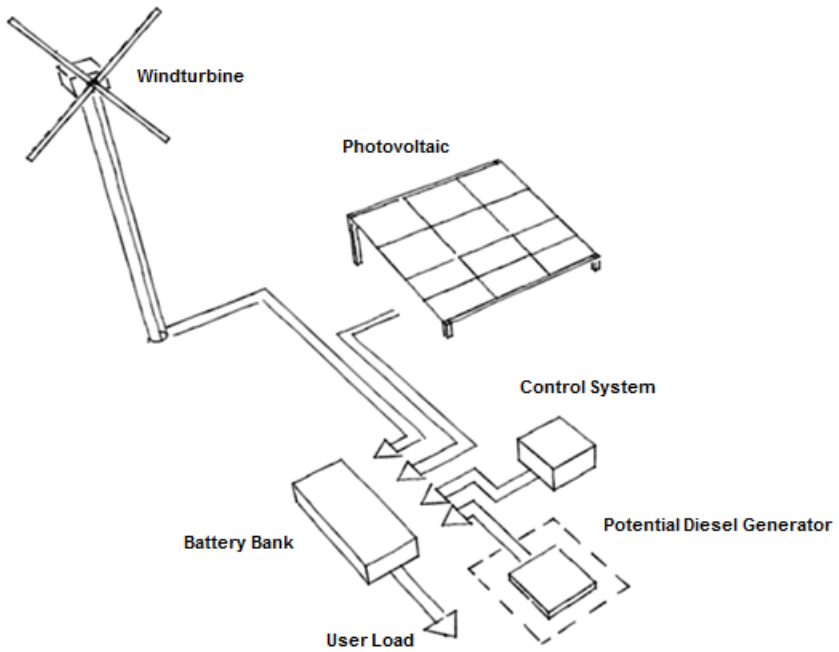

Figure 12.1 – Main components of the Off-grid Simulation Tool

12.2 Weather Data

In order to calculate the hourly output values for photovoltaic (PV) and wind turbine (WT), hourly weather data values must be used. In the *Off-grid Simulation Tool*, the public available weather data known as Danish Design Reference Year (Wang, et al., 2013) is applied. The DRY data was measured by six stations through 2001 to 2010, each station represents a climatological zone within Denmark. The hourly observations through this period have been used to create an annual data set with hourly values, consisting of 11 specific parameters which represent a typical year in Denmark.

As such, the performance of the PV and WT is based entirely on typical data from 2001 to 2010, indicating that the weather data applied is not predictive. Therefore, the calculated performances will without doubt vary from the actual performance, specifically in hourly values. Danish Design Reference Year data is often applied in various simulation tools to create an educated guess on building performance and should therefore create a fairly accurate assessment of the monthly and annually performance of the system.

12.3 Calculation Process

The overall steps of the calculation method in the Excel based *Off-grid Simulation Tool* are illustrated in Figure 12.2, where P is power [W] and Q is energy [kWh].

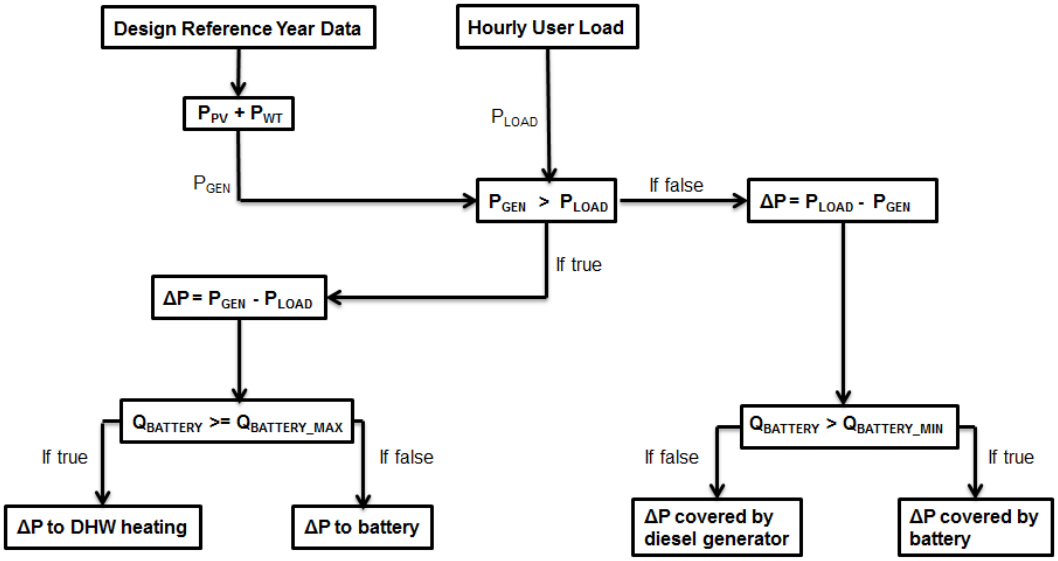

Figure 12.2 – Calculation process of the Off-grid Simulation Tool

The calculation is based on the following steps:

1. An hourly distribution profile for electricity demand and domestic hot water demand is created based on user input of annual consumption. The electrical load for each hour is named P_{USER}
2. Hourly output values for the photovoltaic system named P_{PV} is calculated based on user input regarding the system and the weather data from the Danish Design Reference Year
3. Hourly output values for the wind turbine named P_{WT} is calculated based on user input regarding the system and the weather data
4. If the combined value of P_{PV} and P_{WT} named P_{GEN} is higher than the load P_{USER} the excess electricity is stored in the battery bank. If the battery capacity is at the maximum level, the excess electricity is used as domestic hot water heating through an electric resistor in the water tank

5. If P_{GEN} is lower than the load P_{USER} the missing electricity is discharged from the battery bank. If the battery capacity is at the minimum level, the system will start the auxiliary power, which in this system is a diesel generator to cover the missing load, named ΔP.

In the *Off-grid Simulation Tool* the user will be informed of the following:

- Photovoltaic System
    - Expected investment price
    - Monthly coverage of the electricity demand without a battery bank
    - Missing electricity generation each month, again without a battery bank
- Wind Turbine
    - Wind turbine generation each month and visual overview of the generation over the year
    - Electricity deficit each month without battery storage
- Battery System
    - Minimum required battery capacity to cover the electricity demand every hour of the year based on the applied weather data and performance of PV and WT systems
    - Depth of discharge for every discharge of the year, based on either the calculated minimum capacity or a user specified capacity
    - Lifetime of the battery depending on choice of battery type
    - Total investment cost for the batteries over a 20-year period
- Domestic Hot Water System
    - Monthly coverage of the DHW demand by excess electricity generation
    - Missing excess energy to cover remaining DHW demand

The above exchange of input and output allows the user to evaluate a specified system. The system does not contain an algorithm which automatically optimizes the system, but instead the user is advised to change the individual component sizes in order to identify the best system and component combination for the individual user.

12.4 General Observations of the Off-grid Simulation Tool

Unless the annual electricity consumption is sufficiently low compared to the design sizes of the components (e.g. less than 1000 kWh electricity annually for a combined design capacity of PV + WT of 2 kW) a high battery capacity will be necessary during December – February, compared to the battery capacity necessary for the rest of the year. Therefore, if the house is without grid connection, a battery system worth 3-5 days of electricity consumption can result in a high additional investment, only to ensure sufficient electricity for a very a short period.

A small gasoline or diesel generator of 1.5 kW can be purchased for 1,500 DKK and will easily cover the electricity demand during a period without wind or solar power. While using fossil fuels is not considered sustainable or renewable, it should only be used for few hours during a 20 year period, whereas the additional batteries would be used to some extent, thus needing replacement resulting in an additional investment cost. As batteries are toxic and difficult to decompose, using a diesel generator when or if necessary might be more economically and environmentally sustainable seen over the household lifetime.

13 Design of off-grid system for Ebeltoft

This chapter presents the process of designing a proposal for an off-grid energy system to the houses at *Project Grobund* near Ebeltoft. The developed *Off-grid Simulation Tool* (described in chapter 11) is used to analyze the energy generation and storage for different combinations of photovoltaic panels, wind turbine, batteries and accumulation tank for domestic hot water. In the first part of the chapter, the final proposal for the system is presented with the purpose of showing what the goal of the process described in the rest of the chapter is. This is thought to give the reader a better understanding of the chapter.
After the presentation of the final system, the chapter presents analyses the following topics:

- Evaluation of the solar radiation and wind speeds during respectively winter and summer periods
- Electricity coverage with only a photovoltaic system combined with different battery capacities
- Electricity coverage with only a wind turbine combined with different battery capacities
- Electricity coverage for a system with combined PV and WT – first without battery and then with different battery capacities
- Analysis of a system with battery capacity for all-year electricity coverage and of the utilization of excess electricity generation for production of DHW
- Investigation of battery life-time cost for the system and evaluation of a system with low battery capacity and back-up generator
- Discussion of off-grid systems at other locations and a market analysis for small wind turbines

13.1 Final proposed system for Off-grid house at Ebeltoft

In the following sections, the electricity and DHW coverage for an off-grid house located near Ebeltoft will be evaluated discussed. The assumptions/inputs used for the calculations are as follows:

- Wind data: Design Reference Year 2001-2010 measurements from Assens adjusted to location near Ebeltoft as described in Section 9.2.2.
- Solar radiation: Design Reference Year 2001-2010 measurements from Års Syd (Section 8.1).

Assumed energy demands for each month			
	Electricity	**Space Heating**	**Domestic Hot Water**
Jan	70	516	98
Feb	59	429	88
Mar	66	308	98
Apr	54	116	95
May	56	0	98
Jun	48	0	95
Jul	49	0	98
Aug	56	0	98
Sep	54	0	95
Oct	66	0	98
Nov	63	338	95
Dec	70	488	98
Sum	713	2195	1150

Table 13.1 – Assumed energy demands. The demands are estimated chapter 3

With these input data, the developed *Off-grid Simulation Tool* is used to evaluate the hourly balance between electricity generation, consumption and storage over the year in order to design an energy system which can cover the electricity demand. The excess electricity (that cannot be stored in the battery bank), is utilized for heating of domestic hot water.

If it is a requirement that the system should rely only on the energy sources at the location (i.e. no generator or similar for back-up) the following system is proposed based on the analysis:

- Photovoltaic system with 5 m^2 panels orientated directly south with a tilt of $50°$. Corresponding to a production of 768 kWh.
- A wind turbine with a power-curve corresponding to that stated for the 1 kW (24 V) 'Air Force 1' on Figure 10.1 and a 10-m tower. Corresponding to yearly production of 1287 kWh at the location.
- Battery bank with 10.1 kWh of capacity (based on GEL deep cycle batteries).
- A 200 L DHW tank with immersion heater and heat spiral connected to the mass oven.
- Mass oven to produce space heating and DHW in the winter season.

With this system, the entire electricity demand of 713 kWh is covered, while 86 % of the domestic hot water is covered by the excess electricity generation. The remaining 158 kWh of DHW and the space heating demand of 2195 kWh is covered by the mass oven.

13.2 Process of designing the system for Off-grid house at Ebeltoft

This section contains the analysis of the individual components which lead to the design of the proposed system presented in the previous section.

13.2.1 Evaluation of wind and solar conditions at Ebeltoft

Graph 2 and Graph 3 shows the wind speed and solar radiation for two periods respectively in the winter and summer. As most household wind turbines have a cut in wind speed around 3-4 m/s, a line at 3 m/s indicates when the wind velocity is sufficient for electricity generation. Graph 2 indicates periods in the winter with almost no solar radiation or usable wind - the longest period during the year is seven days (indicated on Graph 2). Graph 3 indicates, that the solar radiation is relatively continuously and reliable during the summer.

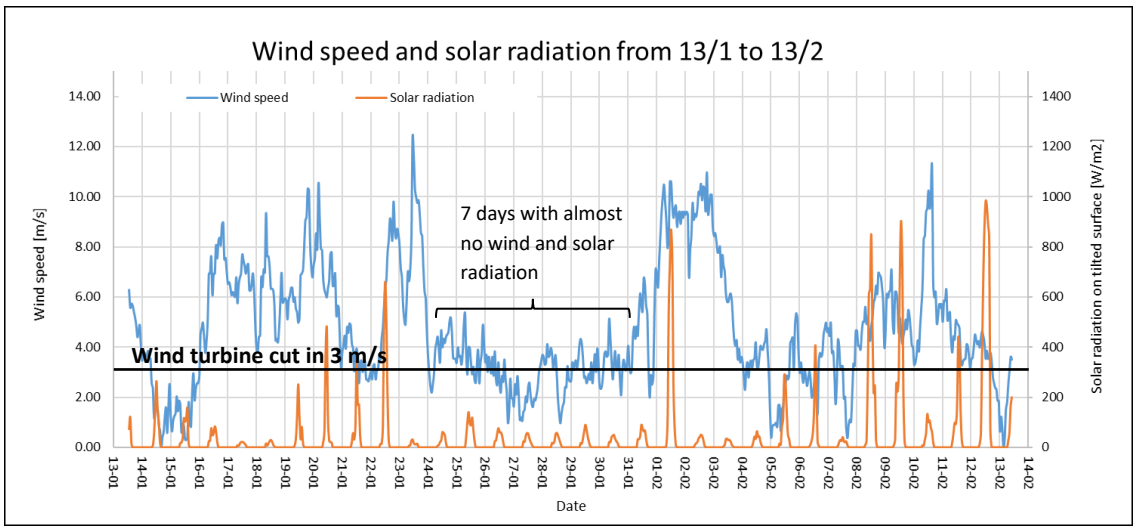

Graph 2 – Wind speed and solar radiation from 13/1-13/2 at location near Ebeltoft.

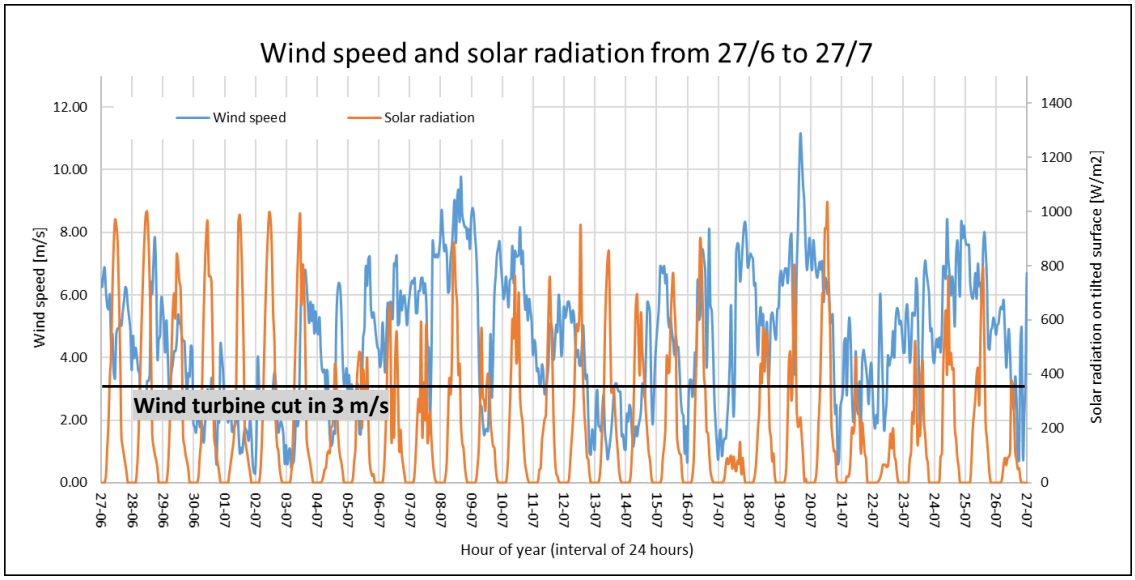

Graph 3 - Wind speed and solar radiation from 27/6-27/7 at location near Ebeltoft.

13.2.2 Evaluation of PV-system electricity coverage at Ebeltoft – No wind turbine

The yearly electricity demand for the off-grid house is estimated to 712 kWh (daily value of 1.6-2.3 kWh) in section 3.2, which is distributed over each hour of the year. Graph 4 shows the electricity deficit (uncovered electricity of the 712 kWh) as a function of photovoltaic area and battery capacity and the total possible electricity generation from the photovoltaic system – there is no other electricity source than the solar panels.

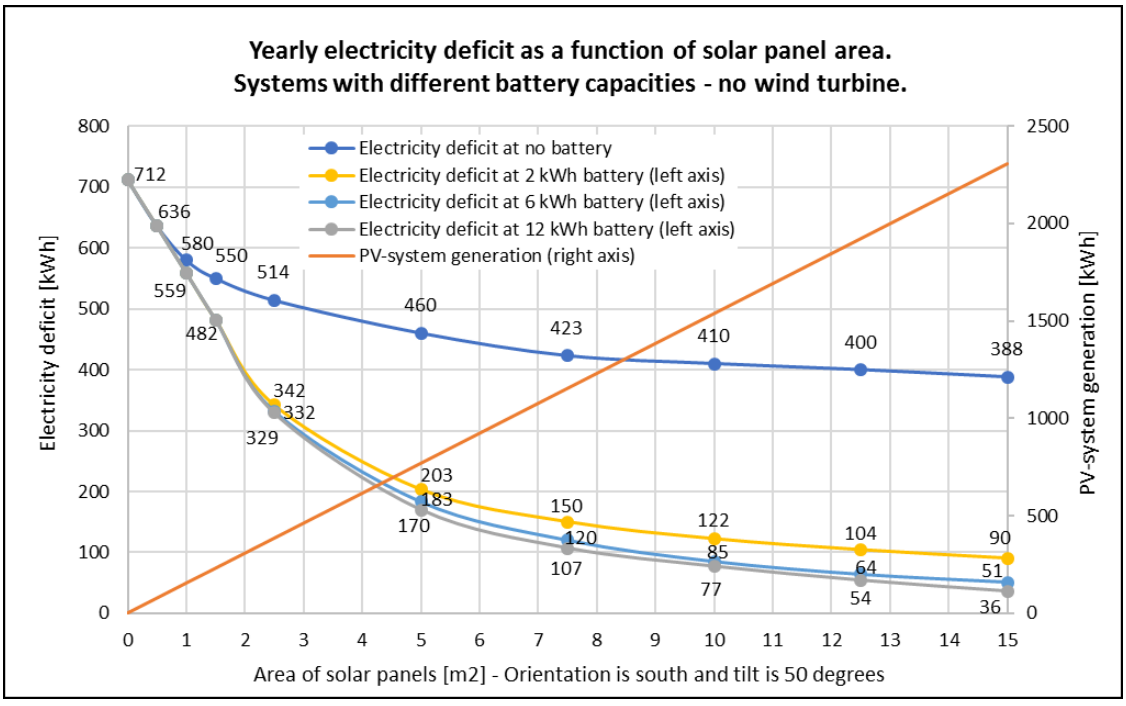

Graph 4 – Yearly electricity generation and electricity deficit as a function of solar panel area.

The graph illustrates, that the implementation of a battery capacity of just 2 kWh reduces the electricity deficit significantly. The reason for this is mainly, that the battery can cover the electricity demand during the nights in periods with excess photovoltaic electricity generation during the day. Increasing the battery capacity further still decreases the deficit, but the efficiency becomes relatively smaller.

The graph also shows that 5 m^2 of solar panels generate approximately 770 kWh of electricity, which is sufficient to cover the yearly demand if the battery capacity is large enough. The required capacity to cover the entire annual demand with a 5 m² PV system would be 182 kWh. Even with 20 m^2 of solar panels (yearly generation of 3072 kWh) a battery capacity of 28 kWh is needed to cover the entire annual electricity demand (this is not illustrated on Graph 3).

13.2.3 Evaluation of wind turbine electricity coverage at Ebeltoft – No PV-panels

The calculations of wind turbine generation presented in this chapter are made based on the stated power curve for a specific 1 kW turbine called 'Air Force 1' – the power curve is illustration in Figure 10.1. This turbine model was initially thought to be a good solution and used for the calculations, but after a later investigation of the efficiencies of small wind turbines, the stated power curve was found to be quite overestimated.
In Appendix R the real efficiencies of small wind turbines are discussed and the Air Force 1 is found to have a realistic generation of around 50 % of the stated power curve. This means, that in order to get the simulated generation presented in this chapter it is actually necessary to install two Air Force 1 turbines – or another turbine with around twice the output. As this increases the cost of the wind system significantly, the Air Force 1 might not be a good choice. However, due to Danish legislation and the market range and price of reliable small wind turbines, the options are very limited - the possibilities are discussed in the last section of this chapter.

- This does not mean, that the simulations are wrong, but that the specific Air Force 1 turbine cannot deliver the simulated generation. In reality a larger (or more) wind turbines are needed, which has been taken into account in the later discussions of the price of the system.

Graph 5 shows the electricity deficit (uncovered part of the 712 kWh yearly electricity demand) as a function of a wind turbine factor. The wind turbine factor expresses the yearly electricity generation relative to a 1 kW (24 V) Air Force 1 wind turbine at 10 m height, that generates 1287 kWh a year. Thus, a factor of 1.6 means, that the yearly production is 2061 kWh - 60 % higher than 1287 kWh. In practice, a higher factor could represent both a higher wind turbine, a wind turbine with a larger rotor area or a location with better wind conditions. The relation is illustrated for three different battery capacities of respectively 0, 2 and 6 kWh.

The graph shows, that the combination of the wind turbine and a battery capacity of 6 kWh can reduce the electricity deficit to almost nothing or entirely depending on the wind turbine factor. The 1 kW Air force 1 wind turbine at 10-meter tower height (corresponding to a factor of 1 on the graph) is thought to be suitable/practical for this particular system. At this generation of 1287 kWh per year, a 14.5 kWh battery would be needed to eliminate the electricity deficit (this is not illustrated on Graph 4)

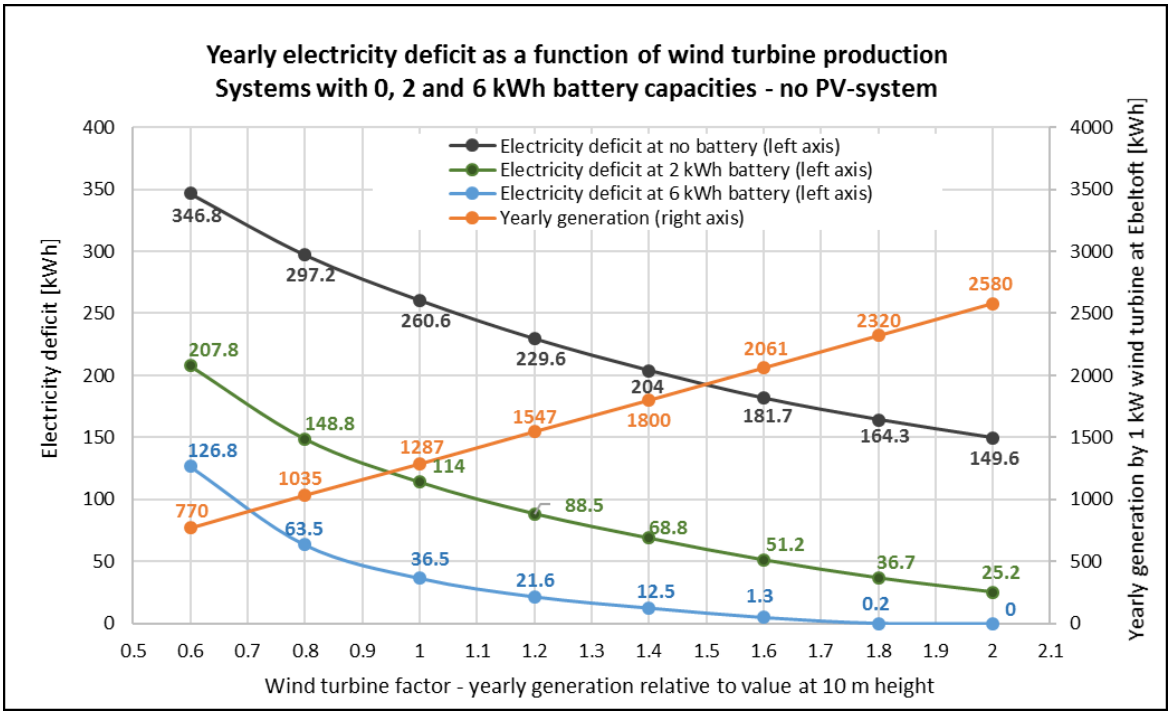

Graph 5 – Yearly electricity generation and electricity deficit as a function of wind turbine factor (relative to 1 kW Air Force 1 at 10 m).

In practice, the wind turbine generation can be increased/decreased either by changing the height of the tower, choosing a model with a different rotor area or changing the location. With the wind conditions at Ebeltoft, the wind turbine factor on Graph 5 from 0.6 – 2 corresponds to the 1 kW Air Force 1 wind turbine at heights from 4.4-33 meter. When using a height of 10 meter and changing the wind data from Karup (lowest mean wind zone in the DRY weather data) to Thyborøn (highest mean wind) the yearly electricity generation changes from 823 to 2628 kWh.

13.2.4 Evaluation of system with wind turbine and solar panels at Ebeltoft – no battery

Based on the evaluation of a photovoltaic system and wind turbine in the previous sections, a system with a combination of the two is evaluated in this section. The chosen system has $5\ m^2$ PV-modules (15 % efficiency) facing directly south with a tilt angle of $50°$ and 1 kW Air Force 1 wind turbine (model 24 V with 3.0 m/s cut-in speed) on a 10-meter-high tower. The simulation is made with wind conditions as calculated for location near Ebeltoft and wind turbine power curve stated by the manufacturer. For a system **without** an installed battery, the annual values are:

- Electricity generation – Wind: 1287 kWh, Solar: 768 kWh
- Electricity demand: 712 kWh
- Uncovered demand (deficit): 166 kWh
- Excess/unused electricity – this will be utilized for DHW: 1508 kWh

These numbers show that the total amount of generated electricity is far beyond the demand, but the deficit is still 166 kWh due to periods with low or no generation. Graph 6 shows the electricity generation and consumption from the 13/1 to the 13/2. The graph shows, that there are some hours with none or very little

production, but also hours with a significant excess of electricity – especially from the wind turbine. The most critical period during the year (seven days with almost no generation) is marked on the graph.

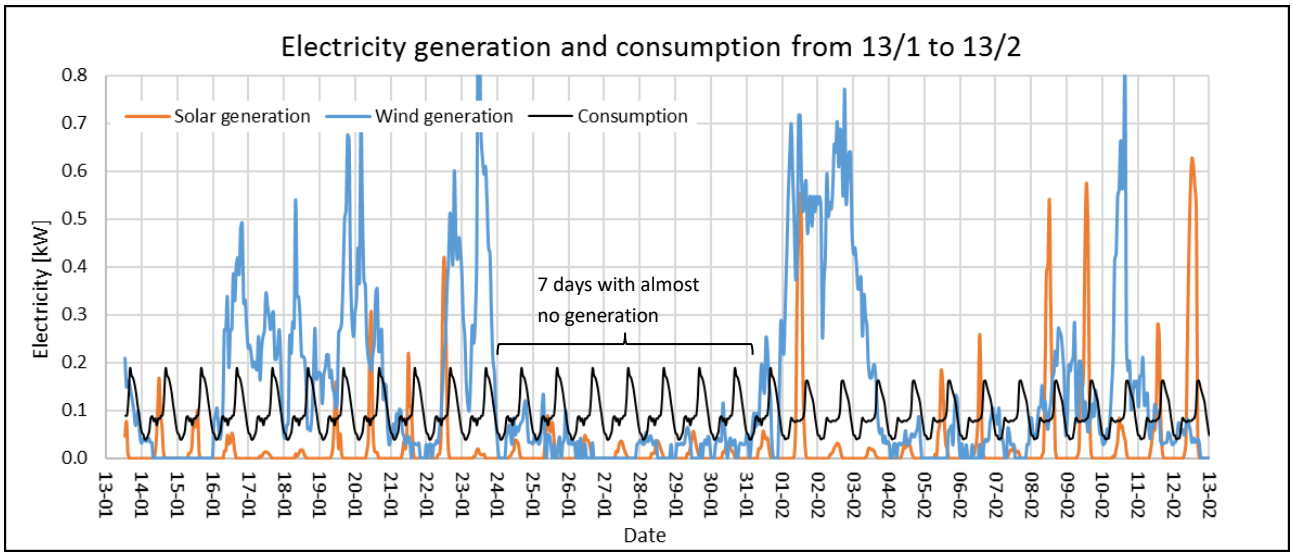

Graph 6 – Electricity generation and consumption for the period 13/1-13/2 with combined PV-panels and wind turbine system. For the period the wind generation is 103 kWh, the solar generation is 20 kWh, the demand is 68 kWh and the uncovered demand is 25 kWh.

Graph 8 shows the electricity balance (generation minus consumption) for the same period. The areas below the red line (0) are electricity deficits, while areas above the red line are excess electricity.

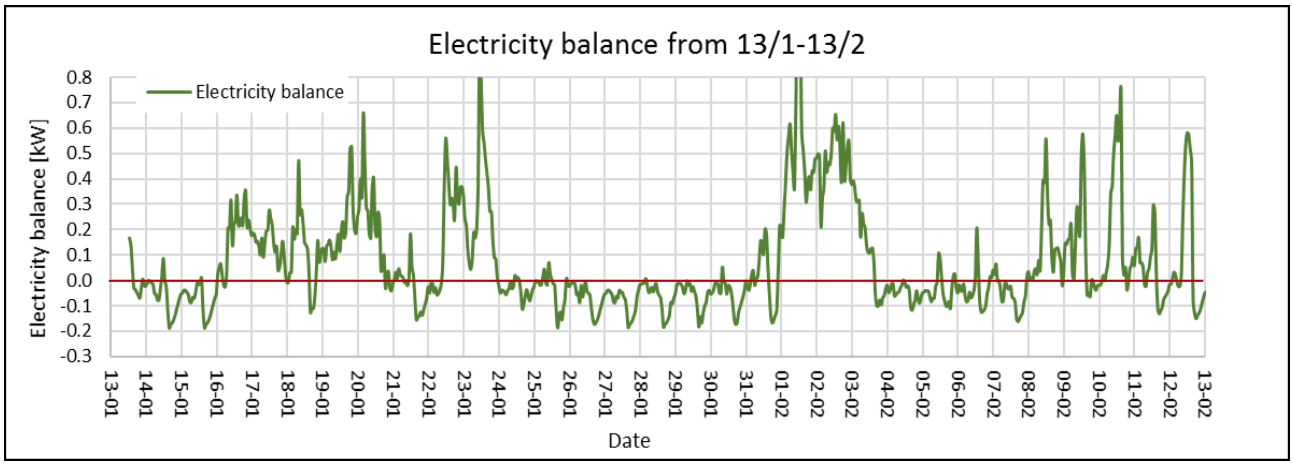

Graph 7 - Electricity balance (hourly generation minus consumption) for the period 13/1-13/2

The summed numbers for the period (13/1-13/2) are:

- Electricity generation – Wind: 102.7 kWh, Solar: 19.8 kWh.
- Electricity demand: 68 kWh.
- Uncovered demand (deficit): 25.1 kWh.
- Excess (unused) electricity: 79.4 kWh.

These numbers indicate, that even for this critical period the total amount of generated electricity is far beyond the demand, but it is distributed inefficiently.

The period from hour 560-730 (around 7 days), where the generation is less than the demand almost all the time, is the most critical period during the year. In some of these hours, a larger PV-system and/or a larger/higher wind turbine, could solve a part of the problem. In the hours with none or very little solar or wind power, a battery is needed to cover the demand – or some other method of electricity generation.

To show the influence of the solar panels in the summer, Graph 8 illustrates the electricity generation, consumption and balance in the period from 27/6-27/7. The electricity balance shows, that overall there is a large excess of electricity (146 kWh), but during nights with no wind, the demand cannot be instantaneously covered. Utilization of the excessive amount of excess electricity is discussed later in this chapter and in Appendix B .

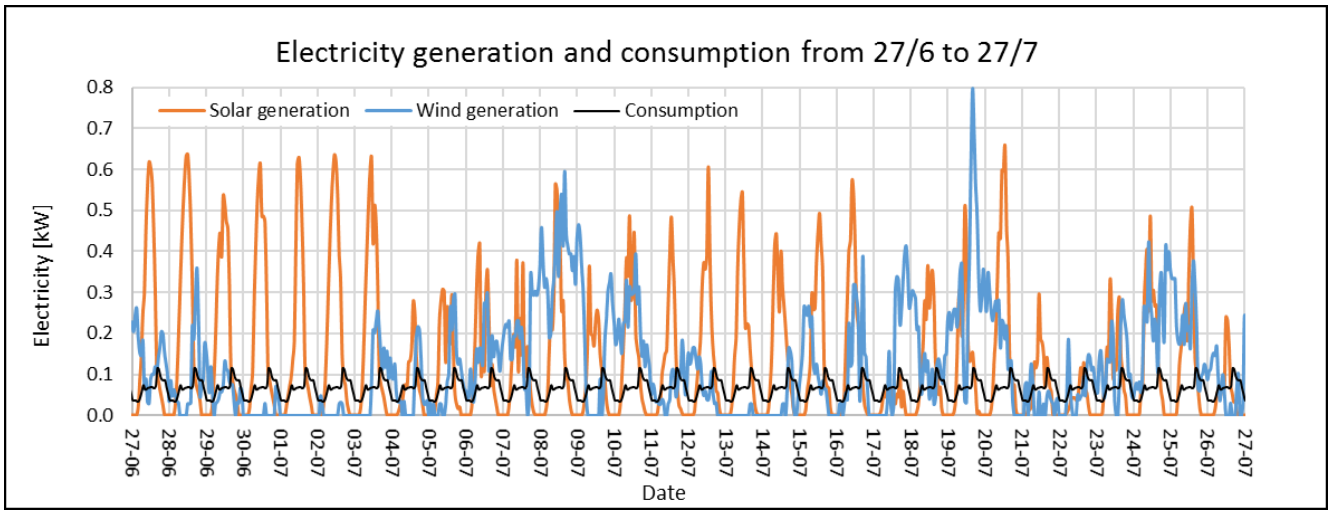

Graph 8 - Electricity generation and consumption for the period 27/6-27/7 with combined PV-panels and wind turbine system. For the period the wind generation is 91 kWh, the solar generation is 99 kWh, the demand is 50 kWh and the uncovered demand is 5.3 kWh.

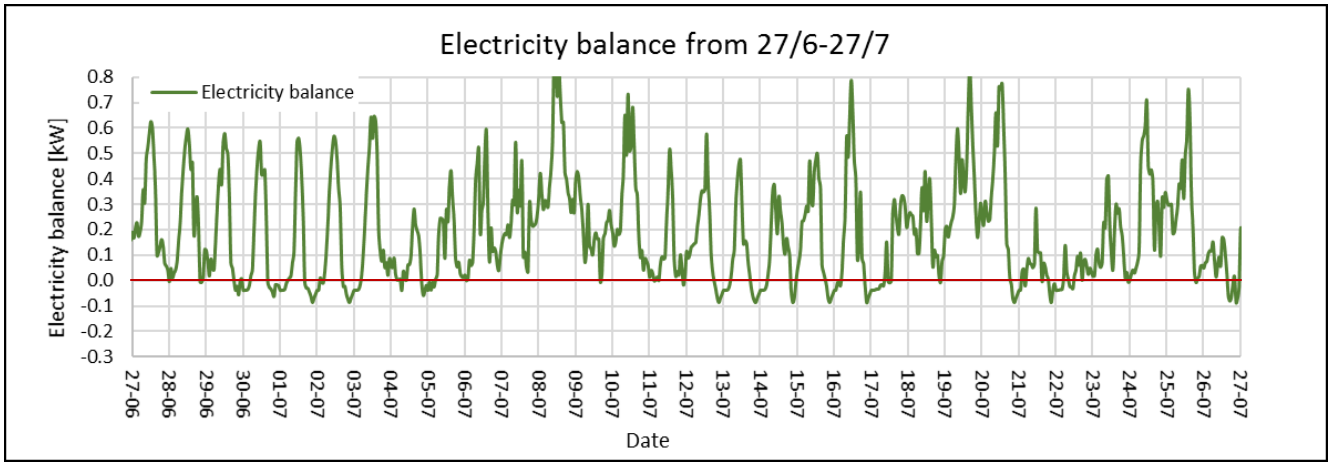

Graph 9 – Electricity balance (hourly generation minus consumption) for the period 27/6-27/7

13.2.5 Addition of battery bank to system

The evaluation of the combined system shows, that overall there is a high excess of electricity generation, but periods with insufficient coverage – especially in the winter, when the solar radiation is low. To utilize the generation more efficiently and eliminate the electricity deficit, a battery bank can be added to the system. Graph 10 illustrates the yearly electricity deficit for the system and the investment cost per year (i.e. investment divided by assumed lifespan) for the battery bank (based on GEL deep cycle batteries (Viva Energi - GEL, u.d.)) as a function of battery capacity.

The battery lifespan is very dependent on the number of discharge cycles and on the depth of the discharges. A larger battery capacity means, that most discharge cycles are less deep, which gives the batteries a longer lifespan. The lifespan for the different battery capacities on Graph 10 are estimated as described in Section 11.1 and will be discussed further later in this chapter for specific systems.

The graph shows that a battery capacity of 10 kWh is needed to eliminate the electricity deficit completely and that it is the first 0-2 kWh of added battery capacity, that makes far the largest difference. This means, that the elimination of the remaining deficit from around 25 to 0 kWh becomes relatively very expensive.

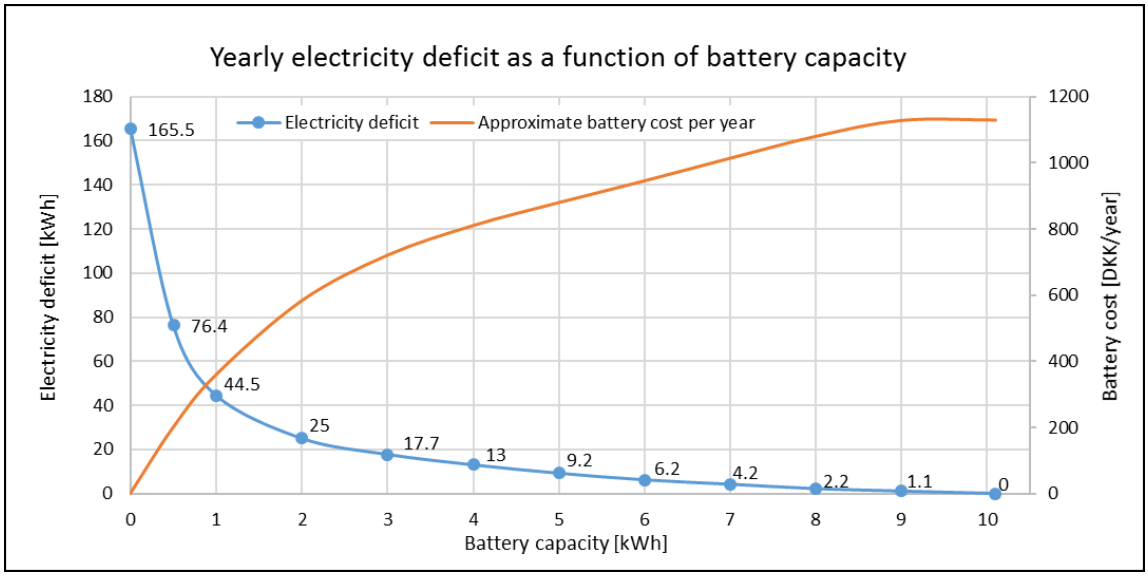

Graph 10 – Yearly electricity deficit for combined PV and wind turbine system as function of battery capacity

Graph 11 illustrates the periods with deficit electricity demand for the system with 2 kWh battery capacity. If the battery capacity is increased, the 'deficit spikes' on the graph is reduced with the same amount. This is illustrated by the orange line which indicates the 'neutral balance' for respectively 4 and 6 kWh battery capacity. If the battery capacity is increased 6 kWh, only two deficit periods of respectively 4.2 and 2 kWh remains.

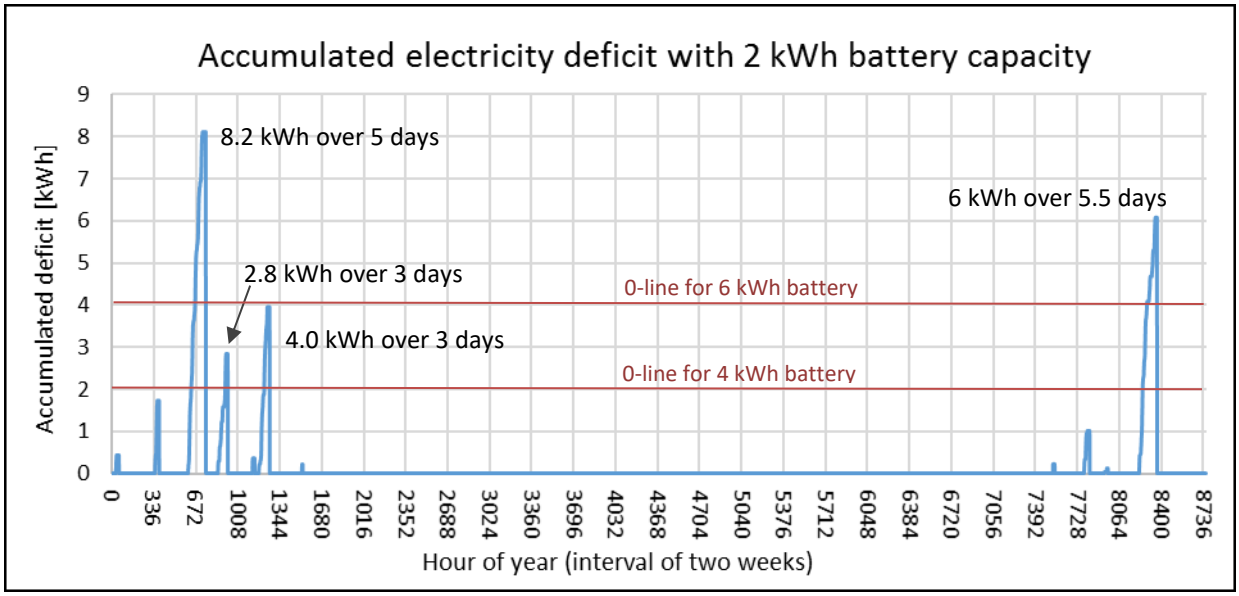

Graph 11 – Periods with accumulated electricity deficit for respectively 2, 4 and 6 kWh of battery capacity.

Graph 10 and Graph 11 shows, that if a few periods without electricity or some additional method to generate electricity (such as a small gasoline generator) is acceptable, the battery capacity can be reduced significantly compared to the 10.1 kWh required for complete annual electricity coverage.

13.2.6 System for Ebeltoft with full battery cover of 10.1 kWh

A lot of combinations can be made and the optimal solution depends on the location and the criteria for the system. In the following discussion, a requirement of 100 % electricity coverage is assumed and the battery capacity of 10 kWh, identified in the previous analysis, is applied. The yearly summed numbers for this system is:

- Electricity generation – Wind: 1287 kWh, Solar: 768 kWh
- Electricity demand: 713 kWh
- Uncovered demand (deficit): 0.0 kWh
- Excess (unused) electricity: 1342 kWh

These numbers show that there is a large electricity excess of 1342 kWh in the system. This excess electricity could be used to heat domestic hot water (DHW). The DHW demand is assumed to be identical in every month and in Section 3.4 the daily demand is estimated to be 3.15 kWh. Graph 11 illustrates the amount of daily excess electricity and the DHW demand. It is seen, that there is a high potential for using the excess electricity to cover the DHW demand. The graph is based on instantaneous cover, thus in Graph 8 no storage of the DHW is possible.

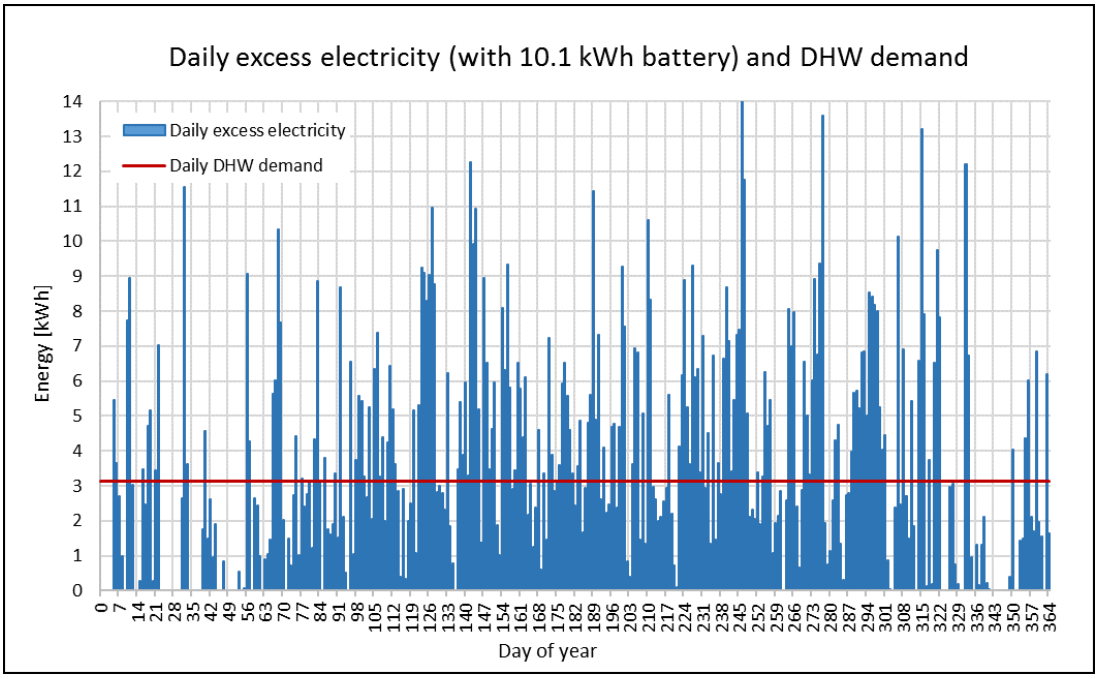

Graph 12 – Daily excess electricity and DHW demand for system with 10 kWh battery capacity.

In Appendix A , a number of simulations are presented where electricity generation is used to heat DHW with a submersion heater, when the battery is fully charged. Systems with different sizes of DHW accumulation tanks are investigated in the appendix, and a 200 Liter tank with a maximum temperature of 90 °C (corresponding to an energy storage of approximately 16 kWh) is found to be sufficient to give a good DWH coverage. The tank is assumed to have a heat loss of 0.74 W/K (100 mm insulation). Graph 13 shows the remaining DHW deficit each day of the year, when the excess electricity is utilized to cover the domestic hot water demand through the tank.

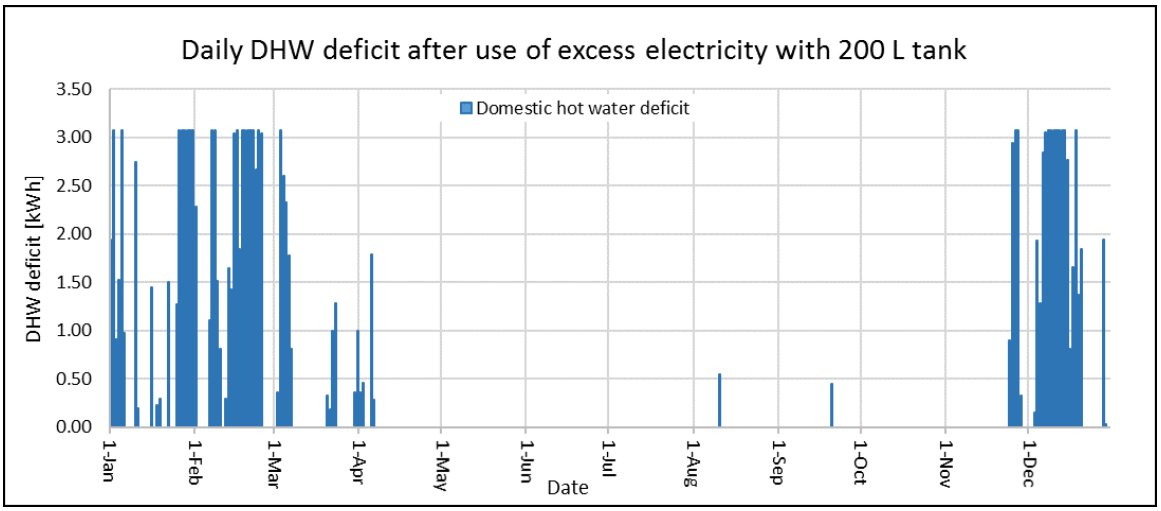

Graph 13 – Daily DHW deficit after use of excess electricity. System with 10.1 kWh battery.

From early April and until late November, most of the DHW demand can be covered by the excess electricity. In addition, there are periods in the winter, where the excess electricity covers all or most of the DHW demand. The yearly DHW demand including loss from the accumulation tank is 1344 kWh and the deficit is only

158 kWh, when the excess electricity is utilized. This means, that only 155 kWh of electricity from the entire 1342 kWh yearly electricity excess is not utilized. In total, 92.5% of the annual electricity generation is utilized for electricity and DHW demands.

In the evaluation of the DHW tank volume, the space heating demand was considered, as the DHW demand that cannot be covered by excess electricity, must be covered by the mass oven. According to Section 3.3.1 the off-grid house has the following space heating demand (a total of 2195 kWh):

Month	Jan.	Feb.	Mar.	Apr.		Nov.	Dec.
Space heating demand [kWh]	516	429	308	116		338	488

Table 13.2 – Space heating demand for Off-grid house

Thus, the system should seek to cover the DHW demand from May through October by other means than the mass oven - as is done with excess electricity in this system suggestion - in order to eliminate any need for using the mass oven when there is no space heating demand. As illustrated by Graph 13, the system with a 200 liter DHW tank shows a distribution of remaining DHW deficit, that fits well with the space heating demand.

When the system is designed with an accumulation tank with a maximum temperature of 95 ℃, the system must have a temperature controlled mixing, so the DHW can be supplied at around 55 ℃, when the tank temperature is high. If the tank should be able to supply 55 ℃ DHW when the total energy content is low and still be able to utilize the entire volume for storage of water at high temperature in other periods, it could be necessary with a submersion heater both at the top and bottom of the tank. This is not investigated further in this report. Graph in Appendix A shows the mean temperature in the tank over the year.

13.2.7 Analysis of battery lifetime cost

A battery bank of 10 kWh GEL deep cycle batteries has an investment cost of approximately 14-16,000 DKK (Viva Energi - GEL), which is a significant part of the total system cost. The lifetime of the batteries depends strongly on the number of discharge cycles, the depth of the discharges and the battery operation temperature.

The optimal operation temperature for a battery is 20-25 ℃ and a rule of thumb is that the lifespan of the batteries decreases with 3-4 years for every 10 ℃ increase in temperature (Viva energy - Batteries). This means, that it is very important to place the batteries in a way, so that they are ventilated and do not heat up during usage.

Graph 14 illustrates the number of deep cycles before the battery is worn out as a function of the depth of discharge. The numbers from 30-100 % discharge is stated at (Viva Energi - GEL), but for the interval 0-30 % an extrapolation is assumed. Based on different sources such as (Civic solar), the actual tendency seems to be, that the gradient increases further from 30 % towards 0 %, which means that the extrapolation is conservative with regard to the number of cycles.

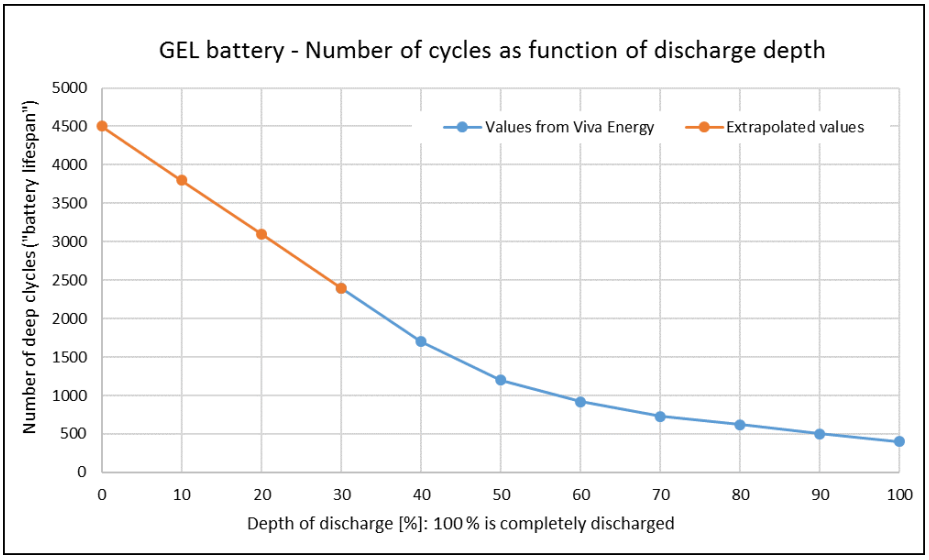

Graph 14 – Number of deep cycles ("battery life") as function of depth of discharge for GEL deep cycle battery (Viva Energi - GEL)

By estimating the number of deep cycles and their depth during the year, the battery lifetime can be estimated. For PV-systems it can be assumed, that there is one deep cycle each day (charging during the day and discharging during the night), but with a wind turbine, the balance can fluctuate significantly. Graph 14 shows, that the battery lifetime is strongly dependent on the depth of the discharges.

In practice, there will be a variation of different discharge depth. Sometimes the battery will be discharged almost completely and other times, it will only be discharged a few percentage. Graph 15 shows the daily minimum battery charge level in percentage of the full battery capacity. Most of the discharge cycles use less than 20% of the capacity and the average daily minimum charge level is 91 %.

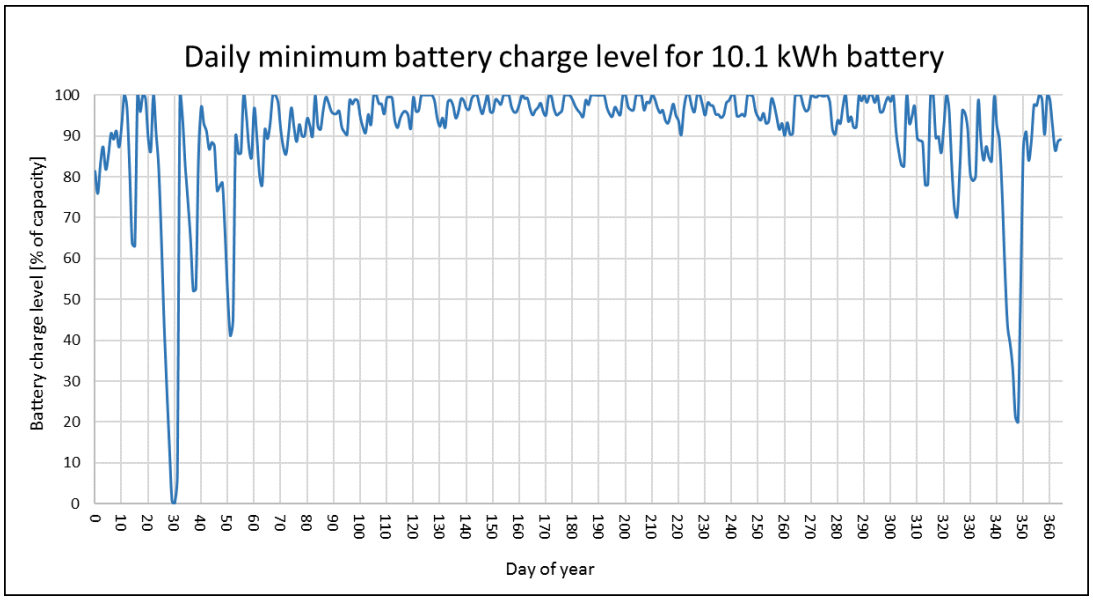

Graph 15 – Daily minimum battery charge level (discharge depth) during the year.

The lifespan of the battery can be roughly estimated by taking the depth of each discharge cycle and weight it according to the relative "lifespan impact" at that discharge depth, as indicated by Graph 14.

When making this evaluation over the year, the 10.1 kWh battery bank is estimated to be worn out after approximately 11.5 years. The investment price for 10.1 kWh batteries is approximately 15,000 DKK, which gives a yearly cost of 1300 DKK for the battery bank.

13.2.8 System with low battery capacity and generator

Graph 15 (above) shows, that with 10.1 kWh of battery capacity, only around 10 % of the capacity is used in average and only for five periods during the year (a total of 404 hours), more than 30 % capacity is used.

Graph 10 and Graph 11 illustrated that if a few periods without electricity or some additional method to generate electricity (such as a small gasoline generator) is acceptable, the battery capacity can be reduced significantly compared to the 10.1 kWh for full annual electricity coverage. At respectively 2, 4 and 6 kWh battery the total electricity deficits were only 25, 13 and 6.2 kWh.

Graph 16 shows the daily minimum battery charge level in percentage of the full battery capacity for a 2 kWh battery bank. The average daily minimum charge level is 68 %, but there is 114 days with discharges below 50 % capacity, indicating much higher use of the battery compared to the previous battery of 10.1 kWh.

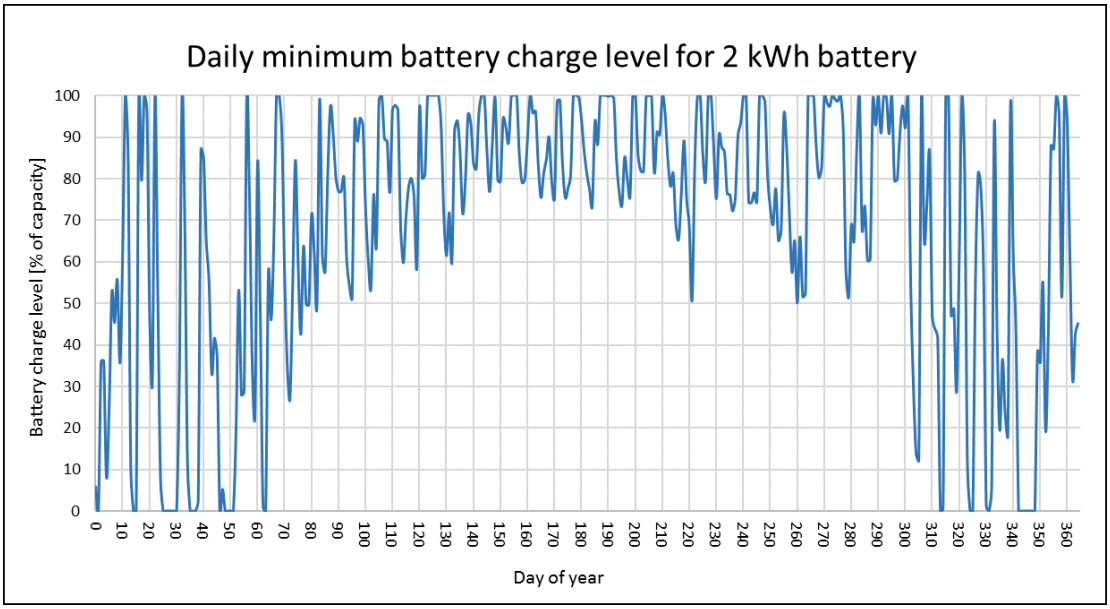

Graph 16 - Daily minimum battery charge level (discharge depth) during the year.

For an annual lifespan evaluation, the 2 kWh battery bank is estimated to be worn out after around 4 years. The investment price for 2 kWh batteries is around 4,000 DKK, resulting in a yearly cost of 1000 DKK for the battery bank (compared to the 1300 DKK/year for the 10.1 kWh battery).

A 1.5 kW gasoline generator can be bought for 1,500 DKK and has a fuel cost of around 5-6 DKK/kWh electricity (Powergenerator, u.d.). This could be a cheap alternative to a part of the battery capacity.

At 2 kWh battery capacity, with a yearly electricity deficit of 25 kWh distributed over approximately 16 days, the fuel cost with a generator is around 140 DKK/year. If the generator is assumed to have a lifespan of 10 years, the cost of 2 kWh battery bank and generator plus fuel is 1290 DKK/year. This solution is not noteworthy cheaper than the solution with a battery bank of 10.1 kWh.

An unknown factor that can affect the system performance is, how much capacity the batteries loose during their lifespan. This could give higher electricity deficits at the later year of the battery banks lifetime. This uncertainty is not investigated in this report, but it could be countered by installing additional battery capacity (over-capacity in the beginning).

As described, the simulations are made based on the weather conditions from the Design Reference Year 2001-2010 (described in Sections 8.1 and 9.1), which is a mean year. In reality, the weather is never the same, and some years can have periods, where the evaluated combination of PV-panels, wind turbine and battery cannot cover the demand – even though the seven-days period contained in the DRY-data with almost no generation is thought to be a rare case. Further, the PV-system or wind turbine could fail and be out of operation for a period. So, if complete security for 100 % coverage of the electricity demand is wanted, a back-up generator or similar should be installed.

13.2.9 Discussion of alternative Off-grid systems and systems at other locations

The energy system designed in this chapter is based on simulations with the weather data estimated for the location near Ebeltoft (based on the Design Reference Year 2001-2010 dataset (DRY-10)). If an off-grid house is placed in another location, the weather conditions can be different.

The solar radiation in Denmark only varies a little (plus/minus around 4 % as described in Section 8.1). The highest yearly radiation for an area in the DRY-10 is only 6 % higher than the lowest – except for Bornholm, where it is 9 % higher. Off course, there could be objects casting shadows on the solar panels, which could reduce the generation. The wind conditions on the other hand, can be very different in Denmark. In the DRY-10 the general wind conditions (due to the roughness of the terrain) measured in a relatively open area varies from a mean wind speed of 4 m/s in inland Jutland (measured at Karup) to 6.5 m/s at the west coast (measured at Thyborøn). When the wind is evaluated hourly over the year, the yearly energy in the wind is around four times higher at the area with high wind speeds (as the energy is dependent on the third power of the wind speed).

For a 1 kW wind turbine with a power curve corresponding to the one stated for the Air Force 1 (Figure 10.1) with a 10-meter tower, the yearly electricity generation with the estimated wind at Ebeltoft is 1287 kWh. If the DRY-10 wind data for Thyborøn is used, the generation is calculated to 2628 kWh and for Karup the generation is 828 kWh. In addition, there can be local obstacles, which can reduce the wind speed significantly. If the off-grid house was located at Thyborøn with the same wind turbine, the battery capacity could be reduced from 10.1 to 5.6 kWh or the PV-system could be removed entirely, while keeping the battery capacity at 9.9 kWh.

If the off-grid house was placed at Karup, the wind turbine power must be approximately 1.5 higher than at Ebeltoft at the same wind speed, to generate the same amount of power. This can be achieved with a larger rotor area (approximately 1.5 times larger). Alternatively, the height of the wind turbine can be increased to around 20 meter, which would create wind conditions corresponding to Ebeltoft. Other solutions are to keep the same wind turbine, but increase the battery capacity to from 10.1 to 15.1 kWh or the solar panel area from 5 to 16 m^2.

If the house is located in a place with very bad wind conditions, the electricity demand could be covered by a larger area of solar panels and a generator alone (as illustrated by Graph 4). With a 10-kWh battery and 15 m^2 solar panels (no wind turbine), the generator must cover a deficit of 42 kWh and with 20 m^2 solar panels, the deficit is 25 kWh. In addition, there is still at good DHW coverage outside the heating season. As discussed in the last section of this chapter, small reliable wind turbines are quite expensive (40-50,000 DKK) and the options are limited.
This means, that a system with more solar panels and a limited use of the generator as described above could be 25-35,000 DKK cheaper, than a system with a wind turbine. If no generator is allowed, it would require around 30 m^2 solar panels and 14.6 kWh of battery to have full electricity coverage. Depending on the wind conditions, this could both be cheaper or more expensive than a system with a wind turbine – at Ebeltoft it is approximately the same price.

Another very important parameter is the electricity demand of the off-grid house. The discussion above is based on the yearly demand of 712 kWh that is estimated in SECTION. This demand is quite low, and based on the vision of low-energy-living in *Project Grobund*. If the demand is increased to twice the amount (1424 kWh) a system with 30 m^2 solar panels, a 1 kW wind turbine and 18.3 kWh of battery capacity is needed to have full electricity coverage.
A system with only solar panels becomes unrealistic if a generator is not allowed. With 30 m^2 solar panels, it would require 94 kWh of battery (around 250,000 DKK over 20 year) to cover the demand during the winter and even with 70 m^2 solar panels (unrealistic area) 26.2 kWh of battery capacity is still needed.
If a generator is allowed one solution could be a system with 30 m^2 solar panels, a low battery capacity of 2-10 kWh and a generator to supply 115-305 kWh electricity per year depending on the battery size. A system like this can be up to 55,000 DKK cheaper than the combined system, but is dependent on the generator.

Overall it must be said, that the best solution for an off-grid system in Denmark based on sun and wind energy, depends completely on the requirements for the system and the wind conditions at the location. If the price is an important factor and a limited generator use is acceptable, a wind turbine might not be a good solution – unless it is a do-it-yourself turbine build from scratch. If sustainable energy generation is the critical parameter, the combination of solar, wind and battery is a good solution.

13.2.10 Summary of market analysis for 1-2 kW wind turbines in Denmark

As described in Appendix H all wind turbines in Denmark with a rotor area above $5\ m^2$ must be type-certified (including specific tower and foundation) according to the Danish *Announcement 73 73* (Energistyrelsen - Cert.). In addition, all wind turbines most have documentation of noise measurements during operation, as they must conform to the law.
After a review of the market for wind turbines below this limit – and the experiences with them – it is clear, that most turbines of this size show poor performance and durability. When it comes to reliable turbines with reasonable performance only a few products could be found. One is the Excel 1kW wind turbine made by the American company Bergey Wind Power with a price in Europe of around 39-43.000 DKK without tower (renugen)**.** Another possibility could be the Kestrel e230i 0.8 kW. It is relatively cheap in USA (14,000 DKK), but the price in Europe is not known. Some data for the mentioned turbines can be found in Appendix S .

A possibility could also be a small certified wind turbine with an area above $5\ m^2$. However, the list at the Danish Energy Agency shows, that only two wind turbines below 5 kW is certified (as of 06-01-2017). These are the Kestrel e300i 1kW and the Windspot 3.5kW. However, none of them seems to be available on the market anymore and both certificates expire in 2017 (Kestrel in January and Windspot in May).
Turbines such as the Windspot 1.5 kW are certified in other European countries according to the international standards, but they still need the special Danish certification. It could be a solution to design a system with tower and foundation for one of the turbines and get it certified, but according to (DTUwind, 2017), a type-certification costs at least 50,000 DKK. If a larger number of turbines are needed, this could be a possibility. Some data for these turbines can be found in Appendix S .

The last possibility is to make a do-it-yourself wind turbine. The legal requirements are the same as stated above, so with a rotor area below $5\ m^2$ only the demand for noise documentation applies. At Scoraig Wind Wind (Piggott), information, books and workshops about how to build wind turbines from scratch can be found. It is a well-tested design and according to (Woods-Bryan & Bryan) a wind turbine with a rotor area of 11 m^2 (corresponding to rated power of 2-2.5 kW) can be built for around 10,000 DKK including tower, when you make everything yourself (carve the blades, make the coils in the generator, etc.). They show quite good productions and have an estimated lifespan of 20-25 years.

The conclusion for small wind turbines in the context of off-grid systems in Denmark must be that the possibilities are limited. One could by a very expensive turbine such as the Bergey Excel 1 or take a chance with one or two cheaper turbines such as the Air Force 1 or Kestrel e230i. However, the cheaper turbines are probably worn out relatively fast, which could make the long-term cost significantly higher. The last possibility is to build a small wind turbine from scratch, but this is surely not a solution for everyone.

13.3 Validation of Off-grid Simulation Tool

To validate the calculation method in the *Off-grid Simulation Tool* the commercial analysis tool Homer Pro (Homer Energy) has been used. Homer Pro is globally recognized and validated through multiple studies, including several of the studies discussed in the literature review in this report. The simulation in Homer validates the hourly performance of the photovoltaic and wind turbine systems along with the hourly balance between generation, storage and user load.

In Homer, the system proposed for *Project Grobund* has been modeled and the DRY weather data has been applied. The annual results of Homer compared to the results of the *Off-grid Simulation Tool* is shown in Table 13.3.

	PV Performance kWh/yr	**WT Performance** kWh/yr	**Excess Electricity** kWh/yr	**Average State of Battery** %
Off-grid Simulation Tool	768,0	1287,4	1341,6	94,7
HomerPro Microgrid Analysis Tool	776,8	1309,2	1345,7	95,1
Deviation [%]	1,1	1,7	0,3	0,4

Table 13.3 – Annual performance for Off-grid Simulation Tool and Homer Pro

The annual results are very identical; however Homer calculates a slightly higher performance for both the PV and WT systems. Figure 13.1illustrates the charge-state in percentage of full capacity for the battery during the entire year, as simulated by respectively the *Off-grid Simulation Tool* and Homer Pro.

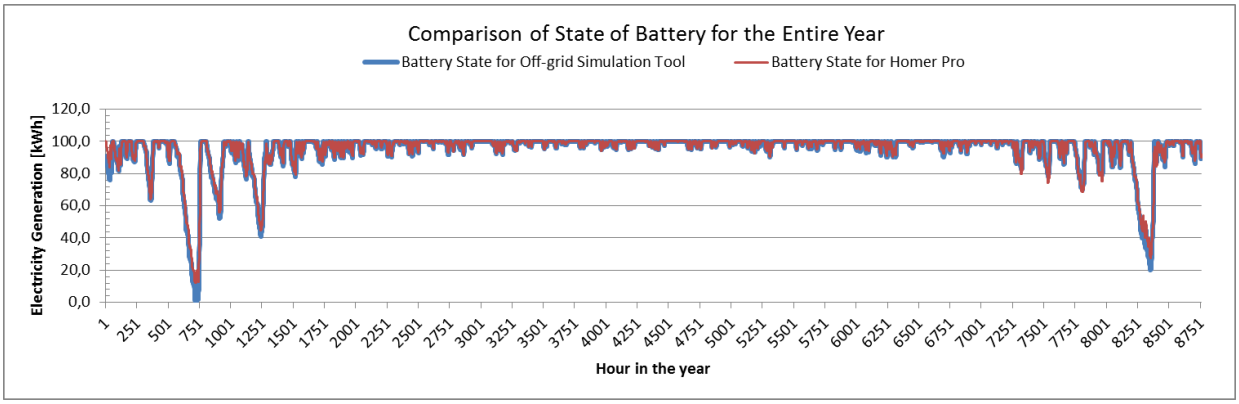

Figure 13.1 – Comparison of state of the battery for the entire year

The development of the state of the battery is very identical as well. Slight differences can be found during the critical periods, where the *Off-grid Simulation Tool* calculates lower state of discharge than Homer. As the results are very identical, the calculation methods implemented in the Off-grid Simulation Tool are validated, and the results can be assumed to be correct. The tool is a bit conservative compared to Homer Pro, which is thought to be preferable compared to an overestimation

Further comparison can be found in Appendix Q .

13.4 Calculation of System Specific Cost of Electricity

The cost of electricity for the designed system can be seen in Table 13.4.

Component	Total Investment Cost [DKK]	Operational Cost [DKK/kWh]	Maintenance Cost [DKK]	Total Annual Electricity Generation [kWh]	Cost of Electricity Over 20 Years [DKK/kWh]	Usable Annual Electricity Generation [kWh]	Effective Cost of Electricity [DKK/kWh]
Photovoltaic [750 W]	11,224	0	0	767.0	0.7	356.4	1.6
Wind Turbine [1000 W]	50,000	0	500	1287.0	2.3	356.4	8.4
Controller System	3,630	0	0	0.0	0.0		
Batteries [24VDC 420A]	36,281	0	0	0.0	0.0		
Wires, fuses, diodes etc.	2,000	0	100	0.0	0.0		
Total System	**103,135**	**0.001**	**600**	**2,054**	**2.80**	**713**	**8.07**

Table 13.4 - Cost of electricity [DKK/kWh] for the specified system

The economic assumptions can be found in Appendix E.2. The most uncertain value is maintenance cost for the wind turbine, as this can vary greatly depending on the use of the system. The variation in the system's cost of electricity as a function of the maintenance cost of just the wind turbine can be seen in Figure 13.2.

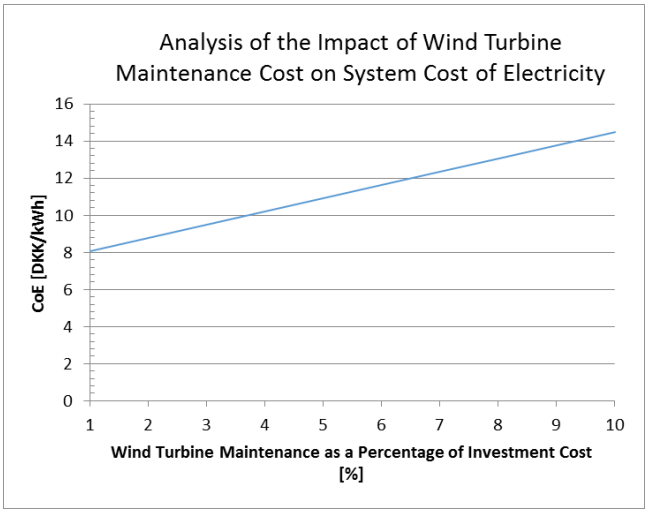

Figure 13.2 - The impact of wind turbine maintenance cost on total CoE

As can be seen from Figure 13.2 the CoE varies from 8.07 to 14.46 DKK/kWh depending on the maintenance cost as a percentage from 1-10 of the wind turbine investment cost. To calculate the CoE in Table 13.4, a percentage of 1.0% has been applied, this assumption is accounted for in Appendiks E.1.6.

The CoE of 8.07 DKK/kWh is 100% higher than the typical grid-connected electricity CoE price (Danish Energy Regulatory Authority). The main reason is the low annual electricity consumption compared to the high investment price. The system seen in Table 13.4 is capable of delivering significantly more electricity than the demand of 713 kWh.

14 Legislation in the Context off-grid Living in Denmark

Concerning off-grid living in Denmark, there is a lot of legislation which must be considered. This is both in the context of private energy production and with regard to connections to the energy and water grids. Further, the law regulates construction permission for buildings and what technical requirements the houses must fulfill. This chapter gives a brief overview over the most important legislation. Allotment gardens (danish: *kolonihave*) and summer houses are not considered, as they are not meant for year-round residence and special laws apply.

The current legislations and their impact on the project can be found in detail in Appendix H .

14.1 Summary of Legislation

If a house in Denmark should be off-grid and the owners will avoid charges for connections to public grids, a location without public heating supply - and without public water and sewage if this is important – must be found. Such locations are mostly found in rural areas with solitary buildings, where it is almost impossible for the municipal council to give a building permission. So, depending on the wanted off-grid-degree, the realistic possibilities is to find an existing house in a rural area and disconnect it from the electricity supply, or build a new house in connection to a small village, where there is no public heating grid.

14.1.1 Suitability of Location at Ebeltoft for Off-grid Living

Based on the above information about the obligations in the local area plan, the area is thought to be unsuitable for both off-grid living and for buildings with alternative designs and building materials. A new local area plan must be made, if the area should be usable for Project Grobund. Nothing specific could be found about household wind turbines in urban zones, but based on the general frame for the area, it is thought to be unrealistic, that the municipal council would allow it.

15 Master Thesis Discussion

15.1 Discussion of Results

The analysis performed throughout this report indicates, that the best solution for off-grid electricity generation for a small household in Denmark, is the combination of photovoltaic panels, a wind turbine and battery storage. This is in agreement with the findings of many similar studies, which are discussed this report. For small-scale operations, solar and wind power technologies are by far the most common applications. This means, that the technologies are improved continuously and the production cost is decreased.

The current house design suggested by *Project Grobund* has been analyzed in various calculation and simulation tools in order to identify the hourly, monthly and annual energy demands. The space heating demand was analyzed in BSim using a floor-heating system to demonstrate the operation of the house-integrated mass oven. This method increases the heating demand compared to a typical household system, as it is much more difficult to adjust the required heating demand since the mass oven only operates between 7 and 9 am. The annual heating production from the mass oven is 2180 kWh, corresponding to 34.1 kWh/m² per year. An alternative house design is suggested in this thesis, which can reduce the heating demand to 426 kWh or 6.9 kWh/m² per year.

The domestic hot water and electricity demand is based on several assumptions discussed throughout this report which are highly dependent on the behavior of the occupants. The daily hot water demand is estimated to 54 liters corresponding to an annual demand of 1344 kWh (21 kWh/m² per year), including losses. The electricity demand is based on assumptions regarding lighting, refrigeration and small electrical appliances, resulting in an annual demand of 713 kWh (11.1 kWh/m² per year). In total, the current house design uses 66 kWh/m² per year, or 39 kWh/m² per year with the alternative house design.

Simulation in the Danish Be10 tool, which is a part of the Danish Building Regulations, shows an annual energy demand of 48.3 kWh/m² per year; 30.5 for heating, 17.3 for hot water and the remaining 0.5 for a small circulation pump. These results are fairly identical to the values of BSim and the deviations are due to a series of fixed assumptions in Be10. This indicates that the heating demand of the house must be reduced in order to conform to current building regulations (approximately 30 kWh/m² per year).

Several off-grid electricity technologies have been analyzed in this report including thermoelectric generators, which have been thoroughly tested both under laboratory and real-life conditions. The laboratory tests showed a conversion rate (thermal to electrical power) of 3.92%. This corresponds to an output of 16.6 W, whereas the manufacturer states a conversion rate up to 6% and output of 21.7 W is possible under ideal conditions. In-field tests of a thermoelectric generator on a mass oven showed almost no output could be achieved by placing the module directly on the mass oven, mainly due to the low thermal conductivity of the mass oven materials and a maximum surface temperature of approximately 150°C. The testing of the thermoelectric generators was concluded, stating that the performance on the mass oven due to the construction principle was insufficient to appeal for further analysis.

Thermoelectric generators, methanol fuel cells, steam engines, biogas generators and stand-alone photovoltaic or stand-alone wind turbines technologies were found to be un-suitable for small-scale household application due to several factors including; unreliable/fluctuating performance, high maintenance or fuel cost,

required technical skills for operation and maintenance or immature/underdeveloped technology resulting in low efficiency and/or high investment costs.

The combination of photovoltaic panels and a wind turbine was found to be the best hybrid-solution, but results in an unreliable and fluctuating system, where the electricity generation depends entirely on the current weather conditions. This sporadic nature of the energy sources means, that the system requires a high storage capacity in order to ensure, that the electricity consumption can be covered in all periods. Especially winter periods with low solar radiation and low wind speed increases the necessity for a high battery capacity. In the applied weather data, Danish Design Reference Year, the longest period without significant solar or wind power is 7 days, as illustrated previously in the report.

The *Off-Grid Simulation Tool* developed during this thesis is a dynamic Excel-based tool which calculates an hourly balance of demand, generation and storage. The tool establishes an hourly distribution of the specified electricity and DHW demand. Weather data is used in order to calculate the hourly electricity generation of both a photovoltaic system and a wind turbine. The user is able to change angle, orientation and size of the PV system, and change the power curve and terrain roughness to adjust the performance of the wind turbine. Based on the demand and generation the tool identifies the electricity balance, be it direct use of generated electricity, storage of electricity generation in the battery or the hot water tank, or use of the stored energy.

The *Off-grid Simulation* Tool is applied for the houses in *Project Grobund.* The proposed system is a 1 kW and 10 meters high wind turbine, 5 m² of solar modules and a 10.1 kWh battery. This system is able to cover the annual electricity demand of 713 kWh under conditions similar to the applied weather data. The total annual electricity generation is 2055 kWh, resulting in an excess generation of 1342 kWh.

The proposed system has been modeled in a commercial analysis tool called Homer Pro in order to validate the calculation methods and results. The comparison showed very identical results with the highest annual deviation of 1.7% for the wind turbine performance. Therefore, the calculation process and results of the *Off-grid Simulation Tool* are found to be very realistic.

It is suggested to install a 200 L hot water tank with an immersion heater, thereby heating the domestic hot water with excess electricity. The design of a system is suggested in this report showing that 86% of the estimated domestic hot water demand can be covered by the use of excess electricity. Incorporating this can increase the utilization of generated electricity from 34.7 to 92.5%, resulting in an annual excess of 155 kWh out of the total generation of 2055 kWh.

The cost of electricity for the suggested system was estimated to be 8.07 DKK/kWh, which could be reduced to 7.06 DKK/kWh by incorporating a gasoline generator into the system, thus decreasing required battery capacity.

To achieve 100% annual coverage a battery of 10.1 kWh is required, but a battery capacity of merely 2 kWh would result in a low annual electricity deficit of 25 kWh. This deficit can be covered by a more reliable back-up technology, such as a generator running on gasoline or diesel fuels. Not only could this reduce the cost of electricity for the system by approximately 25% (due to lower battery investment cost), but also increase the security of electricity supply in the system.

As the weather can vary compared to the used data and the PV-system and wind turbine could be out of operation for periods due to repair or maintenance, the integration of a small back-up generator is thought to be a good solution in any case. While the use of fossil fuels is a non-renewable technology, the annual deficit of 25 kWh equals to approximately 14 liters of gasoline for a generator. The use of electrical batteries - and especially the break-down of these - have a negative impact on the environment. Whether the use of a small amount of fossil fuels is less sustainable than an increased use of batteries is debatable – this is not investigated in this report.

If the demand of either electricity or domestic hot water for the proposed houses should change, the *Off-Grid Simulation Tool* can be used in order to re-calculate the system component sizes. Should the user require an annual electricity demand of less than 300 kWh, a system with only a wind turbine and batteries (no photovoltaic panels) results in a lower cost, and is still able to cover the demand. For annual demands above 300 kWh it is recommended to combine solar and wind power and to increase the area of the photovoltaic instead of investing in a more powerful wind turbine.

As discussed in section 13.2.10, the combination of the comprehensive Danish legislation for wind turbines with a rotor area above $5\ m^2$ and the limited possibilities for quality small wind turbines on the market, makes a small wind turbine is an expensive solution. If wind turbines up to 10 m^2 rotor area were allowed without Danish type certification (for turbine, tower and foundation), more attractive models could be used, which could decrease the cost of electricity significantly. According to Steen Møller from *Project Grobund*, it is also a possibility to build small wind turbines from scratch as a part of the project. This could reduce the investment price and thus cost of electricity significantly.

15.2 Recommended Further Work

The following section contains multiple topics within the project, which can be further developed or improved. The topics are:

- Complete component dimensioning of the electrical system, revolving charge controller etc.
- Re-design of the house to decrease heating demand and improve indoor climate
    - Design ideas to improve these areas are suggested in Appendix C .
- Validation of wind performance method by wind velocity measurements and wind turbine performance tests
- Complete/alternative utilization of excess electricity generation in the system. This topic is discussed shortly in Appendix B
- Evaluation of fresh water supply through gathering and storage of rain water
- Evaluation of sewerage design including storage and fermentation of green house

16 Master Thesis Conclusion

The main components for the proposed system for the households in *Project Grobund* are illustrated in Figure 16.1.

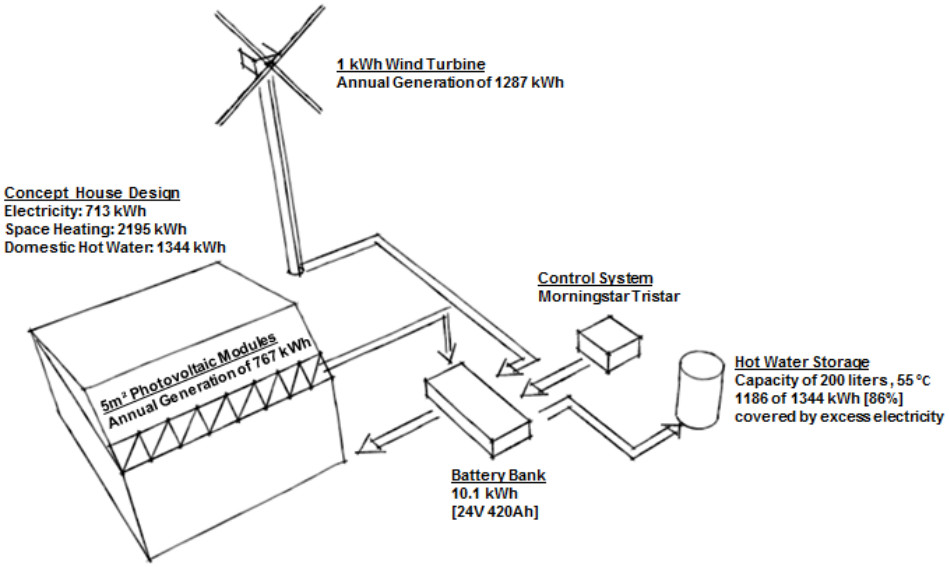

Figure 16.1 – Main Components of the Proposed System

This thesis set out to identify an off-grid energy system for a series of households intended to be constructed near Ebeltoft, Djursland, as a part of a newly started project named *Project Grobund.* Introductory simulations based upon a series of assumptions regarding construction, design and user behavior lead to the following annual energy demands:

- Electricity: 713 kWh
- Space Heating: 2195 kWh
- Domestic Hot Water: 1344 kWh

Based on the specified requirements to the energy system, the optimal energy system, which is able to cover the entire energy demand, is:

- Space Heating
  - A house-integrated mass oven, which was assumed an essential part of the houses, therefore no other space heating solutions was considered
- Electricity
  - 5 m² photovoltaic modules combined with a 1 kW wind turbine (power curve corresponding to Figure 10.1) and a 10.1 kWh battery capacity (total electricity generation of 2055 kWh)
- Domestic Hot Water
  - Summer period (April to November)
    - Covered by excess electricity generation: 769 kWh
  - Winter period (November to April)
    - Covered by excess electricity (387 kWh) and mass oven (188 kWh)

The above system leads to an annual utilization of generated electricity of 92.5%. The dimensioning of the system was conducted in an Excel-based simulation tool developed during the thesis, which can be used in future work to design off-grid systems with a combination of wind turbine, photovoltaic panels, battery storage and domestic hot water production from excess electricity. The tool is based entirely on the user defined electricity demand, the geographic location and the house specific information.

The cost of electricity for the system over a 20-year period is 8.07 DK/kWh. For a grid-connected electricity system the cost of electricity over a 20-year period is 3.25 DKK/kWh including connection fees, which is approximately 60% lower than the proposed system.

Additionally, it was found that the cost of electricity for the system could be reduced by approximately 25% by using a gasoline generator in periods with low solar and wind power, thus reducing the required battery capacity, which decreases the investment cost significantly.

17 References

ADoEC, 2009. *ADEC Guidance re AERMET Geometric Means,* s.l.: Alaska Department of Environmental Conservation.

Adroja, N., Mehta, S. & Shah, P., 2015. Review of thermoelectricity to improve energy quality. *International Journal of Emerging Technologies and Innovative Research* .

Aggerholm, S. & Grau, K., 2016. *SBI-ANVISNING 213 - BYGNINGERS ENERGIBEHOV,* s.l.: s.n.

Ampair, u.d. [Online]
Available at: http://marinewarehouse.net/images/ampair/Ampair%20Catalogue%20Web%20(2010).pdf
[Senest hentet eller vist den 12 2016].

Bechmann, A. et al., 2015. *Shelter models and observations,* s.l.: s.n.

Beckers, R., u.d. [Online]
Available at: http://www.solacity.com/small-wind-turbine-truth/
[Senest hentet eller vist den 1 2017].

Bianchini, A. et al., 2014. *Optimization of a PV-wind-diesel hybrid system for a remote stand-alone application.* s.l., Department of Industrial Engineering.

Bolius - Well, u.d. [Online]
Available at: https://www.bolius.dk/private-vandboringer-19247/

Building Agency, u.d. [Online]
Available at: http://bygningsreglementet.dk/br15_01/0/42

Bullis, K., u.d. *MIT Technology Review.* [Online]
Available at: https://www.technologyreview.com/s/518516/an-inexpensive-fuel-cell-generator/
[Senest hentet eller vist den 12 2016].

Chong, L. W. et al., 2016. Hybrid energy storage systems and control strategies for stand-alone renewable energy power systems. *Renewable and Sustainable Energy Reviews,* Årgang 66, pp. 174-189.

Civic solar, u.d. [Online]
Available at: https://www.civicsolar.com/support/installer/questions/which-one-has-higher-life-cycle-gel-or-agm-batteries
[Senest hentet eller vist den 12 2016].

Close-up engineering, u.d. [Online]
Available at: http://energy.closeupengineering.it/en/lighting-up-thanks-to-the-body-heat-the-peltier-tiles/5238/
[Senest hentet eller vist den 12 2016].

Danish Energy Regulatory Authority, u.d. *elpris.dk.* [Online]
Available at: www.elpris.dk
[Senest hentet eller vist den 2 October 2016].

DB-VVS, u.d. [Online]
Available at: http://www.dbvvs.dk/shop/med-isolering-19c1.html
[Senest hentet eller vist den 1 2017].

DMI - Mean temp., u.d. [Online]
Available at: https://www.dmi.dk/klima/klimaet-frem-til-i-dag/danmark/temperatur/
[Senest hentet eller vist den 1 2017].

DMI. DRY-data., u.d. *Danish Meteorological Institute.* [Online]
Available at: http://www.dmi.dk/fileadmin/user_upload/Rapporter/TR/2013/TR13-19.pdf

Dragsted, J. & Furbo, S., 2012. *Solar radiation and thermal performance of solar collectors for Denmark,* s.l.: s.n.

DTUwind, 2017. *Energistyrelsens Godkendelsessekretariat for Vindmøller* [Interview] (1 2017).

DWIA - Geostrophic wind, u.d. *The Danish Wind Industri Association.* [Online]
Available at: http://www.motiva.fi/myllarin_tuulivoima/windpower%20web/da/tour/wres/geostro.htm
[Senest hentet eller vist den 12 2016].

DWIA - Meteorological wind, u.d. *The Danish Wind Industri Association.* [Online]
Available at: http://www.motiva.fi/myllarin_tuulivoima/windpower%20web/da/tour/wres/siting.htm
[Senest hentet eller vist den 12 2016].

DWIA - Orography, u.d. *The Danish Wind Industri Association.* [Online]
Available at: http://www.motiva.fi/myllarin_tuulivoima/windpower%20web/da/tour/wres/speedup.htm
[Senest hentet eller vist den 12 2016].

DWIA - Roughness rose, u.d. *The Danish Wind Industri Association.* [Online]
Available at: 1) http://www.motiva.fi/myllarin_tuulivoima/windpower%20web/da/tour/wres/rrose.htm
[Senest hentet eller vist den 12 2016].

DWIA - Roughness, u.d. *The Danish Wind Industri Association.* [Online]
Available at: http://www.motiva.fi/myllarin_tuulivoima/windpower%20web/da/stat/unitsw.htm#roughness
[Senest hentet eller vist den 12 2016].

DWIA - Shelters, u.d. *The Danish Wind Industri Association.* [Online]
Available at: http://www.motiva.fi/myllarin_tuulivoima/windpower%20web/da/tour/wres/shelter/guides.htm#r
[Senest hentet eller vist den 12 2016].

DWIA - Tool, u.d. *The Danish Wind Industri Association.* [Online]
Available at: http://www.motiva.fi/myllarin_tuulivoima/windpower%20web/da/tour/wres/shelter/index.htm

DWIA - Weibull, u.d. *Danish Wind Industry Association.* [Online]
Available at: http://www.motiva.fi/myllarin_tuulivoima/windpower%20web/da/tour/wres/weibull.htm
[Senest hentet eller vist den 12 2016].

DWIA - Wind estimation, u.d. *Danish Wind Power Association.* [Online]
Available at: http://www.motiva.fi/myllarin_tuulivoima/windpower%20web/da/tour/wres/dkmap.htm
[Senest hentet eller vist den 12 2016].

DWIA - Wind gradient, u.d. *The Danish Wind Industri Association.* [Online]
Available at: http://www.motiva.fi/myllarin_tuulivoima/windpower%20web/da/tour/wres/shear.htm
[Senest hentet eller vist den 12 2016].

Ebeltoft Fjernvarmeværk, u.d. *Ebeltoft Fjernvarmeværk.* [Online]
Available at: http://www.ebeltoftfjernvarme.dk/
[Senest hentet eller vist den 2 October 2016].

Efoy, u.d. [Online]
Available at: http://www.efoy-comfort.com/da)
[Senest hentet eller vist den 12 2016].

Emarineinc, u.d. [Online]
Available at: https://www.emarineinc.com/Kestrel-e230i-800W-Wind-Turbine
[Senest hentet eller vist den 1 2017].

EMD - Map, 2001. *Vindressourcekort for Danmark,* s.l.: s.n.

EMD - WindPro, u.d. [Online]
Available at: http://www.emd.dk/windpro/windpro-modules/energy-modules/model/
[Senest hentet eller vist den 2016].

EMD & Risø, u.d. *EMD International.* [Online]
Available at: http://www.emd.dk/files/windres/pdf/Middelvinden_i_25m_Danmark.pdf
[Senest hentet eller vist den 2016].

Energistyrelsen - Cert. , u.d. *Energistyrelsens Godkendelsessekretariat for Vindmøller.* [Online]
Available at: http://www.vindmoellegodkendelse.dk/certificering/certificerende-virksomheder/

Energy Alternatives LTD, u.d. [Online]
Available at: http://www.energyalternatives.ca/content/Categories/MicroHydroInfo.asp
[Senest hentet eller vist den 12 2016].

Eventhorizonsolar, u.d. [Online]
Available at: http://www.eventhorizonsolar.com/BergeyWind.html
[Senest hentet eller vist den 1 2017].

Fields, J., Oteri, F., Preus, R. & Baring-Gould, I., 2016. *Deployment of Wind Turbines in the Built Environment: Risks, Lessons, and Recommended Practices,* s.l.: s.n.

Folkecenter - Windspot, u.d. [Online]
Available at: http://www.folkecenter.dk/mediafiles/folkecenter/pdf/Windspot-Pro-.pdf
[Senest hentet eller vist den 1 2017].

Folkecenter, 2012. [Online]
Available at: http://www.folkecenter.net/gb/rd/wind-energy/48006/testfield/windspot/

Future Energy, u.d. *Futurenergy.co.uk.* [Online]
Available at: http://www.futurenergy.co.uk

Gallagher, B., 2016. *U.S. Solar PV Price Brief H1 2016: System Pricing, Breakdowns and Forecasts,* s.l.: Greentech Media.

GBenergy, u.d. [Online]
Available at: http://www.gbenergy.it/acquista-il-kit-minieolico-di-gb-energy/
[Senest hentet eller vist den 1 2017].

Ginnerup, S., 2015. *SBI-ANVISNING 260 - TILGÆNGELIGE FRITLIGGENDE BOLIGER - INDLEDENDE SPØRGSMÅL,* s.l.: s.n.

Gram Mortensen, B. O., 2016. Forsyningspligt og aftagepligt: Et offentligretligt studie. I: *Ret på flere felter: forvaltning, governance, retsskikkerhed.* s.l.:s.n.

Green steam engine, u.d. [Online]
Available at: http://www.greensteamengine.com/products.htm
[Senest hentet eller vist den 12 2016].

Green Steam Engine, u.d. *Green Steam Engine.* [Online]
Available at: http://www.greensteamengine.com/
[Senest hentet eller vist den 20 December 2016].

Gribble, u.d. [Online]
Available at: https://www.gribble.org/cycling/air_density.html
[Senest hentet eller vist den 12 2016].

Grobund, 2017. *Grobund.* [Online]
Available at: www.grobund.org
[Senest hentet eller vist den December 2017].

Grønvold, F. O. et al., 1982. *SBI-ANVISNING 129 - KORROSIONSFOREBYGGELSE I VVS-INSTALLATIONER,* s.l.: s.n.

Homer Energy, u.d. *Homer Energy.* [Online]
Available at: http://www.homerenergy.com/HOMER_pro.html
[Senest hentet eller vist den January 2017].

Hossain, M., Mekhilef, S. & Olatowima, L., 2016. Performance evaluation of a stand-alone PV-wind-diesel-battery hybrid system feasible for a large resort center in South China Sea, Malaysia. *Sustainable Cities and Society,* Årgang 28, pp. 358-366.

Ingeniøren, u.d. *Ingeniøren.* [Online]
Available at: https://ing.dk/artikel/negative-elpriser-vi-forsoemmer-bruge-stroemmen-fra-vores-vindmoeller-173239
[Senest hentet eller vist den 20 December 2016].

J. Moran, M., N. Shapiro, H., D. Boettner, D. & B. Bailey, M., 2012. *Principles of Engineering Thermadynamics.* 7 red. s.l.:John Wiley & Sons.

James, M. & James, B., 2016. *Passive House in Different Climates: The Path to Net Zero,* New York: Routledge.

Jensen., R. L., Nørgaard, J., Daniels, O. & Justesen, R. O., 2011. *Person- og forbrugsprofiler: bygningsintegreret energiforsyning,* s.l.: s.n.

Kavadias, K. A., 2012. Stand-alone Hybrid Systems. *Earth Systems and Environmental Sciences,* Årgang 2, pp. 623-655.

Kestrel, u.d. [Online]
Available at: http://www.kestrelwind.co.za/content.asp?PageID=484
[Senest hentet eller vist den 1 2017].

LaMonica, M., u.d. *IEEE Spectrum.* [Online]
Available at: http://spectrum.ieee.org/energywise/green-tech/fuel-cells/ge-claims-fuel-cell-breakthrough-starts-pilot-production
[Senest hentet eller vist den 12 2016].

Larsen, T., Jensen, R. J., Andersen, M. R. & Daniels, O., 2011. *EnergiParcel, Måling af indeklima og energiforbrug - Endelig rapport,* s.l.: s.n.

Larsen, T. S., 2010. *Måleresultater fra Komfort Husene - Ikke udgivet,* s.l.: s.n.

M. Vanek, F. & D. Albright, L., 2008. *Energy System Engineering – Evaluation & Implementation.* s.l.:Mc Graw Hill.

Madaci, B., Chenni, R., Kurt, E. & Hemsas, K. E., 2016. Design and control of a stand-alone hybrid power system. *International Journal of Hydrogen Energy,* 41(29), pp. 12485-12496.

Michael, A. C., u.d. [Online]
Available at: https://www.ndsu.edu/pubweb/~klemen/Bergey_XL.1_Power_Curve.htm
[Senest hentet eller vist den 1 2017].

Ministry of Environment and Food, u.d. [Online]
Available at: http://svana.dk/vand/vand-i-hverdagen/genbrug-af-vand/regnvand-og-overfladevand/
[Senest hentet eller vist den 1 2017].

Mobil energi, u.d. [Online]
Available at: http://www.mobil-energi.dk/104/Br%C3%A6ndselsceller/EFOY%20Comfort%20210?category_id=308&product_id=3975
[Senest hentet eller vist den 12 2016].

Munch-Andersen, J. & Andersen, B. M., 2004. *Halmhuse - Udformning og materialeegenskaber,* s.l.: s.n.

Nature Agency - Wind , 2015. *Vejledning om planlægning for og tilladelse til opstilling af vindmøller,* s.l.: The Danish Nature Agency.

Navitron - Windspot, u.d. [Online]
Available at: https://www.navitron.org.uk/forum/index.php?topic=20453.0

Navitron, u.d. [Online]
Available at: http://www.navitron.org.uk/forum/index.php?topic=18371.0
[Senest hentet eller vist den 1 207].

Nema, P., Nema, R. K. & Rangnekar, S., 2009. A current and future state of art development of hybrid energy system using wind and PV-solar: A review. *Renewable and Sustainable Energy Reviews,* 13(8), p. 2096–2103.

Nord Energy A/S, u.d. *nord energi net A/S.* [Online]
Available at: http://www.nordenerginet.dk/default.aspx
[Senest hentet eller vist den 2 October 2016].

NSW Government, 2010. *The wind energy fact sheet,* s.l.: Department of Environment, Climate Change and Water NSW.

Ogunjuyigbe, A. S. O., Ayodele, T. R. & Akinola, O. A., 2016. Optimal allocation and sizing of PV/Wind/Split-diesel/Battery hybrid energy system for minimizing life cycle cost, carbon emission and dump energy of remote residential building. *Applied Energy,* Årgang 171, pp. 153-171.

Ovesen, N. et al., 2000. *Afstrømningsforhold i danske vandløb,* s.l.: s.n.

Piggott, Hugh - Kestrel, u.d. [Online]
Available at: http://scoraigwind.co.uk/2011/11/kestrel-e400i-wind-turbine-on-scoraig/
[Senest hentet eller vist den 1 2017].

Piggott, Hugh - Tristar, 2017. [Online]
Available at: http://scoraigwind.co.uk/installing-and-configuring-a-tristar-controller-for-a-wind-system/
[Senest hentet eller vist den 1 2017].

Piggott, H., u.d. [Online]
Available at: http://scoraigwind.co.uk/
[Senest hentet eller vist den 1 2017].

Powergenerator, u.d. [Online]
Available at: http://www.powergenerator.dk/benzin-generatorer/benzin-generator-1.500-w-/-230v
[Senest hentet eller vist den 12 2016].

PVsyst , u.d. *PVsyst Photovoltaic Software.* [Online]
Available at: http://www.pvsyst.com/en/
[Senest hentet eller vist den December 2016].

RAoE, 2016. *The Royal Academy of Engineering.* [Online]
Available at: http://www.raeng.org.uk/publications/other/23-wind-turbine

Renewables First, u.d. *Renewables First.* [Online]
Available at: http://www.renewablesfirst.co.uk/windpower/windpower-learning-centre/how-much-does-a-wind-turbine-cost-to-operate/
[Senest hentet eller vist den 18 December 2016].

renugen, u.d. [Online]
Available at: http://www.renugen.co.uk/bergey-xl-1-1000-watt-wind-turbine/
[Senest hentet eller vist den 1 2017].

Retsinfo. - Authorization, 2014. [Online]
Available at: https://www.retsinformation.dk/forms/r0710.aspx?id=162734
[Senest hentet eller vist den 1 2017].

Retsinfo. - Building, u.d. [Online]
Available at: https://www.retsinformation.dk/forms/R0710.aspx?id=183662
[Senest hentet eller vist den 12 2016].

Retsinfo. - Certification, u.d. [Online]
Available at: https://www.retsinformation.dk/forms/R0710.aspx?id=145252
[Senest hentet eller vist den 12 2016].

Retsinfo. - Connection, u.d. [Online]
Available at: https://www.retsinformation.dk/forms/R0710.aspx?id=183381
[Senest hentet eller vist den 12 2016].

Retsinfo. - Electricity, u.d. [Online]
Available at: https://www.retsinformation.dk/forms/R0710.aspx?id=174909
[Senest hentet eller vist den 12 2016].

Retsinfo. - Energy, u.d. [Online]
Available at: https://www.retsinformation.dk/Forms/R0710.aspx?id=184376#idd6841d59-07a4-4854-8116-c9a60a86b4e0
[Senest hentet eller vist den 12 2016].

Retsinfo. - Environment, u.d. [Online]
Available at: https://www.retsinformation.dk/Forms/R0710.aspx?id=184047

Retsinfo. - Heating, u.d. [Online]
Available at: https://www.retsinformation.dk/forms/r0710.aspx?id=165652
[Senest hentet eller vist den 12 2016].

Retsinfo. - Planning, u.d. [Online]
Available at: https://www.retsinformation.dk/forms/r0710.aspx?id=176182
[Senest hentet eller vist den 12 2016].

Retsinfo. - VVM, u.d. [Online]
Available at: https://www.retsinformation.dk/Forms/R0710.aspx?id=175836
[Senest hentet eller vist den 12 2016].

Retsinfo. - Waste water, u.d. [Online]
Available at: https://www.retsinformation.dk/Forms/R0710.aspx?id=180360

Retsinfo. - Water, 2016. [Online]
Available at: https://www.retsinformation.dk/Forms/R0710.aspx?id=180348#id342059c8-fdcb-477d-91fa-cf1206023bdf
[Senest hentet eller vist den 1 2017].

Retsinfo. - Water, u.d. [Online]
Available at: https://www.retsinformation.dk/Forms/R0710.aspx?id=184065
[Senest hentet eller vist den 12 2016].

Retsinfo. - Wind, u.d. [Online]
Available at: https://www.retsinformation.dk/eli/lta/2015/1736

Rezk, H. & Dousoky, G. M., 2016. Technical and economic analysis of different configurations of stand-alone hybrid renewable power systems - A case study. *Renewable and Sustainable Energy Reviews,* Årgang 62, pp. 941-953.

Rivers, Collyn. Fuel cells., u.d. [Online]
Available at: http://caravanandmotorhomebooks.com/fuel-cells-for-caravans/
[Senest hentet eller vist den 12 2016].

Rivers, Collyn. Truma., u.d. [Online]
Available at: http://caravanandmotorhomebooks.com/truma-vega-fuel-cell-is-no-more/
[Senest hentet eller vist den 12 2016].

Rørcenter, 2012. [Online]
Available at: http://bygningsreglementet.dk/file/269499/Brug-af-regnvand.pdf
[Senest hentet eller vist den 1 2017].

Scanboiler, u.d. [Online]
Available at: http://www.scanboiler.dk/media/11197/Varmtvandsbeholder-mindre-end-250.pdf
[Senest hentet eller vist den 12 2016].

Scoraig Wind , u.d. *Scoraig Wind Electric News.* [Online]
Available at: http://scoraigwind.co.uk/buy-a-charge-controller/
[Senest hentet eller vist den 20 December 2016].

Seas-NVE, u.d. *seas-nve.* [Online]
Available at: http://www.seas-nve-net.dk/seas-nve-net/priser-og-gebyrer/oevrige-priser/tilslutningspriser
[Senest hentet eller vist den 2 October 2016].

Shaw, S., Rosen, A., Beavers, D. & Korn, D., 2008. Status Report on Small Wind Energy Projects Supported by the Massachusetts. *Renewable Energy Trust.*

Silva, S. B.; Severino, M. M.; de Oliveira, M. A. G.;, 2013. A stand-alone hybrid photovoltaic, fuel cell and battery System: A case study of Tocantins, Brazil. *Renewable Energy,* Årgang 57, pp. 384-389.

Solicity, u.d. [Online]
Available at: http://www.solacity.com/docs/Bergey/XL1spec.pdf

Solutions Energies, u.d. [Online]
Available at: http://www.solutions-energies.fr/lang-en/171-bergey
[Senest hentet eller vist den 1 2017].

Sonkyo - Cert., u.d. [Online]
Available at: http://uk.windspot.es/technology-wind-turbines/technology/104/certifications

Sonkyo Energy, u.d. [Online]
Available at: http://uk.windspot.es/
[Senest hentet eller vist den 1 2017].

Syddjurs Kommune, L300, u.d. [Online]
Available at: http://soap.plansystem.dk/pdfarchive/20_1053686_APPROVED_1191580411614.pdf
[Senest hentet eller vist den 12 2016].

Syddjurs Kommune, Plan, u.d. [Online]
Available at: http://kommuneplan.syddjurs.dk/dk/kommuneplan-2016/maal-og-retningslinjer/oversigt-over-alle-retningslinjer-og-generelle-rammer-samt-byraadets-maalsaetninger-og-prioriteringer/samlet-oversigt-over-retningslinjer-og-generelle-rammer-samt-byraadets-maalsaet
[Senest hentet eller vist den 12 2016].

Tegmart, u.d. *Tegmart.* [Online]
Available at: http://www.tegmart.com/thermoelectric-modules/
[Senest hentet eller vist den December 2016].

Troen, I. & Petersen, E., 1989. *Eutopean Wind Atlas,* s.l.: s.n.

Tsuanyo, D., Azoumah, Y., Aussel, D. & Neveu, P., 2015. Modeling and optimization of batteryless hybrid PV(photovoltaic)/diesel systems for off-grid applications. *Energy,* Årgang 86, pp. 152-163.

U.S. Department of Energy, u.d. [Online]
Available at: https://energy.gov/energysaver/microhydropower-systems
[Senest hentet eller vist den 12 2016].

Vindmølle Industrien, u.d. *Vindmølle Industrien.* [Online]
Available at: http://www.windpower.org/da/energipolitik_og_planlaegning/offshore.html
[Senest hentet eller vist den 20 December 2016].

Viva Energi - GEL, u.d. *Viva Energi.* [Online]
Available at: http://www.vivaenergi.dk/solcelle-webshop/LiFePO4_batteri
[Senest hentet eller vist den November 2016].

Viva energy - Batteries, u.d. [Online]
Available at: http://www.vivaenergi.dk/Batteri_teknologier
[Senest hentet eller vist den 12 2016].

Viva energy - GEL, u.d. [Online]
Available at: http://www.vivaenergi.dk/solcelle-webshop/12V_GEL_Solar_batteri/12V_100Ah_GEL-_Gel%C3%A9_Solar_deep_cycle_batteri
[Senest hentet eller vist den 12 2016].

VivaEnergy - PV, u.d. [Online]
Available at: http://www.vivaenergi.dk/solcelle-webshop/store-solcellepaneler?PID=1753
[Senest hentet eller vist den 1 2017].

Wang, P. G. et al., 2013. *2001– 2010 Danish Design Reference Year - Reference Climate Dataset for Technical Dimensioning in,* s.l.: s.n.

Warwick Wind Trials, u.d. *Warwick Wind Trials.* [Online]
Available at: http://www.warwickwindtrials.org.uk/resources/Warwick+Wind+Trials+Final+Report+.pdf
[Senest hentet eller vist den October 2016].

Wikipedia. Thermoelectric., u.d. *Wikipedia.* [Online]
Available at: https://en.wikipedia.org/wiki/Thermoelectric_effect#Seebeck_effect
[Senest hentet eller vist den 12 2016].

Wind Energy The Facts, u.d. *Wind Energy The Facts.* [Online]
Available at: https://www.wind-energy-the-facts.org/operation-and-maintenance-costs-of-wind-generated-power.html
[Senest hentet eller vist den 18 December 2016].

Wind measurement int., u.d. *wind measurement international.* [Online]
Available at: http://www.windmeasurementinternational.com/wind-turbines/om-turbines.php
[Senest hentet eller vist den 18 December 2016].

WindpowerProgram, u.d. [Online]
Available at: http://www.wind-power-program.com/small_turbines.htm
[Senest hentet eller vist den 1 2017].

Windworks, u.d. *Windworks.org.* [Online]
Available at: http://www.wind-works.org/cms/index.php?id=68&tx_ttnews%5btt_news%5d=61&cHash=5257f2f1a83dd2cac9880becfb680f90
[Senest hentet eller vist den October 2016].

Woods-Bryan, S. & Bryan, L., u.d. [Online]
Available at: http://www.echorenovate.com/wind-energy.php
[Senest hentet eller vist den 1 207].

YourHome, Australian Government, u.d. *Australia's Guide to Environmentally Sustainable Houses.* [Online]
Available at: www.yourhome.gov.au/materials/embodied-energy
[Senest hentet eller vist den 8 September 2016].

18 Table of Appendices

Appendix A Analysis of DHW tank

Table 18.1 shows the monthly DHW deficit for different combinations of accumulation tank volume and PV-panel area calculated with the *Off-grid Simulation Tool*.

DHW deficit for combinations of DHW tank and PV-panels [kWh]					
	Volume of DHW tank [L] and total area of solar panels [m^2]				
Month	**100 L, 5 m^2 PV**	**200 L, 5 m^2 PV**	**300 L, 5 m^2 PV**	**100L, 7 m^2 PV**	**200L, 7 m^2 PV**
Jan.	48	38	32	42	31
Feb.	57	47	44	47	37
Mar.	30	15	10	14	5
Apr.	12	4	3	6	0
Maj.	4	0	0	1	0
Jun.	4	0	0	0	0
Jul.	1	0	0	0	0
Aug.	7	1	0	1	0
Sep.	8	0	0	1	0
Oct.	7	0	0	2	0
Nov.	30	10	3	24	8
Dec.	55	44	40	50	38
Sum	265	158	132	188	120

Table 18.1 – Domestic hot water deficit for combinations of accumulation tank and PV-panels after utilization of excess electricity.

In the evaluation of the DHW tank volume, the space heating demand was considered, as the DHW demand that cannot be covered by excess electricity, must be covered by the mass oven. According to Section 3.3.1 the off-grid house has the following space heating demand:

Month	Jan.	Feb.	Mar.	Apr.		Nov.	Dec.
Space heating demand [kWh]	516	429	308	116		338	488

This means, that the system should be designed, so that there is no DHW deficit from May through October. In Table 18.1, it is only the systems with a 100 L accumulation tank, that does not fulfill this requirement. The 200 L tank combined with 5 m^2 solar panels is thought to be sufficient in this evaluation, despite of the 1 kWh deficit in August.

If the system should be dimensioned conservatively (DHW consumption and excess electricity can vary) the difference between a 200 L and 300 L accumulation tank is only around 650-1200 DKK depending on the type of tank (DB-VVS).

Alternatively, additional solar panels are around 1200 DKK per m^2 (VivaEnergy - PV). As the additional solar panels affects the electricity coverage, the battery capacity could be reduced from 10.1 kWh to 9.5 kWh, if the system has 7 m^2 instead of 5 m^2 solar panels. This is a theoretical saving around 1000 DKK in investment, but it might not be practically achievable, depending on the design of the battery bank.

Graph 17 shows the daily mean temperature in 200 liter DHW tank for proposed energy system. In reality, there is a temperature gradient in the tank, so the temperature is highest in the top and lowest in the bottom. It is estimated, that when the mean temperature is below around 21 ℃, the temperature in the top is too low for DHW, and the tank is seen as 'empty' with regard to stored energy. This is the reason why the temperature on Graph 17, is ever below 21 ℃.

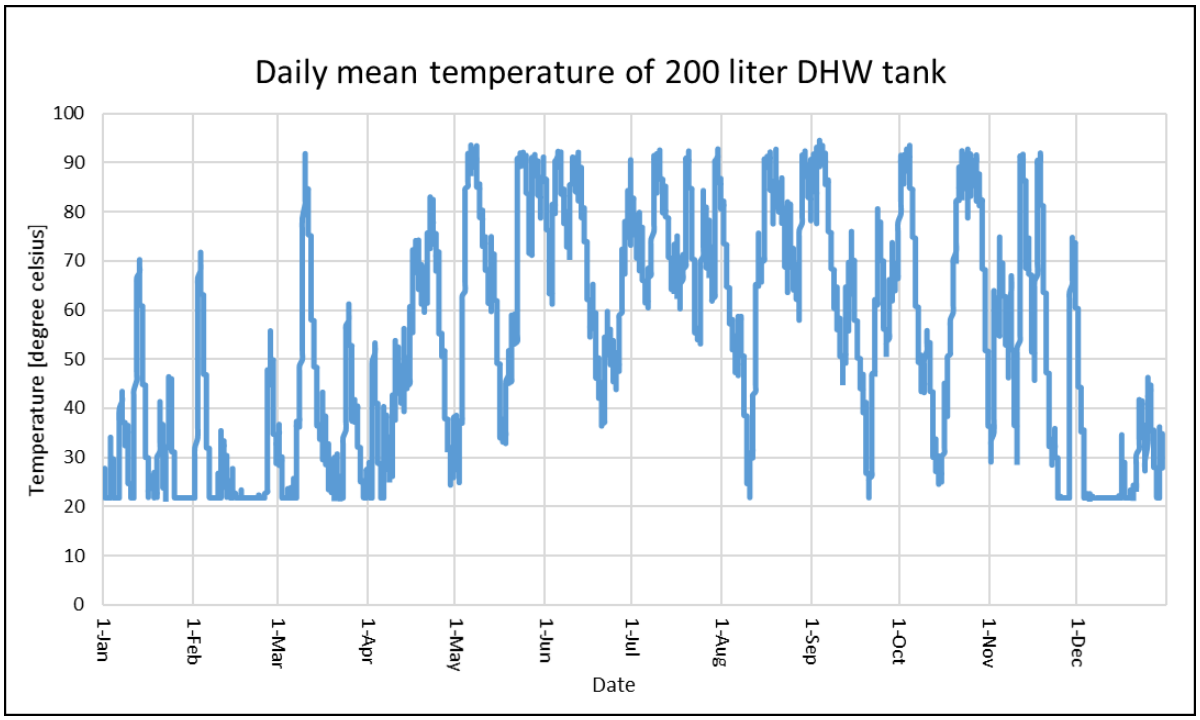

Graph 17 – Daily mean temperature in 200 liter DHW tank for proposed energy system. In reality, there is a temperature gradient in the tank, so the temperature is highest in the top and lowest in the bottom.

Appendix B Additional Utilization of Excess Electricity

The excess electricity generation from renewable sources in certain periods is a challenge in this project - and on regional or global levels as well. In Denmark, the still increasing Wind Farms (Vindmølle Industrien, u.d.) often generate more electricity than the Danish population can consume, resulting in a negative grid electricity price (Ingeniøren, u.d.). This is a significant problem and a great challenge for the Danish energy industry which is constantly looking for technologies to efficiently store the excess electricity.

In *Project Grobund* excess generation is an issue as well due to the fluctuating nature of both solar and wind power. The implemented heating of domestic hot water is a way to deal with the excess electricity, but heating water with electricity in a 1:1 ratio is not energy efficient.

Instead, a common house can be constructed in the area intended for the project. In this building, high powered electrical appliances such as washing machines and dryers for common use can be installed. The periodical electricity consumption of such a building will be too high to cover entirely with renewable sources and therefore the house would require a grid connection.

If the energy systems from each individual off-grid house are connected to the common house, the appliances can be used instead of 'expensive' grid electricity during periods with high amounts of excess electricity generation. As all houses are assumed to have the same setup, photovoltaic and wind turbine, the amount of excess electricity can become quite high in periods with decent amounts of solar and wind power. If the inhabits are willing to conform to a way of living, where we as humans use the energy when it is available instead of making the energy available when we need to use it, the laundry can be done without charge for large periods of the year, if the appliances are used wisely.

Appendix C Alternative House Design

An alternative house design aiming to decrease the heating demand to near zero will be discussed in this section. The "passive" house will rely on the same building techniques and materials as the conceptual design, the only difference in materials is improved exterior windows. The windows in the *passive* house are of the brand HeatMirror and have the following properties:

- Model: HeatMirror IG
    - 2 airtight chambers filled with krypton gassed separated by lightweight film
- U-value center of window: 0,16 W/m²K
- G-value (SHGC): 0,51
- LT-value: 70%

Similar windows with properties corresponding to the above can obviously produce the same result.

The window area in the *passive* design is reduced by 69% compared to the concept design.

The passive house design is illustrated in Figure 18.1.

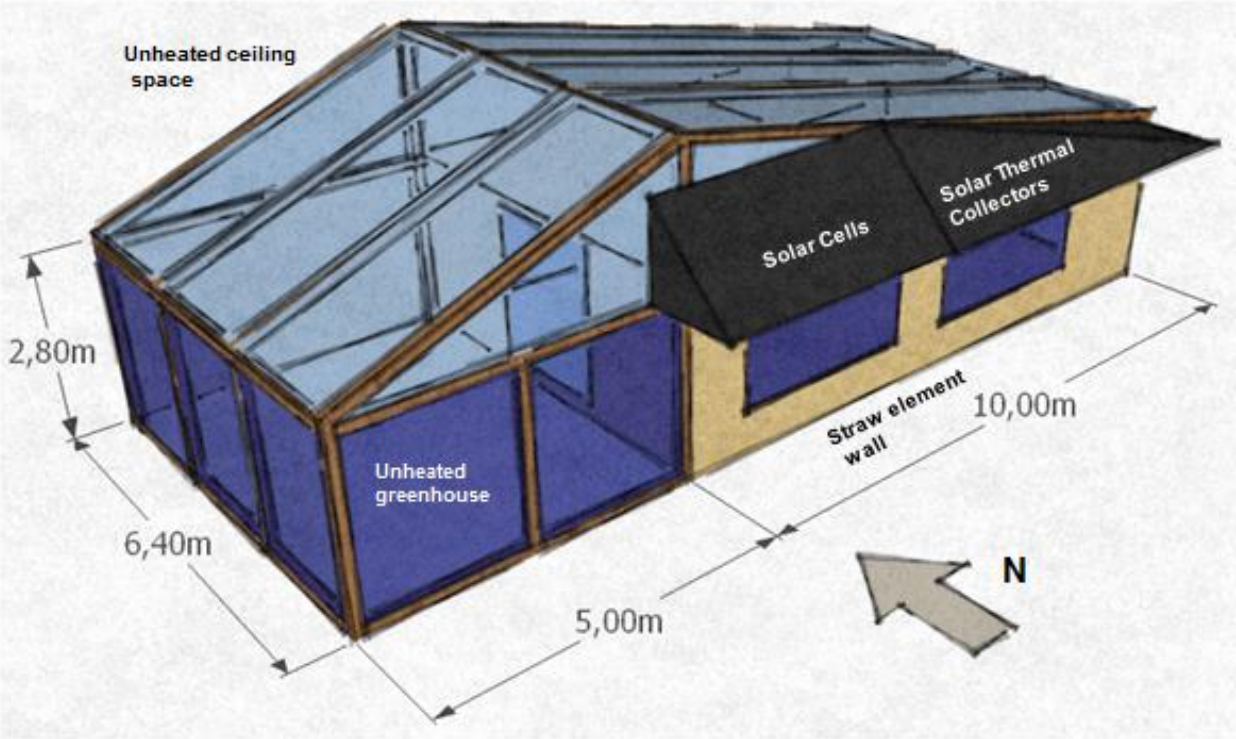

Figure 18.1 – Alternative House Design

The BSim model used for the calculations can be seen in Figure 18.2.

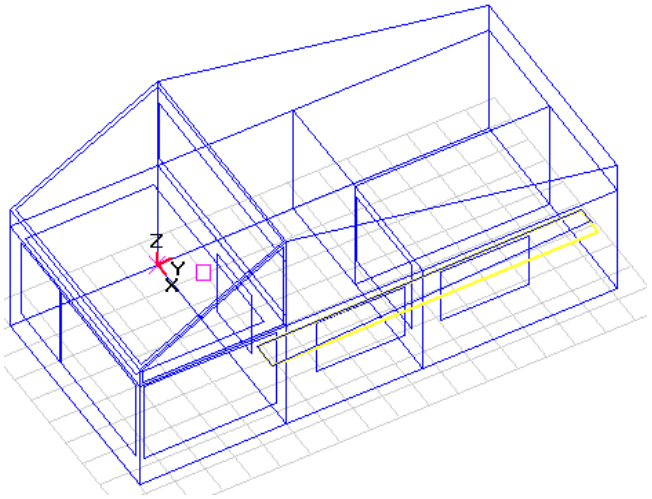

Figure 18.2 – BSIm Model for the Alternative House Design

The geometry and orientation of the house has been altered, resulting in a more rectangular design, but without changing the net floor area of the house or greenhouse. Changing the window properties, window area and orientation has a significant impact on the energy performance and indoor climate of the house.

The heating demand is reduced by 80%, operative temperature hours above 26°C is reduced by 86% and the daylight conditions remains reasonable, as seen in Table 18.2.

Design	Annual Heating Demand [kWh]	Annual Heating Demand [kWh/m²]	Hours Above 26°C [Hours]	Hours Above 27°C [Hours]	Average Daylight Factor [%]
Conceptual	2195.0	34.3	774	492	7.0
Passive	425.5	6.9	107	0	3.6

Table 18.2 – Comparison of Results between Concept and Alternative Design

Table 18.2 clearly shows how these simple changes, which can be done without increase or possibly even a decrease in investment cost, can reduce the heating demand and improve the indoor climate by reducing overheating, while still maintaining an excellent visual climate.

The mean daily operative temperatures for two designs are plotted according to the limits in DS/EN 15251, Figure 18.3.

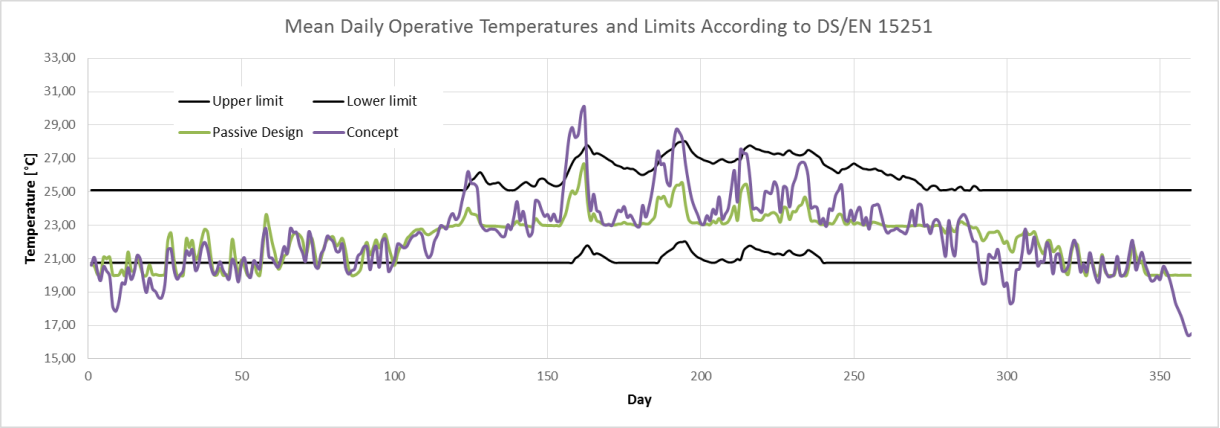

Figure 18.3 – Mean Daily Operative Temperatures for Concept and Alternative Design

The heating set point is set to 20°C, as such both designs fall below the 'Lower limit', while the operative temperature of the *passive* design is seen to remain more stable and also within the 'Upper limit' the entire year.

Achieving a better indoor climate and reducing the heating demand is mainly due to these implementations, which are different than the properties of the conceptual design.

- Increased direct solar radiation from south, as the shading device only block summer sun
    - Allows for plenty of passive solar heating during fall, winter and spring, but blocks strong summer sun when outdoor temperatures are high
        - Conceptual design does not allow for direct solar radiation from south due to the placement of the greenhouse which blocks or reduces the solar radiation significantly
- Changes in greenhouse design
    - Greenhouse receive similar amount of solar radiation even though glazing area towards south is reduced.
    - A reduced interior window area between greenhouse and kitchen/living room reduces chances for overheating in the living room
    - Northern oriented façade of greenhouse is straw element, improves temperature stability
- High insulating windows reduces heat loss, but the high 'solar heat gain coefficient' still allows for passive heating through solar radiation

The ideas to change the current house design described in this section will be presented for *Project Grobund* at an appropriate time.

Appendix D Notes from ”Project Grobund”

In this appendix notes from meetings with Steen Møller from *Project Grobund* are listed as these notes have had an impact on assumptions regarding user behavior and house design.

Appendix D.1 Electricity Consumption

Steen Møller estimates the annual electricity consumption for the houses to be less than 500 kWh, personally he estimates that he can consume 100 kWh annually. This number is based on Steen Møller’s personal experience from living under similar conditions. The houses are intended to include a refrigerator, lights and outlets all running on a 24V direct current system. The oven is intended to run on gas. *Project Grobund* intends to design the houses and their systems to conform to this very low electricity consumption, as such users will find it difficult to consume more electricity than what the system is designed for.

In this thesis, the annual electricity value is based on light level demands simulated in BSim, an annual consumption for an actual refrigerator, along with an estimation of usage of the outlets of 6 hours per day, with an average of 200 Watts, which is conservative according to Steen Møller’s assumptions. As the annual electricity consumption is assumed to be 713 kWh.

Appendix E Economic Assumptions

The following prices have been applied in the project, current October 2016.

Funds are available for purchase of solar installation, hence no bank load.

- Connection fee to electricity net: 15,000 DKK (Seas-NVE) (Nord Energy A/S)
- Electricity price when connected: 2.20 DKK/kWh (Danish Energy Regulatory Authority)
- Photovoltaic prices are assumed to decrease by 12.5% by 2018 (Gallagher, 2016)
- Connection fee to district heating: 25,000 DKK (Ebeltoft Fjernvarmeværk)
- District heating price when connected: 0.45 DKK/kWh (Ebeltoft Fjernvarmeværk)

Appendix E.1 Cost of Electricity for Individual Technologies

The cost of the individual technologies can be seen in Table 18.3.

The table is based on the project annual electricity consumption of 713 kWh, where each technology is assumed to generate 50% of the total annual electricity.

Technology	Total Investment Cost [DKK]	Operational Cost [DKK/kWh]	Maintenance Cost [DKK]	Total Annual Electricity Generation [kWh]	Cost of Electricity Over 20 Years [DKK/kWh]	Usable Annual Electricity Generation [kWh]	Effective Cost of Electricity [DKK/kWh]
Photovoltaic [1500 W]	18,500	0	0	1562.0	0.6	356.5	**2.6**
Thermoelectic Generator [35 modules]	10,500	0	600	356.5	3.2	356.5	**3.2**
Steam Engine [3000 W]	15,000	0	1,500	356.5	6.3	356.5	**6.3**
Biogas Generator [-]	-	-	-	-	-	-	**-**
Fuel Cell [105 W]	43,000	33		356.5	39.0	356.5	**39.0**
Wind Turbine [1000 W]	50,000	0	500	1287.0	2.3	356.5	**8.4**

Table 18.3 – Cost of Electricity for Individual Technologies

Appendiks E.1.1 Photovoltaic

For photovoltaic systems the inverter is typically the only component which requires maintenance or replacement during the lifetime, therefore no maintenance cost is added to the PV system. Calculation of the price of the specific PV system is illustrated in Figure 18.4. The figure is based on current prices for multiple PV system in different sizes in Denmark Q4 2016, along with the expected price drop in 2018 according to (Gallagher, 2016). In table Table 18.3 a 10 m² PV system is suggested.

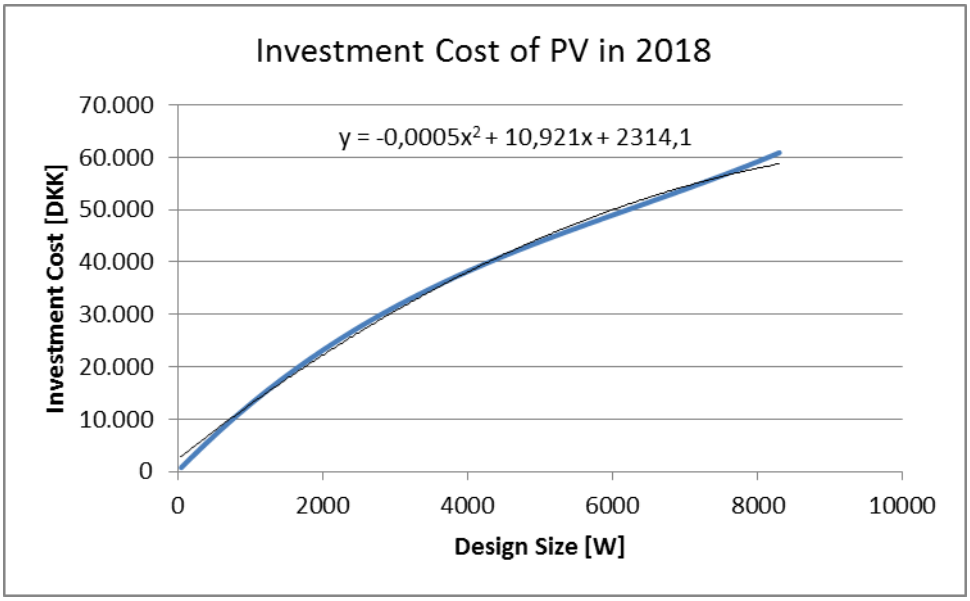

Figure 18.4 – Investment versus Capacity for Photovoltaic System

Appendiks E.1.2 Thermoelectric Generators

For the thermoelectric generators little to no maintenance or replacement can be expected according to the literature study. The required amount of modules is 35, as stated in Section 6.2.

The investment cost of the modules is expected to be 300 DKK (Tegmart) and the maintenance is conservatively set to replacement of 2 modules (600 DKK) per year.

Appendiks E.1.3 Steam Engine

According to (Green Steam Engine, u.d.) a steam engine can be assembled for approximately 3,000 DK while a ready-to-use steam engine of 7.45 kW can be purchased for approximately 15,000 DKK. Besides the steam engine this technology requires a lot of additional equipment such as pipes, valves and several security measures. For a self-assembly engine including the necessary additional equipment the total investment price is estimated to 15,000 DKK. Additionally the maintenance of the system is expected to be quite high due to the high pressure of the system and several moving parts which increases the risk of repairs, thus the annual maintenance cost is estimated to be 10% of the investment cost.

Appendiks E.1.4 Biogas Generator

Prices for biogas generators are very difficult to track down, as the technology is typically implemented to developing countries were components are bought in stores or made at the site. The systems located in the Western World, mostly U.S.A, are found to be individual for every user and therefore the components are very different. It was found to difficult to estimate prices for the biogas system within a reasonable time limit.

Appendiks E.1.5 Fuel Cell

The prices regarding this technology have been mentioned in Section 5.7.

Appendiks E.1.6 Wind Turbine

The investment price for a small wind turbine is discussed Section 13.2.10.

The annual maintenance cost of the wind turbine as an expression of the total investment cost varies from 1 to 10% according to several sources, see below. The choice of maintenance cost has great impact on the CoE of the technology, see Figure 18.5.

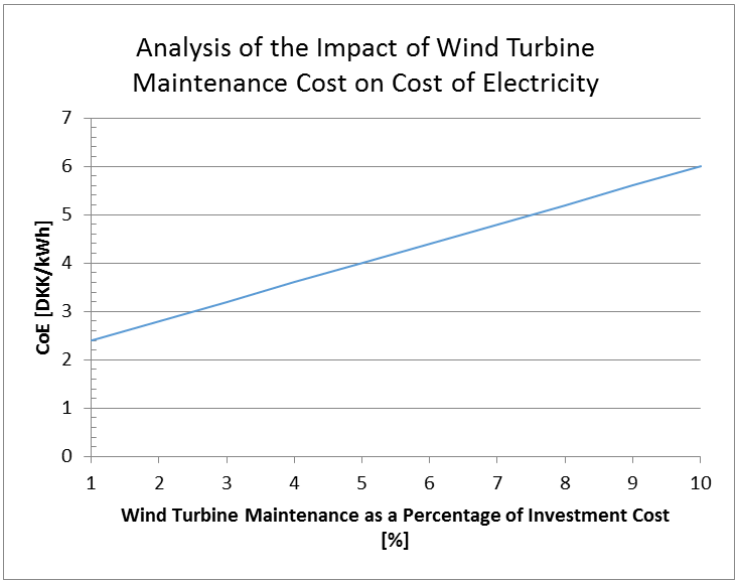

Figure 18.5 – Analysis of Maintenance Cost's Impact on CoE

The CoE of the wind turbine varies from 2.4 to 6.0 DKK/kWh depending on a range of 1-10% annual maintenance cost of the total investment cost. According to (Wind measurement int.), (Renewables First) and (Wind Energy The Facts) the annual maintenance cost can either be calculated based on system size [kW], lifetime electricity generation [kWh] or investment cost [DKK]. Some key numbers in the sources are:

- 0.1125 DKK/kWh, electricity over total lifetime generation
- 435-556 DKK/kW installed size, decreasing as the size of the wind turbine increased
- 1.5-3% of investment cost, decreasing for modern wind turbines

While these numbers are mostly for larger wind turbines, as the maintenance costs for household wind turbines is difficult to track down, the sources mention that a large part of the maintenance is salary for service or labor work, which can be avoided in a household system. Therefore an annual maintenance cost of 1.5% of the total investment cost is found reasonable.

Appendix E.2 Cost of Electricity for the Proposed System

The cost of electricity for the proposed electricity system, over a 20 year period, can be seen in Table 18.4.

Component	Total Investment Cost [DKK]	Operational Cost [DKK/kWh]	Maintenance Cost [DKK]	Total Annual Electricity Generation [kWh]	Cost of Electricity Over 20 Years [DKK/kWh]	Usable Annual Electricity Generation [kWh]	Effective Cost of Electricity [DKK/kWh]
Photovoltaic [750 W]	11,224	0	0	767.0	0.7	356.4	1.6
Wind Turbine [1000 W]	50,000	0	500	1287.0	2.3	356.4	8.4
Controller System	3,630	0	0	0.0	0.0		
Batteries [24VDC 420A]	36,281	0	0	0.0	0.0		
Wires, fuses, diodes etc.	2,000	0	100	0.0	0.0		
Total System	**103,135**	**0.001**	**600**	**2,054**	**2.80**	**713**	**8.07**

Table 18.4 – Cost of Electricity for the system over a 20 year period

It can be seen from the calculations that a cost of electricity (CoE) of 2.80 DKK/kWh can be achieved if the entire electricity generation can be utilized. Although in the current system only 713 kWh of electricity is used, resulting in an effective CoE of 8.07 DKK/kWh. For a grid-connected system with the same consumption, a CoE of 3.25 DKK/kWh can be achieved (Danish Energy Regulatory Authority, u.d.). If instead the system includes a gasoline generator, and the battery capacity is decreased to 1 kWh, the CoE can be improved as seen in Table 18.5.

Component	Total Investment Cost [DKK]	Operational Cost [DKK/kWh]	Maintenance Cost [DKK]	Total Annual Electricity Generation [kWh]	Cost of Electricity Over 20 Years [DKK/kWh]	Usable Annual Electricity Generation [kWh]	Effective Cost of Electricity [DKK/kWh]
Photovoltaic [750 W]	11,224	0	0	767.0	0.7	330.0	1.7
Wind Turbine [1000 W]	50,000	0	500	1287.0	2.3	330.0	9.1
Controller System	3,630	0	0	0.0	0.0		
Batteries [24VDC 420A]	14,985	0	0	0.0	0.0		
Diesel Generator [1500 W]	1,500	5.1	0	53.0	0.0	53.0	6.5
Wires, fuses, diodes etc.	2,000	0	100	0.0	0.0		
Total System	**83,339**	**0.379**	**600**	**2,107**	**2.64**	**713**	**7.06**

Table 18.5 – Cost of Electricity with Back-up Generator

A decrease in battery capacity and use of a back-up generator can reduce the CoE to 7.06 DKK/kWh.

The price calculations for PV and WT are discussed earlier in this appendix. The controller system consists of: Morningstar Tristar 3 charge controller, Tristar Digital Meter and a Relay Driver, the price can be function and price can be found at (Scoraig Wind , u.d.).

Wires, fuses, diodes etc. is an estimated price which covers the remaining components necessary in the electric system. It is assumed that there is a risk of breaking a fuse or smaller component during usage, therefore a small maintenance cost of 100 DKK/year is added.

Appendix F Theory for the Obstacle Model in the *Off-grid Simulation Tool*

The method used in the *Off-grid Simulation Tool* to calculate the effect of shelters is an empirical expression called *The 2D infinite fence model* by Perera (1981). It is basically the same model that is used in the European Wind Altlas software WAsP, but implemented in a more refined way than in the *Off-grid Simulation Tool.* The model is described in (Bechmann, et al., 2015) and calculates the wind deficit behind a 2D shelter of infinite lateral dimensions (i.e. an infinite wall) based on the following equations.

$$\frac{\Delta v(z)}{v_0(h)} = \Gamma \cdot \tilde{C}_h \cdot \left(\frac{x}{h}\right)^{-1} \cdot G(\zeta) \quad \text{with} \quad G(\zeta) = c_a \cdot \zeta \cdot \exp(-a_g \cdot \zeta^{1.5})$$

where $\Gamma = 12.1875$, $\tilde{C}_h = 0.8 \cdot (1-\varphi)$, $c_a = \left[\ln\left(\frac{h}{Rl_0}\right)/2\kappa^2\right]^{1/(n+2)}$, $a_g = 0.67 \cdot c_a^{1.5}$, $\zeta = \left(\frac{z}{h}\right) \cdot \left(\frac{x}{h}\right)^{-1/(n+2)}$ and $n = \ln(z/Rl_0)^{-1}$.

The parameters in these expressions are as follows:

$\Delta v(z)$ is the velocity difference because of the obstacle at the height of interest, z. That is, the undisturbed velocity minus the obstacle-disturbed velocity.
$v_0(h)$ is the undisturbed velocity at the obstacle height, h.
Γ is a factor of 12.1875.
$\tilde{C}_h = 0.8 \cdot (1-\varphi)$ where φ is the porosity of the obstacle in the interval 0 (solid) to 1 (nothing).
x is the distance to the obstacle.
Rl_0 is the roughness length of the terrain (this affects how the wind flows around the obstacle).
κ is the von Kármán constant of 0.4.

The term $\Delta v(z)/v_0(h)$ is called a normalized velocity deficit. In order to estimate the effect of the obstacle at the height of interest (z) the following expression can be used.

$$\frac{v(z)}{v_0(z)} = 1 - \frac{\Delta v(z)}{v_0(h)} \cdot \frac{v_0(h)}{v_0(z)}$$

Here $v_0(h)/v_0(z)$ is a relation of the undisturbed wind velocity at the obstacle height (h) and the height of interest (z). This can be found from Equation 9-1 as:

$$\frac{v_0(h)}{v_0(z)} = \frac{\ln(h/Rl)}{\ln(z/Rl)}$$

Now the speed-up/down factor at a specific height due to an infinite 2D obstacle can be calculated as the term $v(z)/v_0(z)$. To account for the fact, that real shelters are not infinite in the lateral dimension a correction parameter is stated in the European Wind Atlas (Troen & Petersen, 1989, p. 61).

$$O_{cor} = \begin{cases} (1 + 0.2 \cdot \frac{x}{L})^{-1} & for \quad \frac{L}{x} \geq 0.3 \\ 2 \cdot \frac{x}{L} & for \ \frac{L}{x} \leq 0.3 \end{cases}$$

where L is the lateral dimension of the obstacle and x is the distance from the location to the obstacle.

For estimation of the porosity of an obstacle the following intervals are stated in the European Wind Atlas (Troen & Petersen, 1989, p. 59) and some examples of the corresponding obstacle types are given in (DWIA - Shelters, u.d.).

Class	Example	Porosity
Solid	House, wall	0
Very dense	Dense vegetation	≤ 0.35
Dense	Vegetation (trees in summer is 0.5)	0.35 – 0.5
Open	Open vegetation (trees without leaves)	≥ 0.35

Appendix G Optimizing the Photovoltaic Performance

Appendix G.1 Tracking of the Solar Module Angle

In advanced PV systems axis tracking can be incorporated to enhance the performance. Dual tracking allows automatic change of the tilt and orientation angles of the PV modules according to position of the sun, resulting in higher irradiance for all hours during the year. While dual axis tracking systems are expensive, a simple system could be implemented, where adjustment of the tilt angle of the modules could be changed according to the optimal angle for each month.

To assess the potential monthly increase in performance the following situation is applied to the Excel Simulation Tool:

- Zone 1 according to the radiation data.
- Latitude of 57° and longitude of 10°.
- Orientation towards south.
- 10 m² of PV modules with a 15% efficiency.
- No energy storage system.

In Figure 18.6 the monthly available electricity output from the PV systems is illustrated for two systems: A system with a permanent tilt angle of 50° (highest annual output) and a system where the tilt angle is adjusted in 5° increments in the range of 0-90° according to the best monthly performance.

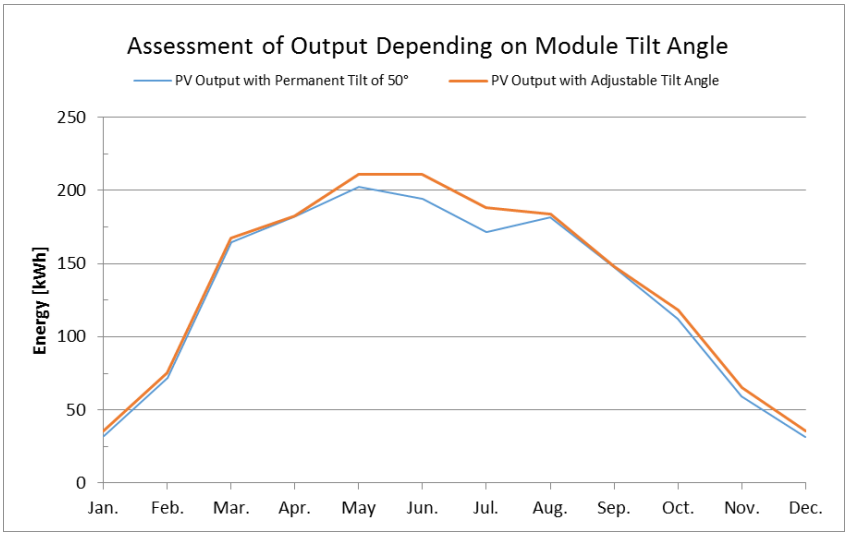

Figure 18.6 – Monthly output of PV system depending on module tilt angle

The monthly generation can be increased by up to 11.87% by adjusting the tilt angle of the PV panels, this results in an annual increase of 70.4 kWh or 4.54%. The optimal tilt angle of the modules for each month can be seen in Table 18.6.

Month	Jan.	Feb.	Mar.	Apr.	May	June	July	Aug.	Sep.	Oct.	Nov.	Dec.
Tilt Angle °	80	70	65	45	25	0	0	35	55	70	75	80

Table 18.6 – Module tilt angle for optimal monthly PV output

In an off-grid system, battery capacity significantly reduces the amount of the PV generation that can actually be utilized. The percentage of available versus usable PV generation typically ranges between 15-30% depending on the installed battery capacity. Even with a high battery capacity, 30% usable electricity results in 21.22 kWh additional annual electricity.

A system where the PV modules can be changed manually by the user increases not only the investment cost but also the risk of additional repairs on the system due to the added complexion. By upgrading the system from 10 to 11 m², approximately 1500 DKK additional investment price, the annual electricity generation can be increased by 9.98% or 154.9 kWh.

The single tracking system allowing the tilt angle of the photovoltaic system to be manually adjusted is found not to yield an increase in electricity generation which can justify the added investment cost and increased risk of reparation and maintenance work.

Appendix G.2 Dual-direction Modules

A PV system made up of two sections with different orientation has been assessed in order to see, if dual orientation can yield a higher annual usable PV generation.

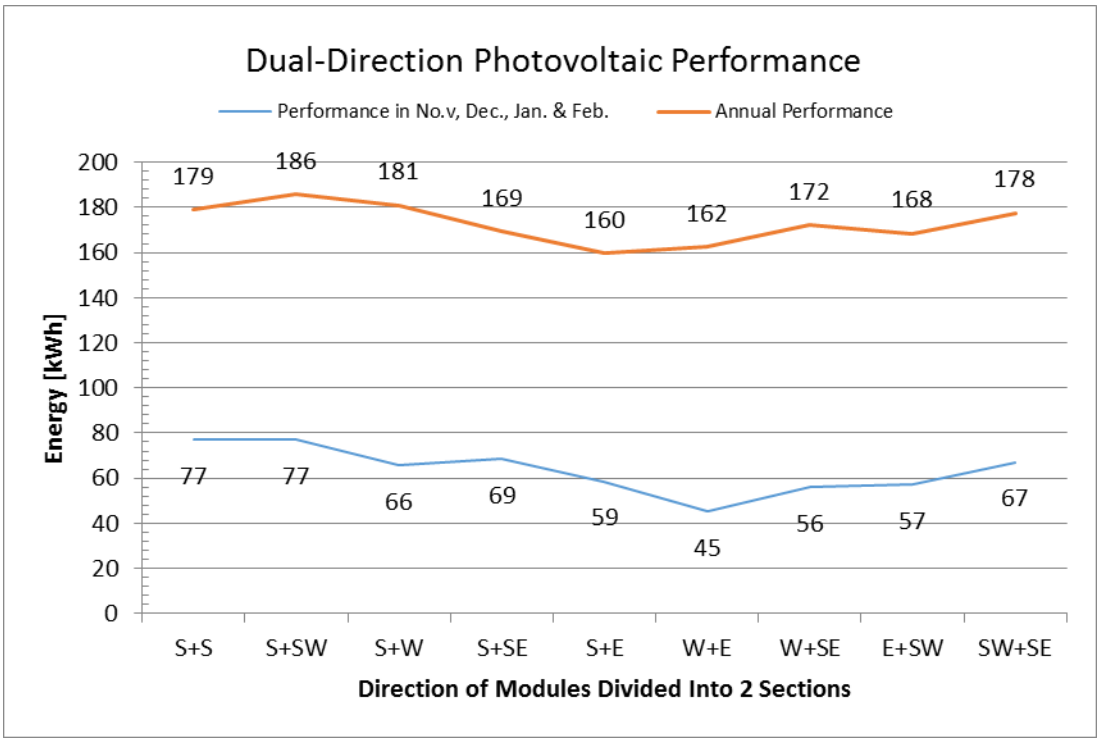

Figure 18.7 – Dual-Direction Photovoltaic Results

Figure 18.7 shows the results for two sections each of 1 m² with different orientation combinations. The highest performance is found with 1 m² facing south with a tilt angle of 50° and 1 m² facing southwest with a tilt angle of 65°. Applying the values from the designed system for the household with an annual electricity demand of 713 kWh, the S+SW option requires a battery capacity of 10.2 kWh, while the S+S option requires

a 10.1 kWh battery capacity. Therefore the best option is to keep the modules facing south with a tilt angle of 50°.

Appendix H Legislation in the Context off-grid Living in Denmark

Concerning off-grid living in Denmark, there is a lot of legislation which must be considered. This is both in the context of private energy production and with regard to connections to the energy and water grids. Further, the law regulates construction permission for buildings and what technical requirements the houses must fulfill. This chapter gives a brief overview over the most important legislation. Allotment gardens (danish: kolonihave) and summer houses are not considered, as they are not meant for year-round residence and special laws apply.

Appendix H.1 Legislation about Grid Connections

In the context of off-grid, the most interesting part of the legislation is whether there are any requirements that demands connection to the different energy grids; district heating, natural gas and electricity. In the Danish laws regarding energy supply there are both consumer rights, such as the right to be supplied by electricity, and grid connection obligations. The reasons for demanding consumers to connect to an energy grid are to obtain the social economic most feasible solution and to secure the economic foundation of the supply company, as it has large investments. Further there can be environmental consideration behind the demand - for example that a common (large scale) energy supply is more efficient than a lot of individual supplies. (Gram Mortensen, 2016, p. 336)

In the legislation, there is a difference between having a *demand for connection* and a *demand for consumption.* This means that a house owner can be instructed to be connected to a energy grid, but can always choose not to use the service.

Electricity

In the Danish '*Law of Electricity Supply*' there is no demand for connection to the electricity grid, as almost every existing and new houses are connected and most people would never live without a connection.

To the contrary, the law states that "A consumer of electricity can freely choose between electricity dealers and electricity products" (Retsinfo. - Electricity). According to (Gram Mortensen, 2016), this statement indicates a common right to be supplied by electricity no matter the location in Denmark. Before October 2015 the formulation was "Everyone has the right to be supplied by electricity, against payment, in this country."

Heating

For district heating and natural gas grids, the '*Law of Heat Supply*' §11 (Retsinfo. - Heating), the '*Law of Planning*' §15 (Retsinfo. - Planning) and the '*Law of Connection to Public Heating Grids*' §2 (Retsinfo. - Connection) gives the Danish municipalities the right to demand connection to the heating/gas grids for both existing and new buildings. The reasons for these demands are especially environmental considerations and economic security for the supply company. There is no demand for consumption in the law, but as fixed connection fees must be paid, it is in most cases economic unfeasible not to use the grid supply. The '*Law of Connection*

to Public Heating Grids' §15 states a number of cases, where grid connection cannot be demanded for existing building. This applies for example to buildings supplied by sustainable energy and waste energy and to low-energy buildings. (Gram Mortensen, 2016, p. 338)

Water

According to the '*Law of Water Supply'* §29 (Retsinfo. - Water) the municipal can demand buildings connected to an existing public water grid, if this is thought to be a desirable solution considering the local circumstances.

The municipal can also plan new public water supply grids for areas, where the existing water supply is found to be unsatisfying. It is however the *Minister of Environment and Food*, that based on the plan from the municipal decides whether the new public water supply grid should be installed.

It seems that the only allowed private supply of drinking water (for drinking and other household applications) is through a private water well, that conforms to the demands and is controlled according to the Danish *'Announcement of water quality and supervision with water supply systems'* (Retsinfo. - Water, 2016). The price for the establishment of a private well is estimated to be around 120,000 DKK (Bolius - Well).

Allowed use of rainwater

According to the Danish *'Announcement of water quality and supervision with water supply systems'* (Retsinfo. - Water, 2016) all water for household use must conform to a number of quality demands and the supply must be subjected to regular controls. An exception is, that rainwater used in toilets and/or washing machines is allowed, when the installation conform to the technical instructions in *'Rørcenter-anvisning 003'* (Rørcenter, 2012). Further, according to 'Law of authorization' (Retsinfo. - Authorization, 2014), the installations must be done by an authorized company. In existing one family houses a rainwater system can be install without permission, but in new houses and all other types of dwellings, a permission from the granted by the municipal. More information can be found at the Danish *Agency for Water and Nature Management* (Ministry of Environment and Food). Whether a dispensation can be obtained in special cases so that rainwater can be filtered and cleaned and used for drinking water is not known.

Waste water

With authority in the '*Law of Protection of the Environment'* (Retsinfo. - Environment) the '*Announcement of Waste Water Permissions'* (Retsinfo. - Waste water) describes the rules for disposal of waste water.

According to §12, house owners within areas served by a water treatment facility are obliged to be connected to the system. For areas with no sewerage system, there are a few different solutions, that the municipal can permit depending on the local conditions – such as the soil type. These solutions are accumulation tanks, seepage systems with a settling tank, biological/chemical cleaning systems and willow waste water cleaning systems with settling tank. For all the systems, the accumulation/settling tanks must be emptied when full, and the municipal council can demand the use of a public service for the disposal.

Appendix H.2 Legislation about Private Energy Production

Photovoltaic systems
For photovoltaic systems, there can be limitations in some areas set by the municipal council in the local plans (with authority in the '*Law of Planning'* §11a). In some municipalities, a building permission is required to install PV-modules on the roof of a building or on the ground. According to the Building Regulation, PV-systems and solar heating systems must be installed in a technically secure manner.

Household wind turbines (Nature Agency - Wind , 2015)
Larger wind turbines require a planning process by the municipal council, but household wind turbines (wind turbines under 25 m high) in rural areas can be installed based on a rural-area-permission alone, if they are placed in immediate connection to an existing building, approximately 20 meters.
In rural areas, the municipal council cannot make directions that prohibit household wind turbines in general, but they can condition rural-area-permission for example with regard to the appearance of the wind turbine. In urban zones (and summer house zones) the municipal council can prohibit household wind turbines by deciding this in the frame for the municipality plan. Further, there can be regulations in local area-plans made by the municipal council, that regulates the possibility for household wind turbines.
All electricity producing wind turbines must fulfill the regulations in *Announcement of Noise from Wind Turbines* (Retsinfo. - Wind).

Solitary wind turbines with a rotor areal under 5 m^2 are not included by the '*Announcement for assessment of environmental effects'* (Retsinfo. - VVM). For all other wind turbines, a screening for assessment obligation must be made. Normally there will not be any assessment obligation in rural areas, but it can be the case if there is a risk of annoying neighbors with shadows or noise, or the project includes more than one wind turbine.

According to '*Announcement for Technical Certification of Wind Turbines'* (Retsinfo. - Certification) all wind turbines with a rotor area above 5 m^2 must be type-certified (for turbine including specific tower and foundation) after the announcement by an instance approved by the Danish Energy Agency. Different rules apply for wind turbines with rotor areas under respectively 40 m^2 and 200 m^2. Paragraph four of the announcement defines some cases, where the Danish Energy Agency can give dispensation for the certification demand for wind turbines with up to 40 m^2 rotor area. This is in context of research and educational purposes or for home build wind turbines (build by the owner) on a defined land area.

Subsidies for sustainable energy production
The '*Law of Promotion of Sustainable Energy'* (Retsinfo. - Energy) describes the price supplements for grid connected sustainable technologies (and the requirements for obtaining the subsidy). In the context of off-grid, these rules are not relevant.

Appendix H.3 Legislation about Building Sites and Technical Requirements

The '*Law of Planning*' (Retsinfo. - Planning) regulates the municipal councils' authority to give permission to new buildings. In general, permissions to new buildings can only be given for areas, that are connected to existing urban zones or villages. It is almost impossible to plan new buildings in the open land.

With authority in the '*Law of Building*' (Retsinfo. - Building), the '*Building Regulation*' (Building Agency) defines the requirements for new buildings and renovations with regard to dimensioning, energy use, indoor climate, technical installations and the like.

Appendix H.4 Available Information about Decided Municipal Area Plans

On the webpage Plansystem.dk by the Danish Business Authority, a lot of information is available about for example municipal area plans, protected areas, heating plans and water plans.
For most – if not all – municipalities, the general municipal plan and local area plans can also be found on the municipal webpage.

Appendix H.5 Summary of Legislation

If a house in Denmark should be off-grid and the owners will avoid to pay for connections to public grids, a location without public heating supply - and without public water and sewage if this is important – must be found. Such locations are mostly found in rural areas with solitary buildings, where it is almost impossible for the municipal council to give a building permission. So, depending on the wanted off-grid-degree, the realistic possibilities is to find an existing house in a rural area and disconnect it from the electricity supply, or build a new house in connection to a small village, where there is no public heating grid.

Appendix H.6 Municipal Plans for Building Area at Ebeltoft

The building area of interest for 'Project Grobund' is located just southwest of Ebeltoft in Syddjurs Kommune, as illustrated by Figure 18.8.

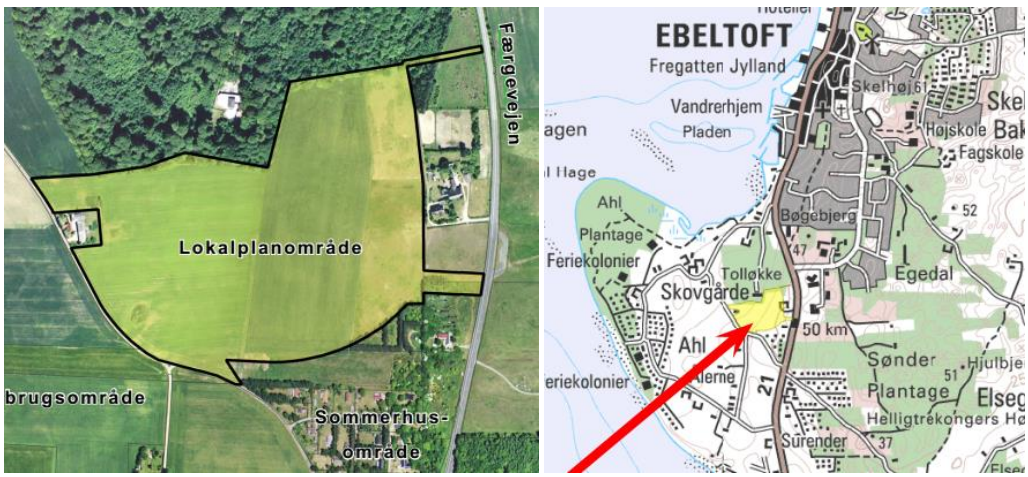

Figure 18.8 – Local area plan L300 in Syddjurs Municipality (Syddjurs Kommune, L300)

According to local area plan LP300 (Syddjurs Kommune, L300) the area has been designated as a housing area in urban zone, with the following obligations (among other):

- Buildings must be connected to Ebeltoft District Heating A.m.b.a
- Buildings must be connected Syddjurs water supply and to the public sewer system
- The external walls of buildings must be made of bricks and the maximum slope of the roofs is 5 %.
- No part of the building must be higher than 7.5 meter.
- The municipal council can give dispensations for small changes deviations, that is not against the overall principals of the area plan.
- Household wind turbines and PV-systems are not mentioned in the local plan.

In the general municipal plan (Syddjurs Kommune, Plan) only the following are stated with regard to private energy production.

- When placing PV-systems in the open land, the influence on the landscape should be considered.
- When placing PV-systems on flat roofs, the panels should not rise more than 1 meter above the roof.
- Household wind turbines can be placed outside the designated wind turbine areas, in connection to solitary buildings, if it is considered to be acceptable with regard to the protection of the open land.

Appendix H.7 Suitability of Location for Off-grid Living

Based on the above information about the obligations in the local area plan, the area is thought to be unsuitable for both off-grid living and for buildings with alternative designs and building materials. A new local area plan must be made, if the area should be usable for Project Grobund. Nothing specific could be found about household wind turbines in urban zones, but based on the general frame for the area, it is thought to be unrealistic, that the municipal council would allow it.

Appendix I Literature Review of TEG's

As it is considered to integrate thermoelectric generators with the proposed mass oven, a short literature study regarding the thermoelectric technologies is performed in order to better assess the potential of this technology as an integrated part of the household's energy production.

Only a few papers have focused on heat recovery through heating of water simultaneously with electricity generation. As early as in 1996 a fairly similar study was conducted in Northern Sweden.

In this study (Killander, 1996), a number of rural house far from the electricity grid, was surveyed in order to establish the population's needs and requirements. The general opinion was that a small off-grid unit able to generate 12V light, enable television transmission for a few hours a day and operate a fresh water pump, would satisfy the requirements of such rural houses, households with fairly similar presumptions as the houses in *Project Grobund*. This study used a wood-stove with the cold side of the TEG towards ambient air. They found that the generator reached 10 Watts of power in the morning, when the ambient temperature was low, decreasing to 4 Watts during the day. Interestingly, the study experienced that as long as a constant temperature difference across the elements was obtained, a decrease in the average temperature could lead to twice the increase in power, due to the figure-of-merit (ZT-curve) of the thermoelectric element. This experience can be used with great advantage in our experiments, as it has been shown, that working in lower temperature ranges can be beneficial.

In a review of thermoelectric generator studies (Gao, Huang, Li, Qu, & Zhang, 2016), a similar conclusion is reached, as shown in Table 18.7 – Commercial TEG modules (Gao, Huang, Li, Qu, & Zhang, 2016) Figure 18.9 – TEG output (Gao, Huang, Li, Qu, & Zhang, 2016). It is clearly illustrated, that as long as ΔT remains the same, a decrease in average temperature results in higher electricity generation. Furthermore, this study establishes an overview of the results of previous tests, as shown in Table 18.7. As can be seen, experiments with forced convection by water have been carried out, achieving between 2.1 to 10.0 Watts with a ΔT of approximately 100K.

Heat sink	Watt /module	ΔT	Module	Manufacturer	References
Air natural convection	1 W	100	HZ-20	Hi-Z	Nuwayhid et al. [24].
Air natural convection	4.2 W	256	HZ-20	Hi-Z	Nuwayhid et al [25].
Air natural convection	3.4 W	127	HZ-20	Hi-Z	Nuwayhid et al [26].
Air natural convection	2.4 W	150	TEP1-1264-3.4	Thermonamic	Lertsatitthanakorn [27]
Air forced convection	3.5 W		HZ-20	Hi-Z	Killander et al. [29,30].
Air forced convection	N/A	-	HZ-20	Hi-Z	Bass and Thelin [31]
Air forced convection	5–10 W		HZ-14	Hi-Z	Mal et al. [49].
Air forced convection	5 W		HZ-14	Hi-Z	Srivastava et al. [52–54].
Air forced convection	5.3 W	210	TEG 12610-5.1	Tecteg	O'Shaughnessy et al. [47].
Air forced convection	4 W		TEP1-12656-0.6	Thermonamic	Mastbergen et al. [40].
Air forced convection	1.7 W	160	TEP1-12656-0.8	Thermonamic	Champier et al [58].
Water natural convection	2.3 W	160	TEP1-12656-0.8	Thermonamic	Champier et al. [58].
Water natural convection	7.6 W	120	TEP1-12656-0.6	Thermonamic	Champier et al. [59,60].
Water natural convection	3.4 W	158	G1-1.4-219-1.14	Tellurex	Juanicó et al. [63].
Water forced convection	5.7 W	100	G1-1.4-219-1.14	Tellurex	Rinalde et al. [64].
Water forced convection	7.9 W		TEP1-12656-0.6	Thermonamic	Goudarzi et al. [65].
Water forced convection	2.1 W	112.8	TEG-127-230-32e	Thermalforce	Brazdil and Pospisil [66].
Water forced convection	10 W		HZ-20	Hi-Z	Allen et al. [67,68].

Table 18.7 – Commercial TEG modules (Gao, Huang, Li, Qu, & Zhang, 2016)

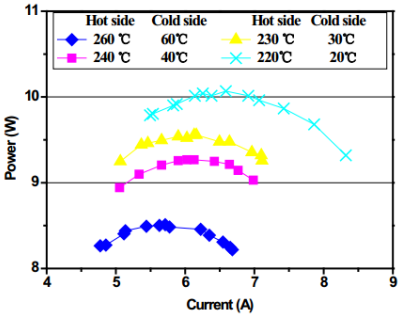

Figure 18.9 – TEG output (Gao, Huang, Li, Qu, & Zhang, 2016)

In the paper of (Sornek, Filipowicz, & Rzepka, 2016), a stove-fireplace with heat accumulation was established in order to test the performance of a TEG under prolonged conditions with lower flue gas temperature. The system took a forced water cooled approach, but found a limiting factor to the TEG potential, as the fairly low air velocity required for heat storing purposes in the brick mass, decreased the output significantly as the operating range was limited. In this study, a flow of cold water was constantly in contact with the TEG

and produced a temperature increase of 6K at a flow of 5 L/min. Similarly, this study found that TEG's with lower operating temperatures are found to be better at generating steady electricity outputs. Also noteworthy from this paper was that the electrical outputs in the experiments corresponded to less than 50% of the outputs recorded under laboratory conditions of the tested TEG's.

Additionally, several papers report more studies of TEG's in general and all papers agree on a future potential for this technology. Among these are smaller TEG's relying on a ΔT of as little as 10K to operate sensors or small actuators (Glosch, Ashauer, Pfeiffer, & Lang, 1999). While another paper, reports of large scale operations generating up to 185 MWh of electricity per year, by recovering waste heat from a large scale Thermal Oil Heater of 40 MW, this paper suggest small improvement can yield a TEG efficiency of approx. 8%.

Although most papers report little to no economic value in technology as of the current state, unless the TEG's are combined with a form of heat recovery, in which case 4% electrical efficiency and 60-80% thermal efficiency can be achieved (Zheng, Yan, & Simpson, 2013), (Zheng, Liu, Yan, & Wang, 2014).

Overall, the papers are positive of the direction of the thermoelectric generators and believe this technology can be become an important element in the future energy generation on a global level, for large scale solar power plants and waste heat recovery systems, as well as small scale generators for rural villages or off-grid houses.

Appendix J The geostrophic wind

The geostrophic wind is around 1-1.5 km above ground and is not particularly affected (slowed down) by friction from the terrain (DWIA - Geostrophic wind). Figure 18.10 shows that the mean geostrophic wind over Denmark is around 10-11 m/s and that it decreases from west towards east. In advanced wind calculation software this wind can be used to calculate the wind conditions at different heights based on the general roughness of the terrain. This method was used by Energy- and Environment Data (EMD) and Research Center Risø to develop a wind resource map over Denmark, which is seen in Figure 18.11 for a height of 25 meter. The map shows, that there are significant differences in the mean wind speed in Denmark, with the highest values at the coasts and the lowest in the inland regions. The map does not include the effect of local obstacles.

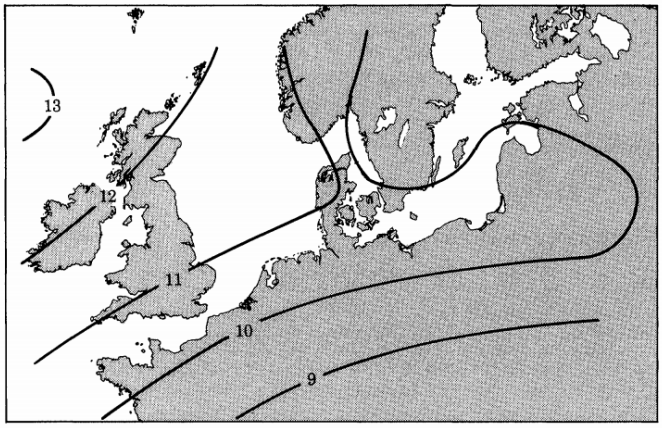

Figure 18.10 – Mean geostrophic wind over Northern Europe in m/s. (Troen & Petersen, 1989, p. 31)

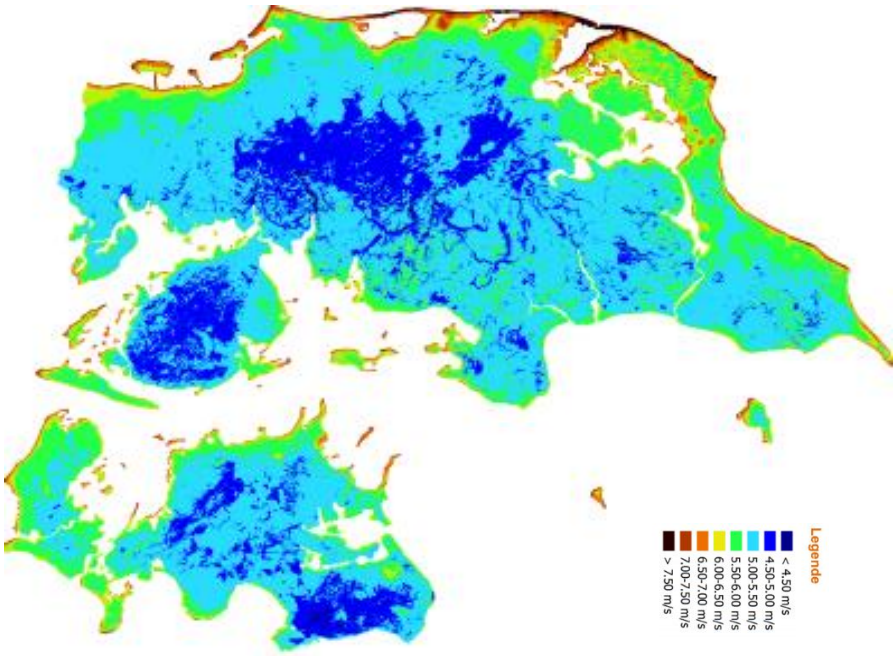

Figure 18.11 – Wind resource map for Denmark (EMD & Risø, u.d.)

Appendix K Adjustment of wind data for change of roughness

The European Wind Atlas (EWA) (a wind resource map developed by Risø National Laboratories and the Technical University of Denmark) is based on a computer model called *Wind Atlas Analysis and Application Programme* (WAsP). The model is based on the transformation of measured wind data and a method for changes of roughness is described. This theory will be explained in this section and implemented in a simplified way in the *Off-grid Simulation Tool* (compared to WAsP, where the method is more refined and detailed). (Troen & Petersen, 1989). The simplifications will give a higher uncertainty for the calculations and if a very detailed evaluation is wanted, a more sophisticated method/software should be used.
Figure 18.12 shows the wind profile before and after a change of roughness in the terrain. The effect of the change increases with the distance x .The height h_{bl} of the developing internal boundary layer can be found from Equation 18-1. Above h_{bl}, the wind profile is equal to that before the roughness change.

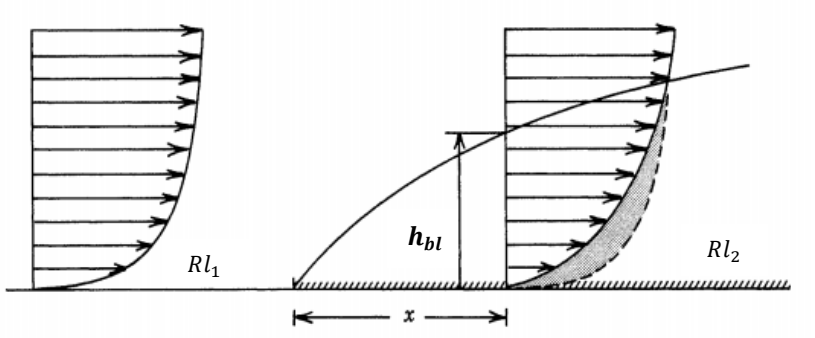

Figure 18.12 – Change of wind profile after a change in roughness (Troen & Petersen, 1989). Rl_1 and Rl_2 is the roughness lengths before and after the change, h_{bl} is the height of the internal boundary layer and x is the distance after the change.

$$v = v_{ref} \cdot \frac{\ln(h_{ref}/Rl_2) \cdot \ln(h_{bl}/Rl_1)}{\ln(h_{ref}/Rl_1) \cdot \ln(h_{bl}/Rl_2)}$$

Equation 18-1

where v_{ref} it the wind speed at the reference height h_{ref} with roughness length Rl_1. v is the wind speed at h_{ref} with the new roughness length Rl_2. h_{bl} is the boundary layer height.

The height of the internal boundary layer depends on the roughness and the distance after the change. It can be found from the following relation or a graph in The European Wind Atlas (page 83).

$$\frac{h_{bl}}{Rl_{max}} \cdot \left(\ln\left(\frac{h_{bl}}{Rl_{max}}\right) - 1\right) = 0.9 \cdot \frac{x}{Rl_{max}}$$

Equation 18-2

The method behind Equation 18-1 is, that it applies Equation 9-1 twice. First it calculates the factor for the wind speed at the boundary layer height from the reference height and the initial roughness length. Then it calculates the factor from the boundary layer height and down to the reference height again with the new roughness length. In other words; it follows the wind profile for the initial roughness length up to where the

wind can be seen as unaffected by the terrain, and then it follows the wind profile for the new roughness length down to the reference height again. Because of this, Equation 18-1 can also be used to change the wind profile between roughness classes for different locations, which will be used later in this chapter.

Neglecting significant obstacles close to the location (within 1000 meter) for now, the actual wind profile at a location is the result of the terrain and its different roughness types upwind from the location, which changes with the direction. In wind resource maps, such as the European Wind Atlas, the purpose is to show the wind resources on a general scale. To do this the measurement data has been adjusted in order to remove influences of obstacles and local terrain roughness. Most of the measurements are recorded at heights around 6-12 meter above ground (Troen & Petersen, 1989, p. 112) and it is stated, that in this context the roughness of the terrain is relevant in a radius of 10-20 km around the location (called the *equilibrium distance*). The reason for this is, that the boundary layer approaches an equilibrium between the pressure gradient force and the friction. The longer away from the location, the less impact does the surface friction have on the equilibrium profile at the location (Troen & Petersen, 1989, p. 571). In this report, a 15 km equilibrium distance is used as radius for the roughness estimations.
When describing the terrain around a location, it is normally divided into 12 sections of 30 degrees. For each of these sections the roughness is evaluated and the entire circle is called the *roughness rose* (DWIA - Roughness rose, u.d.). In order to estimate the wind profile in Ebeltoft with the available DRY data, roughness roses for both the measurement station in Assens and the project location in Ebeltoft have been made. These roughness roses can be seen in Appendix T and Appendix U .

Figure 18.13 shows an example of most of sector one, two and three from the DMI measurement station at Assens. The terrain closest to the location must be given a high weight in the roughness model, so the first kilometer is considered separately later. In the distance from 1-15 kilometer upwind, Sector 1 is divided into two areas. The first area ($A_{1.1}$) is the small town Assens with a roughness length of $Rl_{1.1} = 0.4$. Around 4.7 km upwind the terrain changes and area two ($A_{1.2}$) is farmland with a lot of hedgerows, some scattered forest areas and small villages – roughness length is estimated to be $Rl_{1.2} = 0.3$. In this sector there are relatively uniform terrains within the two areas. In cases where there are parts with different terrain types that cannot be divided into different areas, an area weighted mean of the roughness length is calculated for each of these parts.

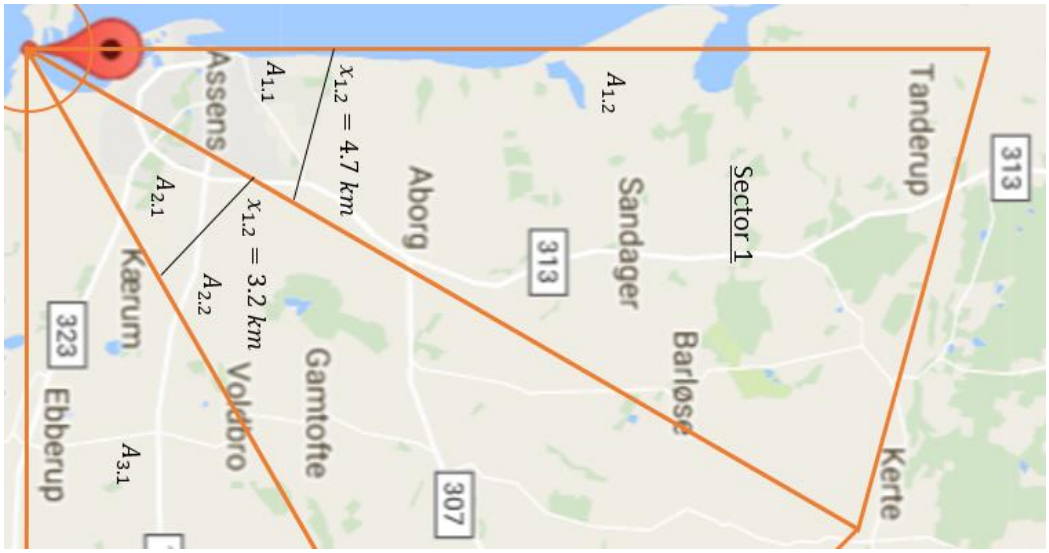

Figure 18.13 – Sector 1, 2 and 3 of roughness rose around DMI measurement station in Assens

After the classification of the roughness lengths in the sector, the average/effective roughness length must be calculated. Because of the mentioned equilibrium in the boundary layer, the roughness of the terrain must gradually lose importance the farther away we get from the location.
In the European Wind Atlas (p. 573), this is obtained by applying an exponential distance factor to the areas, but the method is not described in details, so it cannot be implemented in this report. Instead a method of inverse-distance weighted geometric mean roughness length is used, as this is described in (ADoEC, 2009). This method weight the roughness of each area in the sector according to its fraction of the total area and the distance from the location – i.e. a weighting value of area-fraction/distance. With these weighted areas, the geometric mean is calculated. Using Sector 1 of Figure 18.13 as an example, the evaluation would be as presented in Table 18.8 and the following calculation.

Terrain type	Area $[km^2]$	Area fraction (Af)	Distance	Weighting (Af / Dist.)	Roughness length
Town	5.65	0.09	2.85	0.033	0.4
Agricultural land w. many obstacles	54.4	0.91	9.85	0.092	0.3
Total	60	1		0.125	

Table 18.8 – Parameters for calculation of the inverse-distance weighted geometric mean roughness length

With these values the inverse-distance weighted geometric mean roughness length is calculated as:

$$\overline{Rl} = (0.4^{0.033} \cdot 0.3^{0.092})^{(1/0.125)} = 0.324$$

As mentioned earlier, the first kilometer around the location is considered separately, because it has relatively high impact on the wind condition. In this way, it can be described more detailed and each sector of the circle can be given its own roughness length based on the inverse-distance weighted geometric mean method. Figure 18.14 shows an example of the first kilometer of Sector 3 from the measurement station at Assens. Here the first 250 meter is water/marsh with a low roughness length, the next 300 meter is town

with a high roughness length and the last 450 meter is open agricultural land. With the weighting method, the mean roughness length becomes 0.13.

Figure 18.14 – Mean roughness length calculation for Sector 3 at Assens

Appendix L Discussion of the Roughness Change Function

In the *Off-grid Simulation Tool* one of the wind data sets from the Design Reference Year (DRY - discussed in section 9.1.1) must be chosen for the calculation. For the chosen data, the general terrain roughness can be changed in order to estimate the production in other locations. To do this, the roughness length for the terrain where the measurements are recorded must first be estimated. With this 'initial' roughness length and the chosen new roughness length, the tool adjusts the wind speed values by using the roughness change equation (Equation 18-1). This estimation of the wind speeds at other locations is very rough, as it in most cases is very difficult to describe the area in a 15 km radius around a location with a single value for roughness length. Further, the data is not adjusted for obstacles at neither the measurement location or the new location – i.e. all the results will assume the same obstacles as the measurement location. The full method for roughness and obstacles evaluation described in Appendix K and Appendix F is a significantly better way to estimate the roughness conditions, but requires extensive work for each location.

Table 18.9 shows the electricity generation from a 1 kW Air Force 1 wind turbine at different roughness classes based on the DRY wind data from Thyborøn. The measurements from Thyborøn are the DRY dataset with the highest mean wind speed. The measurement station is placed between the North Sea and Nissum Bredning (fjord), as indicated by Figure 18.15. The land areas to north, east and south are relatively open agricultural land with scattered houses and hedgerows with an estimated roughness length of 0.055 m. Based on this landscape, the overall roughness length for Thyborøn has been estimated to 0.0024 and this value is used as initial roughness length for Table 18.9.

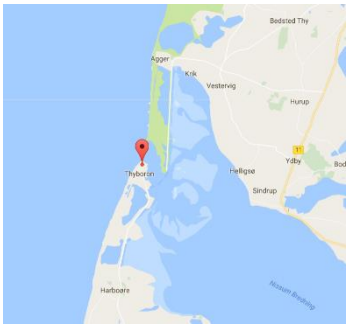

Figure 18.15 – DMI measurement station at Thyborøn

Yearly electricity generation for 1 kW Air Force 1 wind turbine at different roughness classes, based on DMI measurements from Thyborøn with an estimated roughness length of 0.0024 m.			
Class	Length	Terrain type	Generation [kWh]
0	0.0002	Water surface	3626
0.5	0.0024	Smooth surfaces, such as mowed grass.	2985
1	0.03	Open, almost level agricultural land	2057
1.5	0.055	Agl., some houses, few hedgerows (d. 1250 m)	1786
2	0.1	Agl., some houses, more hedgerows (d. 500 m)	1500
2.5	0.2	Agl., many houses and hedgerows (d. 250 m)	1157
3	0.4	Villages, agl. with a lot of tall hedgerows or forests.	809
3.5	0.8	Large cities with tall buildings.	478
4	1.6	Very large cities with very tall buildings.	200

Table 18.9 – Electricity generation from 1 kW Air Force 1 at different roughness classes (based on wind data from Thyborøn)

As seen from Table 18.9 the roughness of the terrain around the location has a high impact on the wind speed and thus the electricity generation from the wind turbine. The only way available in this project to validate the roughness change calculation, is to compare the results with the calculations for the other DRY datasets.

At Holbæk measurement station, the surrounding area is agricultural land with many houses and hedgerows and some areas with cities and forests. A large part of the north-east and east sectors is water surface (fjord). The overall roughness length is estimated to be around 0.2 m, which according to Table 18.9 should give a yearly electricity generation around 1157 kWh. When the actual wind data from the measurement station is used, the electricity generation is calculated to be 1138 kWh.

At Karup measurement station, the landscape is agricultural land with a lot of very close standing hedgerows, larger forest areas and a many small towns. The general mean roughness is estimated to be close to 0.4, which according to Table 18.9 should give a yearly electricity generation around 809 kWh. When the actual wind data from the measurement station is used, the electricity generation is calculated to be 813 kWh.

At Assens measurement station the landscape is agricultural land with a varying roughness length around 0.15-0.3 m from north to north-east, while the rest of the sectors are mainly water surface. It is difficult to combine these different terrains to a mean roughness length, but as the terrain in the directions with prevailing winds (west and south) are water, it is thought to be relatively low - maybe around 0.03-0.05. From Table 18.9 this should give a yearly electricity generation around 2057-1786 kWh. When the actual wind data from the measurement station is used, the electricity generation is calculated to be 2067 kWh.

These considerations show, that the roughness change calculation can be expected to give a realistic result. However, it must be remembered, that it is a rough estimate and that obstacles and local terrain conditions are not taken into consideration. The DMI measurement stations are located at placed in the landscape, with as few close obstacles as possible. This means, that the calculation will deviate from reality, if there is a lot of obstacles at the actual location.

Appendix M Wind Turbine Generation as a Function of Height

When the height of a wind turbine is changed, the production increases or decreases as the wind condition changes. Two factors influence the change of wind speed with height; the general logarithmic wind profile due to the terrain roughness and the obstacles around the location. At a location with a lot of high obstacles, increasing the height of the turbine can have a great value.

Figure 18.16 shows the yearly production from the 1 kW Air Force One wind turbine at the location near Ebeltoft as a function of height. The values are calculated with the *Off-grid Simuation Tool*, where Equation 9-1 (the logarithmic wind profile) has been implemented, so that the user can estimate the electricity generation at different heights. It is seen, that at the location near Ebeltoft, a higher tower can increase the generation significantly.

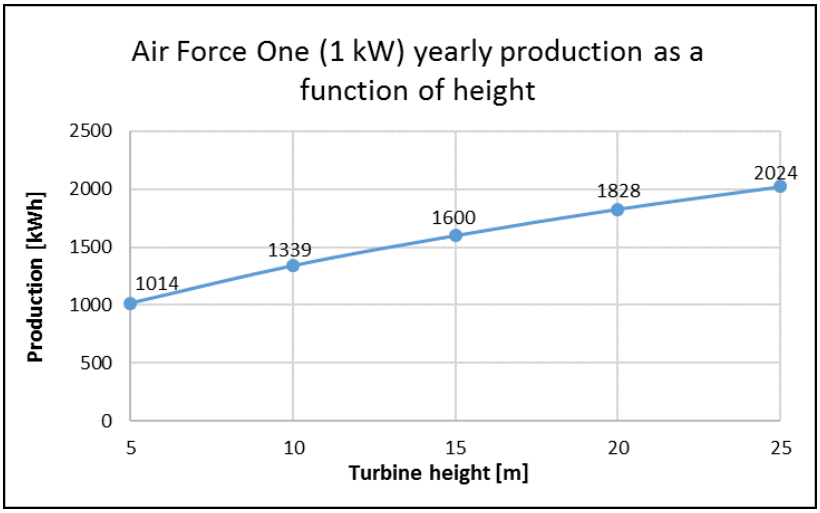

Figure 18.16 – Production from 1 kW Air Force One wind turbine at Ebeltoft for different heights

Appendix N Important effects not included in the *Off-grid Simulation Tool* wind model

Contours of the landscape (orography)

The shape of the landscape can affect the local wind, as the air speeds up or slows down when it is forced over or between hills and mountains. These effects are not included in the simulation tool, as it requires advanced methods to evaluate the terrain from a map with contours and calculate the wind behavior.

One effect is the *tunnel-effect,* where the wind speeds up between two hills or buildings, because the available area is decreased. This effect can increase the wind speed significantly - for example from 6 to 9 m/s. However, depending on the specific conditions the effect can create turbulence that decreases the efficiency of the wind turbine and increases the wear on the mechanics.

Another effect is the *hill-effect*, where the wind speeds up when it is forced over a hill. Due to this, it is generally efficient to place a wind turbine on the top of a hill, as it both increases the height above the terrain and adds the hill-effect. Depending on the form and roughness of the hill, turbulence can also be a problem in this case. (DWIA - Orography, u.d.)

In some cases, these effects can have significant influence on the wind power at a specific site, and special care should be taken if the *Off-grid Simulation Tool* is used in places where these effects could be present.

Atmospheric instability

The logarithmic wind profile relations that are used assume atmospheric stability, which mean that there is no temperature difference between the ground surface and the air. If there is a temperature difference, this will affect the wind flow. In The European Wind Atlas (Troen & Petersen, 1989, p. 567) it is stated that stability modifications are often thought to be relatively unimportant and thus neglected in the context of wind energy.

Wind displacement height

In forests, cities and other places with high and dense terrain the wind profile will not just be slowed down, but will be lifted over the area (i.e. the top of the forest/city can be viewed as the surface). This means that around 66-100 % of the height of the forest/city should be subtracted from the height of the wind turbine in order to get realistic results. (EMD - Map, 2001, p. 8)

This is not included in the *Off-grid Simulation Tool,* but if a wind turbine is placed in for example a forest area, the height of the forest can be subtracted manually from the wind turbine height to account for the effect.

Appendix O Pressure Table for TEG Construction

The following table has been created based on the spring constant of the used piano springs and the distance per round of the bolts on the M6 threaded rods.

Round [mm]	Total Pressure [N]	Total Weight [kg]	Pressure per area [N/cm²]	Weight per area [kg/cm²]
1	207	21	6.59	0.67
2	413	42	13.17	1.34
3	620	63	19.76	2.01
4	826	84	26.34	2.69
5	1033	105	32.93	3.36
6	1239	126	39.51	4.03
7	1446	147	46.10	4.70
8	1652	168	52.69	5.37
9	1859	189	59.27	6.04
10	2065	211	65.86	6.71
11	2272	232	72.44	7.38
12	2478	253	79.03	8.06
13	2685	274	85.61	8.73
14	2891	295	92.20	9.40
15	3098	316	98.78	10.07
16	3304	337	105.37	10.74
17	3511	358	111.96	11.41
18	3717	379	118.54	12.08
19	3924	400	125.13	12.76
20	4131	421	131.71	13.43

Table 18.10 – Pressure table for TEG construction

Appendix P Thermal conductivity test of straw element samples

Five different samples of building elements made of compressed straw were tested with a Guarded Hot Plate Apparatus λ-meter EP500 from (Lambda Messtechnik) at the climate laboratory Aalborg University (Figure 18.17).

Figure 18.17 - λ-meter EP500

The sample for testing is placed between the 'hot' and 'cold' heat plates with insulation around. The samples are wrapped in two layers of plastic foil with thermal gel between to ensure a good connection between the sample and the heat plates.
The apparatus sets a constant temperature difference over the sample with a constant heat flux. When a steady state condition is reached, the thermal conductivity (λ-value) is calculated based on the temperature difference and the heat flow. The steady state condition for all the tests is defined as a maximum change of the calculated λ-value of 0.3 % over 200 minutes.

For each sample, three measurements are made with different temperature sets. All of them have a temperature difference of 15 ℃ between the plates, but with the following temperature sets: $47.5 - 32.5$℃, $32.5 - 17.5$ ℃ and $17.5 - 2.5$ ℃. These temperatures give the samples mean temperatures of respectively 40, 25 and 10 ℃ at steady state.

Appendix P.1 Results of conductivity tests

Sample 1

- Dimensions: 150 x 150 mm
- Thickness: 49.7 mm
- Weight: 356 g

Test temperature set [℃]:	$47.5 - 32.5$	$32.5 - 17.5$	$17.5 - 2.5$
Test mean temperature [℃]:	40	25	10
Measured λ $[W/(m \cdot K)]$:	0.0784	0.0713	0.0677
Deviation	0	0	0
Calculated $\lambda - 10$ $[W/(m \cdot K)]$:	0.0677	TC:	0.3563

Sample 1b

- Dimensions: 150 x 150 mm
- Thickness: 47.5 mm
- Weight: 338 g

Test temperature set [°C]:	$47.5 - 32.5$	$32.5 - 17.5$	$17.5 - 2.5$
Test mean temperature [°C]:	40	25	10
Measured λ $[W/(m \cdot K)]$:	0.0775	0.0704	0.0668
Deviation	0	0	0
Calculated $\lambda - 10$ $[W/(m \cdot K)]$:	0.0668	TC:	0.3553

Sample 2

- Dimensions: 150 x 150 mm
- Thickness: 52.2 mm
- Weight: 336 g

Test temperature set [°C]:	$47.5 - 32.5$	$32.5 - 17.5$	$17.5 - 2.5$
Test mean temperature [°C]:	40	25	10
Measured λ $[W/(m \cdot K)]$:	0.0729	0.0659	0.0623
Deviation	1	1	0
Calculated $\lambda - 10$ $[W/(m \cdot K)]$:	0.0623	TC:	0.3540

Sample 3

- Dimensions: 150 x 150 mm
- Thickness: 53.1 mm
- Weight: 346 g

Test temperature set [°C]:	$47.5 - 32.5$	$32.5 - 17.5$	$17.5 - 2.5$
Test mean temperature [°C]:	40	25	10

Measured λ $[W/(m \cdot K)]$:	0.0767	0.0694	0.0662
Deviation	0	0	0
Calculated $\lambda - 10$ $[W/(m \cdot K)]$:	0.0662	TC:	0.3517

Sample 4

- Dimensions: 150 x 150 mm
- Thickness: 58.1 mm
- Weight: 354 g

Test temperature set [℃]:	$47.5 - 32.5$	$32.5 - 17.5$	$17.5 - 2.5$
Test mean temperature [℃]:	40	25	10
Measured λ $[W/(m \cdot K)]$:	0.0778	0.0693	0.0653
Deviation	0	1	0
Calculated $\lambda - 10$ $[W/(m \cdot K)]$:	0.0653	TC:	0.4147

Conclusion

The thermal conductivity of the tested elements is between 0.0623 and 0.0668 W/mK, the assumed value in the BSim model is set to 0.068 W/mK which is a bit conservative compared to the test results.

Appendix Q Validation of Off-grid Simulation Tool

In order to further compare the results of the *Off-grid Simulation Tool* and Homer the month of January has been analyzed. Table 18.11 shows the annual comparison of the two methods.

	PV Performance kWh/yr	WT Performance kWh/yr	Excess Electricity kWh/yr	Average State of Battery %
Off-grid Simulation Tool	768,0	1287,4	1341,6	94,7
HomerPro Microgrid Analysis Tool	776,8	1309,2	1345,7	95,1
Deviation [%]	1,1	1,7	0,3	0,4

Table 18.11 – Annual Results of Off-grid Tool and Homer Pro

The photovoltaic generation, wind turbine generation and state of battery during the month of January have been illustrated in respectively Figure 18.18, Figure 18.19 and Figure 18.20.

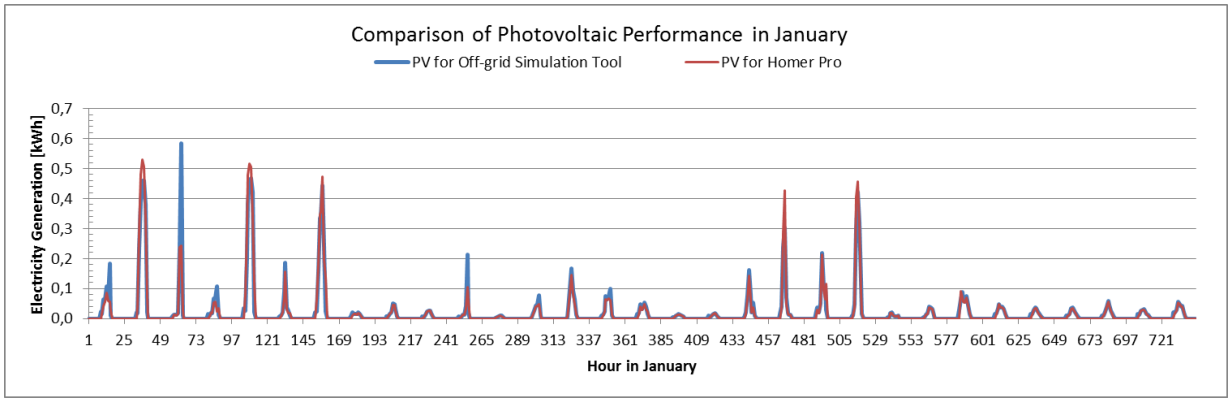

Figure 18.18 – Comparison of photovoltaic performance for January

The PV performance is overall very similar, but in a few cases the *Off-grid Simulation Tool* calculates a slightly higher output. The deviations are found around 3 or 4 pm close to sunset. This indicates that the deviation occurs due to either the calculated angle of the sun or possibly Homer assumes a horizon cut-off (typically 15° in simulation tools) whereas the *Off-grid Simulation Tool* does not take into account any horizontal shading.

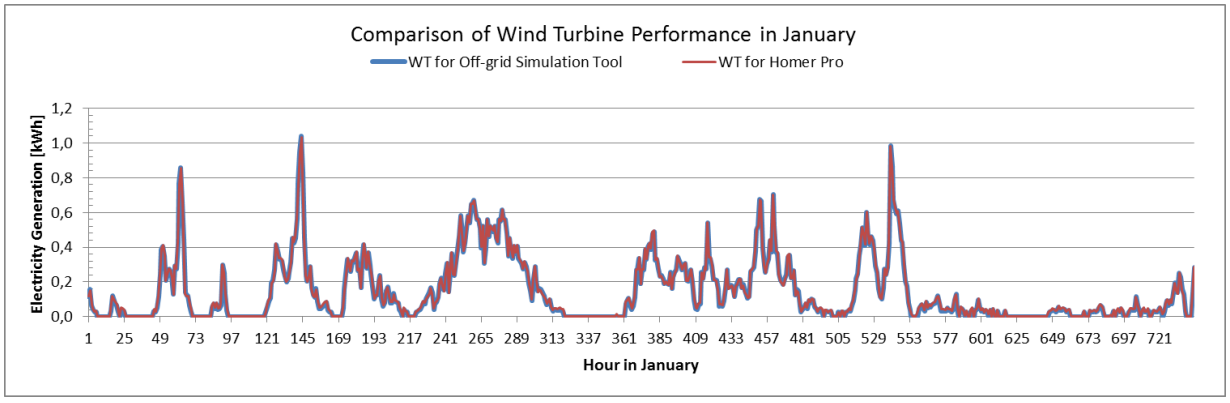

Figure 18.19 – Comparison of wind turbine performance for January

The wind turbine output for January is identical. The deviations which affect the annual outputs are found at high wind speeds (+14 m/s) where the regression method applied in the *Off-grid Simulation Tool* differs slightly from the power curve (which is used in the Homer model).

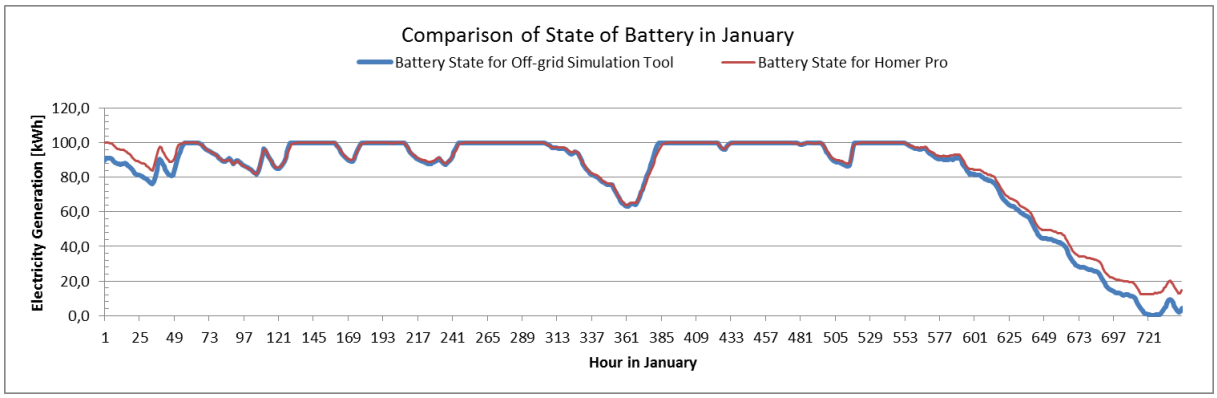

Figure 18.20 – Comparison of state of battery for January

It can be seen from Figure 18.20 that Homer assumes a 100% battery capacity at the first hour of the year (the last hour of the year has a value of 90.31% in Homer and 89.15% in the *Off-grid Simulation Tool*). The *Off-grid Simulation Tool* assumes a 100% capacity at the 1st of June at 12 pm instead, since the electricity generation is higher in this period and therefore 100% capacity is more likely.

The deviation at the end of January is assumed not to be caused by a difference in electricity generation, as it can be seen from the previous figure that these are identical for the period. Instead the deviation might be due to the performance of the battery in either of the methods. Either way, the deviation is found to be acceptable and the calculation method in the *Off-grid Simulation Tool* is thought to give realistic results.

Appendix R Evaluation off stated power curve and real life efficiencies for wind turbines

In Section 10 of this report, the method used for calculating the wind turbine generation in the Off-grid Simulation Tool is described. The method calculates the generation based on the power curve, that the user states in the simulation tool. This means, that if the power curve stated by the manufacturer is not correct the method will calculate unrealistic generations. As mentioned shortly in the initial review of household wind turbines in Section 5.8, most real life tests show generations below the predicted.

If a manufacturer has stated a power curve, the claimed efficiency of the wind turbine can be evaluated by comparing the stated power to the energy in the wind (calculated with Equation 10-3).

This is done for the 1 kW Air Force 1 wind turbine (described in Section 10.2) and the results are presented in Table 18.12. The power in the wind is calculated with two densities of respectively 1.34 kg/m^3 at -10 °C and 1.17 kg/m^3 at 30 °C (Gribble, u.d.), as the conditions under which the power curve is stated is not known. This results in an efficiency interval for each wind speed.

Wind [m/s]	Stated power [W]	Power in wind [W]	Claimed efficiency [%]
3	26	38-44	60-68
4	55	90-103	53-61
5.5	135	234-268	50-58
6.5	227	386-443	51-59
7.2	296	525-602	49-56
8.6	450	895-1025	44-50
9.5	558	1206-1382	40-46
11	768	1873-2145	36-41
12.5	1002	2748-3148	32-36
14	1142	3861-4422	26-30

Table 18.12 – Stated power curve for Air Force 1

Table 18.12 shows that for the Air Force 1 turbine, the claimed efficiency is from 26 to 60 % depending on the wind speed (if we take the low estimate – high air density). As the theoretical Betz Limit (mentioned in Section 10.1) is 59 % and large wind turbines convert up to 45-50 % of the energy in the air at peak efficiency (NSW Government, 2010). These values indicate, that the efficiencies in Table 18.12 are unrealistic.

For smaller wind turbines, the efficiencies are lower due to relatively more turbulence around the blades (WindpowerProgram). At (WindpowerProgram) they tested five small wind turbines and found peak efficiencies of 30-36 %. Likewise, (Beckers) writes that many small wind turbines do not get above 30 % overall efficiencies and uses this number as a 'real-world efficiency' from wind to electricity grid.

Wind turbines are more efficient at some wind speeds than other. This is a combination of the efficiency of the blades and the maximum limit of the generator. Figure 18.21 shows the test results for a 2.4 kW 'Skystream' wind turbine. As seen, the efficiency is highest in wind speeds from around 5-10 m/s and at around

13 m/s, the turbine reaches its peak power, which means that higher winds are not utilized. All wind turbines show an efficiency curve with overall the same form as on Figure 18.21. Some turbines have higher efficiencies at the lower wind speeds and reach a higher peak efficiency (35 %) at wind speeds around 6-7 m/s. It seems, that this is especially the case with larger household wind turbines (10-12 kW). (WindpowerProgram)

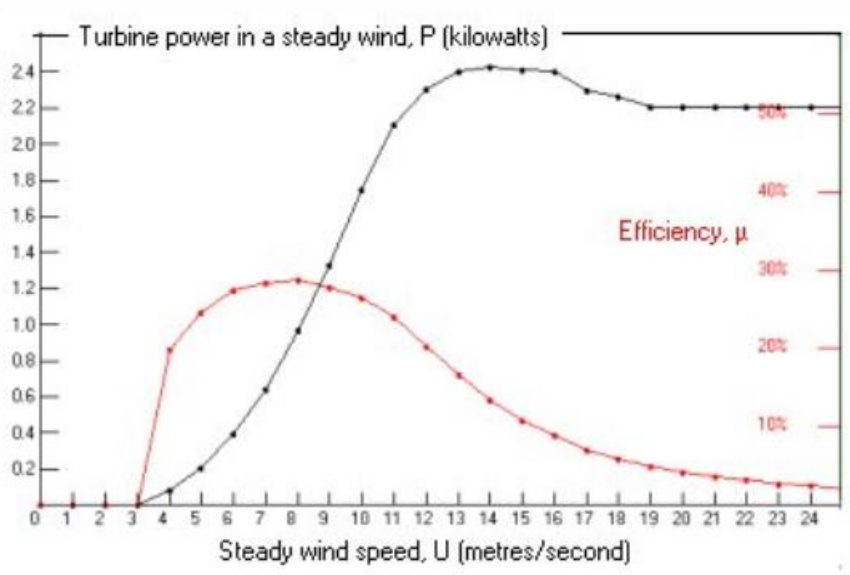

Figure 18.21 – Test results for Skystream wind turbine

To get a realistic calculation of the electricity generation, efficiencies of this order should be used. If the Air Force 1 turbine with wind speed of 3 m/s and a peak power of 1142 W is assumed to be relatively efficient, realistic efficiencies could look like in Table 18.13.

Wind [m/s]	Estimated realistic efficiency [%]	Estimated realistic power [W]	Stated power [W]
3	10	4	26
4	20	19	55
5.5	25	60	135
6.5	28	116	227
7.2	28	157	296
8.6	28	268	450
9.5	28	348	558
11	25	500	768
12.5	20	587	1002
14	16	660	1142

Table 18.13 – Estimated realistic efficiency of Air Force 1 wind turbine

When the efficiencies of Table 18.13 are used instead of the stated power curve for the Air Force 1, the yearly production is reduced from 1253 kWh to 670 kWh – a reduction of 47 %. On a renewable energy forum (Navitron) some real-life measurement with the turbine shows an annual generation of 725 kWh at a mean wind of 5.36 m/s. When the wind in the *Off-grid Simulation Tool* is adjusted to give this mean wind speed, the generation is 880 kWh. This indicates that real life performance might be even worse than the estimated efficiencies of Table 18.13.

This discussion indicates, that the stated performance of small wind turbines cannot always be trusted. This can lead to a generation in the simulation tool that is significantly higher than in real life, which can distort the simulation of the entire energy system and give an unrealistic result. For this reason, an effort should be put into finding a wind turbine with a certified/tested power curve.

Appendix S Investigation of possible options for small wind turbines in Denmark

Excel 1kW turbine

The Excel 1kW wind turbine made by the American company Bergey Wind Power has good reviews and a rotor area of 4.91 m2, which is just below the Danish certification limit of 5 m2.

The wind turbine has the following specifications (Sonkyo Energy):

- Rotor diameter: 2.5 meter
- Rated power (11 m/s): 1 kW
- Cut in speed: 3 m/s
- Weight: 75 kg
- Warranty: 5 Years

The price of the turbine in Europe is around 39-43.000 DKK without tower (renugen) (Solutions Energies) but only around 24,000 DKK in USA (Eventhorizonsolar). Table 18.14 shows both the stated power curve (Solicity) and a power curve stated by (Michael), whom has tested it under standard (real) conditions. As seen the stated efficiencies are high (not impossible), but the real-life efficiencies are significantly lower.

Wind [m/s]	Stated power [W]	Efficiency [%]	(Michael) [W]	Efficiency [%]
3	25	30	0	1
4	66	34	20	10
6	225	34	130	20
7.5	450	35	250	19
9	720	32	440	20
10.5	1000	28	650	18
12	1220	23	820	15
13.5	1220	16	980	13
15	1150	11	1010	10
18	980	5	1000	6

Table 18.14

The Kestrel e230i 800 W wind turbines

The South African company Kestrel makes a wind turbine with a rotor area of 4.2 m^2, that could be an interesting possibility (Kestrel). Some of the larger Kestrel turbines have good reviews (Piggott, Hugh - Kestrel) and as seen below, the stated power curve has realistic efficiencies. The turbine could not be found on the European market during this research (06-01-2017). The price without tower in the United States is around 14,000 DKK, but it can be significantly higher in Europe. (Emarineinc). The wind turbine has the following specifications:

- Rotor diameter: 2.3 meter
- Rated power (12.5 m/s): 800 W
- Cut in speed: 2.5 m/s
- Weight: 45 kg
- Warranty: 2 years

Wind [m/s]	Stated power [W]	Calculated efficiency [%]
3	20	29
4	50	30
6	130	23
8	300	23
10	520	20
12	765	17
14	820	12
16	820	8

Windspot turbines

The Spanish company Sonkyo Energy makes 1.5 kW and 3.5 kW wind turbines, that look like good proposals for off-grid wind turbines. They are designed and tested according to international standards (Sonkyo - Cert.) and have good reviews such as (Navitron - Windspot) and according to (Folkecenter - Windspot), the annual production of the 3.5 kW is actually noteworthy higher than claimed.

Including controller and dumb load, the 1.5 kW can be bought for around 36,000 DKK and the 3.5 kW for 47.000 DKK (GBenergy). This is prices in Italy without tower and without transport to Denmark. In the following, some more information about the two wind turbines are stated. The crucial problem is, that the turbines have a rotor area above 5 m2 and there is no “turbine-on-tower” systems certified in Denmark available.

Windspot 1.5 kW wind turbine from the Spanish Sonkyo Energy

The wind turbine is certified in France according to the international standard IEC 61400-2 for small wind turbines. It has not been type-certified in Denmark by one of the companies approved for making certifications (Energistyrelsen - Cert. , u.d.). The wind turbine has the following specifications (Sonkyo Energy, u.d.):

- Rotor diameter: 3.3 meter
- Rated power (12 m/s): 1.5 kW
- Cut in speed: 3 m/s
- Weight: 155 kg
- Estimated annual production:
  - Mean wind 5 m/s: 2383 kWh
  - Mean wind 7 m/s: 4850 kWh

Wind [m/s]	Stated power [W]	Calculated efficiency [%]
3	40	28
4	100	29
6	300	26
8	700	26
10	1150	22
12	1550	17
14	1650	11
16	1625	7
18	1580	5
20	1600	4

The efficiencies of this power curve seem realistic compared to the previous discussion. The company claims a yearly production of 2383 kWh at a mean wind of 5 m/s. At this mean wind, the *Off-grid Simulation Tool* gives 2385 kWh which indicates, that it is a realistic number.

Windspot 3.5 kW wind turbine from the Spanish Sonkyo Energy

Certified in Denmark with tower from the company LS Stoker until the 16th of May 2017, but LS Stoker seems to be closed. According to (Folkecenter, 2012), Windspot 3.5 kW from LS Stoker had a price of 200.000 DKK. The wind turbine has the following specifications (Sonkyo Energy, u.d.):

- Rotor diameter: 4.05 meter
- Rated power (12 m/s): 3.5 kW
- Cut in speed: 3 m/s
- Weight: 185 kg
- Warranty: 5 Years
- Estimated annual production:
  - Mean wind 5 m/s: 3610 kWh
  - Mean wind 7 m/s: 7350 kWh

Wind [m/s]	Stated power [W]	Calculated efficiency [%]
3	120	46
4	250	49
6	750	43
8	1600	39
10	2600	32
12	3500	25
14	3720	17
16	3600	11
18	3500	7
20	3550	6

Appendix T Roughness classification and obstacle description for Assens

Roughness classification (15 km radius) and obstacles description for DMI measurement station at Assens, Denmark.

In order to estimate the wind conditions at different locations with the hourly wind data from Assens the roughness of the terrain around the location are described, so that the data can be adjusted according to other local conditions.

The roughness classification is presented in the first part of the appendix as a roughness rose with a radius of 15 km and is divided into 12 sectors of 30 degrees. These sectors are shown three at a time in on the figures on the following pages.

For each sector the terrain is divided into areas with more or less the same roughness. The division is in the upwind direction (i.e. lines over the width of the sector) and the distances from the location are stated on the figures. For areas with different terrain types where a division is impossible an area weighted mean value is found for the area. The roughness lengths for the areas are estimated based on more detailed photo-maps (Google Maps) than the map used for the figures. The roughness estimates are stated at under the figures together with a description of the areas.

The estimated roughness lengths in a radius of one kilometer around the location are shown on Figure, where the resolution of the map is higher.

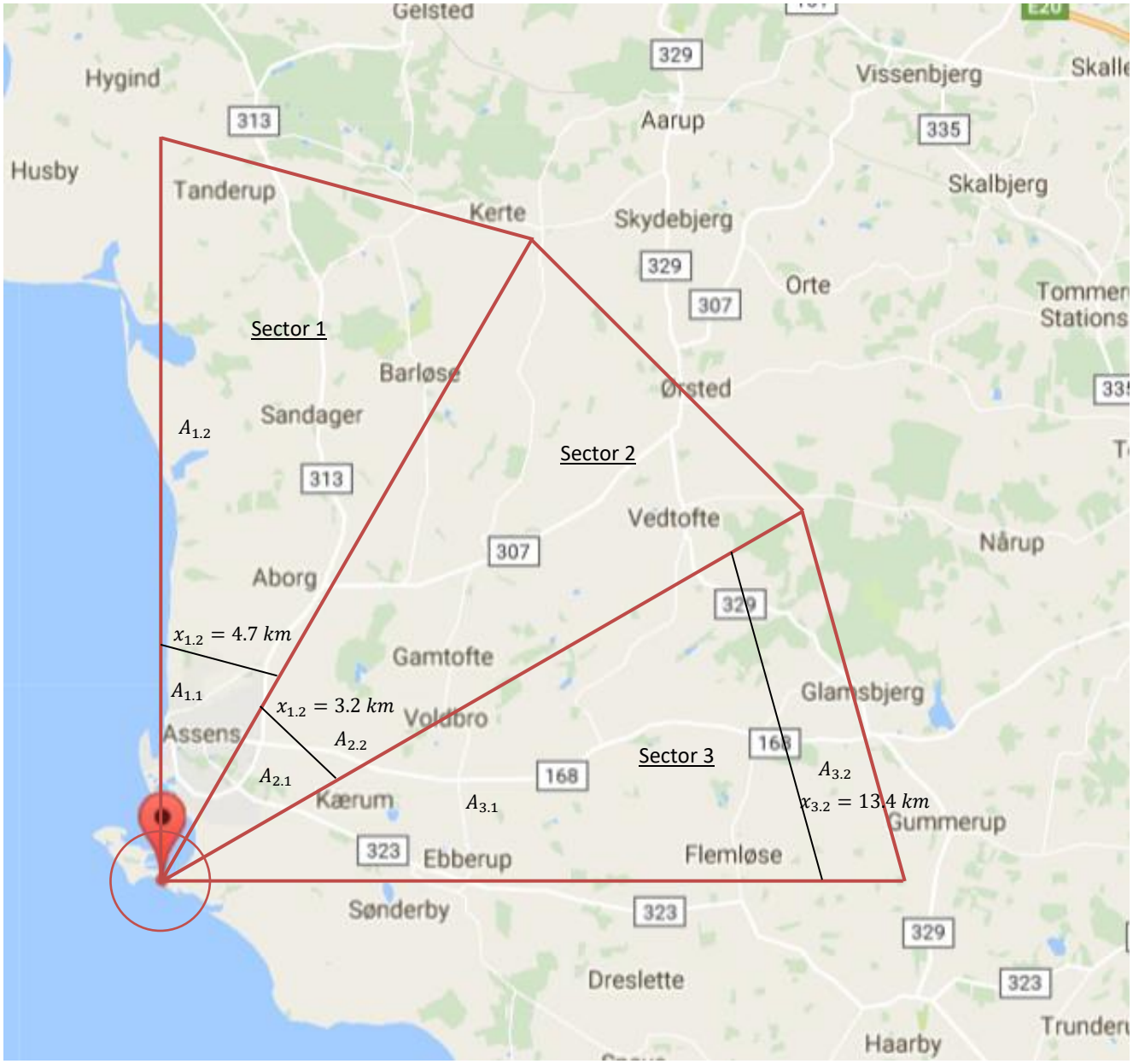

Sector 1: $A_{1.1}$ is the small town Assens with $Rl_{1.1} = 0.4$. $A_{1.2}$ is farmland with a lot of hedgerows, some scattered forest areas and small villages - roughness is estimated to be $Rl_{1.2} = 0.3$.

Sector 2: $A_{2.1}$ is a part of the small town Assens and some farmland with hedgerows, scattered forest areas and small villages - roughness is estimated to be $Rl_{2.1} = 0.3$. $A_{2.2}$ is farmland with hedgerows and a few forest areas - roughness is estimated to be $Rl_{2.2} = 0.2$.

Sector 3: $A_{3.1}$ is more open farmland, but still with hedgerows and small villages - roughness is estimated to be $Rl_{3.1} = 0.15$. $A_{3.2}$ is a mix of forest area, the village Glamsbjerg and farmland - roughness is estimated to be $Rl_{3.2} = 0.35$.

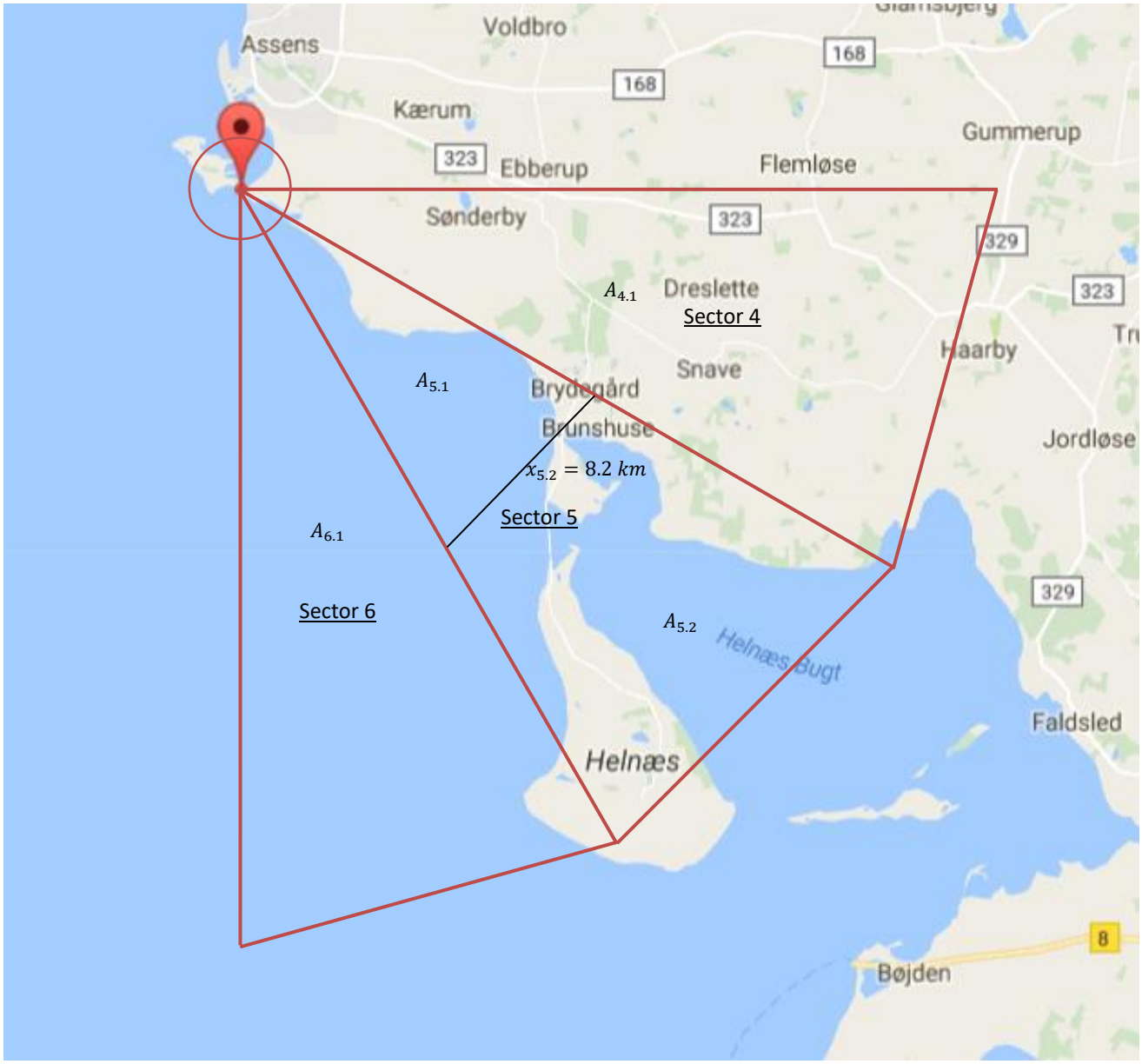

Sector 4: $A_{4.1}$ is farmland with a lot of hedgerows, some scattered forest areas and small villages - roughness is estimated to be $Rl_{4.1} = 0.3$.

Sector 5: $A_{5.1}$ is water surface with $Rl = 0.0002$ and 10 % farmland with $Rl = 0.2$. This gives an area weighted mean for $A_{5.1}$ of $Rl_{5.1} = 0.9 \cdot 0.0002 + 0.1 \cdot 0.2 = 0.02$. $A_{5.2}$ is estimated to be 50 % water surface and 50 % farmland with a lot of hedgerows, forest areas and small villages (roughness 0.35). This gives an area weighted mean for $A_{5.2}$ of $Rl_{5.2} = 0.5 \cdot 0.0002 + 0.5 \cdot 0.35 = 0.18$.

Sector 6: $A_{6.1}$ is water surface with $Rl_{6.1} = 0.0002$.

Sector seven and eight covers only water, which gives them roughness class 0 (roughness length 0.0002).

Area $A_{9.1}$is water surface with roughness lenght of 0.0002. Area $A_{9.2}$ is mostly farmland with a lot of hedge-rows, some forest areas and a small summer house area. This is estimated to have a roughness between class 2.5 and 3 with a roughness length of 0.28. The area also contains around 10 % water surface, with a roughness length of 0.0002. The area weighted length is calculated to be $0.9 \cdot 0.28 + 0.1 \cdot 0.0002 = 0.252$.

Sector 10: $A_{10.1}$ is water surface with $Rl = 0.0002$. $A_{10.2}$ is estimated to be 55 % water surface and 45 % farmland with a lot of hedgerows, scattered forest areas and small villages (roughness 0.35). This gives an area weighted mean for $A_{10.2}$ of $Rl_{10.2} = 0.55 \cdot 0.0002 + 0.45 \cdot 0.35 = 0.16$.

Sector 11: $A_{11.1}$ and $A_{11.3}$ are water surfaces with $Rl = 0.0002$. $A_{11.2}$ is estimated to be 65 % water surface and 35 % farmland with some hedgerows and scattered forest areas (roughness 0.3). This gives an area weighted mean for $A_{11.2}$ of $Rl_{11.2} = 0.65 \cdot 0.0002 + 0.35 \cdot 0.35 = 0.11$.

Sector 12: $A_{12.1}$ is assumed to be water surface with $Rl = 0.0002$. Considering the neglected land areas in $A_{12.1}$, area $A_{12.2}$ is assumed to be farmland with a lot of hedgerows and forest areas - roughness $Rl_{12.2} = 0.35$.

Roughness and obstacle description for each of the twelve 30-degree sectors in a 1 km radius around DMI measurement station at Assens, Denmark.


$Rl_{12.0} = 0.0003$
$Rl_{1.0} = 0.0003$
Nyhuse
$Rl_{11.0} = 0.081$
$Rl_{2.0} = 0.0005$
Torø
Fiskepladsen Torø
$Rl_{10.0} = 0.06$
$Rl_{3.0} = 0.13$
Københavns Lærerforenings...
Torø Huse
Thorøhuse Forsamlingshus
$Rl_{9.0} = 0.0003$
$Rl_{4.0} = 0.13$
$Rl_{8.0} = 0.0002$
$Rl_{5.0} = 0.0009$
$Rl_{7.0} = 0.0002$
$Rl_{6.0} = 0.0002$
Google


Measurement tower

Appendix U Roughness classification and obstacle illustration for location at Ebeltoft

Roughness classification (15 km radius) for Christianslundvej 1, 8400 Ebeltoft.
In the context of calculating the wind conditions at the possible building site for Project Grobund, a roughness classification has been made as a roughness rose as seen on the figure below. The used method is the same as described in Appendix T . The roughness values for the areas are stated in the table below with the notation of "sector-number.area-number" counting the areas from the location and outward.

$Rl_{1.1}$: 0.38	$Rl_{2.1}$: 0.35	$Rl_{2.2}$: 0.135	$Rl_{3.1}$: 0.3	$Rl_{3.2}$: 0.0002	$Rl_{4.1}$: 0.35	$Rl_{4.2}$: 0.0002
$Rl_{5.1}$: 0.38	$Rl_{6.1}$: 0.2	$Rl_{6.2}$: 0.0002	$Rl_{7.1}$: 0.15	$Rl_{7.2}$: 0.0002	$Rl_{8.1}$: 0.15	$Rl_{8.2}$: 0.0002
$Rl_{8.3}$: 0.15	$Rl_{9.1}$: 0.35	$Rl_{9.2}$: 0.0002	$Rl_{9.3}$: 0.17	$Rl_{10.1}$: 0.4	$Rl_{10.2}$: 0.25	$Rl_{11.1}$: 0.35
$Rl_{11.2}$: 0.0002	$Rl_{11.3}$: 0.35	$Rl_{12.1}$: 0.0002	$Rl_{12.2}$: 0.4			

Roughness and obstacle description for each of the twelve 30-degree sectors in a 1 km radius around DMI measurement station at Assens, Denmark.